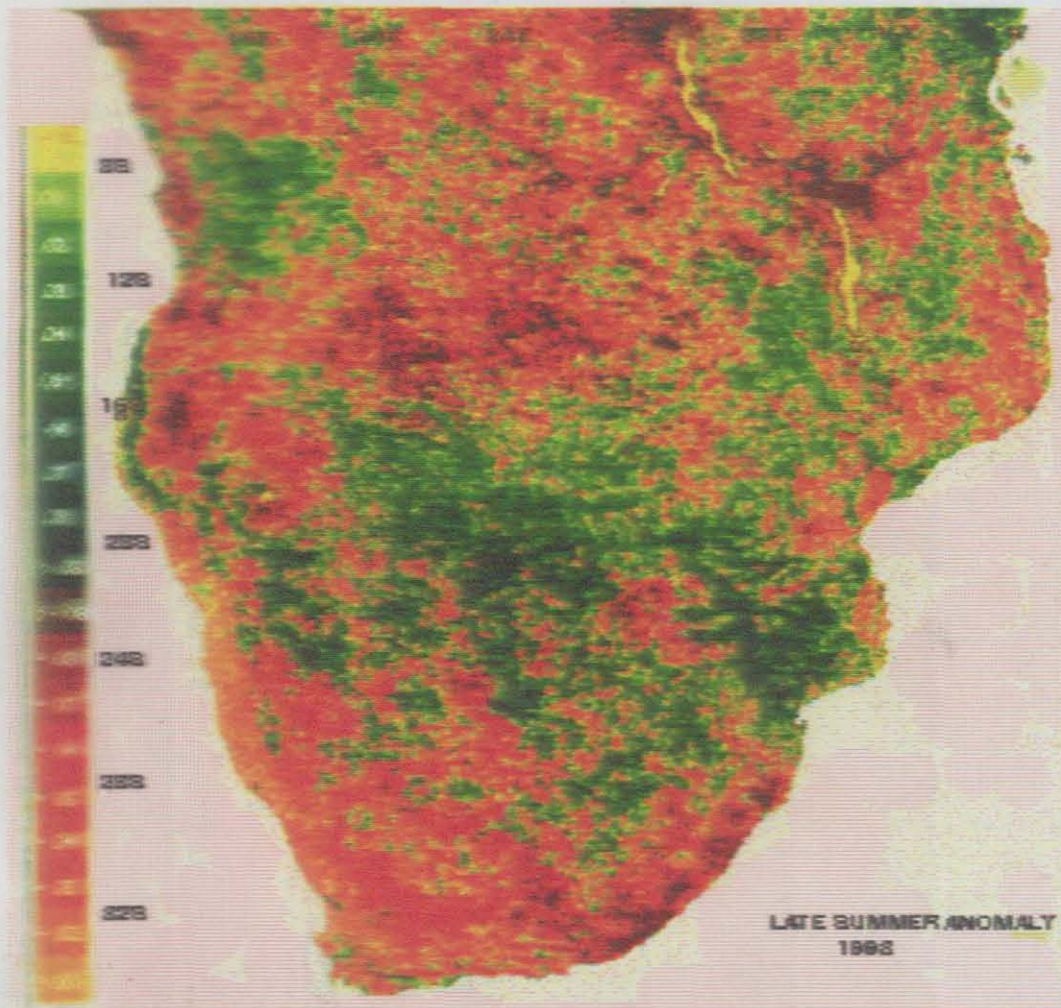


**Causes, structure and impacts of the 1992/93 drought in  
KwaZulu/Natal**

**Lawrence Thembokwakhe Dube**



**Supervisor : Professor Mark Jury**

**Department of Geography and Environmental Studies  
University of Zululand**

**December 1998**

**Thesis submitted in fulfillment of the requirements for the  
degree of Doctor of Science**

## **DECLARATION**

The whole thesis is the researcher's original work, unless specifically indicated to the contrary in the text, and has not been submitted in part or in whole to any other university for degree purposes. The research work was carried out in the Department of Geography and Environmental Studies, University of Zululand, under the supervision of Professor Mark Robert Jury.

Softly and quietly across the waiting mountains,  
    Softly and quietly and while we slept in sorrow,  
Sure of its way even in the heart of darkness,  
Came the redeeming rain:  
Came even as sleep to strained and weary eyeballs,  
Came even as rest to toil-racked limbs and tired,  
Came even as love to souls in desolation,  
So came the rain

*From drought* by Jan van Avond

## ACKNOWLEDGEMENTS

The success of a piece of research work of this magnitude cannot be attributed to one man's effort. The outstanding supervision of Professor Jury is appreciated. His thorough reading of each submission made, constructive comments, suggestions and new ideas he shared with me have been useful tools for the final output of this work. His quality of supervision has made me enjoy my work and given me an inspiration to work on the project harder.

Acknowledgements are given to ECMWF data processed at the Oceanography Dept, University of Cape Town and a note of thanks is given to the university for resources and facilities. Mr Emmanuel Mpeta mentored and familiarised me with data processing in Cape Town and his contribution to this work is also appreciated. Mr Henry Mulenga's suggestions during the course of the project have been vital and appreciation for this is herein recorded. The social company I was given by Mark Majodina during my visit in Cape Town for data analysis gave me the edge to travel and relax in a rather unfriendly weather. His efforts to ensure the availability of some of the station data from the South African Weather Bureau are also acknowledged.

NCEP/NOAA website and data processing via internet at UZ are also appreciated. Station climatic data have been made available with courtesy of Dr W. Alexander, a hydrologist at the University of Pretoria. Mrs Veronica Botha, Lydia Meyer and Anna Kozakiewics are thanked for cartographic expertise they have displayed in the annotation of some graphs in this thesis. Funding by FRD for computer facilities and network at UZ via the Centre for Environmental Studies is also recorded. Appreciation for DAAD funding and the University of Zululand's Research Committee funds are also registered. Moral support given to me by members of Geography and Environmental Studies at the University of Zululand and my family over years is appreciated.

## **DEDICATION**

This research project is dedicated to my mother, Thembekile Mama Christina Dube, who has been a pillar of strength throughout my life, Nompumelelo, my daughter Luyanda, and son Nelani.

## OUTLINE

	Page
Preface	xx to xxii
Abstract	xxiii to xxv
 <b>CHAPTER 1: INTRODUCTION</b>	
1.1 Introduction	1-1
1.2 Background to the study area	1-1
1.3 Problem statement	1-2
1.4 Hypotheses	1-3
1.5 Research objectives	1-4
1.6 Description of data and research methods	1-5
1.7 Background to drought climatology	1-6
1.8 National review of the 1992/93 drought	1-7
1.8.1 Extent of the drought in South Africa	1-7
1.8.2 Economic costs of the drought for South Africa	1-9
1.8.2.1 Sugar cane	1-10
1.8.2.2 Timber	1-10
1.8.2.3 Maize and wheat	1-11
1.8.2.4 Water supply	1-11
1.9 Drought impact studies in the SADC and elsewhere	1-12
1.10 Conclusion	1-13
 <b>CHAPTER 2: LITERATURE REVIEW: CLIMATE VARIABILITY</b>	
2.1 Introduction	2-1
2.2 Major rainfall-producing systems over SE Africa	2-2
2.3 El Nino and the Southern Oscillation (ENSO)	2-3
2.3.1 Dry and wet spells over South Africa	2-4
2.4 Some indices of climate variability over southern Africa	2-5
2.4.1 Southern Oscillation Index	2-5
2.4.2 February Rainfall Index	2-6

	Page
2.4.3 Transvaal Rainfall index	2-6
2.5 Influence of monsoons and wave perturbations on circulation regime	2-7
2.6 The climatic dipole over southern Africa and the Indian Ocean	2-8
2.7 Climatic trends	2-8
2.8 Relationships between the NDVI/OLR and climate over southern Africa	2-10
2.8.1 Mean spatial patterns of OLR and NDVI over southern Africa	2-10
2.8.2 Convective trends and OLR	2-11
2.8.3 SSTs and OLR correlations	2-11
2.8.4 NDVI as an indicator of temporal climate variability over Africa	2-13
2.9 Interannual variability of convective activity over South Africa and SSTs	2-14
2.9.1 Relative significance of SSTs in climate variability	2-14
2.9.2 Mechanism underlying rainfall variability over southern Africa	2-16
2.9.3 The role of the QBO in rainfall response	2-18
2.10 Teleconnection patterns associated with summer rainfall over South Africa	2-19
2.10.1 Correlation of rainfall and global indices	2-20
2.10.2 Regional SST teleconnection patterns	2-21
2.10.3 Regional OLR teleconnection patterns	2-22
2.10.4 Regional wind teleconnection patterns	2-23
2.11 The simulation and prediction of drought	2-24
2.11.1 Statistical predictors	2-24
2.11.2 Numerical simulations	2-26
2.11.3 Predictability of drought over South Africa	2-28
2.12 Environmental implications of drought	2-29
2.12.1 Historical perspective of drought monitoring programmes in Africa	2-29

	Page
2.13 Drought in other parts of the world	2-31
2.13.1 Drought regimes	2-31
2.13.2 Results of numerical drought simulations	2-32
2.14 Conclusions	2-33

### **CHAPTER 3: RESULTS ON LONG-TERM CLIMATE VARIABILITY OVER KWAZULU/NATAL AND THE 1992/93 DROUGHT**

3.1 Introduction	3-1
3.2 Data and methodology	3-1
3.3 Local climate variability over KwaZulu/Natal	3-2
3.3.1 Temperature	3-2
3.3.2 Rainfall	3-3
3.3.3 OLR and NDVI	3-4
3.4 Impacts of the drought	3-4
3.4.1 Midmar and Pongolapoort Dams inflow	3-5
3.4.2 Maize	3-6
3.4.2.1 Climate requirements	3-6
3.4.2.2 Maize and the economy	3-7
3.4.2.3 Maize yield	3-7
3.4.2.4 Sensitivity of maize to climate and importance of forecast	3-8
3.4.3 Sugar cane	3-9
3.4.3.1 Climate requirements	3-9
3.4.3.2 Sugar cane and the economy	3-10
3.4.3.3 Sugar cane yield	3-10
3.5 Conclusion	3-11

**CHAPTER 4: METEOROLOGICAL STRUCTURE OF THE 1992/93 DROUGHT (ECMWF)**

	Page
4.1 Introduction	4-1
4.2 Data and methodology	4-1
4.3 Results	4-2
4.3.1 May 1992 and January 1993 fields and anomalies	4-2
4.3.1.1 Geopotential heights	4-2
4.3.1.2 Temperature, vertical motion and divergence	4-3
4.3.1.3 Vectors of horizontal wind and water vapour flux	4-4
4.3.1.4 Vorticity, vorticity of water vapour flux, divergence of water vapour flux and precipitable water	4-5
4.3.2 Dry spell composites and anomalies	4-6
4.3.2.1 Outgoing longwave radiation	4-6
4.3.2.2 Geopotential heights	4-6
4.3.2.3 Temperature, vertical wind and divergence	4-8
4.3.2.4 Composite vectors of 200 hPa horizontal wind and water vapour flux	4-8
4.3.2.5 Vorticity, vorticity of water vapour flux, precipitable water and divergence of water vapour flux	4-9
4.3.2.6 The 1992/93 summer OLR and NDVI	4-10
4.4 Conclusion	4-11

**CHAPTER 5: HEMISPHERIC SCALE COMPOSITE MEAN AND ANOMALY ANALYSIS OF THE 1992/93 DROUGHT (NCEP/NOAA)**

5.1 Introduction	5-1
5.2 Data and methodology	5-1
5.3 Results	5-2
5.3.1 Anomaly fields	5-2
5.3.1.1 Geopotential heights	5-2

	Page
5.3.1.2 Wind vectors	5-3
5.3.1.3 Outgoing longwave radiation	5-4
5.3.1.4 Precipitable water	5-4
5.3.1.5 Vertical motion	5-5
5.3.1.6 Streamfunction	5-5
5.3.1.7 Velocity potential and divergence	5-6
5.3.1.8 Sea surface temperatures	5-7
5.3.1.9 Surface air temperature	5-7
5.3.2 Vertical sections anomaly fields	5-8
5.3.2.1 Vertical motion	5-8
5.3.2.2 Zonal winds	5-9
5.3.2.3 Meridional winds	5-9
5.3.2.4 Velocity potential and divergence	5-9
5.3.2.5 Streamfunction	5-10
5.4 Conclusion	5-10

## **CHAPTER 6: CAUSES OF THE 1992/93 DROUGHT**

6.1 Introduction	6-1
6.2 Antecedent (SON) conditions	6-1
6.2.1 Geopotential heights	6-1
6.2.2 Wind Vectors	6-2
6.2.3 Outgoing longwave radiation	6-3
6.2.4 Sea surface temperatures	6-3
6.2.5 Precipitable water	6-4
6.2.6 Vertical motion (Omega)	6-4
6.2.7 Streamfunction	6-5
6.2.8 Velocity potential	6-5
6.3 Discussion of 1992/93 (DJF) drought	6-6
6.3.1 Jet stream influence	6-6
6.3.1.1 Jet stream dynamics	6-7

	Page
6.3.2 Tropical influences	6-9
6.3.3 Effects of local topographic circulations	6-10
6.3.4 Budget calculations	6-11
6.3.5 Regional climatic patterns	6-12
6.4 Synthesis	6-13
6.5 Conclusion	6-15

## **CHAPTER 7: SUMMARY AND CONCLUSIONS**

7.1 Summary	7-1
7.2 Recommendations	7-3
7.3 Conclusions	7-5

<b>REFERENCES</b>	Ref-1 to Ref-23
-------------------	-----------------

<b>APPENDIX</b>	A-1 to A-12
-----------------	-------------

## **APPENDIX A3: STATISTICAL PREDICTION OF RAINFALL AND CROP YIELDS**

A3.1 Rainfall over the Swaziland-KwaZulu/Natal region	A-1
A3.2 Maize yield over South Africa	A-1
A3.3 Sugar cane yield over KwaZulu/Natal	A-1

### **A3 TABLE**

Table A3.1: Predictor definitions	A-2
-----------------------------------	-----

## **APPENDIX A4: DEFINITIONS AND CALCULATION OF SOME ATMOSPHERIC VARIABLES**

A4.1 Vorticity and divergence	A-3
A4.2 Precipitable water	A-4
A4.3 Streamfunction	A-5
A4.4 Velocity potential	A-5

	Page
A4 FIGURES	A-6 to A-11
A4 TABLE	
Table A4.1: Meteorological pentads	A-12

## LIST OF FIGURES

	Page
Fig. 1.1: Location map of KwaZulu/Natal and its bioclimatic groups	1-14
Fig. 1.2: Historical variation in the Southern Oscillation Index	1-15
Fig. 1.3: Map of South Africa showing provinces, major towns and cities of the country	1-15
Fig. 1.4: Food production chart to account for the way drought can affect production activities	1-16
Fig. 2.1: Smoothed departures of monthly central Indian Ocean SST and the global SOI	2-34
Fig. 2.2: Schematic illustration of wind circulation for (a) wet, and (b) dry summer scenarios	2-34
Fig 2.3: Schematic illustration of zonal, vertical circulations for below normal South African summer rainfall	2-35
Fig. 2.4: (a) Composite OLR difference for wet – dry summers (b) The two core regions representing ENSO related interannual rainfall anomalies	2-35
Fig. 2.5: Desertification map for southern Africa	2-36
Fig. 2.6: Southern Africa rainfall trends from 1900-01 to 1995-96 as percent anomalies from the 1962-90 average	2-36
Fig. 2.7: Southern Africa temperature trends from 1897 to 1995 expressed as anomalies from the 1961-90 average	2-37
Fig. 2.8: (a) Correlations between Jan-Feb-Mar SST principal component scores in the ocean to the east and south east of South Africa and rainfall. (b) Envisaged circulation adjustments associated with warm events in the region	2-37

	Page
Fig. 2.9: (a) Correlations between Jan-Feb-Mar SST principal component scores in the western equatorial Indian Ocean and rainfall. (b) Envisaged circulation adjustments associated with warm events in the region	2-38
Fig. 2.10: Correlation map of SST vs SAF rainfall for the preceding Oct (lag -4 months, (a)) and Feb (0 lag, (b))	2-38
Fig. 2.11: Correlation map of OLR vs SAF rainfall for the preceding Oct (lag -4 months, (a)) and February (0 lag, (b))	2-39
Fig. 3.1: Climatological data districts of South Africa	3-12
Fig. 3.2: Seasonal cycle of maximum temperature over the KwaZulu/Natal coastal region	3-13
Fig. 3.3: Historical maximum temperature anomalies over the KwaZulu/Natal coastal region from 1960 to 1996	3-13
Fig. 3.4: (a) Distribution of rotated PC4 of normalised DJF rainfall and (b) associated time series of coefficients. (c) Estimated cross-correlations of U200 (PC4, loaded at 32°E/30°S) and KwaZulu/Natal temperature	3-14
Fig. 3.5: KwaZulu/Natal rainfall seasonal cycle	3-15
Fig. 3.6: KwaZulu/Natal rainfall departures (18 pt smoothed) from 1960 to 1996	3-15
Fig. 3.7: KwaZulu/Natal rainfall departures (3 pt smoothed) from 1960 to 1996	3-16
Fig. 3.8: Variation in KwaZulu/Natal's vegetation index (January to March 1982-1994) for grid points 30°S/30°E and 27.5°S/32.5°E	3-16
Fig. 3.9: Average OLR for DJF pentads (1975-94) at the point 30°E/30°S	3-17
Fig. 3.10: Location of major dams of South Africa	3-17
Fig. 3.11: Midmar Dam inflow seasonal cycle	3-18
Fig. 3.12: Midmar Dam inflow (1964-1996)	3-18

	Page
Fig. 3.13: Pongolapoort Dam inflow (1930-1996)	3-19
Fig. 3.14: Periodogram of Pongolapoort Dam inflow	3-19
Fig. 3.15: Comparison of rainfall and maize in KwaZulu/Natal (1972-1996)	3-20
Fig. 3.16: Sugar cane growing areas in South Africa	3-20
Fig. 3.17: Sugar cane yield per hectare in KwaZulu/Natal (1950-1995)	3-21
Fig. 4.1: Geopotential heights and anomalies (gpm) at 850, 500 and 200 for May 1992 and January 1993	4-12
Fig. 4.2: Anomalies of temperature at 850 hPa, vertical motion at 500 hPa and divergence for May 1992 and January 1993	4-13
Fig. 4.3: Horizontal wind anomaly at 200 hPa for (a) May 1992, and (b) January 1993	4-14
Fig. 4.4: Anomaly of water vapour flux vectors integrated between 1000 and 300 hPa for May 1992	4-15
Fig. 4.5: Anomaly (from the 1980-94 mean) of water vapour flux vectors integrated between 1000 and 300 hPa for January 1993	4-16
Fig. 4.6: Anomalies of vorticity at 200 hPa, integrated vorticity of water vapour flux between 1000-500 hPa and integrated precipitable water between 1000-300 hPa for May 1992 and January 1993	4-17
Fig. 4.7: Means and anomalies of divergence of water vapour flux integrated between 1000 and 300 hPa for May 1992 and January 1993	4-18
Fig. 4.8: OLR time series for Dec 92 – Feb 93 (30°S, 30°E)	4-19
Fig. 4.9: (a-d) OLR departures from the 1980-94 DJF mean for pentads 70 (1992), 01, 03, 07 and 12 (1993); (e) mean composite OLR for DJF pentads (a-d)	4-20

	Page
Fig. 4.10: Pentad composite geopotential heights and anomalies at 850, 500 and 200 hPa for DJF 1992/93 dry spell	4-21
Fig. 4.11: Pentad composites and anomalies of temperature at 500 hPa, vertical wind at 500 hPa and divergence at 200 hPa for DJF 1992/93 dry spell	4-22
Fig. 4.12: Composite of (a) horizontal wind field vectors at 200 hPa, and (b) water vapour flux vectors integrated between 1000 – 300 hPa, for the DJF 1992/93 dry spell	4-23
Fig. 4.13: Pentad composites and anomalies of vorticity at 200 hPa, integrated vorticity of water vapour flux between 1000 – 500 hPa and integrated precipitable water between 1000 – 300 hPa for DJF 1992/93 dry spell	4-24
Fig. 4.14: Pentad composite and anomaly of divergence of water vapour flux integrated between 1000 – 300 hPa for DJF 1992/93 dry spell	4-25
Fig. 4.15: Satellite photographs of the anomalies NDVI over southern Africa for the 1992/93 early summer, and late summer periods	4-26
Fig. 5.1: Geopotential heights (a) mean and (b) anomaly at 850 hPa for DJF 1992/93	5-12
Fig. 5.2: Geopotential heights (a) mean and (b) anomaly at 500 hPa for DJF 1992/93	5-13
Fig. 5.3: Geopotential heights (a) mean and (b) anomaly at 200 hPa for DJF 1992/93	5-14
Fig. 5.4: (a) Mean and (b) anomalies of wind vectors and speed at 850 hPa for DJF 1992/93	5-15
Fig. 5.5: (a) Mean and (b) anomalies of wind vectors and speed at 500 hPa for DJF 1992/93	5-16
Fig. 5.6: (a) Mean and (b) anomalies of wind vectors and speed at 200 hPa for DJF 1992/93	5-17
Fig. 5.7: (a) Mean and (b) anomalies of OLR for DJF 1992/93	5-18

	Page
Fig. 5.8: Columnar precipitable water (a) mean and (b) anomaly for DJF 1992/93	5-19
Fig. 5.9: (a) Mean and (b) anomalies of vertical motion at 500 hPa for DJF 1992/93	5-20
Fig. 5.10: Streamfunction (a) mean and (b) anomalies at the 0.995 sigma level for DJF 1992/93	5-21
Fig. 5.11: Streamfunction (a) mean and (b) anomalies at the 0.2101 sigma level for DJF 1992/93	5-22
Fig. 5.12: Velocity potential (a) mean and (b) anomalies at the 0.995 sigma level for DJF 1992/93	5-23
Fig. 5.13: Velocity potential (a) mean and (b) anomalies at the 0.2101 sigma level for DJF 1992/93	5-24
Fig. 5.14: (a) Atlantic and Indian, and (b) Pacific Ocean anomalies of sea surface temperature during DJF 1992/93	5-25
Fig. 5.15: (a) Mean and (b) anomalies of air temperature at 1000 hPa over land and sea during DJF 1992/93	5-26
Fig. 5.16: DJF 1992/93 vertical motion anomalies between 1000 and 100 hPa levels at (a) 30°E and (b) 15°S	5-27
Fig. 5.17: DJF 1992/93 zonal wind anomalies between 1000 and 10 hPa levels at (a) 30°E and (b) 30°S	5-28
Fig. 5.18: DJF 1992/93 zonal wind anomalies between 1000 and 10 hPa levels at (a) 60°E and (b) 15°S	5-29
Fig. 5.19: DJF 1992/93 meridional wind anomalies between 1000 and 100 hPa levels at (a) 60°E and (b) 15°S	5-30
Fig. 5.20: DJF 1992/93 velocity potential anomalies between the 0.9950 and 0.2101 sigma levels at (a) 30°E and (b) 30°S	5-31
Fig. 5.21: DJF 1992/93 streamfunction anomalies between the 0.9950 and 0.2101 sigma levels at (a) 60°E and (b) 15°S	5-32
Fig. 6.1: Geopotential heights (a) mean and (b) anomaly at 850 hPa for SON 1992	6-17

	Page
Fig. 6.2: Geopotential heights (a) mean and (b) anomaly at 500 hPa for SON 1992	6-18
Fig. 6.3: Geopotential heights (a) mean and (b) anomaly at 200 hPa for SON 1992	6-19
Fig. 6.4: (a) Mean and (b) anomalies of wind vectors and speed at 850 Pa for SON 1992	6-20
Fig. 6.5: (a) Mean and (b) anomalies of wind vectors and speed at 500 hPa for SON 1992	6-21
Fig. 6.6: (a) Mean and (b) anomalies of wind vectors and speed at 200 hPa for SON 1992	6-22
Fig. 6.7: (a) Mean and (b) anomalies of OLR for SON 1992	6-23
Fig. 6.8: (a) Atlantic and Indian, and (b) Pacific Ocean anomalies of sea surface temperature during SON 1992	6-24
Fig. 6.9: Columnar precipitable water (a) mean and (b) anomaly for SON 1992	6-25
Fig. 6.10: (a) Mean and (b) anomalies of vertical motion at 500 hPa for SON 1992	6-26
Fig. 6.11: SON 1992 vertical motion (omega) anomalies between 1000 and 100 hPa levels at (a) 30°E and (b) 15°S	6-27
Fig. 6.12: Streamfunction anomalies at the (a) 0.995, and (b) 0.2101 sigma levels for SON 1992	6-28
Fig. 6.13: Velocity potential anomalies anomalies at the (a) 0.995, and (b) 0.2101 sigma levels for SON 1992	6-29
Fig. 6.14: (a) Schematic illustration of the positions of the subtropical and subpolar jet streams, and (b) wind circulation patterns, during the 1992/93 dry summer over South Africa	6-30
Fig. 6.15: Scheme of westerly jet producing dry conditions over South Africa during the 1992/93 dry summer season	6-30

	Page
Fig. 6.16: Air and dew-point temperatures variations over KwaZulu/Natal along a section from the Drakensberg to Durban during DJF 1992/93. The warming effect with altitude decrease is apparent from the Figure	6-31
Fig. 6.17: Conceptual model of the influences of jet streams, meso-scale circulation and tropical effects on mid-summer precipitation over KwaZulu/Natal	6-31
Fig. A4.1: DJF 1992/93 geopotential height at 30°S latitude at the (a) 1000 hPa level, and (b) 10 hPa level	A-6
Fig. A4.2: DJF 1992/93 geopotential height anomalies at (a) 35°S latitude at the 1000 hPa level, and (b) 10 hPa level	A-7
Fig. A4.3: DJF 1992/93 streamfunction anomalies at 30°S latitude at the (a) 0.9950 sigma level, and (b) 0.2101 sigma level	A-8
Fig. A4.4: DJF 1992/93 streamfunction anomalies at 35°S latitude at the (a) 0.9950 sigma level, and (b) 0.2101sigma level	A-9
Fig. A4.5: DJF 1992/93 velocity potential anomalies at 30°S latitude at the (a) 0.9950 sigma level, and (b) 0.2101 sigma level	A-10
Fig. A4.6: DJF 1992/93 velocity potential anomalies at 35°S latitude at the (a) 0.9950 sigma level, and (b) 0.2101 sigma level	A-11

## LIST OF TABLES

	Page
Table 1.1: Bioclimatic groups of KwaZulu/Natal	1-17
Table 2.1: ENSO and anti-ENSO events from 1950 to 1998	2-39
Table 2.2: Jan-Mar rainfall variance in the summer rainfall region accounted for by variations in JFM SST with and without the phase of the QBO taken into account	2-40
Table 3.1: Maize last planting dates	3-21
Table 3.2: Sugar cane-growing areas in KwaZulu/Natal	3-21
Table 6.1: Evaporative losses over KwaZulu/Natal during the dry 1992/93 summer	6-32
Table 6.2a: SON 1992 and DJF 1992/93 departures of meteorological fields from their respective composite means for KwaZulu/Natal	6-32
Table 6.2b: SON 1992 and DJF 1992/93 departures of meteorological fields from their respective composite means for core centres of activity and areas indicating teleconnections to the 1992/93 KwaZulu/Natal drought structure	6-33 to 6-34
Table 6.3: Conceptual model of jet streams influence on mid-summer rainfall over eastern parts of South Africa	6-35
Table A3.1: Predictor definitions	A-2
Table A4.1: Meteorological pentads	A-12

## PREFACE

Of all the natural environmental hazards on earth, drought is possibly the most insidious. By its nature it develops slowly, frequently occupying vast areas and persisting for lengthy periods. In addition to the loss of life and destruction of vegetation, serious damage can also occur to top-soil under drought conditions, thus resulting in enhanced desertification. Despite the widespread and repetitive nature of drought, research into its origins and precursor mechanisms has been surprisingly limited. Drought research has received sporadic encouragement, normally at times of major drought episodes and, in general, much research connected with drought has been incidental to other climatic problems.

Drought is a normal feature of climate and its occurrence is inevitable. The widespread occurrence of severe drought during the past three decades underscores the vulnerability of both developed and developing societies to its ravages. Societies and government have in the past chosen to react to drought rather than employing timely risk management skills. The 1991/92 drought provides a good example of this. Governments in Zimbabwe and other southern African states were warned in advance of the looming drought by meteorologists but they resorted to waiting till the crisis had taken its toll.

Widespread and sustained droughts that have periodically afflicted southern Africa over the past three decades are those in 1964, 1968, 1970, 1982, 1983, 1984, and 1987 often in association with the El Nino. Recent drought in southern Africa has renewed concern about possible man-made climate change. A large majority of the population here relies on agriculture at a subsistence level for food, or at a more advanced level to generate income,

and are therefore particularly susceptible to changes in rainfall and climate. This problem is exacerbated by the high degree of inter- and intra-seasonal rainfall variability over the southern African subcontinent. Another factor compounding the drought problem is the growing population of southern Africa which is placing increasing pressure on already limited water resources. Improving the understanding and methods of prediction of the rainfall systems affecting southern Africa will be of great assistance to engineers, hydrologists and agriculturalists in the planning development of effective water management policies.

This seven-chapter thesis provides a detailed account of the 1992/93 drought. It seeks to describe the causes, structure and impacts of the drought. Chapter 1 is an introduction to the study wherein the regional setting is described, background to the problem, hypotheses and general objectives of the study, as well as the background to the 1992/93 drought in KwaZulu/Natal and elsewhere are outlined.

Chapter 2 reviews works pertaining to climate variability over southern Africa and other parts of the world with emphasis on the more recent ones. Atmosphere-ocean interaction studies relevant to below-normal rainfall events are emphasised. Linked to these studies is the predictability of drought occurrence using general circulation models (GCM). The use of GCMs initialised using predicted sea surface temperature changes in the South Atlantic and Indian Oceans in the Africa region holds promise for the timeous forecasting of drought conditions over southern Africa. However, further work must be done to reduce the uncertainties associated with the use of global climate models to predict seasonal or within-seasonal rainfall.

Chapter 3 gives a perspective on historical climate variability of KwaZulu/Natal utilising data obtained from the SAWB. Parameters used to assess climate variability are temperature, rainfall and satellite outgoing

longwave radiation (OLR) which has been used as a proxy for convective activity over the region. The stations data date back as far as 1960. The impact of the 1992/93 drought is also presented in this Chapter in terms of dam inflows and agricultural output. For both long-term climate variability and impacts of the drought, means and anomalies of climatic variables are computed.

Details on the datasets utilised (rainfall, tropospheric wind, OLR, etc.) are given in Chapters 4 and 5 which also present the analysed data on climate variability over KwaZulu/Natal and the meteorological structure of the 1992/93 drought, respectively. The data are obtained from European Centre for Medium-Range Weather Forecasting (ECMWF) and National Centres for Environmental Prediction / National Oceanic and Atmospheric Administration (NCEP/NOAA). These data are also analysed for means and anomalies, and comparisons between the two datasets undertaken in Chapter 5. Links with previous research by other authors and plausible explanations are given for the observed circulation patterns.

The causes of the drought are discussed in Chapter 6 in the context of the results of the analyses and literature review. Antecedent SON analysis is undertaken on NCEP/NOAA data to detect the 'memory', if any, in the circulation regime contributing to below normal rainfalls during the peak summer of 1992/93. The overall summary and recommendations are given in Chapters 7 reflecting on the objectives of the study and the challenges that lie ahead in drought studies. Emphasis is placed on the need for improved forecasting skills and timely planning so as to better prepare for the drought as it occurs.

## ABSTRACT

A majority of the population in southern Africa rely on agriculture at a subsistence level for food, or at a more advanced level to generate income, and are therefore susceptible to changes in rainfall and climate. The high incidence of drought since the 1970's (Jury, 1996), and particularly the devastating droughts of 1982/83 (Jury and Levey, 1997) have laid a ground of motivation for a study on circulation changes associated with the 1992/93 drought over KwaZulu/Natal and its impacts.

This research analyses the historical context of the 1992/93 drought in KwaZulu/Natal using ECMWF and NCEP/NOAA data at a resolution of  $2.5^{\circ}$  x  $2.5^{\circ}$ . To outline the causes and structure of the drought surface and upper-level meteorological data are utilised and impacts are assessed using agricultural production and water resource data. Pentad synoptic weather data for the drought period are composited to establish patterns of circulation and convection over the region, and departures from the historical mean computed. Satellite and conventional data sources are used and time series analysis is undertaken. Outgoing longwave radiation (OLR) and normalised difference vegetation index (NDVI) are used as a proxy for convective intensity and for the identification of impacted areas over South Africa. Wind data and derived parameters are employed to explore large-scale dynamical structures. Pongolapoort and Midmar Dams inflow levels, and agricultural production output data from sugar cane and maize industries are used to gauge the severity of the drought.

Data analysis indicates that increased westerly winds with surface marine lows and continental highs prevailed over southern Africa. Anomalous

divergence and subsidence occurred over the eastern subcontinent. This was coupled with reduced tropical moist inflows. Anticyclonic vorticity and subsidence via upper level convergence suppressed convection over KwaZulu/Natal. Mid-latitude winds played a significant role in producing the drought over KwaZulu/Natal through the northward (southwards) movement of the subpolar (subtropical) jet streams which limited the supply of moisture into this region. The area of reduced water vapour flux extended from 15-33°S and 15-35°E.

The 1992/93 DJF analysis of OLR reflects a SE-NW oriented wave-train pattern over southern Africa with KwaZulu/Natal and Malawi anti-phase with the wet Zambezi. Negative anomalies of the streamfunction are obtained between 35°S and 15°S associated with anticyclonic circulation at the 50°E longitude. These are areas where negative SSTs are observed to the east. It is thus apparent that a Hadley cell is a driving mechanism behind the 1992/93 drought over parts of southern Africa south of 20°S.

The atmospheric wave train pattern during SON is aligned in the same axis as in the DJF season but the anomaly values are higher in the latter season. This is an indication that even during the pre-summer season convection is suppressed over KwaZulu/Natal and parts of southern Africa south of 20°S. No propagation of these wave trains is observed. The values of below normal precipitable water within these axes increase in the peak summer season. During the DJF (summer) season, the Indian and Atlantic Oceans were anti-phase at the surface and upper levels, but show in-phase tendencies in the pre-summer velocity potential anomaly field.

Surface temperatures over southern Africa led to evaporative losses which contributed to a decline in vegetation cover, dam and streamflow levels. The 1992/93 agricultural season was characterised by crop failure and inadequate food resources in some areas. Sugar cane yields in particular were the worst

on record during the 1992/93 drought period compared to those of the past three decades. Midmar dam level inflows plunged from 100 mil m<sup>3</sup> at the end of 1990 to 0.5 mil m<sup>3</sup> during the 1992/93 summer season.

The analysis suggests that the 1992/93 drought was not a strong El Nino-induced climatic event. There are signs observed in the velocity potential and divergence fields showing resemblance to an El Nino type of influence but most parameters analysed do not suggest patterns typical of ENSO. The westerly mid-latitude winds coupled with a prominent Hadley cell overturning at 15°S had a profound influence on the occurrence of drought during the 1992/93 summer season than SSTs. Furthermore, budget calculations indicate that kinematic (rotational) properties of the circulation structure had more contribution to the occurrence of the drought than thermodynamic properties. The north-south Hadley overturning between South Africa and the Zambezi implied an anti-phase circulation regime. This together with mesoscale internal dynamics in the meteorological structure of KwaZulu/Natal, sustained the drought for at least three years. As a result, substantial reduction in crop yield and streamlevel inflows had a deleterious repercussions on the community in KwaZulu/Natal.

## CHAPTER 1

### 1: INTRODUCTION

#### 1.1 INTRODUCTION

The rainfall over much of southern Africa has a well-defined annual cycle with the largest values occurring during summer (October-March). Substantial increases or decreases in summer rainfall can have devastating effects, particularly for agriculture which constitutes up to 25% of GDP in South Africa (Jury, 1997), and as much as 75% in some countries in Africa (Eakin, 1996; Goddard and Graham, 1997).

It has been estimated that due to rapid population growth and economic activities, coupled with prolonged droughts, water demand in South Africa will exceed the total available supply around the year 2020 (Bruyere, 1997). Summer rains over the central plateau are highly variable at all scales, and take the form of wet spells of 3 to 7 d duration at near-monthly intervals from November to March. Each major wet spell can contribute up to 25% of the seasonal total (Jury and Levey, 1997). Water storage systems periodically fail during drought periods. These points highlight the need to further the understanding drought-producing processes in South Africa which is the purpose of this study.

#### 1.2 BACKGROUND TO THE STUDY AREA

KwaZulu/Natal is located along the south-east coast of South Africa (Fig. 1.1). Climatologically it is classified as a summer rainfall region. The altitude ranges from sea level to over 3 000 m, affecting a considerable range in temperature. Topography varies from the undulating plains of Maputaland to

the rugged, broken terrain of the Valley of Thousand Hills and the Drakensberg Mountains. The rainfall also varies considerably, from 500 mm to over 2 000 mm per annum. River systems of the province run west to east cutting through geological layers and resulting in deeply incised valleys. Mean maximum annual coastal temperatures range from 22°C in the north to 19°C in the south. Table 1.1 and Figure 1.1 summarise the physical characteristics of KwaZulu/Natal as defined by its bioclimatic groups (le Roux, 1993; Camp *et al.*, 1995; Camp, 1997). A bioclimatic group is a demarcated area throughout which there are recurring patterns of topography, soils, vegetation and climate (Camp *et al.*, 1995; Camp, 1996).

With this great variation in topography, geology and climate, KwaZulu/Natal possesses enormous diversity of natural resources. In recent years, however, increased water demand from the urban, industrial, and agricultural centres has placed untenable burden on the environment. Following the 1992/93 drought, urban water restrictions were in force, many farmers were bankrupt, and there were major economic repercussions thereof. A study of the climatological patterns underlying drought is necessary to assist in planning and managing water resources, and to provide guidance in agricultural production

### 1.3 PROBLEM STATEMENT

The climate of Africa south of 15°S has received increasing attention since the devastating drought of 1982 to 1984, when national values of maize crop yields declined to 10% of historical values and numerous sources of water dried up (Jury and Levey, 1997). Major wet spells over South Africa in summer contribute up to 25% of the seasonal total and are associated mainly with frontal systems, cyclonic vortices, ITCZ, etc. (Preston-Whyte and Tyson, 1988; Jury and Levey 1997). The intensity of these systems is influenced by interannual variability of the atmospheric circulation and related

anomalies. The problem statement underpinning this study is the need to enhance the understanding of the meteorological processes that produce below-normal rainfall scenarios as it impacts negatively, particularly on agriculture which constitutes a remarkable fraction of South Africa's GDP.

#### 1.4 HYPOTHESES

Summer (November-March) rains over the plateau of southern Africa (23-30°S, 23-30°E) (Fig. 1.3) are usually sufficient to support dryland agriculture, which makes a vital contribution to the economy of the region. Interannual rainfall cycles range between 2-20 years (Jury, 1992) and the amplitude of variability is typically two times the standard deviation, even for regional averages. A poor season can result in crop failure and inadequate food resources (Jury *et al.*, 1996a). This study seeks to test the following hypotheses:

- (a) Increased upper-air westerly winds with surface marine lows and continental high contribute to drought. Concurrently the tropical easterly flow weakens in agreement with documented El Nino influences.
- (b) During the period of drought in 1992/93 in KwaZulu/Natal pressures throughout the troposphere over South Africa are above normal, while falling to the south. Anomalous divergence and subsidence occurs over the subcontinent.
- (c) The subtropical jet stream is displaced northward during dry years limiting the supply of moisture into South Africa.
- (d) A lack of tropically-sourced inflow of moist air is one of the key causes of the drought.
- (e) During the drought period above normal surface temperatures over southern Africa lead to evaporative losses which contribute to a decline in agricultural production, vegetation cover, and dam and stream-flow levels.

## 1.5 RESEARCH OBJECTIVES

The 1991-1992 summer saw the presence of a strong negative value of the SOI (Fig. 1.2) and one of the worst droughts over southern Africa in the historical record. Other countries in southern Africa, particularly Zimbabwe, were also hard hit (Jury and Majodina, 1997). The 1991/92 early-summer season was comparable to the 1982/83 season although the mid-summer period was better for the former (South African Weather Bureau, 1992a).

Anomalies in precipitation and temperature of South Africa during the period of 1992 to 1993 can be associated with changes that occurred in the atmospheric circulation around the hemisphere. It is the purpose of this thesis to provide a detailed analysis of these anomalies in the circulation system of South Africa. One motivation for the study is the increase in the incidence of drought and flood in the last three decades.

Various studies have been carried out to describe the temporal behaviour of previous droughts and the associated anomalies over the region and surrounding oceans (Tyson, 1984; 1986; Jury and Levey, 1993; Jury and Lutjeharms, 1993). The satellite-derived normalised vegetation index (NDVI) has been used to assess the impact of year-to-year climate fluctuations in southern Africa (Jury *et al.*, 1997). The contribution of this thesis to drought studies is:

- (a) To analyse the historical context of the 1992/93 drought using historical data and to outline the cause and structure of the drought using surface and upper-level meteorological data.
- (b) To assess the impacts of drought on agricultural production and water resources.
- (c) To assist in the further understanding of mechanisms governing drought-producing systems which can aid improved forecasting models and procedures.

## 1.6 DESCRIPTION OF DATA AND RESEARCH METHODS

To achieve the objectives of the study pentad ECMWF and NCEP/NOAA synoptic weather data, at a resolution of  $2.5^\circ \times 2.5^\circ$  each, have been composited for the drought period to establish patterns of circulation and convection over the region. Departures of the drought scenario from the historical mean are computed. From the satellite and conventional data sources consulted, time series analysis has been undertaken. OLR is used as a proxy for convective intensity and for the identification of areas of sympathy and opposition to convection over South Africa. Wind data and derived parameters are employed to explore large-scale tropical dynamical structures. Plausible explanations are offered for the observed associations and links made with established research. Dam levels and streamflow, and agricultural production output data from sugar cane and maize industries are used to gauge the severity of the drought. Maize has been selected because of its importance in the South African economy and sugar cane because it is almost exclusively grown in KwaZulu/Natal. In addition these crops have a direct dependence on precipitation. Details on data and methodology are given in Chapters 3 to 5.

Since local climate has the power to influence vegetation cover, climate-vegetation relationships are investigated in this study through analyses of satellite-derived OLR and NDVI data. Two radiation channels from the polar orbiting satellite are used for NDVI calculation *viz.* channel 1 (visible,  $0.55\text{-}0.68 \mu\text{m}$ ) and channel 2 (near infrared,  $0.725\text{-}1.10 \mu\text{m}$ ) (Sakamoto and Steyaert, 1987). The strength of OLR or rainfall forcing reflects on the spatial and temporal distributions of vegetation. OLR-NDVI relationships are explained in terms of rainfall in that a reduction (increase) in OLR, which indicates an increase (decrease) in rainfall, may cause an increase (decrease) in NDVI. Through this relationship, a high OLR is associated with bare, reflective, unvegetated surfaces with great atmospheric subsidence, frequent

clear skies, high sensible heat flux and low rainfall. Areas with low OLR are usually regions of high occurrence of cloud cover (since clouds are near-perfect absorbers of OLR), deep convection (Gondwe and Jury, 1997), and high soil moisture hence evapotranspiration.

## 1.7 BACKGROUND TO DROUGHT CLIMATOLOGY

During an El Nino event tropical surface ocean temperatures are high, creating changes in zonal pressure gradients. Over southern Africa upper-level confluent westerlies enhance surface divergence and diminishes the occurrence of easterly waves and lows. Pressures increase over the subcontinent and the area of maximum tropical heat release and the zone of preferred occurrence of major cloud bands shifts eastward from South Africa to the Indian Ocean. The input of westerly momentum into the subtropical jet decreases the potential for meridional fluxes of energy (Preston-Whyte and Tyson, 1988). This research studies and analyses circulation anomalies of the 1992/93 drought and compare results with studies undertaken in South Africa and elsewhere.

The importance of the El Nino-Southern Oscillation phenomenon (ENSO) in modulating the variability of South Africa's rainfall has been demonstrated (Harrison, 1986; Mason and Lindsay, 1993). Changes in the wave configuration and frequency of westerly Rossby waves are other factors of fundamental importance in controlling the variability of rainfall south of about 20°S over the subcontinent (Harrison, 1986; Jury and Levey, 1993). In Chapter 2 these topics are reviewed in detail.

The empirical agreements between regional precipitation anomalies in southern Africa and Indian Ocean sea surface temperature (SSTs) have been discussed by Jury *et al.*, (1996) based on observational data. A detailed review and synthesis of the characteristics and mechanisms of the rainfall

variability over southern Africa is discussed in Chapter 2. ENSO teleconnections are generally significant in the African sector (Jury and Lyons, 1994) and those associated with the 1992/93 drought have been reported in other parts of the world. For example, anomalies in precipitation and temperature were observed from 1991 to 1995 over South America related to the extended El Nino event (Cavalcanti, 1997).

The need to understand and predict climate variability over Africa has led to the formation of programmes like CLIVAR (1995), a WCRP project whose aim is to gain an understanding of relationships between seasonal rainfall and ENSO through knowledge of ocean-atmosphere coupling over the tropical Atlantic and Indian Oceans. Priorities in this programme are given to observations, diagnostic analysis and predictive modelling. Drought can result in large-scale crop failure and food shortages, vegetation and animals perish (Glantz, 1987; Msengezi and Chenje, 1994; Hulme, 1996). Such impacts were observed in the past (e.g. 1982-84 drought) and were expected to contribute to the 1992/93 regional drought due to sustained negative values of the Southern Oscillation Index (SOI) (Hulme, 1996) (Fig. 1.2) which accounts for about 30% of the regional rainfall variance (Jury and Lyons, 1994). Previous studies have linked drought to the El Nino. Thiao (1996) found that during the past three decades, crop yields in Zimbabwe were well related to rainfall during El Nino episodes, with a correlation coefficient of 0.64.

## 1.8 NATIONAL REVIEW OF THE 1992/93 DROUGHT

### 1.8.1 EXTENT OF THE DROUGHT IN SOUTH AFRICA

Drought severity can be defined as  $S = (Q_n - Q_d)/Q_n$ , (Vlachos and James, 1983), where  $Q_n$  is water available during a normal season, and  $Q_d$  is the amount of water available during the drought. The vulnerability of the supply

to drought may be indexed as the probability that the drought severity will exceed some tolerable value  $S^1$ . The losses depend on  $S$ , the duration of shortfall, and the time distribution of water availability within the duration.

One of the greatest concerns during the 1992/93 drought period was the low-level of surface and ground water reserves. Curbs were imposed on water use in many parts of the country (Financial Mail, 1993a), farmers had to drill bore-holes and destroy trees to conserve water (Gittens, 1993). The rainfall in the North-West Province (Fig. 1.3) from July 1992 to June 1993 was 369 mm, less than 75% of normal, and below the 418 mm for the 1991/92 drought period. The South African Weather Bureau (1992) defines a drought area as any region getting less than 75% of its normal rainfall. Under this definition, most of the country was suffering some sort of drought, including most of KwaZulu/Natal, the Eastern Cape, the Karoo (except the Little Karoo), Gordonia, Griqualand West and Northern Cape, the western half of the Free State and the Northern Province (Fig. 1.3) (Financial Mail, 1993a).

The areas suffering the most serious drought conditions (less than 75% of normal rainfall for two years running) were northern and southern KwaZulu/Natal, coastal Eastern Cape, the central and upper Karoo, parts of the northern Cape, south-western Gauteng and north-western Free (Fig. 1.3). Only in the winter rainfall areas, such as the Western Cape, was the general water and agricultural situation satisfactory. Bloemfontein's rainfall of 274 mm was less than its previous low of 324 mm in 1984. December was the driest on record for some stations, especially in the Eastern Cape, where Somerset East recorded only 2.4 mm. Its previous low was 4 mm in 1884 (Financial Mail, 1993a).

The 1991-93 drought period was one of the most severe in the recorded climatological history of the Kruger National Park, with an average of 44.1%

of the long-term mean annual rainfall received (Zambatis and Biggs, 1995). There was a 50% decline in the number of days on which rain occurred. Two-thirds of the year experienced maximum temperatures of a significantly higher intensity than normal. This together with slightly increased minimum temperatures and a significant increase in the number of days with daily temperatures above 30°C, resulted in a hotter than normal year (Zambatis and Biggs, 1995). The persistent dry period which extended from 1991 to 1994 was followed by higher rainfalls that occurred since December 1995 over South Africa (Rautenbach, 1997a). An extensive domain of well above-normal SST anomalies developed south-west of South Africa during mid-December 1995 and strong easterly winds from the midlatitudes maintained a steady flux of moisture over the eastern and central interior of South Africa.

## 1.8.2 ECONOMIC COSTS OF THE DROUGHT FOR SOUTH AFRICA

Drought combined with poor land practices can initiate or accelerate desertification. A drought can affect on-farm storage, labour migration, the use of inputs such as fertilizers, labour supply, farm income, imports, etc. Figure 1.4 depicts how climate can affect food production.

Drought in 1992 cost the South African economy R4.55 billion in terms of the gross domestic product (Financial Mail, 1993b). In 1993 the expected growth estimated at 0.5% turned out to be -2%. In 1992 food inflation rose by 30% p.a. (Landbouweekblad, 1993; Financial Mail, 1993d). The drought relief fund for 1992 was 3.8 billion which was 3% of the total budget for the country (van Zyl, 1993; Farmer's Weekly, 1993). The current account of the balance of payments was adversely affected by the rise in imports and a decline in exports. A review of the national economic costs of the drought on sugar cane, timber, maize and wheat yields, and water supply in South Africa is presented below.

### 1.8.2.1 SUGAR-CANE

Agricultural products had to be imported (Financial Mail, 1993c) but prospects for a better 1994 season were high at the end of 1993 (Financial Mail, 1993d; The South African Sugar Association, 1993g). A total of 75 000 tons of imported sugar arrived in South Africa from Australia (30 000 tons) and Swaziland (45 000 tons) in early October 1993 (The South African Sugar association, 1993j). In the sugar industry, the *Eldana* pest exacerbated crop yields (The South African Sugar Association, 1993a, b) and the worst affected areas were along the south coast where less than 50% of the normal yield was obtained. Least affected areas were Pongola and Mpumalanga. The growers' revenue declined by R790 million over the two dry seasons (The South African Sugar Association, 1993c). Sugar price was increased by 14.5% from June 1992 (The South African Sugar Association, 1993e).

### 1.8.2.2 TIMBER

During the 1992/93 financial year timber prices increased because it had to be imported as timber growers were savaged by two years of drought. The Forest Owners' Association surveyed 758 140 ha of South Africa's 1.2 million ha planted to timber and determined that the drought cost growers R455 million (Financial Mail, 1993c). More than 30 000 ha had to be replanted at the end of the drought season and an additional cost of R2000 ha<sup>-1</sup> had to be borne to clear trees and plant new ones. Growers lost 6.7 million m<sup>3</sup> or 42% of a year's crop (Financial Mail, 1993c).

### 1.8.2.3 MAIZE AND WHEAT

The maize farmers' combined debt was not accurately known but estimated as responsible for most of the R17 billion total that farmers owed in the 1992/93 financial year. According to Nampo (National Maize Producers' Organisation), it cost R970 ha<sup>-1</sup> on average to produce the maize crop that was reaped. Of that R650 was for direct costs (fuel, labour, seed, fertiliser and pesticides) and the rest for items such as interest, depreciation and management. The wheat harvest in 1992 was 1.26 mega-tonnes (about 1 MT below South Africa's annual consumption) which was the worst crop harvest in 20 years (Financial Mail, 1993c). This necessitated imports of 1 million tonnes at a cost of R550 million (van Zyl, 1993).

### 1.8.2.4 WATER SUPPLY

While urban dwellers faced tightening water restrictions as the level of the province's dams sank, thousands of rural dwellers also bore the brunt of the scorching two-year drought. They had to rely on emergency water supplies, delivered by several government and non-government organisations, including the sugar industry. Long queues formed daily as rural people, mostly women, trudged many kilometers from their homes daily with containers to collect water to survive (The South African Sugar Association, 1993f). With the launching of "Operation *Amanzi*" which subsidised the transport costs of getting water into rural areas in KwaZulu/Natal in 1992, 13 million litres of water were delivered over 50 000 km (The South African Sugar Association, 1993i). Water for domestic consumption and irrigation was rationed in the urban areas of Pietermaritzburg and Durban (The South African Sugar Association, 1993h).

## 1.9 DROUGHT IMPACT STUDIES IN THE SADC AND ELSEWHERE

Drought impact studies carried out in Africa and elsewhere reveal the complexity and seriousness of the problem. The high population growth rates that plague Africa and poor land-use practices exacerbate the problem in this region. In Zimbabwe during the 1991/92 drought, 90% of the inland dams dried up, 6.2 million communal farmers in rural areas who depend on agriculture for survival were severely affected. As a result of the drought 5.5 million (which is 75% of the rural population) had requested for drought relief assistance by November 1992 (Glantz, 1996; Glantz *et al.*, 1997). Nicholls (1985) has examined and modelled decadal variations in the Australian climate in the form of prolonged drought and impact upon agricultural production. Heathcote (1991) reports that the 1982/83 drought in Australia cost \$7500 million.

Because most of sub-Saharan African economies are driven by agriculture, so the effects of meteorological droughts are direct and can be large. In such countries, a majority of the population is employed in the agricultural sector which contributes substantially to foreign exchange earnings. The ramifications of drought are thus extended throughout the economy. In Zimbabwe, 1992 GDP fell by 8% in real terms with the agricultural sector directly accounting for the 3% decline in GDP (Glantz, 1996). The SADC's grain shortfall, which had been predicted in March 1991 to be approximately 3 million tonnes, turned out to be a 6 million tonnes shortfall. Botswana's sorghum crop was 11 000 tonnes (one third of the previous year's harvest). Zimbabwe's maize harvest reached 133 000 tonnes and Zambia a low of 464 000. Zimbabwe's communal maize sector yield averaged an abysmal 0.16 T ha<sup>-1</sup> (normal average is about 1 T), while yields in South Africa reached 0.85 T ha<sup>-1</sup>, compared to its potential yield of 3 T ha<sup>-1</sup> (Glantz *et al.*, 1997).

Maize producer prices in Zimbabwe were more than doubled from Z\$270 to Z\$550 T<sup>-1</sup> in 1992. Imports cost as much as four times the subsidised price that the government sold them to industrial millers for. This cost the government approximately US\$ 300 million, or 11% of GDP for 1991/92 (Glantz *et al.*, 1997). The 1991/92 drought cost the Zambian government US\$300 million, bringing its 1992 deficit to US\$1.7 billion. A 39% decline in agricultural output was a large instigator of the 2.8% decline in GDP. Wages lost value in real terms after inflation took off during 1992. In November 1991, the lowest paid public service worker earned K5 000/month (US\$80), a time when mealie meal cost K250/25kg bag. A year later, the same worker earned K11 000, but mealie meal had gone to K2 000/bag (a 930% increase). The government also had to raise taxes to grapple with increased expenditures and budget deficit problems (Glantz *et al.*, 1997).

Drought impact studies other than the 1992/93 event that have been conducted include those in Portugal (Santos *et al.*, 1983), Sicily (Rossi, 1983), Mexico (Cervera, 1983), Namibia (Hattle and Webster, 1983), Sahel (Hidore, 1983), Australia and Indonesia (Nicholls, 1987), and others.

## 1.10 CONCLUSION

Drought and flood years are an inherent feature of the climate of southern Africa and present significant climate-related risks. While agriculture accounts for less than 10% of the formal sector of the economy (Jury, 1995), rural communities subsist on agriculture and the corresponding rainfall from November to March. It is important therefore to understand drought-producing mechanisms in order to develop improved forecast skills that will enhance opportune planning and help reduce the adverse effects produced by this phenomenon. This thesis will investigate the climatic processes that produced the 1992/93 drought in KwaZulu/Natal and its impacts on local agricultural output.

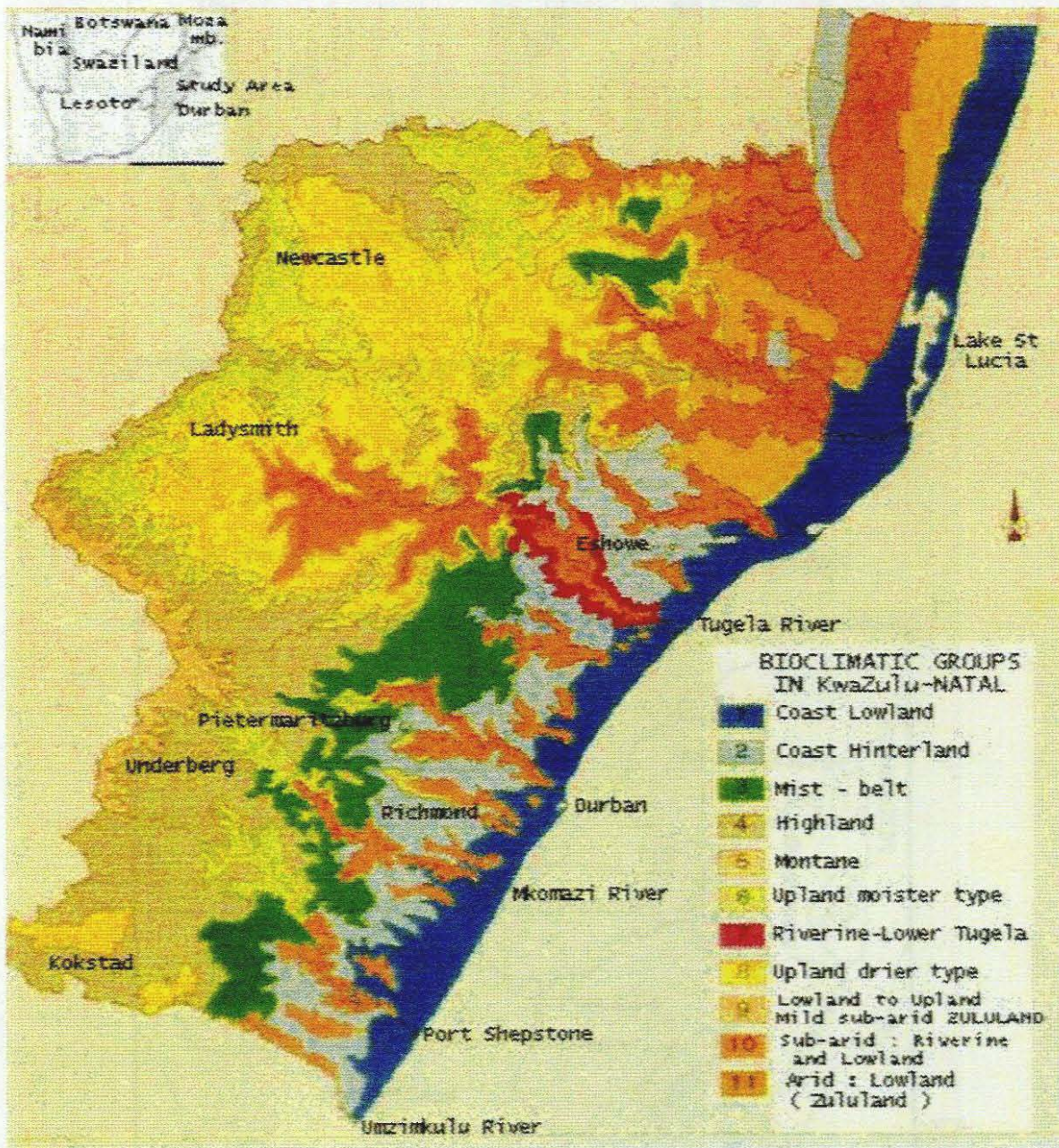


Fig. 1.1: Location map of KwaZulu/Natal and its bioclimatic groups (Source: le Roux, 1993).

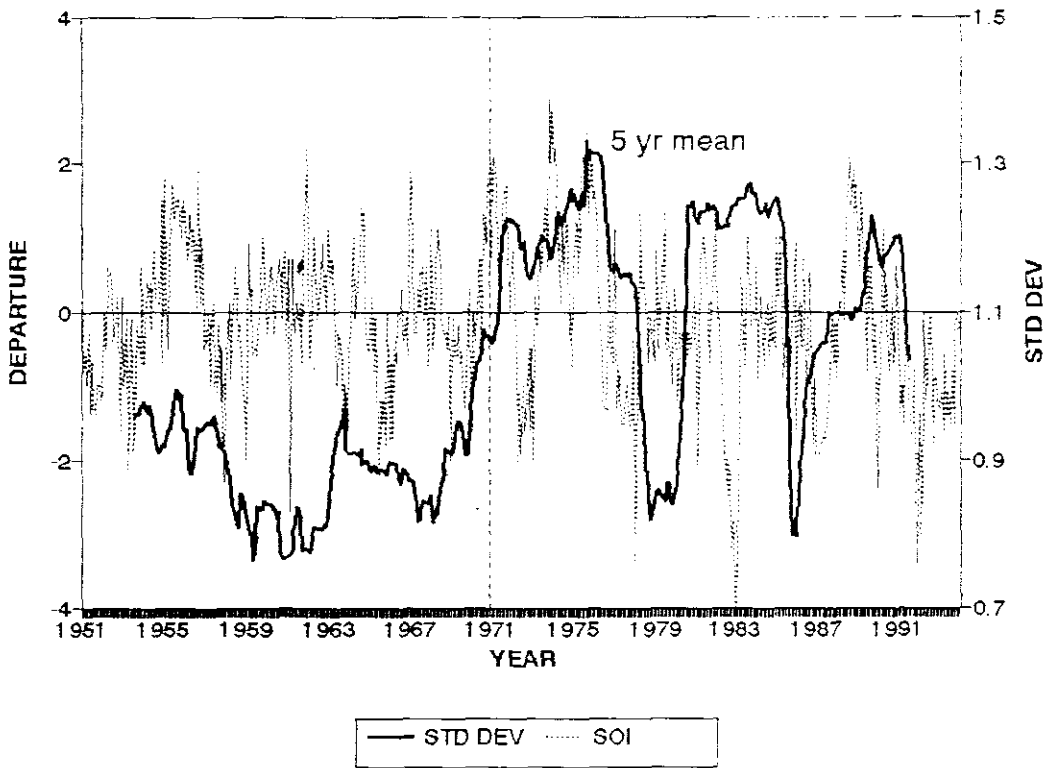


Fig. 1.2: Historical variation in the Southern Oscillation Index.

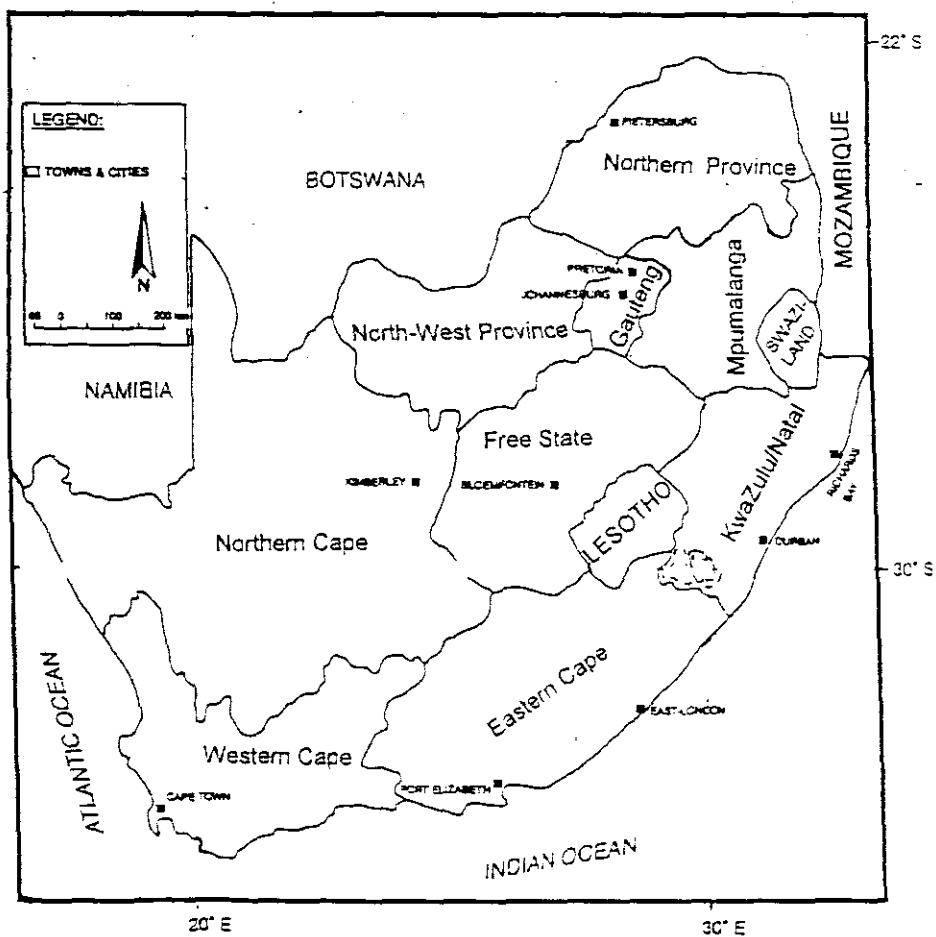


Fig. 1.3: Map of South Africa showing its provinces and major towns and cities.

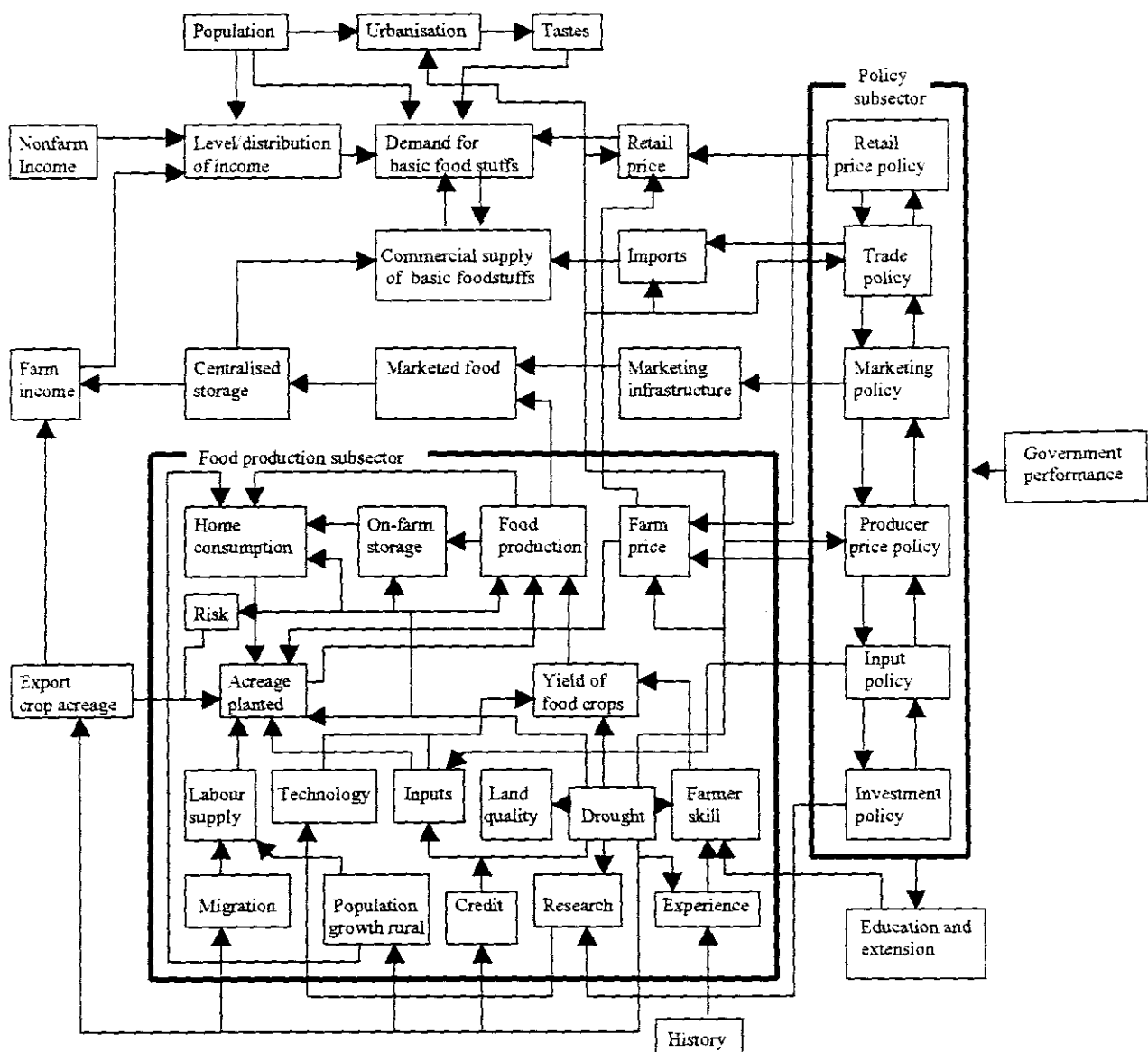


Fig. 1.4: Food production chart to account for the way drought can affect production activities (Source: Glantz *et al.*, 1997).

Table 1.1: Bioclimatic group data of KwaZulu/Natal (Source: le Roux, 1993).

1 Bioclimatic group	Altitude range (m)	Average temperature (°C)	Rainfall range (mm)	Suitability for dryland production	Limitations
Coast lowland	0 – 450	20 – 22.5	850 – 1400	Moderate	Topography, disease, humidity, temperature
2 Coast hinterland	450 – 900	17.5 – 20	850 – 1300	Moderate to high	Topography, subsoil acidity
Mist-belt	900 – 1400	16 – 18	800 – 1600	Moderate to high	Disease, subsoil acidity
3 Highland	1400 – 1950	13 – 15	800 – 1500	Moderate to high	Subsoil acidity, cold, high input costs
4 Montane	1950 – 3400	<13	>1500	Not suitable	Cold, topography
6 Upland, moister type	900 – 1400	16 – 18	800 – 1000	Moderate to high	Disease, subsoil acidity
7 Riverine (Lower Tugela)	300 – 600	17 – 22	700 – 800	Not suitable	Topography, rainfall
8 Upland, drier type	900 – 1400	16 – 18	600 – 800	Low to high	Severe short-term droughts
9 Lowland to upland, Mild sub-arid	150 – 1100	21 – 22	700 – 800	Low	Rainfall
10 Sub-arid, Riverine and Lowland	150 – 900	18 – 23	600 – 700	Not suitable	Rainfall
11 Arid, Lowland	150 – 450	21 – 23	520 – 600	Not suitable	Rainfall

## CHAPTER 2

### 2: LITERATURE REVIEW: CLIMATE VARIABILITY

#### 2.1 INTRODUCTION

The climate of southern Africa is maintained by the position of the subcontinent in relation to the major atmospheric circulation features of the Southern Hemisphere. As a result of its geographic location, rainfall is seasonal over most of the southern continent. Since the mid 1980's rainfall patterns over South Africa have become increasingly variable, when compared with the period 1951-1980 (Crimp *et al.*, 1997) and drought has become more frequent. Summer rainfall over SE Africa is subject to large interannual variability characterised by alternating wet and dry decades and years. The purpose of this chapter is to review the underlying features of climate variability over southern Africa, with particular emphasis on the below-normal rainfall scenario over south-east Africa.

Mainly in the form of literature review, this chapter presents a background and circulation features of importance in the present context. As is it not feasible to give a detailed review of all the works done in this field, brief mention will be made to those believed more pertinent. However, emphasis will be placed on the studies of Lindesay (1988), Walker (1989), Pathack *et al.*, (1993), Jury (1995, 1996a and b, 1997) and Mulenga (1998) as they are the most recent, comprehensive and of direct concern to South African rainfall distribution and variability.

## 2.2 MAJOR RAINFALL-PRODUCING SYSTEMS OVER SOUTH-EAST AFRICA

Southern Africa's position in relation to the tropical, subtropical and mid-latitude pressure regimes is an important factor influencing climate of the subcontinent (Tyson, 1986). The thermally-direct Hadley cell and the thermally-indirect Ferrel cell both descend in the subtropics, producing the quasi-stationary subtropical high pressure belt. The positions of the South Atlantic, South Indian Anticyclones within this zone of high pressure vary throughout the year (Preston-Whyte and Tyson, 1988). Major rainfall-producing systems over South Africa include ridging anticyclones which account for 16 to 25% of the rainfall variance over the region (Preston-Whyte and Tyson, 1988). To the north of the subtropical belt a zone of easterly waves and tropical lows supply the northern regions of southern Africa with tropical moisture and heat. These circulation systems account for between 16 and 49% of the rainfall variance over the northern interior of South Africa (Preston-Whyte and Tyson, 1988).

A cut-off low is an intense form of westerly trough which accounts for many of the flood-producing rains observed over South Africa, such as the KwaZulu/Natal floods of 1987. Its frequency of occurrence shows a semi-annual variation with peaks in March to May and September to November (Preston-Whyte and Tyson, 1988). The combination of a cut-off low and a ridging anticyclone to the south produces widespread rainfall over South Africa.

In all recent classifications of summer rainfall-producing systems which include upper-level forcing, tropical-temperate troughs have been identified as the systems contributing substantially more to the rainfall over southern Africa than any other. Tropical-temperate trough systems contribute about 30% of the October and December rainfall totals, 60% of the January total

and about 39% of the mean annual total, making them important contributors to summer rainfall over the central interior (Crimp *et al.*, 1996; Jury, 1997; van den Heever *et al.*, 1997). They occur preferentially over southern Africa (Madagascar) during wet (dry) southern African summers and are a major conduit for the poleward transfer of tropical moisture and energy. The work of Diab *et al.* (1991) and Preston-Whyte *et al.* (1991) has defined the contribution by various synoptic weather types to the total rainfall budget over South Africa.

### 2.3 EL NINO AND THE SOUTHERN OSCILLATION (ENSO)

In the western tropical Pacific, the SSTs are normally warm (~ 29°C), the sea-level pressure is low and precipitation is heavy whilst the reverse applies in the eastern Pacific. The cold water in the region of the equatorial eastern Pacific persists throughout the year. This normal gradient in SSTs along the equator is associated with westward winds. Although seasonal variations of this pattern occur, conditions are usually warm and wet in the west, and cool and dry in the east (Hastenrath, 1991; National Research Council, 1996); Glantz *et al.*, 1997).

Occasionally, however, the warm pool in the western tropical Pacific begins to spread eastward. Accompanying these changes in SST, the regions of low pressure move eastward with the warm pool, and the eastern and central Pacific become warm and rainy while the western Pacific becomes cooler and drier. This warming of SSTs off Ecuador and Peru is known as El Nino. The Southern Oscillation is a widespread positive correlation of sea-level pressure anomalies near northern Australia that surround the warm pool in the western Pacific and extends into the Indian Ocean, with negative anomalies east of Tahiti in the eastern and central Pacific (Hastenrath, 1991; Glantz, 1996; National Research Council, 1996; Glantz *et al.*, 1997; Mason and Jury, 1997).

### 2.3.1 DRY AND WET SPELLS OVER SOUTH AFRICA

Alternations between the warm El Nino phases and cool La Nina phases of ENSO affect regional precipitation regimes across the globe through changes in the strength and location of the major equatorial convective centres, zonal teleconnections and patterns of wavetrains in higher latitudes (Allan *et al.*, 1997). Seasonal prediction studies of precipitation using Pacific SST in subtropical South America have been undertaken by Montecinos *et al.*, (1997); Mullan *et al.*, (1997); in the extratropical Atlantic such as by Rochail, (1997) and in the Indian Ocean such as by Pathack *et al.*, (1993), Landman (1997) and Thiao and Barnston (1997).

Over South Africa, the El Nino is associated with the warm phase of ENSO and wet conditions with the cold phase. During drought years, the upper-level standing waves in the westerlies are displaced eastward with the preferential locality for the occurrence of trough lines shifting from the west to the east coast region. At the same time the tropical easterly flow weakens, tropical-temperate troughs occur further to the east (Harrison, 1986; Jury *et al.*, 1991; Jury and Levey, 1993), the locus of occurrence of cloud bands associated with tropical-temperate troughs moves eastward off the continent and over the western Indian Ocean. The westerlies also strengthen south of Africa (Harrison, 1986, Jury and Levey, 1993), particularly in the vicinity of Marion Island (Harrison, 1986), and tracks of weaker mid-latitude storms shift northward (Harrison, 1986; Tyson, 1986). Wet periods are characterised by an apposite circulation pattern to that of dry periods (Preston-Whyte and Tyson, 1988; Jury and Levey, 1997). A comprehensive review of ENSO-related below and above normal rainfall circulation patterns over southern Africa is provided in Tyson (1986) and Preston-Whyte and Tyson (1988).

## 2.4 SOME INDICES OF CLIMATE VARIABILITY OVER SOUTHERN AFRICA

Various indices of climate variability have been used in a number of studies in South Africa. Some of the most commonly employed indices are discussed below.

### 2.4.1 SOUTHERN OSCILLATION INDEX

The most commonly used global index is the Southern Oscillation Index (SOI). The influence of ENSO (as measured by the SOI) on summer rainfall has been investigated for different SOI lags by Rocha and Simmonds (1997a). The relationship is such that during the summer following the onset of an ENSO event, south-eastern Africa tends to experience dry conditions. Strongest relationships are found with the SOI leading rainfall by about 3 to 6 months (Rocha and Simmonds, 1997a). Jury (1996) suggests that the spring SOI and late summer QBO (at 30hPa) are slightly better predictors than the mid-summer values and that correlation values are 10% better for seasonal indices (3-month mean) than for individual months, owing to the influences of transient intra-seasonal oscillations. Jury *et al.* (1996a, b) found that when the SOI is strongly negative central equatorial Indian Ocean (CEI) SST typically exceed 30°C, for example in 1970, 1973 and 1983. Conversely, La Nina are associated with CEI SST < 26°C.

Simultaneous variations of SOI and rainfall account for, at most, 20% of rainfall variance over central South Africa. The relationships in this area are such that higher rainfall tends to coincide with the high phase of the Southern Oscillation, and vice versa. The close relationships between summer area rainfall and SOI spectra at both quasi-biennial and Southern Oscillation periods support the physical mechanism linking phase changes of the oscillation with zonal and meridional circulation adjustments over southern

Africa, and thence with rainfall variations over central parts of South Africa (Lindesay, 1988).

#### 2.4.2 FEBRUARY RAINFALL INDEX

An index of normalised departures of February rainfall over northern South Africa (SAF) correlates well with regional patterns of OLR and SST in a study by Jury *et al.* (1996b). Significant correlations are sustained between SST in the central Indian Ocean and February rainfall at lags 0 to -9 months ( $<-0.5$ ). The dynamical link is through the southward advance and intensity of the Indian monsoon trough. The CSIRO4 GCM indicates that anomalous warming of SST in the central Indian Ocean anticipate and sustain drought over southern Africa.

Departures of the SAF index rainfall vary between -1 and +2. Correlations between annual statistics of the SAF index and the SOI and QBO are +0.44 and +0.30, respectively (Jury *et al.*, 1996b), accordance with those reported by Mason (1992). Normalised departures of smoothed monthly CEI SST and SOI are illustrated in Figure 2.1. A close correspondence is noted with minor exception.

#### 2.4.3 TRANSVAAL RAINFALL INDEX

The predictability of summer rainfall in the eastern part of southern Africa has been demonstrated in recent studies by Hastenrath, 1995 Hastenrath *et al.*, 1995). The predictand is an index (TVR) of the December-January-February precipitation over the South African Highveld. The predictors are based on empirical-diagnostic analyses and include the JAS SOI, the preceding JFM value of the 50mb zonal wind over Singapore (U50); an index of the October-November surface westerlies along the Indian Ocean Equator (UEQ); and an index of November SST in the south-western Indian Ocean (UKT). The

training period is 1954-78, and the verification period 1979-90. Regression models using predictors U50, UEQ and UKT account for more than 30% of the variance in the independent dataset. In the neural networking model with U50 and SOI as input, 62% of the variance is explained in the verification period (Hastenrath, 1995 and Hastenrath *et al.*, 1995).

The indices outlined above have been successful in explaining both the below and above-normal rainfall scenario over southern Africa. Other indices such as the Brandon-Marion Index (BMI) (Rocha and Simmonds, 1997a) exist in literature but have proved to be less useful.

## 2.5 INFLUENCE OF MONSOONS AND WAVE PERTURBATIONS ON CIRCULATION REGIME

Correlations between area-rainfall and surrounding winds, and wet-dry wind composites undertaken by Jury (1992) have revealed a number of features which are schematically shown in Figure 2.2a and b. The most prominent is the strength of the low-level NW monsoon to the north of Madagascar. When the NW Monsoon is weak, additional moisture is available to enhance convection downstream over SE Africa, while tropical cyclogenesis is reduced in the central SW Indian Ocean. In the mid-troposphere a standing trough moves westward in wet summers and eastward over the Mozambique Channel in dry summers. In wet summers, upper level easterlies intensify in the subtropical zone and reflect the presence of standing waves. In dry summers, subtropical westerlies encroach equatorwards and become more zonal (Fig. 2.3). Analysis of the velocity potential reveals convergence at 200 hPa over SE Africa in dry summers and convergence at 850 hPa in wet summers. Most significant over the equatorial zone off east Africa, 200 hPa zonal westerlies assist uplift and convection over SE Africa.

## 2.6 THE CLIMATIC DIPOLE OVER SOUTHERN AFRICA AND THE INDIAN OCEAN

A landmark contribution to the modern understanding of drought-producing mechanism over southern Africa has been Pathack *et al.*'s (1993) land-air interaction and Jury's (1992) southern Africa/Indian Ocean dipole interaction theory. According to Pathack *et al.* (1993) the 'coupled' African and Indian Ocean cells involve mass subsidence over southern Africa and ascent over the Indian Ocean in dry summers over South Africa (Fig. 2.3), while a relative reversal corresponds to wet conditions across the central interior of the country. The Indian Ocean connection reflects a dipole-like behaviour between the two areas from a dynamical point of view (Fig. 2.4a), thus confirming results obtained from investigations involving SST and OLR variations with respect to rainfall. These east-west cells develop after November, and gradually intensify to attain peak amplitude about February (Jury, 1992).

The ENSO-rainfall link for a region immediately to the north of the summer rainfall area, in equatorial eastern Africa, exhibits concurrent rainfall anomalies of apposite sign, that is, wet conditions during ENSO events. The east-west opposition of OLR correlations is considered to be a subtropical dipole (Jury, 1992) which teleconnects the CEI monsoon trough with southern African continental rainfall (Jury *et al.*, 1996b). Figure 2.4b shows the two core areas of ENSO related interannual rainfall anomalies occurring at different seasons (Rocha and Simmonds, 1997a).

## 2.7 CLIMATIC TRENDS

Much of southern Africa is prone to desertification which may be triggered or exacerbated by drought (Fig. 2.5). The whole of Botswana and Namibia and more than half of South Africa are rated as potential desert, with large areas

of the Western and Northern Cape Provinces and part of the Northern Province at very high risk (Preston-Whyte and Tyson, 1988). Recent notable meteorological trends include a decrease in the frequency of station days with rainfall  $> 70$  mm and an increase in station days with temperature  $> 38^{\circ}\text{C}$  (Jury and Majodina, 1997). These trends negatively impact run-off and evaporation. Agreement in extreme temperature statistics in all regions suggest that drought is widespread over southern Africa. Variation in rainfall over southern Africa since 1900 is shown in Fig. 2.6.

Global warming may produce prolonged droughts and desertification through reduced vegetation cover due to reduced precipitation, increased temperatures and counter-radiation in a  $\text{CO}_2$  satiated environment. The change in climate, arising from reduced total rainfall amounts in the Sahel since the 1960's, has been found to be attributable to the fact that the SSTs of the three influencing oceans have persistently warmed. Other observed meteorological features like increased albedo, due to possible overgrazing by livestock, may therefore be effects, and probably not the cause, of the persistent drought in the Sahel (Adedoyin, 1997). Over the last century, there has been warming of more than  $1^{\circ}\text{C}$  over South Africa and of  $0.5^{\circ}\text{C}$  over southern Africa as a whole (Hulme, 1996) (Fig. 2.7). GCMs project a warming rate over southern Africa for the period between 1990 and 2059 at  $0.3^{\circ}\text{C}$  per decade (Meadows *et al.*, 1993; Hewtson, 1997; Hunt, 1997; Joubert, 1997; Whetton *et al.*, 1997)

There is an indication that in South Africa the Karoo desert is expanding at a rate of between  $0.4$  and  $2.4$   $\text{km yr}^{-1}$  (Preston-Whyte and Tyson, 1988). Despite this agreement Hoffman (1995) used satellite imagery and survey data, matched ground and aerial photography, and undertook an analysis of historical stock record, but could not find a conclusive agreement as to whether the Karoo is degrading or not. Kruger (1997) shows that there is no

significant trend in rainfall on a regional scale as some areas of the country experience a positive trend and some a negative trend (Gondwe and Jury 1997a; Kruger, 1997; Mulenga, 1998). Further research into these areas needs to be undertaken.

## 2.8 RELATIONSHIPS BETWEEN THE NDVI/OLR AND CLIMATE OVER SOUTHERN AFRICA

### 2.8.1 MEAN SPATIAL PATTERNS OF OLR AND NDVI OVER SOUTHERN AFRICA

OLR and NDVI show marked seasonal and spatial variations over southern Africa and they can indicate long-term climate variability. OLR-NDVI relationships are explained in terms of rainfall in that a reduction (increase) in OLR, which indicates an increase (decrease) in rainfall, will naturally cause an increase (decrease) in NDVI. Through this relationship, a high OLR is associated with bare, highly reflective, unvegetated surfaces with great atmospheric subsidence, frequent clear skies and low rainfall during summer. Areas with low OLR are usually regions of high occurrence of cloud cover (since clouds are near-perfect absorbers of OLR) and deep convection (Gondwe and Jury, 1997a).

Africa south of 15°S is semi-arid and its vegetation is dominated by grassland savanna. To the east of 30°E, tropical and deciduous woodlands are found in response to high humidity and summer rains which fall on steep mountain slopes adjacent to warm seas (Jury *et al.*, 1997). To the west of 25°E and south of 20°S, water vapour content is low and surface temperatures above 40°C are common during summer. The Kalahari Desert for example is characterised by sensible heat fluxes  $> 100 \text{ W m}^{-2}$  and reduced evapotranspiration and cloud cover (Jury *et al.*, 1997).

Mean NDVI shows a distinct sharp boundary between the moist, vegetated areas and the dry western coast and central area. This climatic difference is probably due to the Agulhas and Benguela currents. Vegetation removal may decrease precipitation through a series of feedback mechanisms (Gondwe and Jury, 1997a) and may produce desertification.

### 2.8.2 CONVECTIVE TRENDS AND OLR

The patterns of convection are defined by the OLR with a correlation between area rainfall and coincident OLR departures of -0.93 having been determined (Jury *et al.*, 1993). The OLR difference field (Fig. 2.4a) reveals a dominant centre of convection over SE Africa. A sympathetic NW-SE axis of negative OLR values extends into the oceans adjacent to SE Africa. In contrast, the SW Indian Ocean region shows positive values approaching  $+20\text{Wm}^{-2}$  to the east of Madagascar where tropical cyclones are frequent. This interaction is the climatic dipole discussed previously (Jury, 1992).

Historical OLR-NDVI correlation show that certain areas are more sensitive to climate impacts than others. The southern plateau along  $25^{\circ}\text{E}$  is an area significantly correlated with changes in the surface vegetation. In contrast, the NE highlands of South Africa and the ITCZ region of western Zambia appear to be areas of high rainfall where vegetation is relatively buffered from the effects of climatic fluctuations (Gondwe and Jury, 1997b).

### 2.8.3 SSTs AND OLR CORRELATIONS

Pathack (1993) and Pathack *et al.* (1993) have identified the central South Atlantic (CSA) and the central equatorial Indian (CEI) Oceans as major determinants of rainfall variability over South Africa, while the analysis of

Mason (1992) highlights the Agulhas Current region and its retroflexion. Highest SST vs OLR correlations ( $r = -0.54$ ) are obtained for the CEI, hence oceanic heat anomalies explain about 1/3 of the convective variance in this convective monsoon region during El Nino periods. Pathack (1993) has shown that OLR in the CEI is well correlated with South African rainfall in the late summer ( $r = +0.90$  at lead times  $< 4$  months). CEI SST fluctuations are also highly correlated with eastern equatorial Pacific SST ( $r = +0.75$ ) via the ENSO. The physical link is through diabatic heating and Walker cell overturning following the onset of the NE monsoon in the Indian Ocean (Jury, 1995).

Correlations for CSA SST in respect of the Agulhas Current region (ACR) wind and CEI OLR are  $-0.53$  and  $-0.52$ , respectively, and indicate that warming of the 'upstream' central South Atlantic region is associated with increased easterly winds in the southern Mozambique Channel and deeper monsoon convection in the Indian Ocean. OLR and SST in the Agulhas retroflexion region are positively related, contrary to the principle that SST and convection should increase together. In the higher latitudes and winter season, SST-OLR relationships are often dominated by negative feedback, that is, reduced cloud cover contributes to solar insolation and warmer SST. The OLR vs SST relationship in the CSA is also positive and suggests that elevated SST are associated with locally reduced convection (for example the ocean lags the atmosphere. Jury *et al.* (1993) have shown that the summer rainfall on the south-east coast of Africa is influenced by the proximity and temperature of the adjacent warm Agulhas Current.

#### 2.8.4 NDVI AS AN INDICATOR OF TEMPORAL CLIMATE VARIABILITY OVER AFRICA

Jury *et al.* (1997) have undertaken an assessment of the impact of year-to-year climate fluctuations based on satellite vegetation (NDVI) data. In this study the NDVI has been mapped over southern Africa for the period 1981-1994. Sharp upward and downward trends follow the cycle of summer floods and drought. January to March NDVI values are correlated at +0.82 with harvested maize yield for the North West Province of central South Africa. Departures of late summer NDVI from the historical mean illustrate the distribution and intensity of the influence of the SO, in alternating seasons of vegetative growth and depletion (Jury *et al.*, 1997).

In a PCA study Anyamba and Eastman's (1997) component 7 pattern show that variability in vegetation greenness over Sahel-East Africa region is primarily influenced by the phase of the QBO pattern at 2.0 - 2.5 years and to a lesser extent by ENSO at the 7 year time scale. Vegetation patterns over southern Africa and south-eastern Africa region on the other hand are largely modulated by ENSO variability at time scales ranging from 4-7 years (Anyamba and Eastman, 1997).

From an analysis of monthly NDVI images for the period 1982-1995, Anyamba and Eastman (1997) have demonstrated that recent ENSO-related droughts in southern Africa exhibit two very distinctive spatial patterns. The first is a pattern referred to as the Type 1 ENSO drought, with strong evidence of movement along a path from Namibia to Botswana, to Zimbabwe, to southern Zambia, northwest Mozambique and southern Malawi. Both the 1986/87 and 1994/95 ENSO events exhibit this pattern. The second one, a type 2 ENSO drought, tends to originate from a main cell near southern Mozambique and southern Zimbabwe, and then expands

outwards from this cell as the southern hemisphere summer progresses. The 1982/83 and 1991/92 ENSO warm events are examples of this pattern of drought (Eastman and Anyamba, 1997).

## 2.9 INTERANNUAL VARIABILITY OF CONVECTIVE ACTIVITY OVER SOUTHERN AFRICA AND SSTs

Over the last few years increasing recognition has been given to the importance of sea surface temperature changes in regulating the atmospheric circulation and rainfall over southern Africa (Walker, 1989; Walker and Lindesay, 1989; Thiao, 1996). Sea-surface temperature affects atmospheric variability because of the inherent large spatial coherence and persistent properties of the oceans. Nicholson (1983) suggests that the influence of SSTs may bear more local (e.g. advective) rather than global influences such as the Southern Oscillation. Over Australia SST-forced variability is strong over most of the region, but a maximum in excess of 60% is observed over northern parts (Rocha and Simmonds, 1997d). The pattern is also similar to that of ENSO in the region. In South America SST-forced rainfall variability is dominant over north-eastern parts, explaining more than 80% of the total rainfall anomalies (Rocha and Simmonds, 1997d). Overall these results show that much of the forcing in the three southern continents appear to be linked to ENSO. This section reviews the air-sea interaction mechanism and interannual variability pertinent to southern African summer rainfall

### 2.9.1 RELATIVE SIGNIFICANCE OF SSTs IN CLIMATE VARIABILITY

Rainfall associations with global SST anomalies reveals that areas in the tropical Indian and Pacific Oceans are linked with rainfall changes over the subcontinent. The relationship is such that warm anomalies tend to be followed by dry conditions over much of south-eastern Africa. Strongest

relationships are found when SSTs lead the rainfall season by about 1 to 3 months (Rocha and Simmonds, 1997a).

Well-defined atmospheric anomalies identified during dry south-eastern African summers include, amongst others, anomalously warm tropospheric temperatures and marked low-level cyclonic circulation anomalies over the central Indian Ocean, which generate abnormally weak easterly winds along much of the south-eastern coast of Africa. These perturbations to the low-level flow divert moisture from the continent and result in precipitation decreases (Rocha and Simmonds, 1997a). The SST-rainfall link over the Indian Ocean remains strong after the ENSO effects have been removed, suggesting that the atmospheric circulation anomalies observed over south-eastern Africa during dry summers, are linked mainly to SST anomalies over the Indian Ocean (Rocha and Simmonds, 1997a). Table 2.1 displays ENSO and anti-ENSO events that have occurred since 1950.

Mason (1994) has analysed eight principal components which explain 75% of the sea surface temperature variability over the period 1910 to 1989 if the equatorial region is excluded (Table 2.2). November rainfall, which is important because it is associated with the start of the summer growing season, is positively correlated with SST in the central South Atlantic Ocean at lags of -2 to -4 months and in other areas.

A shift in the correlation patterns has been noted when moving from the November to December rainfall regime. Whereas October and November rainfall variations show generally positive, albeit weak, links with SST variations over most ocean areas, in December the correlations become negative and more significant, particularly with SSTs which are situated further away from the subcontinent. The teleconnections are strongest for rainfall variations during the months of December, February and March, and

are relatively weak in the case of January rainfall. Amongst the SST regions which represent potential for prediction of December rainfall include the Arabian Sea Area, western and Eastern Equatorial Pacific (Pathack *et al.*, 1993).

In general, the CEI area is the most sensitive SST area in the correlation with South African summer rainfall. The association does not, however, hold prior to October (Pathack *et al.*, 1993). Jury *et al.* (1996b) have shown that during the onset of the 1973 and 1982/83 El Nino droughts SSTs in the CEI, were above normal.

The sensitivity of South African rainfall to CEI SSTs has been confirmed by various authors in recent studies. Jury (1996c) has found that the SSTs in the central equatorial Indian Ocean are best correlated with South African rainfall at  $r < -0.6$  at lags -2 (Nov) and 0 (Jan) months in association with the El Nino, while the equatorial central Atlantic upper wind index is correlated at  $r < -0.8$  at lags -4 and -2 months. In ranking the rainfall response to sea surface temperature variability over all years in the period 1953 to 1989 in terms of its statistical field significance for the summer rainfall region as a whole, Mason *et al.* (1994) however, found that it is changes in the central South Atlantic Ocean temperature, those of the South Atlantic subtropical convergence region and those of the western equatorial Indian Ocean which have the greatest effect on South Africa rainfall (Table 2.2).

### 2.9.2 MECHANISM UNDERLYING RAINFALL VARIABILITY OVER SOUTHERN AFRICA

Figure 2.3 schematically depicts the climatological, relative, zonal circulation anomalies corresponding to dry summer conditions across South Africa, as discussed previously. As the Indian Ocean to the south-east of South Africa

warms and cools so the pattern of baroclinic westerly waves over the country adjusts. Anomalous warming is associated with an easterly movement of the locus of most frequent occurrence of upper-level wave troughs (Fig. 2.8a and b). The summer rainfall region becomes drier to the west of the trough (enhanced divergence and subsidence on the trailing side). The pattern of rainfall associated with sea surface temperature variations in the central South Atlantic Ocean in Mason *et al.*'s (1994) analysis suggests that atmosphere-ocean interactions produce changes in the South Atlantic anticyclone and in baroclinic westerly wave configurations that affect rainfall over the subcontinent. Mason *et al.* (1994) suggests that either a shift in the position of standing wave 3 of the southern hemisphere circulation or a change from a wave 3 to a wave 6 pattern would produce a diminution of summer rainfall in association with warming of the ocean in the specific region.

The reverse circulation pattern describes wet summers across South Africa (Pathack *et al.*, 1993). A zonal, vertical cell to the west of southern Africa implies mean rising motion over land and mean sinking over the western Atlantic. This circulation pattern often exists in association with the gradual warming of the sea surface from December through February. A slight increase in the SST of these regions, often noted in response to the low phase of the global El Nino (negative SOI), may be expected to significantly increase the surface vapour pressure over the CEI and induce the circulation anomaly through related thermodynamic processes.

Temperature change in the South Atlantic subtropical convergence region likewise appears to be modulated with the baroclinic westerly waves in such a way that warming of the ocean surface is linked to a significant increase in rainfall over the summer rainfall region, mainly when the QBO is westerly. Warming of the western equatorial Indian Ocean causes pressure to fall over

the ocean forming tropical lows or barotropic easterly waves situated over that area (Fig. 2.9a, b). This occurs irrespective of the QBO and has the effect of shifting the tropical convection pattern eastward. Tropical-temperate troughs form further to the east and major cloud bands linking tropical and temperate regions and their attendant rainfall bands also shift eastward to the Madagascar region. Finally, as sea surface temperature in the Agulhas region increase, so an enhanced moisture influx may occur over northern areas via the tropical easterlies (Jury *et al.*, 1993). Further to the south the strengthened sea surface temperature gradient encourages increased cyclogenesis.

### 2.9.3 THE ROLE OF THE QBO IN RAINFALL RESPONSE

The atmospheric response to sea surface temperature anomalies is not always consistent. One possible reason for this is a modulating effect exerted by the QBO. Given the regular period of the QBO (2.3 years), this global indicator offers additional levels of predictability for southern African rainfall (Jury, 1995). Jury *et al.* (1994) found a correlation between the QBO and tropospheric winds, which corresponds with upper cyclonic, Walker cell descent over southern Africa and ascent over Madagascar in east phase summers in agreement with Fig. 2.3.

Ranking the rainfall response to SSTs according to the QBO phase, it is the Indian Ocean south-east of South Africa (QBO easterly), followed by the South Atlantic subtropical convergence region (QBO westerly) and the Agulhas system (QBO westerly). Ranking rainfall response according to the degree of significance of the correlation between sea surface temperature and rainfall for the 3 cases taken together (i.e. QBO not taken into account, QBO easterly and QBO westerly), then the strongest association between sea surface temperature variability regions and a summer rainfall temperature

response on land is that with the Indian Ocean to the south-east (easterly), followed by the central South Atlantic (unstratified), the South Atlantic subtropical convergence region (unstratified), the western equatorial Indian Ocean (unstratified) and the Agulhas system (QBO westerly) according to Mason *et al.*, 1994.

There is a sympathetic response between the QBO and the upper limb of the Walker cell anomaly. Hence in the wet phase of the QBO, uplift within troughs over SE Africa is enhanced, while westerly shear limits the potential for development of barotropic weather systems of the SW Indian Ocean. In the opposing east phase of the QBO, the upper limb of the Walker cell anomaly is more easterly and subsidence limits the development of troughs over SE Africa (Jury, 1992; Pathack *et al.*, 1993). In the east phase tropical cyclones are particularly frequent and intense in the SW Indian Ocean region (for example in the summers of 1982 and 1984). It is during this phase that the effects of the ENSO may be most readily transmitted from the Pacific to SE Africa.

The patterns of SST discussed above act to support the circulation differences between wet and dry summers presented previously. To the SE of Africa where the warm Agulhas Current flows SST are  $+1^{\circ}\text{C}$  above normal during wet summers and to the SW of Africa near  $40^{\circ}\text{S}$ ,  $10^{\circ}\text{E}$ , SSTs are  $+2^{\circ}\text{C}$  above normal in wet summers (Jury *et al.*, 1993).

## 2.10 TELECONNECTION PATTERNS ASSOCIATED WITH SUMMER RAINFALL OVER SOUTH AFRICA

Convection in the spring-time monsoon trough over the central Indian Ocean is a reliable climatic determinant of teleconnections governing summer rainfall over southern Africa. As the monsoon advances southward from spring to

summer, it establishes a convective 'dipole', which modulates regional convection through east-west differences in Hadley cell mass overturning (Jury, 1996). This subsection discusses correlations of rainfall and global indices, teleconnection patterns of regional SSTs, OLR and wind, pertinent to the study, obtained mainly by Jury (1996).

#### 2.10.1 CORRELATION OF RAINFALL AND GLOBAL INDICES

For January (which refers 0 lag in Jury, 1996)) cross-correlation values and significance levels, for the period 1955 to 1990, with 34 DF for QBO, SOI, South Africa, Namibia, and Zimbabwe rainfall indicated significance at the 99% confidence limit Zimbabwe and South African rainfall ( $r = +0.62$ ). The correlation value for South African rainfall and the SOI is  $+0.57$ , and  $+0.44$  for both Zimbabwe and Namibia rainfall and the SOI. Correlations significant above the 95% limit include Namibia and Zimbabwe rainfall ( $r = +0.39$ ), and Namibia and South African rainfall ( $r = +0.33$ ). Correlations significant above the 90% limit are Zimbabwe rainfall and the QBO ( $r = +0.28$ ).

Analysis of mid-summer atmospheric anomalies by Jury *et al.* (1996b) indicated that the upper-air westerlies increase during dry summers over southern Africa and subsidence increases over the eastern parts of southern Africa. The surface flow over the Mozambique Channel becomes anomalously southerly while the surface flow over equatorial Africa becomes anomalously westerly. The ITCZ moves northwards and the Inter-Ocean Convergence Zone (IOCZ) disappears (Jury *et al.*, 1996b).

Positive SST anomalies over the CTIO (central tropical Indian Ocean) produce large convection which produces world-wide synoptic scale perturbations in Jury *et al.*'s (1996b) GCM circulation. The circulation changes modelled over subtropical Africa appears to be a non-linear response

to the primary convective forcing and results in significant enhancement and northward shift of the midlatitude westerlies. The eastward shift of the upper-air subsidence over southern Africa and reduction of southward moisture flux is the major forcing mechanism for prolonged summer drought when warmer than normal SSTs occur over the CTIO (Jury *et al.*, 1996b).

#### 2.10.2 REGIONAL SST TELECONNECTION PATTERNS

Jury (1996c) has shown that SSTs in the central equatorial Indian Ocean basin are linked with summer rainfall over southern Africa and that changes in SST over CEI are consistent with those associated with the ENSO signal. SST-rainfall correlation patterns at lags -2, which refers to November, are have positive values in the central Atlantic Ocean and a small negative correlated area off equatorial east Africa. Positive correlations occur in the South Indian Ocean in the area 25°-35°S, 60°-90°E at 0 lag (February) (Jury, 1996).

Composite SSTs for the CEI lag the global ENSO during the Indian monsoon transitions before (-6 months) and after the event (+6 to +12 months). On this basis Jury (1996c) concludes that the finding suggests that SSTs of CEI could mislead during the year following a strong El Nino year as in 1992/93. At this time the SST-rainfall correlations are negative in the central South Atlantic in the area 10°-30°S, 10°W-10°E. The values in the Atlantic are weaker than in the Indian Ocean and spatially less extensive at lag 0 (January). A small positive region occurs in the vicinity of 40°S, 10°E to the south of Africa where the warm Agulhas Current splits and returns to the Indian Ocean.

### 2.10.3 REGIONAL OLR TELECONNECTION PATTERNS

The OLR correlations reveal that convection in the spring-time monsoon trough over the central and western Indian Ocean is an important determinant of summer rainfall over southern Africa (Jury, 1996). As the monsoon trough migrates southward during the season, it sets up a 'dipole' which modulates southern Africa rainfall through east-west overturning (Jury, 1993b).

The OLR-rainfall correlation patterns at lags -2 (November) has a positive correlation in the central and western Indian Ocean. The relationship means that reduced (increased) convection in the spring time monsoon transition corresponds with above (below) normal rainfall in the following summer over southern Africa. Convection in the monsoon trough is modulated by the underlying SST which drives an anomalous Walker Cell linked to southern Africa. The positively correlated area is over the western equatorial Indian Ocean (Jury, 1996c).

The January rainfall-OLR correlation pattern has a negative (sympathetic) area over southern Africa, with a distinct NW-SE alignment consistent with subtropically forced cloud bands (Harrison, 1986; Jury, 1996). The band of negative correlations is located over southern Africa. Opposing correlations occur over the South Atlantic (30°W) and the south-west Indian Ocean (60°E) in the latitude band 20°-30°S. This correlation pattern refers to a subtropical hemispheric wave four pattern that modulates convective variability at the interannual scale (Jury, 1996c).

#### 2.10.4 REGIONAL WIND CORRELATION PATTERNS.

Jury (1996c) has found that the most useful circulation index is zonal upper winds over the equatorial Atlantic. This is a signal associated with the SOI, and may refer to a retreat (advance) of the South Atlantic standing westerly wave in La Nina (El Nino) years, through upstream effect of meridional SST gradients in the Pacific on the thermal wind. Harrison (1986) identified the central South Atlantic upper winds as an important modulator of southern African climate, through downstream adjustment of subtropical westerly waves and associated poleward fluxes.

At -2 lag (Nov) the 200 hPa vectors are directed westward over the equatorial Atlantic Ocean between 5°N and 10°S, 40°W-0°. A cyclonic gyre is located over southern Africa with southward directed flow anomalies over the Mozambique Channel. Northward directed correlation vectors at 200 hPa over the central South Indian Ocean between 60° and 90°E, 0°-20°S occur, in conjunction with the area of significant -SST and +OLR correlations. The wind vector correlations at 700 hPa display a similar response, implying that Hadley anomalies may be confined near the surface (Jury, 1996c).

At 0 lag (Jan) the upper wind correlations are dominated by anticyclonic feature to the south of Africa, with westward directed vectors across South Africa. Northward vectors are found to the south of Madagascar, and southward vectors occur over the Benguela region of the south-east Atlantic, a pattern consistent with Hadley and Ferrel cell overturning (Jury, 1996; Tyson, 1986). The 700 hPa correlation vector fields reflect an anticyclonic presence over the Agulhas Current region to the south-east of southern Africa. Flow anomalies indicate south-westward advection of moist unstable air in wet summers, from a source region over the northern Mozambique Channel. Northward vectors over the south-west Indian Ocean imply the

advection of cold dry air into the tropical cyclone zone (Jury, 1996).

In a GCM simulation Rocha and Simmonds (1997a) found that 3 months before dry summers, low tropospheric wind anomalies at 850 hPa are south-easterly over much of south-eastern Africa south of 20°S and north-easterly over south-western Africa. At zero-lag (DJF), the spatial pattern of the meridional wind anomalies changes little but the zonal winds are anomalously westerly in the southern part.

## 2.11 THE SIMULATION AND PREDICTION OF DROUGHT

The preceding discussion has shown that the most widespread and effective drought precursor is large-scale SST anomalies. By far the best known example of an SST anomaly is the El Niño phenomenon which involves warming of 2-4°C in the central and eastern tropical Pacific. Statistical and numerical drought methods have been used to predict summer rainfall over South Africa. A review of literature on prediction of summer rainfall and model simulations over South Africa and other parts of the world is presented below.

### 2.11.1 STATISTICAL PREDICTORS

Statistical drought simulation methods can make useful predictions for limited time-frames, but require separate relations to be derived for each region considered. A variety of statistical methods have now been developed, and some are being used operationally with mixed success. Statistical prediction methods have many attractions being simple and conceptually based. In addition their ability to make predictions for the normal range of climatic variables usually required for practical utility provides a considerable advantage over numerical methods. The major requirement for accurate

rainfall predictions is a good prediction of the spatial and temporal variability of the precursor environment (Hunt, 1991).

The empirical agreements between regional precipitation anomalies in southern Africa and Indian Ocean SSTs have been discussed by Jury *et al.* (1996b) based on observational data. The simulation excluded SST anomalies in the Atlantic and Pacific Ocean basins and results indicate that summer drought over southern Africa may be induced by anomalous warming of the tropical Indian Ocean. Point-to-field correlation analyses of SST and OLR at lags -4 and 0 months (October and February) by Jury (1996c) are shown in Figs. 2.10 and 2.11a and b). SST correlation indicates a large area of coherent negative correlation occurs across the CEI both in October and February, and is 'mimicked' in the eastern tropical Pacific. These statistical relationships indicate that above normal CEI SST underly summer drought over southern Africa (Jury *et al.*, 1996b). An area of positive anomalies is found in the subtropical south-west Indian Ocean. Jury *et al.* (1996b) observed that the fact that a positive correlation is not sustained at lag -4 months (October) suggests that SST in the 'Agulhas gyre' region may reinforce, rather than initiate climate anomalies. Trade winds strengthen over the Agulhas gyre in dry years and serve to limit poleward fluxes of tropical air over Africa (Jury *et al.*, 1993; Jury and Lutjeharms, 1993).

Observed rainfall anomalies which are statistically linked to SST boundary forcing have been validated and reproduced by model results (Rautenbach, 1997b; van Heerden *et al.*, 1997)). In a study by Goddard and Graham (1997), the relative importance of Indian Ocean SSTs to regional precipitation anomalies over southern Africa is examined for observations and for three general circulation model (GCM) simulations. The three GCM simulations with warming of the Indian Ocean produced rainfall anomalies which are consistent with results of Jury *et al.* (1996).

In a study by Rocha and Simmonds (1997d) using rft (ratio between forced and total variability), over southern Africa SST-forced precipitation anomalies account for more than 40% of the total anomalies. This area is coincident to that where ENSO has the strongest signal. Strong forcing is also found over eastern equatorial Africa. The statistical associations reinforce the conclusion that above normal convection and SST in the CEI precedes and sustains summer drought over southern Africa.

### 2.11.2 NUMERICAL SIMULATIONS

Realistic numerical simulations of drought conditions can be obtained with current GCMs, by inserting observed SST anomalies into composite-defined distributions (Barnston, 1997; Wilder *et al.*, 1997). These simulations are capable of reproducing most climatic effects associated with drought as well as the rainfall perturbations.

GCM experiments have been used in which the model has been forced with spatial- and time-evolving SST anomalies characteristic of dry summers over south-eastern Africa. Rocha and Simmonds (1997b) demonstrate that anomalously warm SSTs in the tropical Indian Ocean, which are partly modulated by ENSO, are the most direct cause (only oceanic forcing is considered) of dry south-eastern African summers. They generate a rather strong and well-defined low-level cyclonic anomaly over the central Indian Ocean east of Madagascar. The south-east trades and north-eastern monsoon are weakened, and result in weaker moisture fluxes inland and increased moisture flux convergence over the central Indian Ocean. The rising branch of the Walker Circulation, normally located over southern Africa, shifts to the east towards the Indian Ocean. Reduced convection and precipitation takes place over the subcontinent, whereas the Indian Ocean experiences

abnormally high precipitation rates. Slightly cool and warm oceanic surface waters over the eastern and western parts of the western Pacific Ocean, respectively, contribute to a further eastward shift of the rising branch of the Walker Circulation maximum convection and rainfall anomaly zone.

Relatively warm SSTs in the central and eastern Pacific Ocean have little direct influence on the low-level circulation over the Indian Ocean and south-eastern African sector. However, unlike SST anomalies in other parts of the ocean, they generate quite strong upper-level westerly wind anomalies across much of the tropics between the central Pacific and the central Indian Ocean (Rocha and Simmonds, 1997b).

It has therefore been established that certain patterns of SST anomalies which develop well before the rainy season, and persist during summer, can generate dry conditions over south-eastern Africa. This robustness implies good prospects for forecasting summer rainfall from knowledge of SSTs before the start of summer (Rocha and Simmonds, 1997b).

Studies on the physics of the tropical air-sea interaction processes and the regulation of SSTs (Jury, 1993; Majodina *et al.*, 1997; Peter, 1997) have been undertaken. Peter (1997) has undertaken simulations, using the Australian 4-level, mixed layer CSIRO general circulation climate model, initialised with regional SST anomalies associated with late summer (January to March) drought over southern Africa and the results compare well with observations and circulation patterns discussed in the preceding section. Other studies have looked at the relationships between interannual and decadal fluctuations in rainfall, temperature, the SO and SST over the Pacific and Indian Oceans (Hunt, 1991; Jury and Parker, 1997; Klopper, 1997; Power *et al.*, 1997; Mulenga, 1997 and 1998;).

A CSIRO4 model has been employed by Jury *et al.*, (1996b) to simulate drought over South Africa. The model climatology fields are consistent with observations. Correlation maps for OLR are shown in Figure 2.11 a and b. The positive area shifts southward along 70°E from 0° to 20°S to be located in the South Indian Ocean by February (0 lag). An area of negative OLR correlations develops over southern Africa, in sympathy with co-located rainfall. The east-west opposition of OLR correlations (subtropical dipole (Jury, 1992)) teleconnecting the CEI monsoon trough with southern African continental rainfall is also evident.

### 2.11.3 PREDICTABILITY OF DROUGHT OVER SOUTH AFRICA

Rainfall predictability over south-east Africa is high because as a sub-tropical region, rainfall responds directly to boundary forcing such as SST anomalies, including El Nino events. Rainfall in this region originates from a single well organised quasi-permanent circulation system (Hastenrath, 1995; Thiao and Barnston, 1997) as opposed to the chaotic nature of the circulation regimes of mid-latitudes. The predictability of summer rainfall in the eastern part of southern Africa has been demonstrated in a number of studies (Hastenrath, 1995; Hastenrath *et al.*, 1995; Jury *et al.* 1996; Jury *et al.* 1997; Rocha and Simmonds, 1997a ). Landman (1994) uses canonical correlation analysis of SST fields in the tropical oceans. In a related study, Cane *et al.* (1994) report predictability of maize yield in Zimbabwe from the modelling of tropical Pacific SST.

Partly in response to the devastating effects of the 1991-93 drought in southern Africa the South African Weather Bureau and a number of research groups in the South African universities have begun to release seasonal forecasts in the last few years (South African Weather Bureau, 1992; Hastenrath *et al.*, 1995; Mason *et al.*, 1996; Jury, 1996; 1997). Agriculture,

hydrological and other climate-impacted economic activities can benefit from long-range forecasts based on ENSO teleconnections, so improving the economic growth potential of southern Africa (Jury, 1996; Jury, 1997; Thiao and Barnston, 1997).

The conceptual model given in Figures 2.3 and the subsequent hypothesis (Fig. 2.2) arising from observed links between sea surface temperature anomalies and rainfall over southern Africa (Harrison, 1986; Lindesay, 1986; Jury and Pathack, 1991; Jury, 1993) have been tested using general circulation models. Models used to simulate drought over southern Africa include the Melbourne University General Circulation Model (MUGCM) (Rocha and Simmonds, 1997c), the UKMO Unified Model (Mullan *et al.*, 1997), and the Australian CSIRO 4-level R21 GCM (Lindesay *et al.*, 1993; Peter, 1997; Reason *et al.*, 1997). Atmospheric and ocean GCMs used in various research projects are in agreement with this pattern and suggest that coupled modes of air-sea interaction play an important role in interdecadal variability in the South Indian Ocean region. Statistical links between the warm waters of the Agulhas Current system and the summer climate of southern Africa have been established (Jury *et al.*, 1993).

## 2.12 ENVIRONMENTAL IMPLICATIONS OF DROUGHT

### 2.12.1 HISTORICAL PERSPECTIVE OF DROUGHT MONITORING PROGRAMMES IN AFRICA

Desertification is defined as a progressive soil and vegetation degradation in arid, semi-arid and dry sub-humid lands, not just outright conversion to desert, to which both human and climatic factors may be contributing (United Nations, 1992a; Botha, 1995; Adedoyin, 1997). Desertification and drought affect sustainable development through their interrelationship with social

problems such as poverty, poor health and nutrition, lack of food security, etc. These have affected 25% of the earth's land (Verstraete and Schwartz, 1991). The situation is serious in Africa where 66% of the continent is desert or dryland, and 73% of agricultural dryland are already degraded (United Nations, 1992b).

The 1992 UN Rio Conference on Environment and Development produced an international blue-print for sustainable development into the 21st century, the Agenda 21, which represents the commitment of the international community to address all aspects of the environment and development on global basis. As a result of the Rio Conference, the Desert Margins Initiative (DMI) has emerged to mitigate desertification and drought (Sivakumar, 1995). The purpose of the DMI is to co-ordinate research efforts into desertification and drought in sub-Saharan Africa. The governance mechanisms of the DMI in Africa is organised according to four distinct and complementary levels, *viz.* national, sub-regional (west, southern and east Africa), regional (Africa) and global (UNEP). Drought has become such a priority that drought monitoring efforts throughout Africa are undertaken by the Famine Early Warning System (FEWS) programme sponsored by the United States Agency for International Development (USAID) (Dilley, 1996; Kousky, 1997). The failure to utilise forecasts based on sound scientific knowledge would negate attempts at achieving food security (Mulenga 1998). It is imperative to undertake research to distinguish between anthropogenically-induced drought and drought due to normal climate variability, and assess their severity and persistence as well as the magnitude of their impacts to enable cure programmes to be established. Any scientific approach to the problem of drought and desertification should adopt an integrated approach addressing the physical, biological and socio-economic aspects of these processes.

## 2.13 DROUGHT IN OTHER PARTS OF THE WORLD

### 2.13.1 DROUGHT REGIMES

The droughts of northeast Brazil, which has its rainy season concentrated mainly in March/April, are characterised by an anomalous poleward position of the near-equatorial trough and embedded confluence axis and convergence band, positive SST departures in the tropical North Atlantic, and anomalously cold waters in the south equatorial Atlantic (Hastenrath, 1983; Kousky *et al.*, 1983; Rathor *et al.*, 1983; Valença, 1983; Hastenrath, 1987;). Surface circulation features conducive to drought include the distant position of the convergence band, the cold south equatorial waters and its resulting effects on moisture and instability of the boundary layer flow, and enhanced meridional temperature contrasts across the Equator which drive a thermally-direct meridional circulation cell in the atmosphere, featuring subsidence over the Nordeste (Hastenrath, 1991).

Rainfall variations during the boreal summer half-year in the central American-Caribbean region are related to the position of the north Atlantic high. During drought years, the pressure on the equatorward side of the subtropical high is enhanced, the trades appear stronger, and most of the north Atlantic waters are anomalously cold. The approximately inverse departure configurations are characteristic of abundant rainfall years (Hastenrath, 1991).

Drought in sub-Saharan Africa, which experiences its rainfall at the height of the boreal summer, are associated with anomalously far equatorward position of quasi-permanent circulation features, in particular the surface confluence axis and convergence band, and negative SST anomalies are found in a band across the tropical north Atlantic. Anomalously warm surface waters in the

western Indian Ocean and in the equatorial Pacific also tend to be associated with deficient Sahel rainfall. Empirical diagnostic studies have been complemented by GCM experiments aimed at the Sahel drought problem (Hastenrath, 1991).

Rainfall and SST at the Angola coast shows antecedents of remote forcing by seasonal wind stress relaxation over the western equatorial Atlantic. Strong easterly wind stress relaxation in the remote western region during the preceding months is associated with warm east coastal waters and abundant Angolan rainfall around the March/April maxima in the annual cycle. A strong affinity between interannual variability and annual cycle mechanisms is also indicated in various other tropical regions (Hastenrath, 1991).

#### 2.13.2 RESULTS OF NUMERICAL DROUGHT SIMULATIONS

Voice and Hunt (1984) have run experiments for fixed January conditions and fixed SST anomalies, and obtained ENSO-related droughts over parts of Australia, southern Africa, South America and North America. They were able to relate the rainfall changes to perturbations induced in the low-level synoptic wind distributions. In particular, they showed that while synoptic patterns were disturbed in the Australia region, where the largest forcing occurred, elsewhere only secondary changes were produced. Markham and McLain (1977) have related drought in the north-east Brazil with anomalies in the tropical Atlantic Ocean.

Folland *et al.* (1986) composited the SST for the global oceans for July to September for a number of dry years in the Sahel minus the SST for a number of wet years. The resulting SST anomalies showed warmings, about 1°C for the South Atlantic and Indian Oceans and south-east Pacific Ocean, with the North Atlantic and North Pacific Oceans being colder. Folland *et al.* (1986)

ran their GCM in perpetual July mode with these SST anomalies and observed substantial rainfall reductions throughout the Sahel, indicating the critical impact of the SST anomalies for drought in this region. The principal cause of the rainfall reduction was shown to be a decrease in the low-level meridional flux of moisture from the South Atlantic into the Sahel in agreement with findings by Charney (1975). Owen and Ward (1989) have conducted model studies which suggest that the long-term rainfall decline in the Sahel starting in 1968 was due to SST changes in the Atlantic Ocean.

Trenberth *et al.* (1988) have suggested, on the basis of a GCM, that the 1988 drought precursor in the USA was the SST anomaly patterns in the Pacific Ocean. They showed that a wavetrain could be set up across the North Pacific and North America similar to that observed, and thus consistent with the occurrence of drought. The general characteristics of the drought were well simulated. Detailed comparisons, however, revealed flaws in the simulation, such as the enhanced rainfall from Florida to Mississippi in May, but the increased rain over north-west Canada was well reproduced (Hunt, 1991).

## 2.14 CONCLUSION

This chapter has given a review on climate variability over southern Africa, outlining both the below and above-normal rainfall scenarios. Highlights have been placed on recurrent droughts over southern Africa during the past few years and the need for long-range prediction to help in reducing climate vulnerability in the region. This provides a framework on the underlying processes governing climate variability over KwaZulu/Natal and the repercussions thereof, which are subjects of the following discussion.

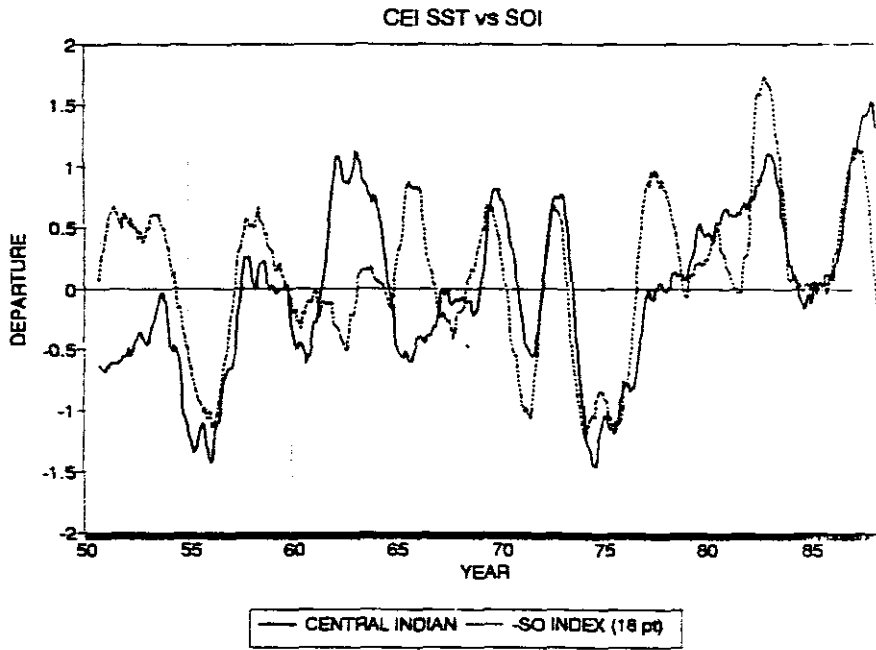


Fig. 2.1: Smoothed departures of monthly central Indian Ocean SST and the global SOI. The SOI has been inverted for comparison and an 18 point running mean applied (Source: Jury *et al.*, 1996b).

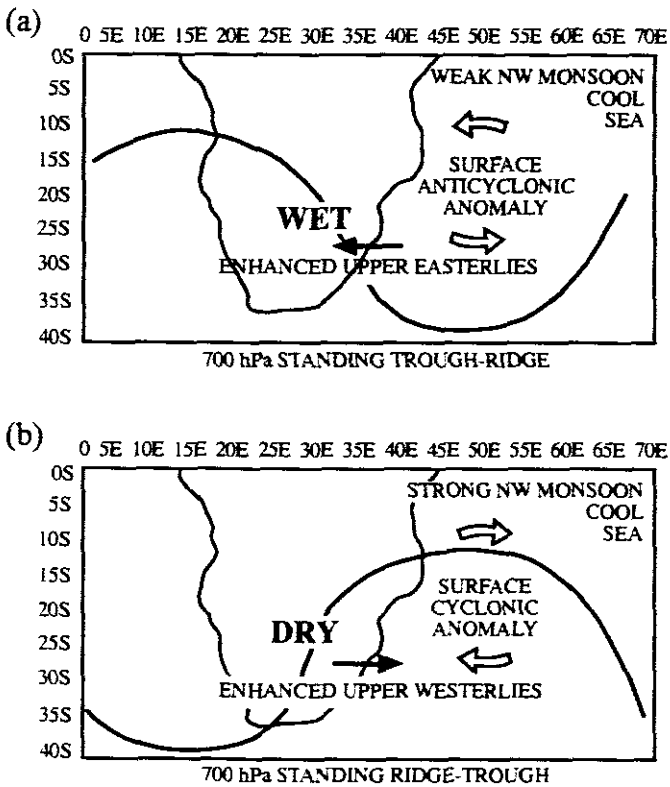


Fig. 2.2: Schematic illustration of wind circulation for (a) wet ,and (b) and (c) dry summer scenarios (Source: Jury, 1992).

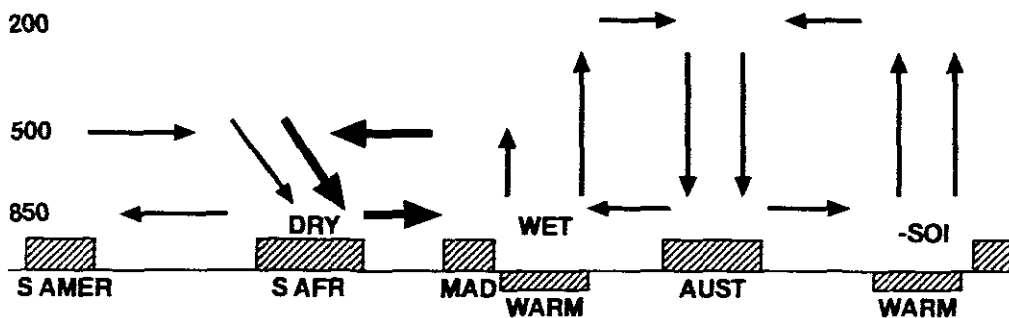


Fig 2.3: Schematic illustration of zonal, vertical circulations for (a) above normal South African summer rainfall (wet), and (b) below normal South African summer rainfall (dry). S AFR, MAD and AUST represent South Africa, Malagasy and Australia (Source: Pathack *et al.*, 1993).

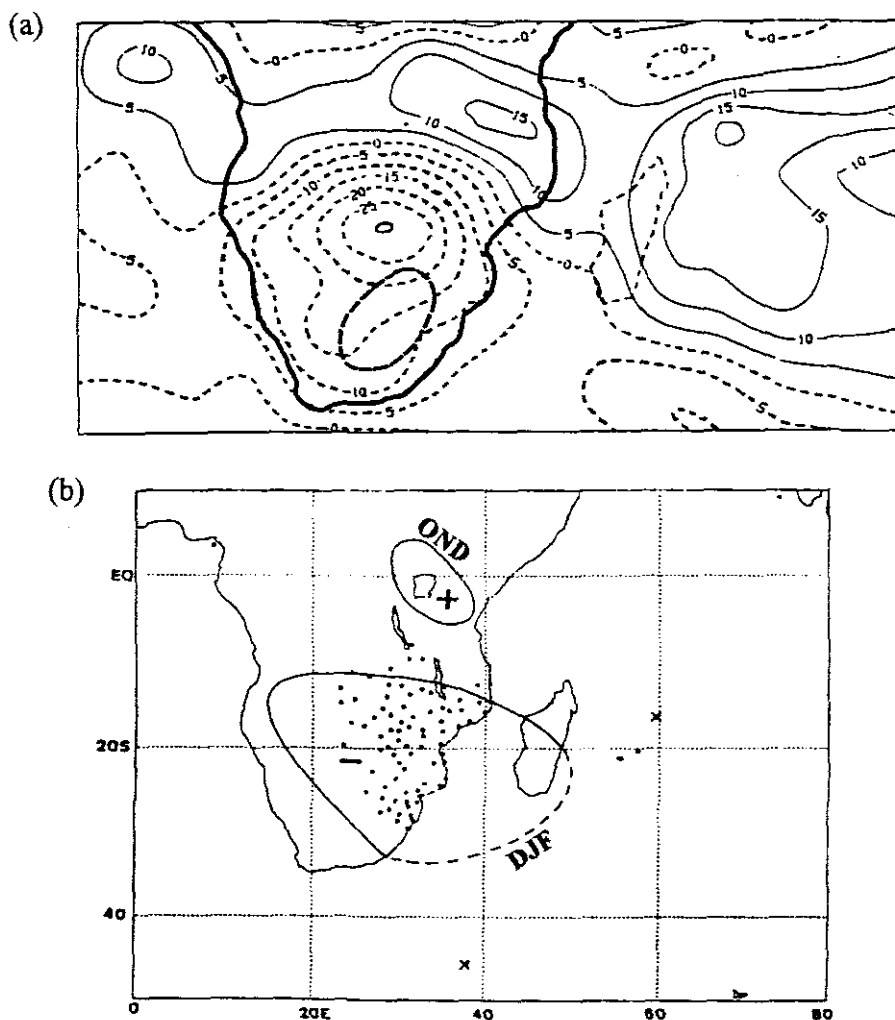


Fig. 2.4: (a) Composite OLR difference for wet – dry summers showing the climatic dipole interaction between South Africa and SW Indian Ocean. The contour interval is 5  $Wm^{-2}$  (Source: Jury, 1992). (b) The two core regions representing ENSO related interannual rainfall anomalies between equatorial (OND) and subtropical southern Africa (DJF). The signs represent those rainfall anomalies during ENSO events. Stars represent data stations and crosses represent the locations of St Brandon and Marion Island (Source: Rocha and Simmonds, 1997a).

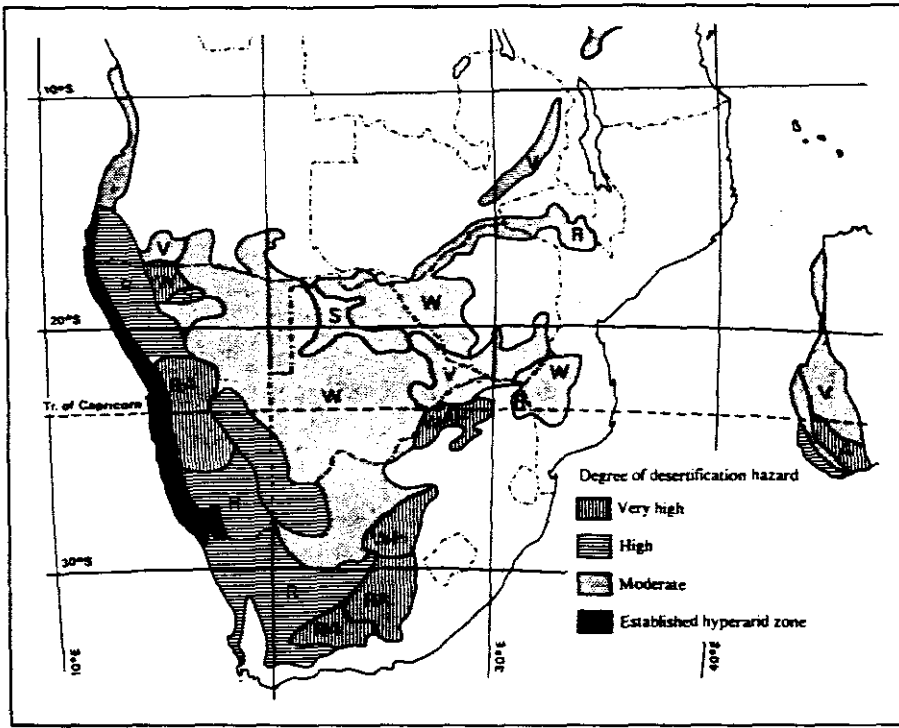


Fig. 2.5: Desertification map for southern Africa. W represents surfaces subject to sand movement; R stony or rocky surfaces subject to aerial stripping by deflation or sheet wash; V alluvial or residual surfaces subject to stripping of topsoil and accelerated runoff, gully erosion on slopes and/or sheet erosion or deposition on flat lands; S surfaces subject to salinisation or alkalinisation; H subject to human pressure; A subject to animal pressure (Source: Preston-Whyte and Tyson, 1988).

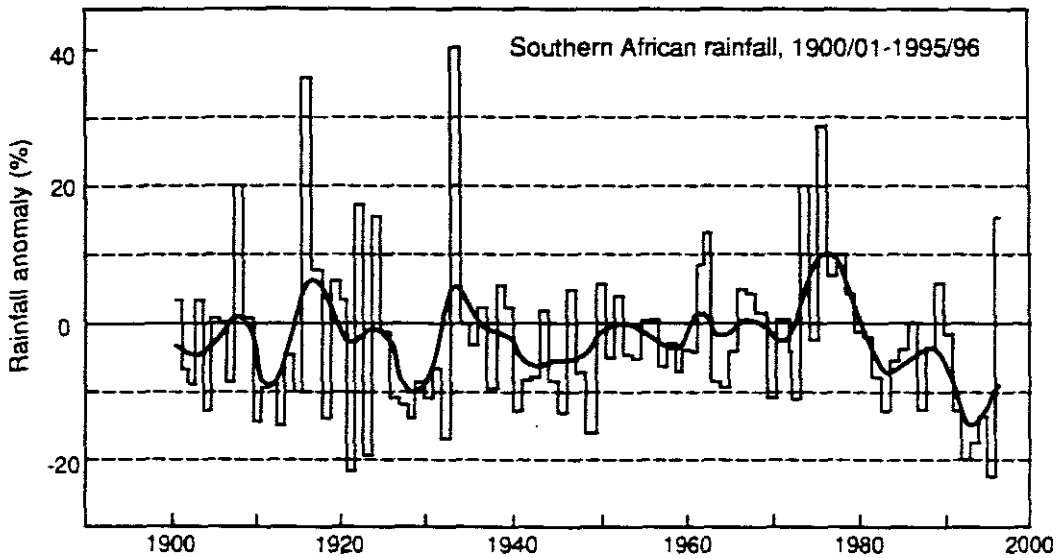


Fig. 2.6: Southern Africa rainfall trends from 1900-01 to 1995-96 as percent anomalies from the 1962-90 average. Annual totals are for the July to June rainfall year. The smooth curve shows variations on time scales longer than ten years. The index is calculated from a gridded data set derived from about 500 rainfall stations (Source: Hulme, 1996).

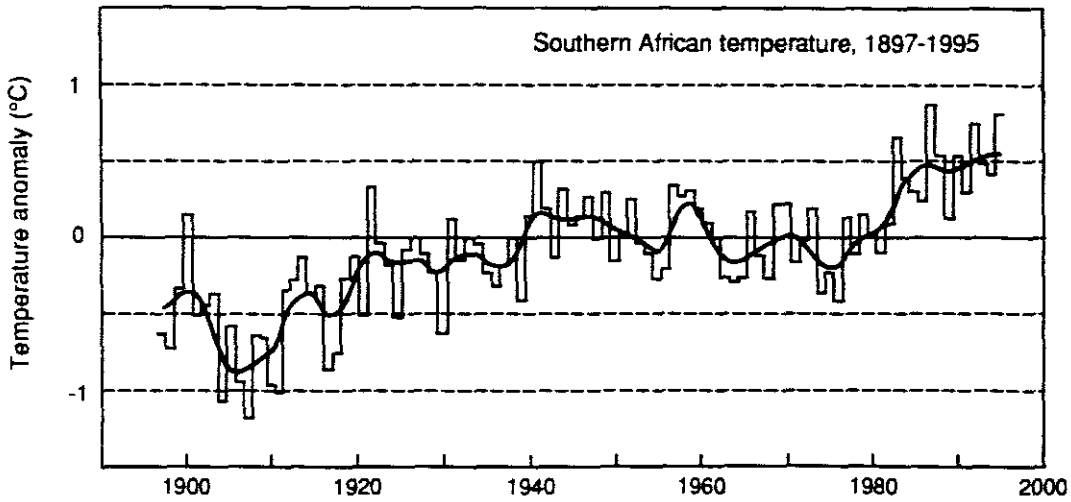
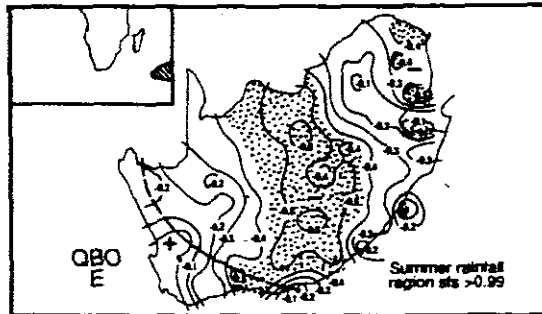


Fig. 2.7: Southern Africa temperature trends from 1897 to 1995 expressed as anomalies from the 1961-90 average. The smooth curve shows variations on time scales longer than ten years. The index is calculated from a gridded data set derived from about 100 temperature stations (Source: Hulme, 1996).

a) Correlation between SST and rainfall



b) Circulation pattern

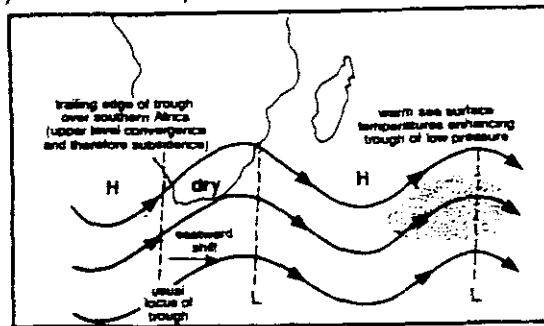
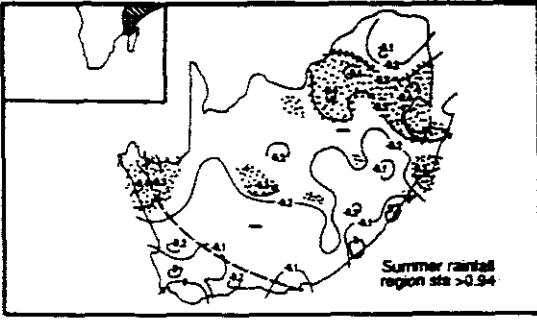


Fig. 2.8: (a) Correlations between Jan-Feb-Mar SST principal component scores in the ocean to the east and south east of South Africa and rainfall. All areas locally significant at the 90% level are shaded. Areas where the summer rainfall region as a whole has a statistical field significance (sfs) exceeding 0.90 are indicated. (b) Envisaged circulation adjustments associated with warm events in the region (Source: Mason *et al.*, 1994).

a) Correlation between SST and rainfall



b) Circulation pattern

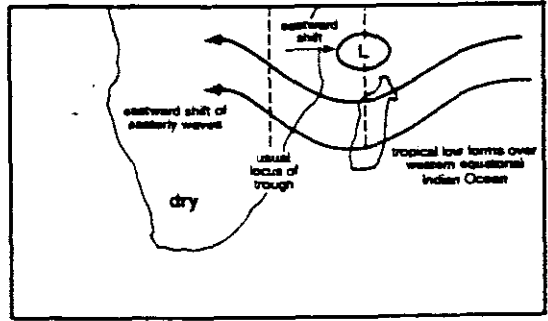


Fig. 2.9: (a) Correlations between Jan-Feb-Mar SST principal component scores in the western equatorial Indian Ocean and rainfall. All areas locally significant at the 90% level are shaded. Areas where the summer rainfall region as a whole has a statistical field significance (sfs) exceeding 0.90 are indicated. (b) Envisaged circulation adjustments associated with warm events in the region (Source: Mason *et al.*, 1994).

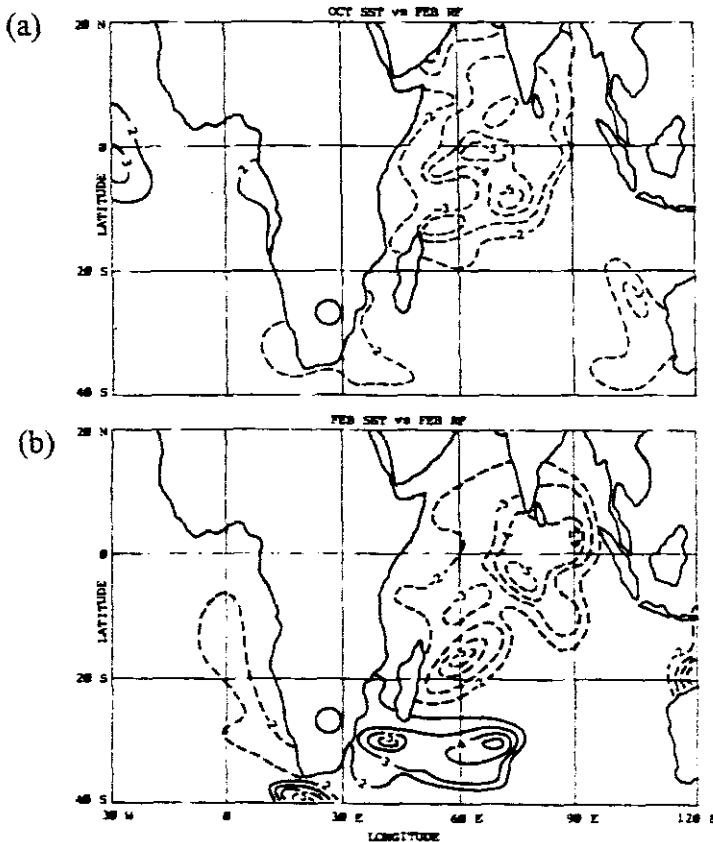


Fig. 2.10: Correlation map of SST vs SAF rainfall for the preceding Oct (lag -4 months, top) and Feb (0 lag). Negative values are dashed and labels multiplied by 10, DF = 36 (Source: Jury *et al.*, 1996b).

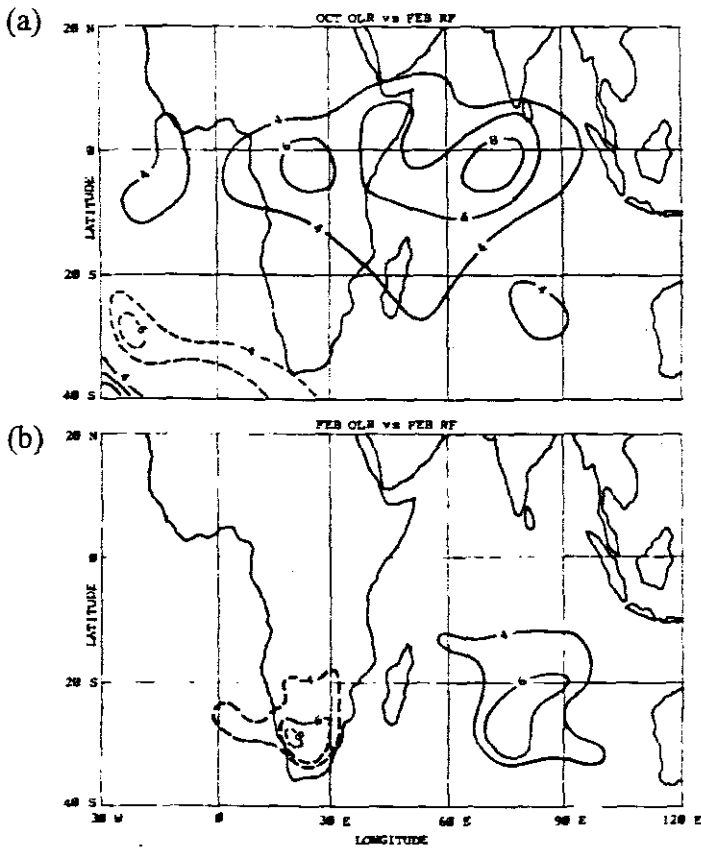


Fig. 2.11: Correlation map of OLR vs SAF rainfall for the preceding Oct (lag -4 months, top) and February (0 lag) as in Fig. 2.28 (Source: Jury *et al.*, 1996b).

Table 2.1: ENSO and anti-ENSO events. Data from 1950 to 1989 have been obtained from Rocha and Simmonds (1997a).

Warm events (ENSO)	Cold events (anti-ENSO)
1952-1952	
1953-1954	
	1954-1958
1957-1958	
1963-1964	
	1964-1965
1965-1966	
1969-1970	
	1970-1971
1972-1973	
	1973-1974
1976-1977	
	1978-1979
1982-1983	
1986-1987	
	1988-1989
1991-1992	
	1996-1997
1997/98	

Table 2.2: Jan-Mar rainfall variance in the summer rainfall region accounted for by variations in JFM SST with and without the phase of the QBO taken into account. Rainfall variance is given as the square of the correlation coefficient of the highest contours in areas where the correlation has a point significance greater than 0.90. The statistical field significance (SFS) for the region as a whole is also given (Source: Mason *et al.*, 1994).

Principal component	Area of occurrence	% SST variance	% rainfall variance; sign of correlation (); sfs for region ()		% rainfall variance with phase of QBO (); sign of correlation (); sfs for region ()		Area where effect most pronounced
1	Benguela system	17,3	16 (-)	(not sig.)	49 (E) (-)	(not sig.)	N, Transvaal
2	Agulhas system	13,0	16 (+)	(not sig.)	16 (W)(+)	(>.90)	Cape, Transkei, parts of Transvaal
3	NE Brazil coast	11,3	9 (-)	(not sig.)	16 (W)(-)	(not sig.)	Scattered
4	Western equatorial ocean	7,5	16 (-)	(>.94)	49 (E)(-) 25 (W)(-)	(not sig.) (not sig.)	NE regions
5	Central S Atlantic Ocean	7,4	16 (-)	(>.97)	16 (W) (-)	(not sig.)	S Cape coastal and adjacent inland areas
6	S Brazil Coast	7,1	16 (+)	(not sig.)	16 (E,W) (+)	(not sig.)	
7	Indian Ocean SE of S Africa	6,2	4 (-)	(not sig.)	36 (E) (-) 16 (W) (+)	(>.99) (>.90)	NW-SE band, Cape Prov NW-SE band, Cape Prov
8	S Atlantic subtropical convergence region	5,2	16 (+)	(>.96)	25 (W)(+)	(>.96)	S Cape coastal and adjacent inland areas

## **CHAPTER 3**

### **3: RESULTS ON LONG-TERM CLIMATE VARIABILITY OVER KWAZULU/NATAL AND THE 1992/93 DROUGHT**

#### **3.1 INTRODUCTION**

The high degree of inter- and intra-seasonal rainfall variability over the southern African bears profound implications for the majority of the population of southern Africa relying heavily on agriculture for subsistence and/or commercial purposes. The last period of South African summer rainfall within 0.5 of the standard deviation for three consecutive years was 1958-1960 (Jury, 1996b). Up to 91% of southern Africa's rainfall is returned to the atmosphere via evapotranspiration, compared to a global average of 65-70% (Gondwe and Jury, 1997b). Hence year-to-year climatic variations have critical impacts on crop yields and the sustainability of water resources. This Chapter provides an account of local climate variability over KwaZulu/Natal, thus laying a foundation for the following Chapter on the meteorological structure of the drought, and outlines the impacts of the 1992/93 drought.

#### **3.2 DATA AND METHODOLOGY**

Various sources of data were used to perform an analysis of long-term climate variability over Kwazulu/Natal and the assessment of the impacts of the 1992/93 drought. Temperature and rainfall data were obtained from the South African Weather Bureau. KwaZulu/Natal rainfall districts used in the analysis were 25, 26, 30, 31, 44, 45 (Fig. 3.1). Temperatures are represented by four coastal stations in Figure 3.1. These data were analysed for mean and anomalies from the established long-term means, and statistical tests of correlation performed. The OLR and NDVI data were obtained from the

Advanced Very High Resolution Radiometer (AVHRR) aboard the NOAA series of satellites. These data were also analysed for long-term and the 1992/93 DJF trends. The entire long-term period (1975-1994) OLR time series was analysed for the 30°S, 30°E grid point to establish climate variability. Mapping NDVI over southern Africa for the period 1981-1994, Jury *et al.* (1997) observed sharp upward and downward trends following the cycle of summer floods and drought. In this study OLR and NDVI data are used as proxy for convective activity over the region. Maize and sugar cane yields, and Midmar and Pongolapoort Dams inflow data were obtained from Dr W. Alexander, a hydrologist of University of Pretoria. These data were also analysed for mean trends and departures to establish the impacts of the drought.

### 3.3 LOCAL CLIMATE VARIABILITY OVER KWAZULU/NATAL

#### 3.3.1 TEMPERATURE

The seasonality of temperature in KwaZulu/Natal displays a peak in summer (November to March) with the highest temperatures occurring in February. Lower temperatures occur in winter with lowest temperatures occurring during the peak winter month of July (Fig. 3.2). Periods of above and below normal temperatures have occurred in the past over KwaZulu/Natal (Fig. 3.3). The period from 1992 to the end of 1993 had exceptionally high positive temperature departures relative to the whole period from 1960 to 1995. The five month running mean at this time are about 1°C greater than those of the drought period of 1982/83, one of the severest droughts in the last four decades.

Mulenga's (1998) PC4 (loaded at 32°E, 30°S) shows large negative loadings over KwaZulu/Natal and explains 6% of the variance in summer rainfall. Positive loadings occur over Mozambique, the Congo Basin and the Western

Cape Province (Fig. 3.4a). Figure 3.4b shows coefficients of this principal component. A correlation ( $r = 0.20$ ) is observed between KwaZulu/Natal temperature and 200 hPa zonal winds at -4 lag (Fig. 3.4c) suggesting that the zonal winds at 200 hPa can be a useful forecast variable for KwaZulu/Natal summer rainfall.

### 3.3.2 RAINFALL

KwaZulu/Natal shows marked seasonality in rainfall, peaking between December and January and least in June/July (Fig. 3.5). The variability between months is low, being about 20 mm in winter and about 40 mm in summer. Rainfall-producing synoptic and meso-scale circulation systems over KwaZulu/Natal have been discussed in Chapter 2.

The rainfall departures indicate that the 1992/93 drought was the worst period during the past four decades (Fig. 3.6). Other major dry years were the periods from 1965 to 1970 peaking in 1968, and the period 1979 to 1983 with a peak in 1983. The intensity of these dry spells is dwarfed by that of 1992/93. Since 1960, three major wet periods occurred in KwaZulu/Natal, and these were from 1971 to 1973, 1975 to 1977, and 1986 to 1990 and again in 1995-97. The temperature for these periods concurs with rainfall. The above normal trend between 1984 and 1985 is short. A contributing factor to the 1984/85 peak is cyclone *Demonia* rainfall. The period 1986 to 1990, with a 1987 peak contributed by cyclonic floods, is a wet period spanning a relatively longer period. The spectral power shows that there has been a three to five year cycle in drought frequency over the past thirty years and the amplitude of the dry spells is intensifying.

The three point smoothing of the rainfall time series for KwaZulu/Natal since 1960 indicates a high climate variability (Fig. 3.7). The period from 1991 to 1993, however, remains the most extended period of drought in any

three consecutive years on record since 1960, peaking in 1992. This is followed by the 1981 to 1983 drought in its magnitude and persistence. Statistical models for predicting rainfall over the Swaziland- KwaZulu/Natal region are given in Appendix A3.

### 3.3.3 OLR AND NDVI

OLR and NDVI are good indicators of the effect rainfall forcing has on the spatial and temporal distributions of vegetation (Gondwe and Jury, 1997). Figure 3.8 shows that a reliable inference can be drawn from the variation in NDVI on periods of dry and wet spells. NDVI responds to annual variations in climate by portraying reduced "greenness" during dry periods and increased values during wet periods. Figure 3.9 shows long-term variation in OLR displaying correspondence to dry and wet periods observed over the past 20 years. Gondwe and Jury (1997) found that KwaZulu/Natal has a weak OLR-NDVI relationship because this region is always relatively green. The presence of the warm current explains the increased rainfall and enhanced vegetation found on the south-east coast of Africa (Preston-Whyte and Tyson, 1988).

### 3.4 IMPACTS OF THE 1992/93 DROUGHT

Despite the inconvenience that drought causes around the world, many drought-producing phenomena are still insufficiently understood in terms of characterisation and impact assessment. Drought impacts have rarely been properly assessed in the past, even in some of the more developed countries. Studies on drought impacts on crop yields have been conducted in Portugal (Santo *et al.*, 1983), Sicily (Rossi, 1983), Mexico (Cervera, 1983), Namibia, (Hattle and Webster, 1983), in the Sahel (Hidore, 1983), and probably elsewhere. This section outlines the 1992/93 drought impacts in KwaZulu/Natal using dam inflows and crop yield data.

### 3.4.1 MIDMAR AND PONGOLAPOORT DAM INFLOWS

Inflow levels into the Midmar and Pongolapoort (or Pongola) Dams (Fig. 3.10) have been used in this study to assess the intensity of the 1992/93 drought period. The Midmar Dam seasonal inflow cycle corresponds to the rainfall seasonal cycle (Fig. 3.11). Maximum inflow occurs in summer, peaking in February, and least inflows occur in winter months. Deviations from mean inflows are consistently low in winter. Standard deviations grow in spring through to summer. This is because of the high incidence of tropical cyclonic and convective rains during these seasons. The seasonal cycle shows September/October and January to March having higher standard deviations since 1960.

The annual series of inflow into Midmar and Pongola Dams correlate with periods of dry and wet spells occurring in the province (Figs. 3.12, 3.13). From 1991 to the end of 1993, inflow into Midmar Dam declined to levels below  $10^7 \text{ m}^3$ . The end of 1992 and 1993 were the worst in this period with inflow levels falling below  $10^6 \text{ m}^3$ . Such low levels were also reached in the summer of 1982 and 1983. The other dry spells identified from the rainfall anomalies in the preceding discussion did not reach such low levels. The contribution of the 1987 floods, cyclone Démonia in 1984 and cyclone Eugénie in 1972 (Preston-Whyte and Tyson, 1988) are some of the events worth noting in the peak inflow levels. Peaks in inflow levels were also contributed by extended wet spells. The mean inflow level up to 1980 had less variability and thereafter dry period frequency increases. For Pongola Dam inflow, significant spectral energy is contained at periods of 18.6, 4.1 and 2.36 years, corresponding to the luni-solar tide, the ENSO and QBO, respectively (Fig. 3.14).

General decrease in inflow levels result in shortages affecting municipal supplies, industry, agriculture, recreation, etc. Consequencies of drought also include increases in pollution because of reduced surface waters, increased salinity in agriculture and ground water, etc.

### 3.4.2 MAIZE

#### 3.4.2.1 CLIMATE REQUIREMENTS

Maize requires a warm to hot, frost-free growing season. In KwaZulu/Natal, the most suitable areas for dryland maize production occur in bioclimatic groups 2, 3, 4 and 6, and under irrigation in Bioclimatic Groups 8, 9, 10 and 11 (Table 1.1) (Smith, 1993). Bioclimatic groups are demarcated areas in which the environmental conditions such as soil, vegetation, climate and to a lesser extent terrain form, are sufficiently similar to permit uniform recommendations of land use and farm practices to be made. This helps to assess the magnitude of crop yields that can be achieved, provide a framework in which an adaptive research programme can be carried out, and to enable land users to make correct decisions (Camp, 1997).

For good yields, a dryland maize crop requires 500 to 700 mm of rain over the growing season (October to March). Peak moisture demand, and thus the greatest likelihood of stress, occurs at tasselling usually in early February, when yield may be reduced by up to 8% per day of stress (Smith, 1993).

The optimum mean daily temperature for the germination of maize is between 18 and 20°C. Optimum temperatures for growth are between 24 and 30°C, within a range of 15 to 35°C. Growth is inhibited below 10°C or above 30°C. The total heat units (sum of mean daily temperatures above a threshold over a season) up to tasselling should be at least 750. Maize requires at least 1500 heat units to achieve an optimum yield during the

growing season. A heat unit of less than 1500 would depress yields, while a total of 1500 to about 1800 would result in increased yields. Where total heat units exceed 1800, yields tend to decline due to high temperatures, hence evaporative losses, and less effective rainfall (Smith, 1993).

Maize requires well-drained, deep soils. Light or heavy texture soils reduce yields. Acid saturation should not exceed 20%. If soil-moisture conditions are favourable for planting, the best yields will be obtained from the early October plantings. Planting late results in tasselling taking place during cooler conditions, with resultant lower yields. The last planting season depends on the bioclimatic group (Table 3.1) (Smith, 1993).

#### 3.4.2.2 MAIZE AND THE ECONOMY

South Africa produces some of the finest quality maize in the world and earns up to R1 000 million in foreign exchange on international markets in good crop years (Whitehead *et al.*, 1993). The maize industry stimulates the economy directly by ensuring a livelihood for more than a million South Africans and provides secondary industries with over R1 500 million worth of business each year (Smith, 1993). Maize is a staple food of southern Africa and has a potential economic value of approximately \$1 billion a year (Glantz *et al.*, 1997).

#### 3.4.2.3 MAIZE YIELD

KwaZulu/Natal is not the main maize-producing region in South Africa. Maize is produced on a smaller scale, relative to national production, in the cooler higher-lying inland areas of the province. As a drought-sensitive crop and contributing substantially to the South African economy, maize offers a good yardstick to gauge the severity of a dry period over the interior of KwaZulu/Natal.

A comparison of maize yield in KwaZulu/Natal and rainfall since 1972 is depicted in Figure 3.15. The correlation is showing an overall positive relationship particularly after 1978. For the period of the 1991-93 drought, the year of minimum yield was 1992. The 1993 drought year shows an increasing yield. This trend occurs because the higher-lying areas of KwaZulu/Natal were not as hard-hit by the 1992/93 drought and recovered earlier than along coastal areas. The climate sensitivity of maize yield is observed in the drought period of the early eighties when sustained negative departures occurred. A model defining the best fit for maize yield over South Africa is given in Appendix A3.

#### 3.4.2.4 SENSITIVITY OF MAIZE TO CLIMATE AND IMPORTANCE OF FORECAST

Since flowering coincides with the peak water requirements of the maize plant, and is also the stage at which the crop is most sensitive to drought, the time of planting needs to be selected to ensure that flowering does not take place when the chance of drought is high. Most early planted maize, however, flowers when the probability of hot dry weather is high. The risk is even high where early planting takes place on soils with dry sub-soils. When pre-planting rains have been good and the profile is saturated, early-planted maize has a better chance of doing well. The decision whether to plant early or late will therefore depend on the soil-water reserves at the time of planting, and also on expectation of the severity and frequency of mid-summer dry spells (Mallett, 1993).

### 3.4.3 SUGAR CANE

#### 3.4.3.1 CLIMATE REQUIREMENTS

Sugar cane is grown in tropical and subtropical regions throughout the world (Experiment Station of the SA Sugar Association, 1977). More than 90% of South Africa's sugar is produced in KwaZulu/Natal near the Indian Ocean Coast with very little production more than 30km from the ocean (Fig. 3.16 and Table 3.2) (Smith, 1978). The residual percentage of sugar cane comes from the lowlands of the Mpumalanga Province. All of South Africa's sugar is produced in the east, made possible by the tempering effect of the Mozambique current, which flows southward along the coast. Nevertheless, inland from the ocean, particularly at higher altitudes, frost is a limiting factor.

Precipitation in the sugar cane areas of KwaZulu/Natal averages about 950 mm, with about 70% of it coming from October through March. Rainfall decreases from south to north, and supplementary irrigation is increasingly used northward from the Mt Edgecombe area. Temperatures in summer (DJF) are favourable for sugar cane growth and since this is the rainy period, cane development is rapid. With the onset of cool and dry weather in April, cane reaches maturity quickly.

Sugar cane can be harvested at any age between 11 and 24 months depending on conditions for growth. Yields between 90 and 100 T ha<sup>-1</sup> are usually obtained during good-rain years. It is profitable to harvest sugar cane when its sucrose content reaches its maximum in September or October. Harvesting usually starts in May onwards (Experiment Station of the SA Sugar Association, 1977).

### 3.4.3.2 SUGAR CANE AND THE ECONOMY

Sugar cane production rose sufficiently in the 1930s to provide for a substantial quantity of sugar for export. About 57% of the production is sold within South Africa. In the development of the Sugar Act in 1936, the South African sugar industry made a moral commitment to supply the home market ahead of exports, a commitment to which it still adheres (Smith, 1978). The gross proceeds of sugar cane for the 1997/98 financial year from exports and local markets is R4.4 billion (of which R3.2 billion is a national earning) making a contribution of about 0.5% to the GDP (Pers. Comm., Chadwick, 1998).

### 3.4.3.3 SUGAR CANE YIELD

Figure 3.17 depicts the sugar cane yield in KwaZulu/Natal for the period 1950 to 1995. The growth in yield from 1950 to the early 1970's is associated with technological advancement. The declining trend in yield since the early 1970's is due to growth in pest infestations mainly *Eldana* borer. The impact of the 1992/93 drought is clear in the figure. Sugar cane yields declined to half those of the mid-sixties in 1992/93. The dry periods identified above, including 1982/83, all correspond with declining yields over KwaZulu/Natal.

Besides crop shortage and losses, drought is known to increase insect activities and predators, multiplying of weeds, perennial and palatable species are replaced by less useful species, increased fire hazard, prime land conversion and a potential transformation to other land uses. The model defining the best fit for sugar cane yield is given in Appendix A3.

### 3.5 CONCLUSION

The climate of KwaZulu/Natal has been characterised by periods of alternating dry and wet years. The 1992/93 drought period has been shown to have adversely affected the economy of KwaZulu/Natal through reduced crop yields and dam inflows. The negative impacts of the drought on vegetation cover, dam levels inflow, maize and sugar cane yields have been the worst on record in the last three decades in KwaZulu/Natal. The following important points pertaining to drought over KwaZulu/Natal and South Africa are noted:

1. The frequency of drought occurrence has increased and intensified over the last three decades.
2. Wet years of lesser intensity and shorter duration tend to follow drought years.
3. Drought affects sustainable development through its interrelationship with environmental and socio-economic problems such as poverty, poor health and nutrition, and lack of food security.
4. Droughts over KwaZulu/Natal have a 3 to 5 year cycle.

Highlights have been made in this Chapter on progress achieved to forecast the climate of KwaZulu/Natal. At present reliable accuracy is up to -6 months lag. Likewise, crop yield models have been formulated and their performance matches the observed yields well. This chapter has laid a framework for Chapters 4 and 5 which detail the meteorological structure of the 1992/93 drought scenario.

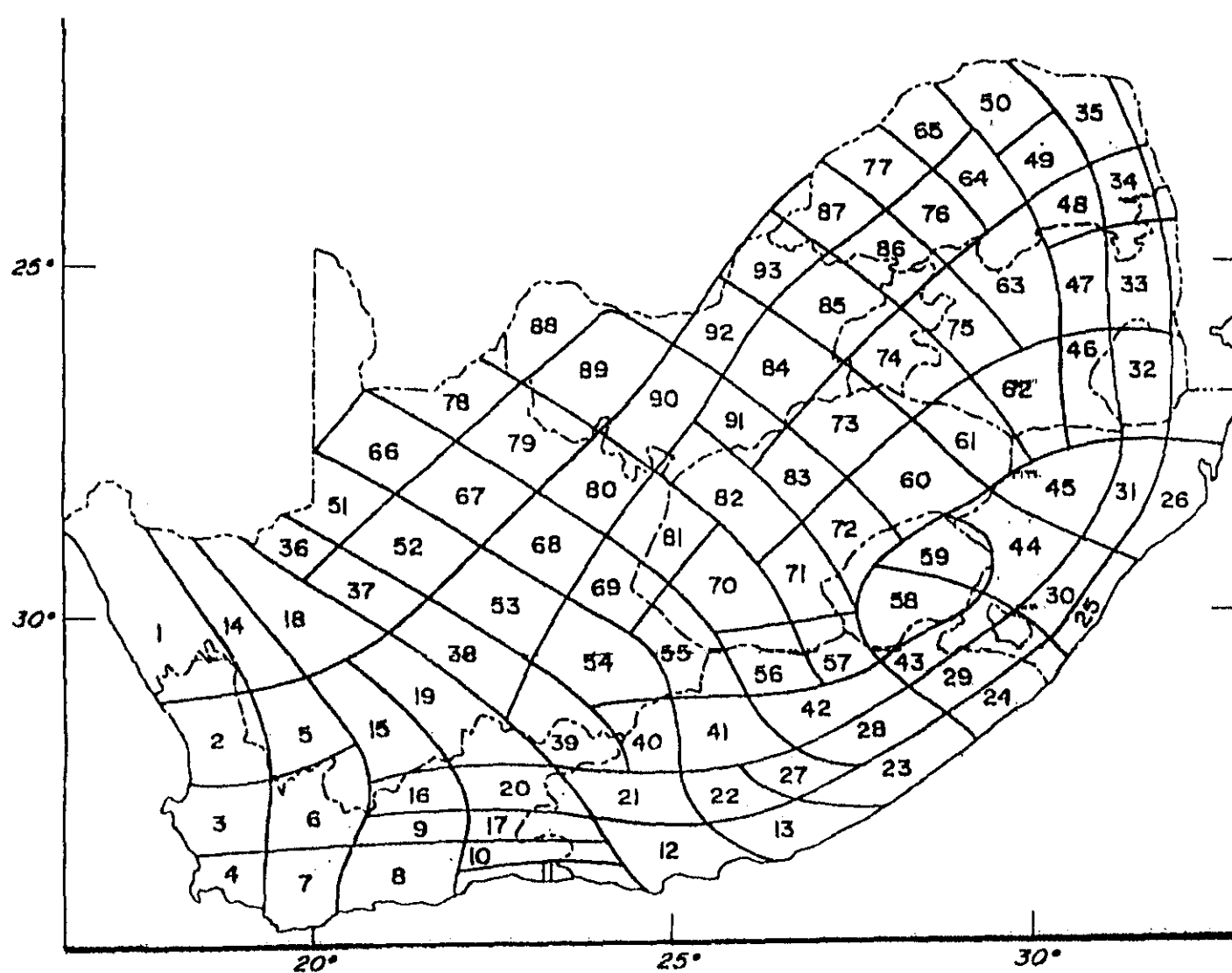


Fig. 3.1: Climatological data districts of South Africa. Rainfall Data from districts 25, 26, 30, 31, 44, 45 were used in the analysis of climatic variability over KwaZulu/Natal.

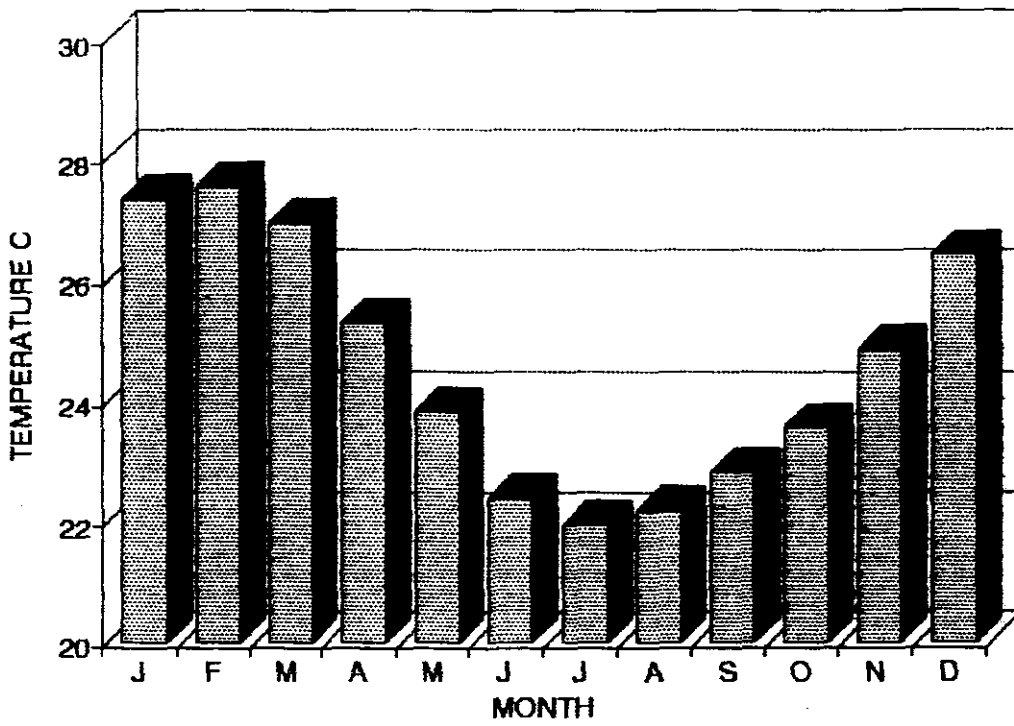


Fig. 3.2: Seasonal cycle of maximum temperature over the KwaZulu/Natal coastal region from station data: Port Shepstone, Durban, Mt Edgecombe and St Lucia (Fig. 3.1)).

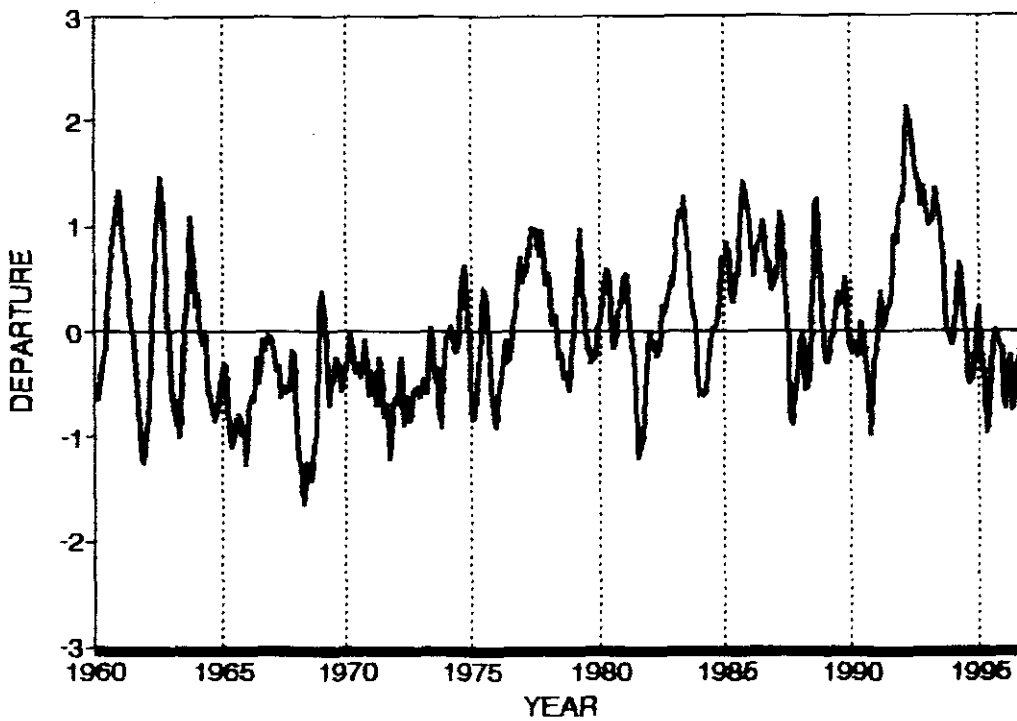


Fig. 3.3: Historical maximum temperature anomalies over the KwaZulu/Natal coastal region from 1960 to 1996 (data stations 25, 26, 30, 31, 44, 45 (Fig. 3.1)).

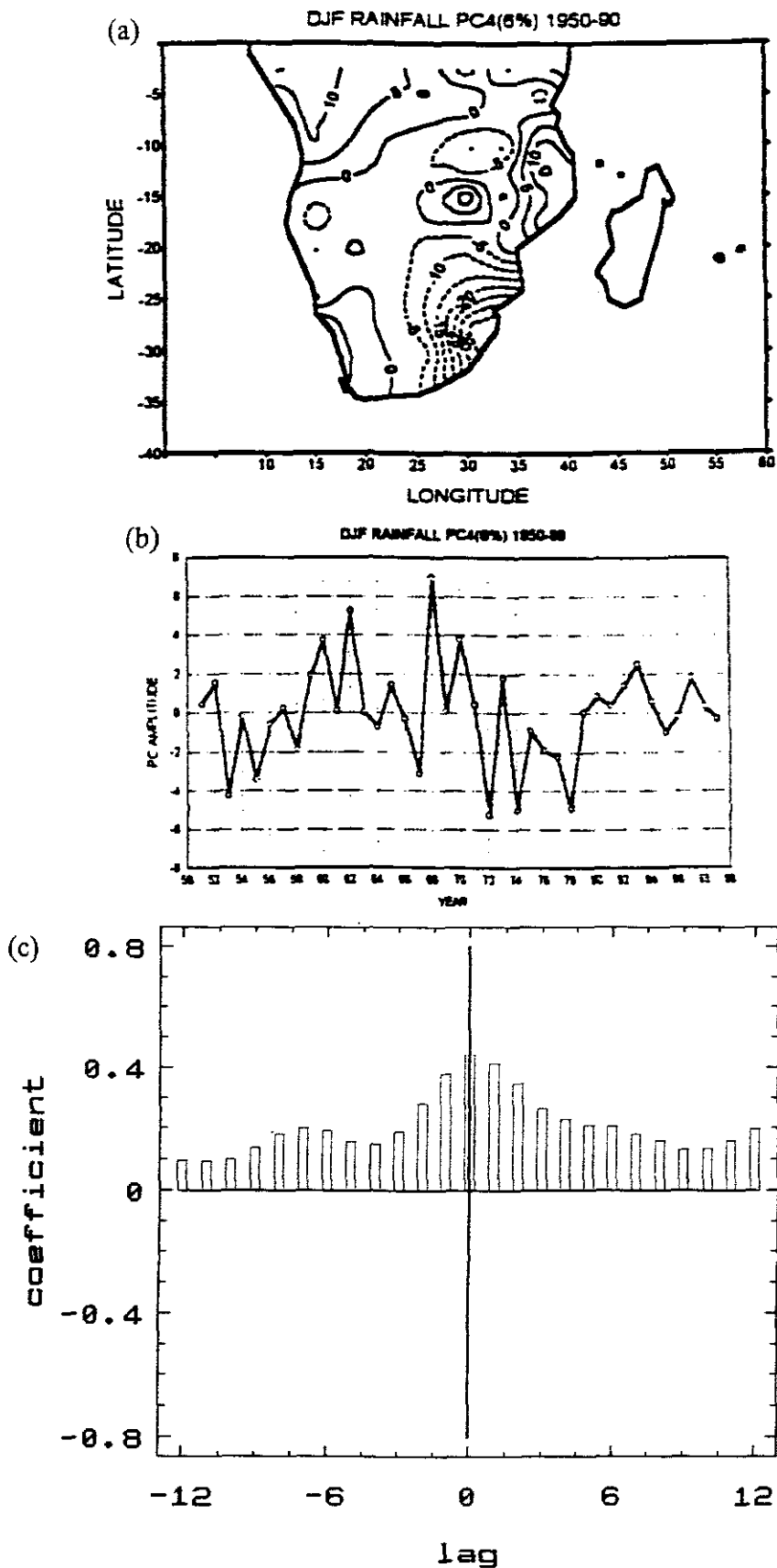


Fig. 3.4: (a) Distribution of rotated PC4 of normalised DJF rainfall and (b) associated time series of coefficients (Source: Mulenga, 1998). (c) Estimated cross-correlations of U200 (PC4, loaded at 32°E, 30°S) and KwaZulu/Natal temperature

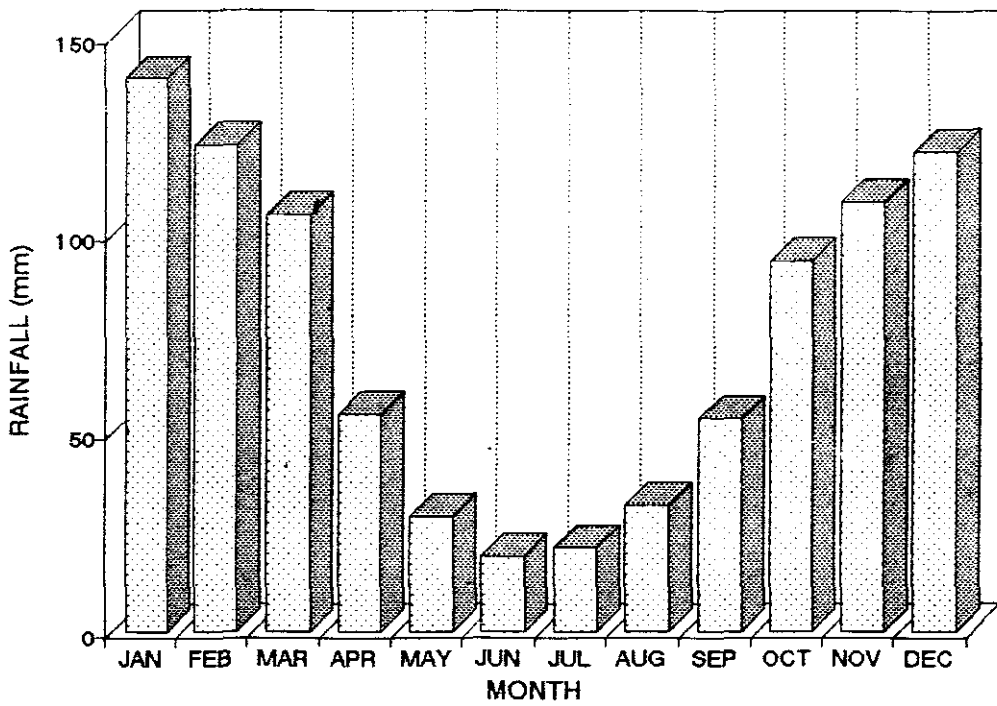


Fig. 3.5: KwaZulu/Natal rainfall seasonal cycle.

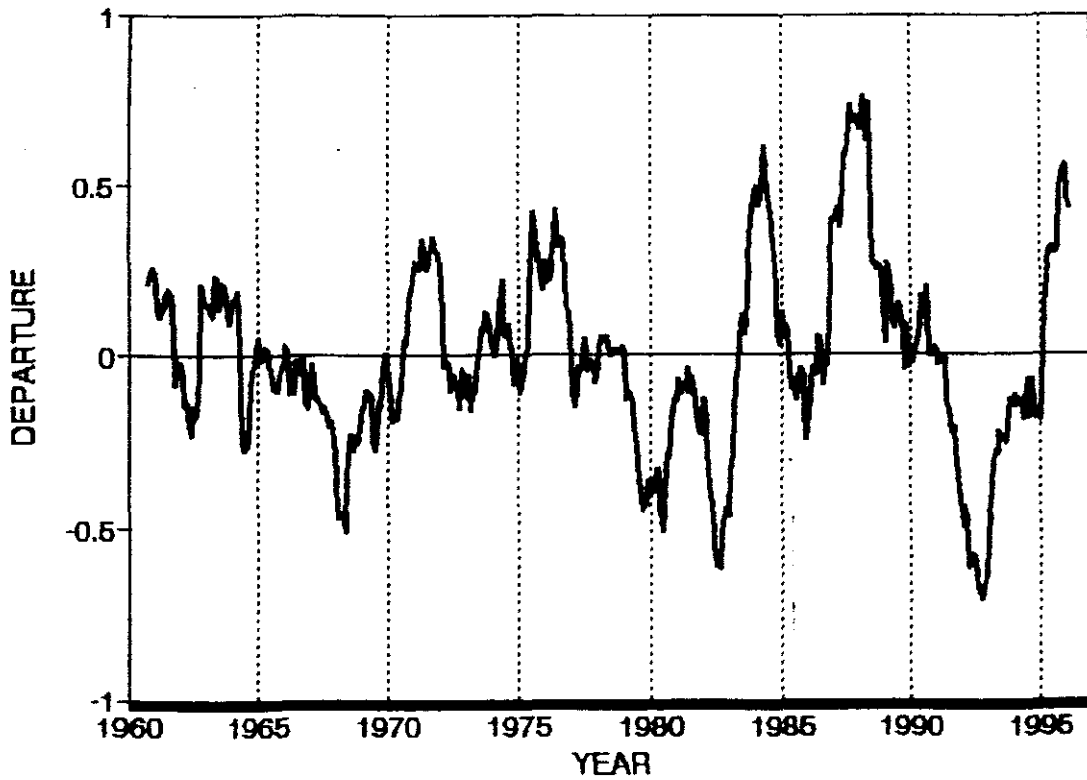


Fig. 3.6: KwaZulu/Natal rainfall departures (18 pt smoothed) from 1960 to 1996 (data stations 25, 26, 30, 31, 44, 45 (Fig. 3.1)).

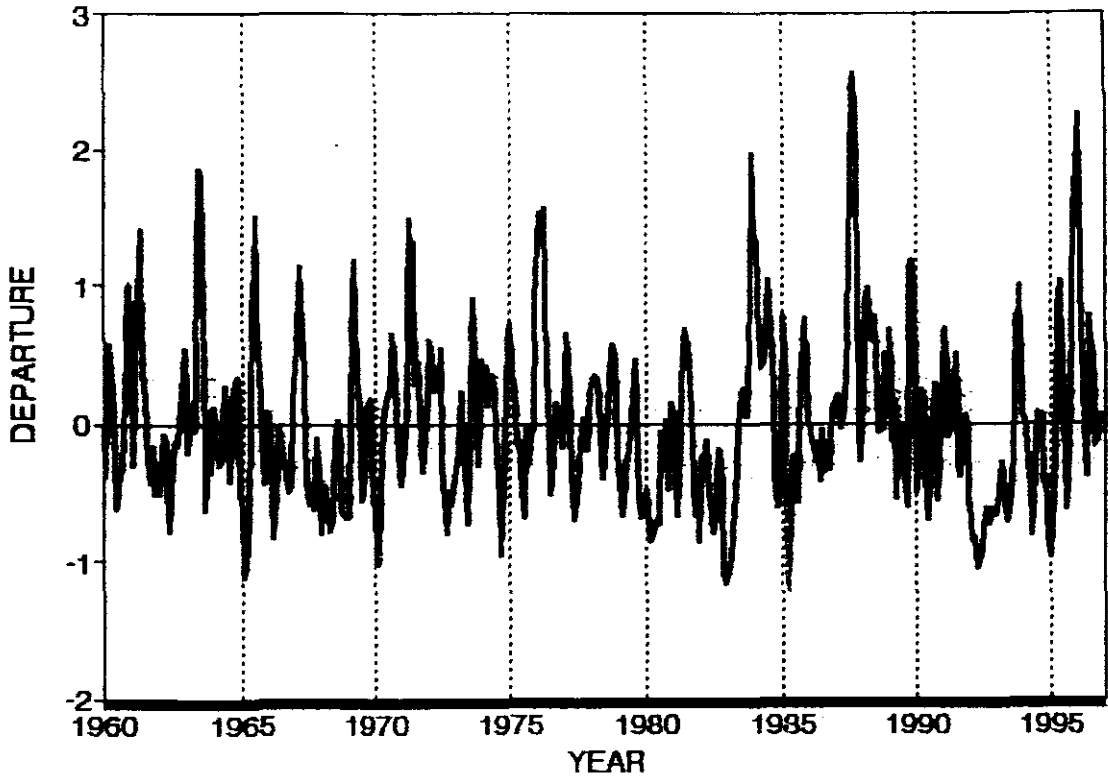


Fig. 3.7: KwaZulu/Natal rainfall departures (3 pt smoothed) from 1960 to 1996 (data stations 25, 26, 30, 31, 44, 45 (Fig. 3.1)).

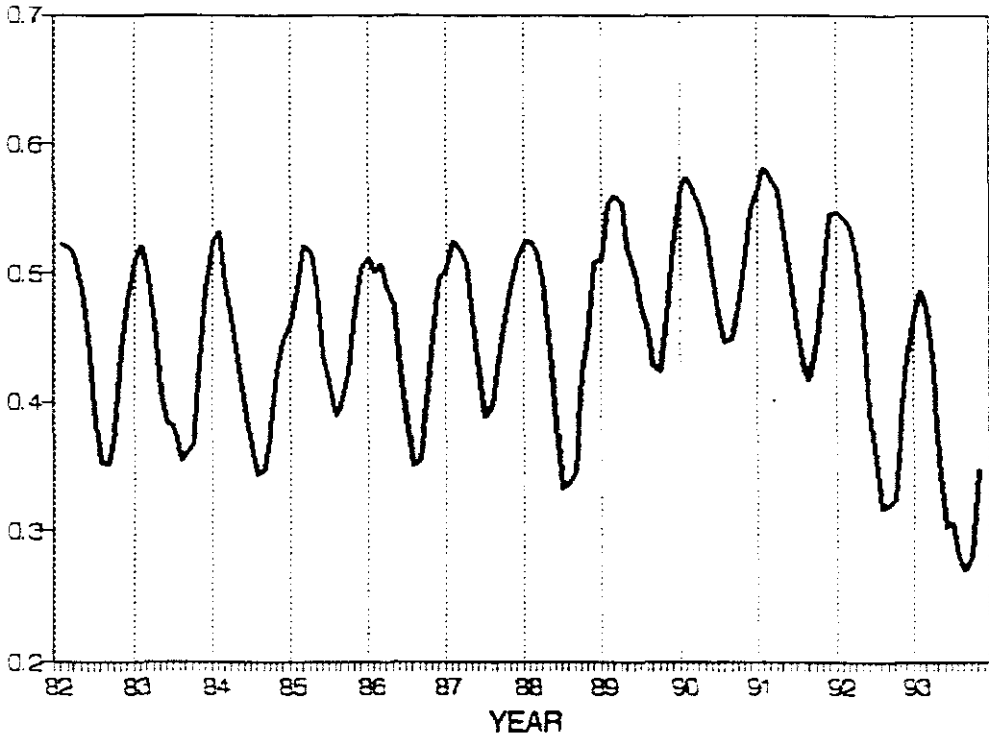


Fig. 3.8: Variation in KwaZulu/Natal's vegetation index (January to March 1982-1994) for grid points 30°S/30°E and 27.5°S/32.5°E.

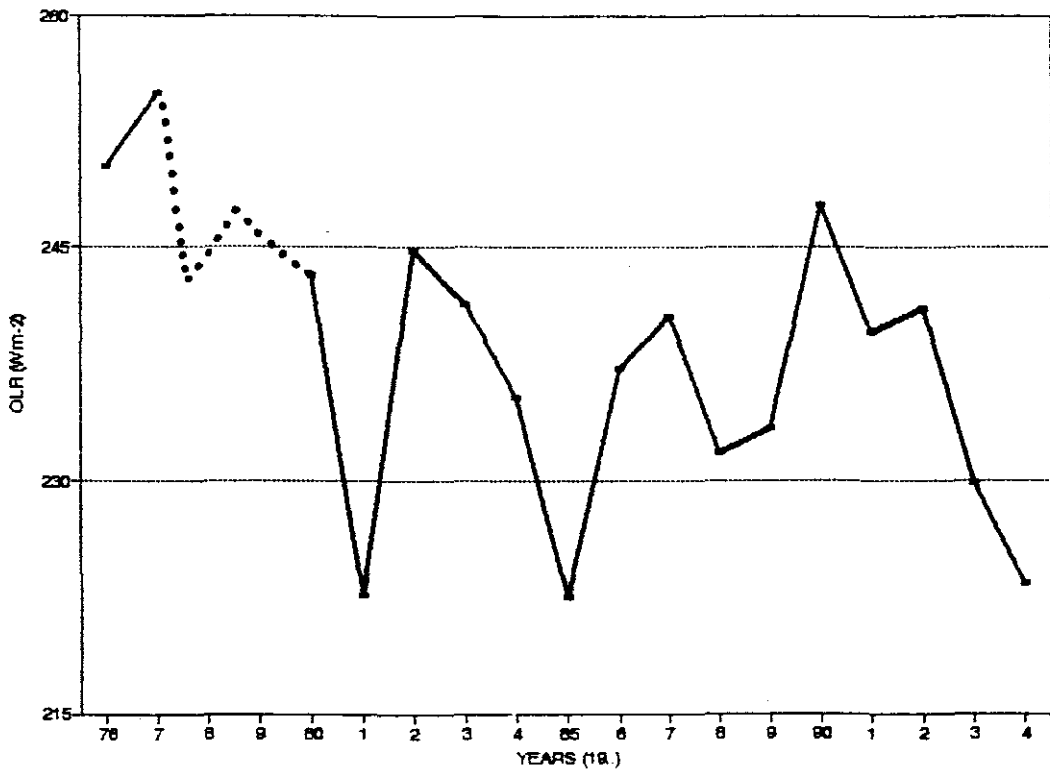


Fig. 3.9: Average OLR for DJF pentads (1975-94) at the point 30°E, 30°S. Dots indicate extrapolated values as data is missing.

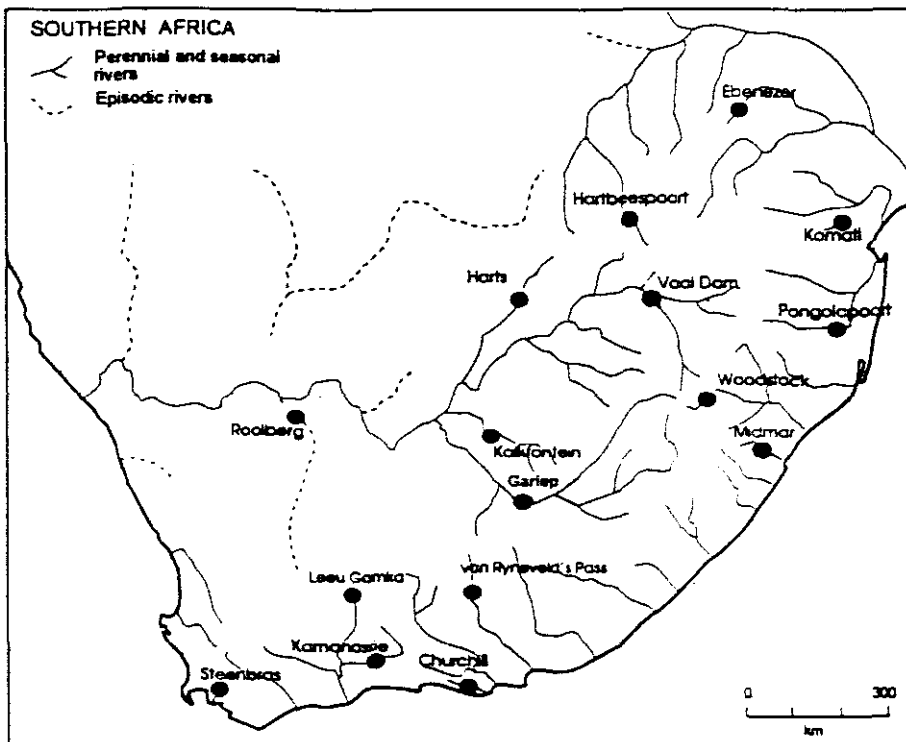


Fig. 3.10: Location of major dams of South Africa. Inflow levels of Midmar and Pongolapoort Dams have been used in the assessment of the 1992/93 drought over KwaZulu/Natal.

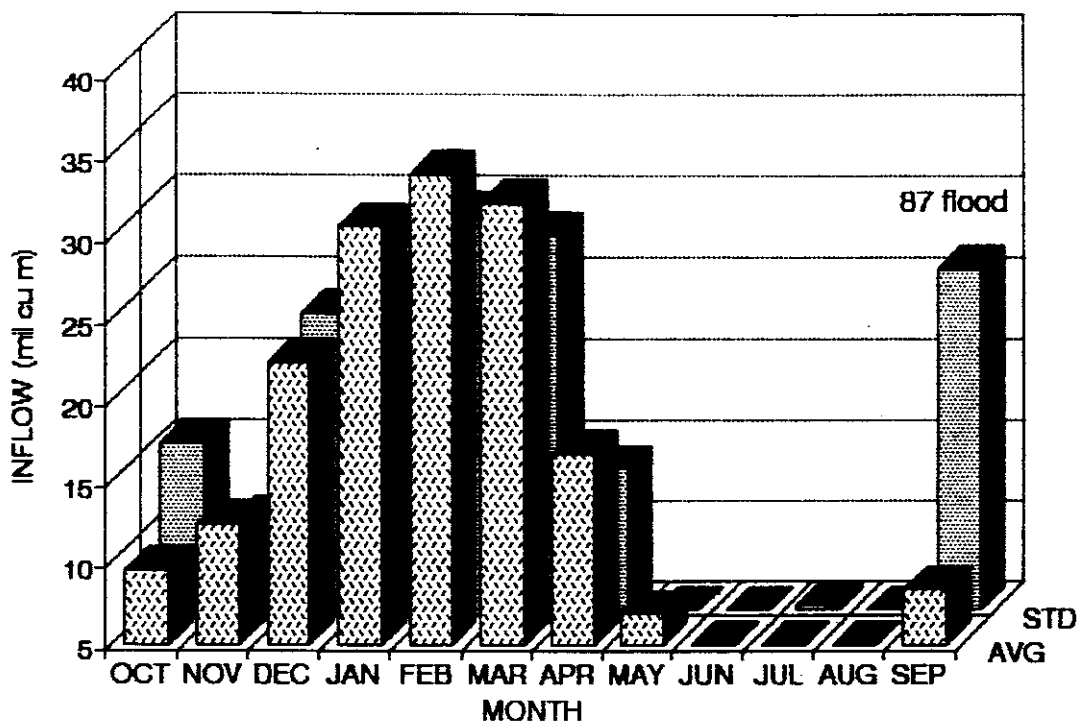


Fig. 3.11: Midmar Dam inflow seasonal cycle.

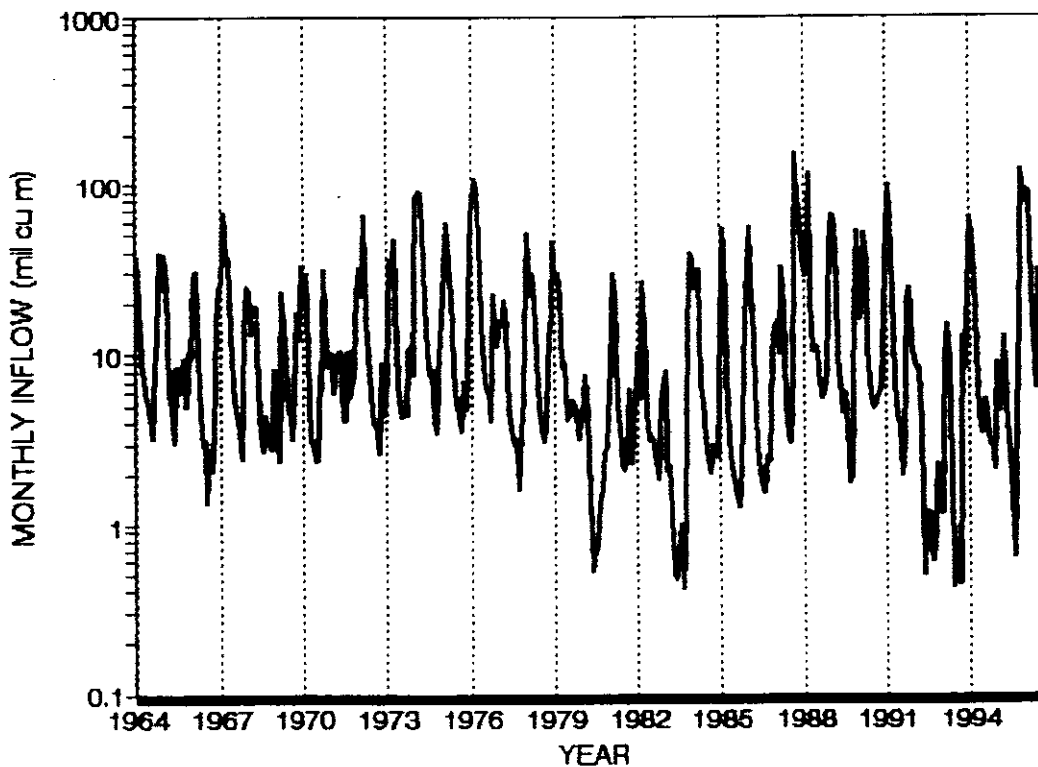


Fig. 3.12: Midmar Dam inflow (1964-1996).

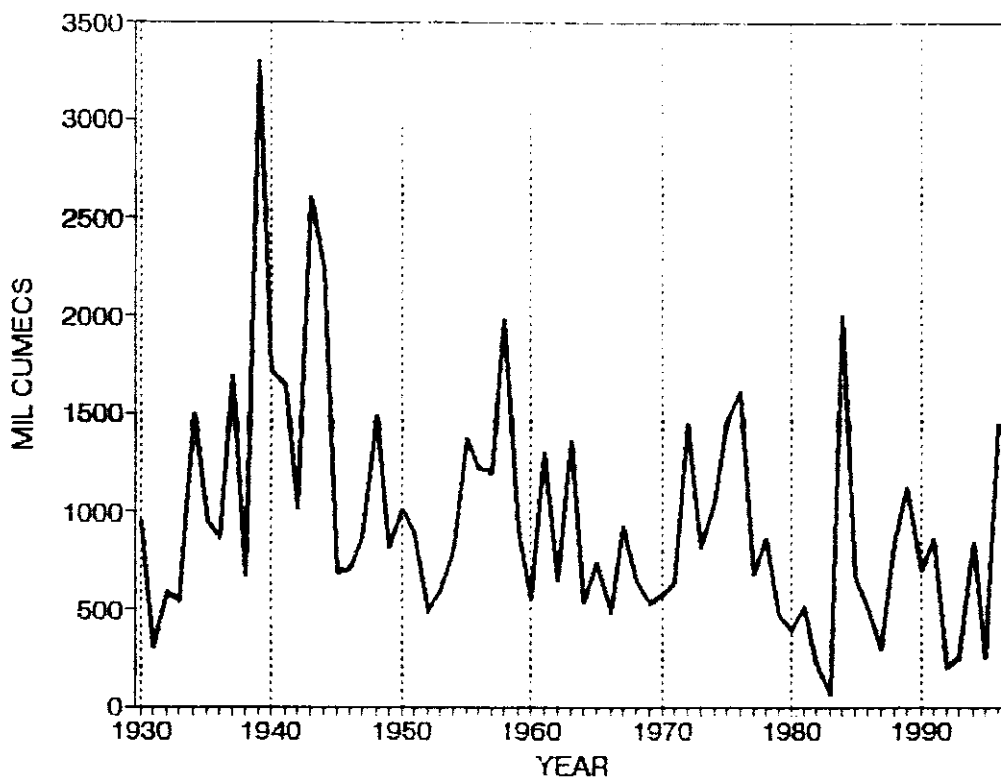


Fig. 3.13: Pongolapoort Dam inflow (1930-1996).

(X 1E6)

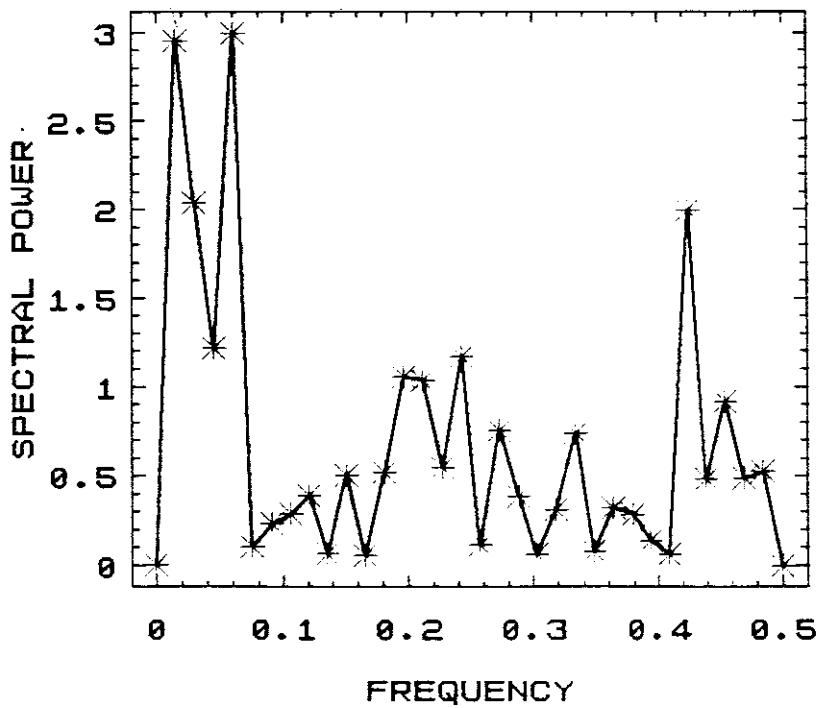


Fig. 3.14: Periodogram of Pongolapoort Dam inflow.

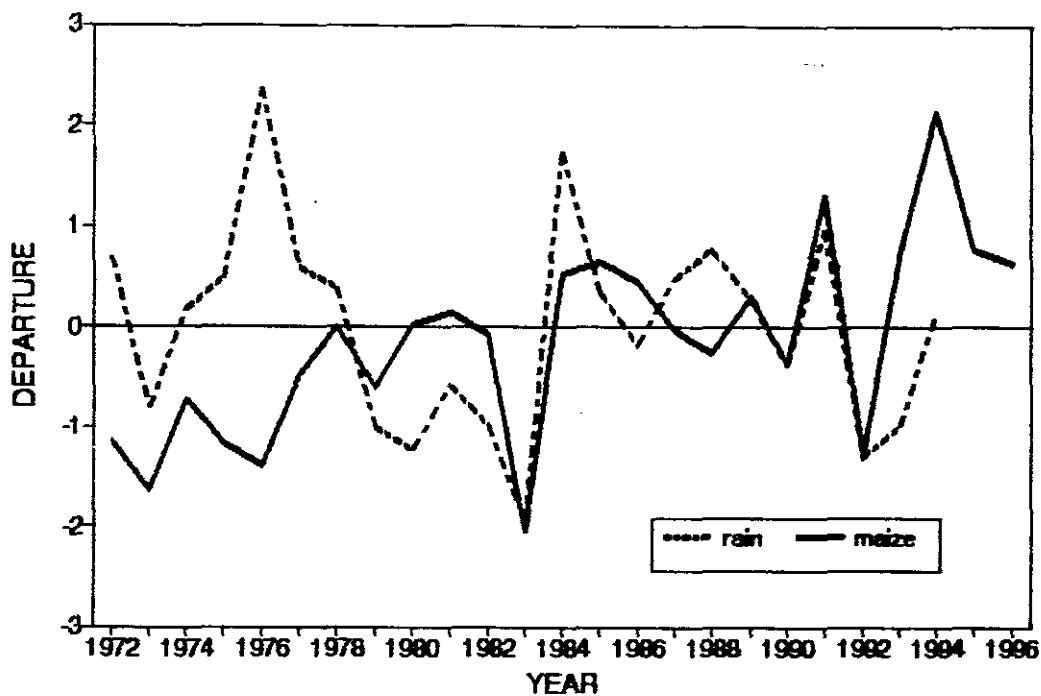
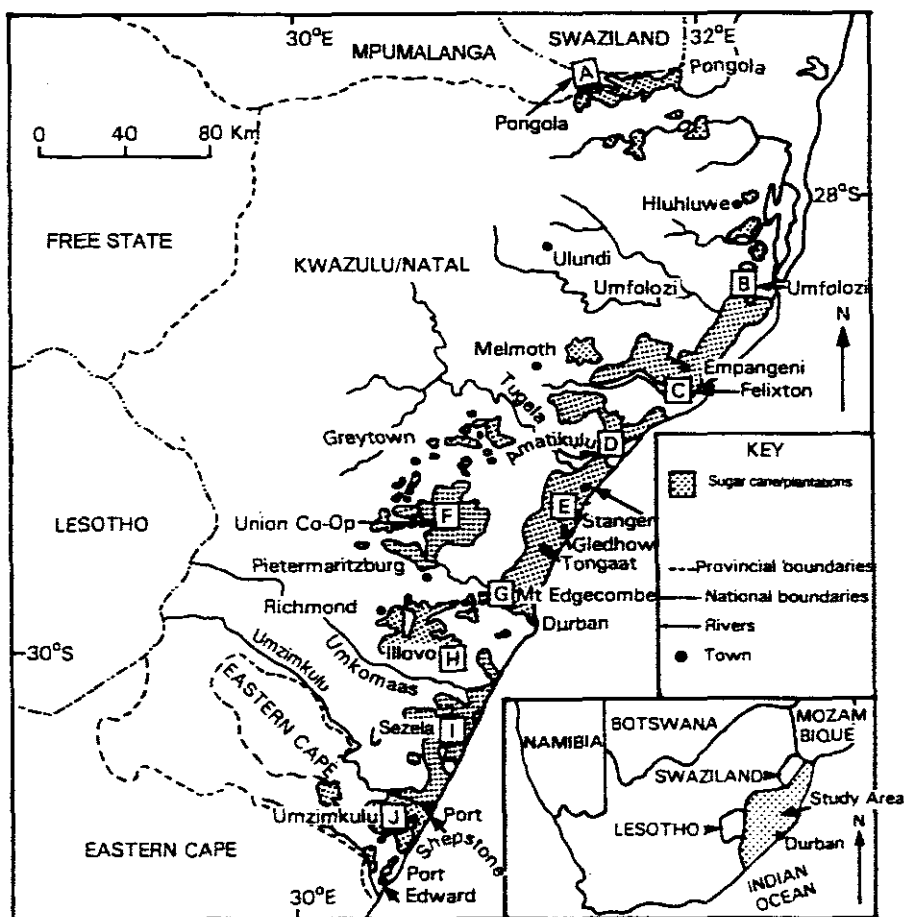


Fig. 3.15: Comparison of rainfall and maize in KwaZulu/Natal (1972-1996).



Fig

Fig. 3.16: Sugar cane growing areas in South Africa (Source: Dewey, 1993).

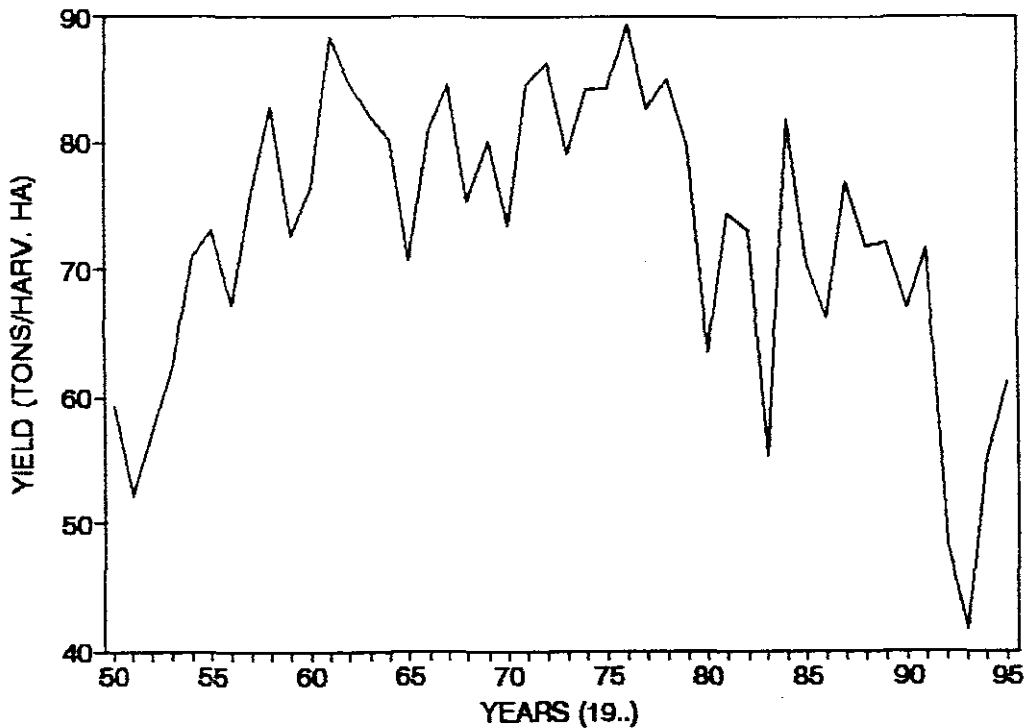


Fig. 3.17: Sugar cane yield per hectare in KwaZulu/Natal (1950-1995).

Table 3.1: Maize last planting dates (Source: Smith, 1993).

Bioclimatic group	2 (Coast hinterland)	3 (Mist-belt)	4 (Highland)	6 (Upland – moister type)
Last planting date	30 November	15 November	05 November	25 November

Table 3.2: Sugar cane-growing areas in KwaZulu/Natal (Source: Godefroy, 1992).

Region	Extent	Total area (hectares)
North Coast	Mt Edgecombe to the Tugela River	111 000
	Tugela River to Umfolozi River	99 000
South Coast	Illovo	5 000
	Sezela	40 000
	Umzimkulu	22 000
Midlands	Between Illovo, Mid-Illovo, Eston and Richmond	25 500
	Richmond, Alverston, Cato Ridge, Umlaas Road and Hillcrest	15 500
	Kraanskop – Pietermaritzburg - Greytown	50 000

## CHAPTER 4

### 4: METEOROLOGICAL STRUCTURE OF THE 1992/93 DROUGHT (ECMWF)

#### 4.1 INTRODUCTION

Circulation changes associated with the 1992/93 drought are analysed and impacts thereof investigated in this Chapter. Associations and comparisons are made with established literature to establish common meteorological trends or disparities.

#### 4.2 DATA AND METHODOLOGY

Selection of the KwaZulu/Natal drought scenario is undertaken on the basis of monthly rainfall, OLR and NDVI, Midmar and Pongolapoort Dams inflow and coastal temperature data discussed in the previous chapter. This suggested May 1992 and January 1993 as dry months suitable for analysis. Anomalies for these drought months with respect to their long term 1980-1994 means are analysed below.

December 1992 to February 1993 pentad OLR values for the 30°S, 30°E grid point were analysed and four peaks for in-season dry spell identified. The entire long term period (1975-1994) OLR time series was analysed for the same grid point. Anomalies for the four dry spells, i.e. 18 dry pentads minus the historical summer mean, were composited.

Data from the European Centre for Medium-Range Weather Forecasting (ECMWF) at resolution of 2.5° x 2.5° were used. The domain for both monthly and pentad analyses was 15°S-45°S and 15°E-45°E for the following parameters: 200 hPa wind and its divergence and vorticity, integrated vectors of water vapour flux between 1000 and 500 hPa and their divergence and

vorticity, geopotential heights at 850, 500 and 200 hPa levels, temperature at 500 hPa, vertical motion at 500 hPa, and integrated precipitable water between 1000 and 300 hPa. The analysis was also performed on NDVI data obtained from the Advanced Very High Resolution Radiometer (AVHRR) aboard the ECMWF series of satellites. The NDVI values were analysed for seasonal means and standard deviations. Definitions and calculation of some of the analysed variables are given on the appendix.

## 4.3 RESULTS

### 4.3.1 MAY 1992 AND JANUARY 1993 FIELDS AND ANOMALIES

May 1992 and January 1993 are months deemed necessary for detailed meteorological analysis from rainfall, OLR/NDVI, dams inflow and temperature data discussed in the previous Chapter. January 1993 exhibit dual circulation systems for most atmospheric variables analysed. Durban was near the centre of these inverse circulation regimes.

#### 4.3.1.1 GEOPOTENTIAL HEIGHTS

A weak trough at 850 hPa was observed over the 30°E longitude of South Africa (Fig. 4.1a) accounting for dry south-west flow anomalies in May 1992. At 500 hPa low geopotential height anomalies to the south-east of South Africa are observed (Fig. 4.1b). The low pressure anomaly over the Indian Ocean is associated with warming of the ocean during dry years which feed anticyclonic subsidence over the continent. The summer rainfall region becomes drier to the west of the trough (consequent upon enhanced divergence and subsidence of air on the trailing side of the trough). At 200 hPa level the gpm anomaly field is much similar to that of the 500 hPa level except that the geopotential minimum to the south is very strong obtaining an anomaly value of -80 at 30-35°E along 45°S (Fig. 4.1c).

In January 1993, at 850 hPa level the low pressure cell over the Indian Ocean and the high pressure to the west of South Africa induce weak southerly flow over KwaZulu/Natal (Fig. 4.1d). At 500 hPa a similar southerly meridional airflow pattern into KwaZulu/Natal associated with negative geopotential height anomalies to the east and south-east of South Africa and positive westward is observed (Fig. 4.1e). At the same time near Cape Town (34°S, 20°E) positive geopotential anomalies are found. At 200 hPa low geopotential heights are concentrated at 45°S, 45°E in the Marion Island region (Fig. 4.1f).

#### 4.3.1.2 TEMPERATURE, VERTICAL MOTION AND DIVERGENCE

In May 1992 the 850 hPa temperature anomaly shows KwaZulu/Natal experiencing above normal temperatures (Fig. 4.2a). To the north-east and south of South Africa below-normal temperatures were observed. A similar anomalous pattern was observed in January 1993 with warming covering a larger domain of southern Africa and the Indian Ocean east of the subcontinent (Fig. 4.2d). Locally above-normal temperatures in the lower atmosphere are typical of drought years. To the south, below normal temperatures are significant.

Vertical motion anomalies at 500 hPa in May 1992 shows weak positive (sinking) velocity anomalies over KwaZulu/Natal (Fig. 4.2b). In contrast, the January 1993 field shows anomalous subsidence south and north of Durban and weak upward velocities to the west (Fig. 4.2e). These patterns are patchy and incoherent. This suggests that individual months may not give a good reflection of the overall atmospheric circulation anomalies during dry years and that composites for dry spells or seasons may give a more consistent output.

A convergence anomaly at 200 hPa is observed throughout South Africa in May 1992 (Fig. 4.2c). Over the oceans nearby positive divergence is found. The January 1993 divergence anomaly field at 200 hPa is positive over KwaZulu/Natal (Fig. 4.2f).

#### 4.3.1.3 VECTORS OF HORIZONTAL WIND AND WATER VAPOUR FLUX

KwaZulu/Natal is characterised by a cyclonic circulation anomaly at 200 hPa in May 1992 (Fig. 4.3a) centred to the north, produced by recurving anomaly of westerly winds. Over the winter rainfall region, an anticyclonic circulation is noted. Westerlies prevail to the south of South Africa producing cyclonic anomalies over the Indian Ocean.

In January 1993, a cyclonic anomaly at 200 hPa is located further north over Botswana (Fig. 4.3b). The anticyclonic anomaly over the west of South Africa drifted east thus dislocating major cloud bands into the Indian Ocean as suggested by Harrison (1983) and Preston-Whyte and Tyson (1988). Over KwaZulu/Natal, weak convergence occurred as a result of anticyclonic streamline anomaly to the south and cyclonic anomaly to the north of the province. The convective zone over Madagascar is characterised by anomalous anticyclonic circulation at 200hPa level.

A divergence anomaly of water vapour flux occurred over KwaZulu/Natal in May 1992 (Fig. 4.4). In January 1993, divergence anomalies accompanied by an offshore flux of water vapour occurred over KwaZulu/Natal (Fig. 4.5). Other centres of strong WVF divergence anomalies over the subcontinent in both months were over Zambia and Namibia. WVF convergence anomalies occurred over the western Cape, Botswana and over the Indian Ocean near Madagascar. The flux of water vapour is down the topography implying that local effects played an important role in inflicting KwaZulu/Natal with

drought during the dry 1992/93 rainfall season (Fig. 4.4 and 4.5). Low-level horizontal moisture flux during the 1992/93 drought indicated maximum anomalous equatorward water vapour flux divergence around 40°S (Fig. 4.3b and 4.4). The positive anomalies in water vapour flux over south-west Africa (Fig. 4.14b) are due to anomalous moisture convergence from the equatorial regions.

#### 4.3.1.4 VORTICITY, VORTICITY OF WVF, DIVERGENCE OF WVF AND PRECIPITABLE WATER

The anomaly of vorticity at 200 hPa in May 1992 over KwaZulu/Natal, particularly north of Durban, favours convergence at this level (Fig. 4.6a) and therefore downward-directed vertical motion dictated by continuity balance (Fig. 4.2b). In January 1993 the anomalous cyclonic vorticity field at 200 hPa prevailed over the section of southern Africa south of 20°S (Fig. 4.6d).

Vorticity of water vapour flux between 850 and 300 hPa in May 1992 shows anticyclonic anomalies almost throughout KwaZulu/Natal (Fig. 4.6b). Negative (cyclonic) vorticities occurred to the north and south of South Africa. In January 1993 vorticity anomaly of water vapour flux exhibits, like most variables analysed for this month, a dipole pattern being anticyclonic south of Durban and cyclonic northward (Fig. 4.6e).

For both May 1992 and January 1993 precipitable water is below normal throughout southern Africa (Figs. 4.6c and f). Centres of high negative precipitable water anomalies are in KwaZulu/Natal and Botswana. KwaZulu/Natal is characterised by positive divergence of water vapour flux fields and anomalies in May 1992 and January 1993 (Fig. 4.7a-d). The surface divergence anomaly in KwaZulu/Natal in May 1992 is stronger than in January 1993. Convectational activity is observed east of Madagascar due

to strong convergence gradients in this zone, particularly in January 1993. A prominent zone of anomalous divergence of WVF is observed over the interior of South Africa in January. Such WVF divergence coupled with below normal precipitable water values ensured reduced convective rainfall over South Africa. North of 20°S the divergence fields are, on the average, negative.

### 4.3.2 DRY SPELL COMPOSITES AND ANOMALIES

#### 4.3.2.1 OUTGOING LONGWAVE RADIATION

An analysis of OLR identified four mean DJF 1992/93 pentads suitable for compositing, viz., 70 of 1992, 01, 03, and 07 of 1993 (Fig. 4.8). Figures 4.9a-d show OLR departure fields for each of these individual pentads. Figures 4.9a and b show similar positive departures over the continent. Figures 4.9b and d both indicate positive departures over the southern parts of the subcontinent and some convection (negative OLR values) further north. The mean composite OLR field for the four pentads (Fig. 4.9f) shows a strong subsidence (positive values) over southern Africa with maximum values centred over Botswana and Namibia. Convective activity occurred over the north-eastern parts of the subcontinent where values below 240  $Wm^{-2}$  were observed. This is consistent with the convective dipole with centres of opposing action located over southern Africa and over east Africa and the SW Indian Ocean.

#### 4.3.2.2 GEOPOTENTIAL HEIGHTS

The composite geopotential height field for the composite 1992/93 dry spell at 850 hPa (Fig. 4.10a) indicates a strong gradient to the south of South Africa and meridional influences elsewhere. KwaZulu/Natal is located in a zone of diffluence produced by cyclonic motion to the east of South Africa

and an anticyclone centred over the western parts (Fig. 4.10d). The geopotential height anomaly field at 850 hPa for the dry spell shows a weak south-east to north-west oriented trough. Southerly meridional flow is suggested in the geopotential height anomaly field over the southern and south-eastern parts of South Africa. A negative pressure cell occurs over the southern Indian Ocean centred over Marion Island.

At 500 hPa level, westerlies are supported (Fig. 4.10b) as is often the case during global El Nino and during winter season (Parker and Jury, 1997). The geopotential height anomaly at this level (500 hPa) shows negative departures oriented on the same axis as at 850 hPa (Fig. 4.10e). Positive departures are evident at both the 850 and 500 hPa levels over the South Atlantic and the central Indian Oceans. The geopotential height field at 200 hPa confirms the prevalence of westerly winds. The anomaly field shows negative departures for the entire subcontinent (Fig. 4.10f) which would oppose convective outflow in a barotropic scenario.

Strong negative pressure anomalies occurring near Madagascar create a dipole consistent with Rocha and Simmonds (1997a). This anomaly dipole is related to the fluctuations of the preferred position of the ridge associated with standing waves 1 and 3 which are often located over the South Atlantic and south-western Indian Oceans, respectively. The anomalies highlight a weakening of the South Atlantic and Indian Ocean highs and a reduction of the surface pressure gradient directed from the oceans to the subcontinent.

Mason *et al.* (1994) showed that such changes in the South Atlantic high are associated with local SST variations. This suggests that atmosphere-ocean interactions produce changes in the South Atlantic anticyclone or in baroclinic westerly wave configurations that affect rainfall over the subcontinent.

#### 4.3.2.3 TEMPERATURE, VERTICAL MOTION AND DIVERGENCE

Negative temperature departures are observed at 500 hPa throughout southern Africa and the adjacent oceans (Fig. 4.11a) during the composite dry spell of 1992/93. The anomaly field shows weak negative departures averaging about 0.4°C over the southern parts of KwaZulu/Natal and the Eastern Cape Province. Cooler mid-tropospheric temperatures are related to a reduction of latent heating (convection) and the equatorward intrusion of mid-latitude air (westerly shear).

Vertical motion fields indicate that much of KwaZulu/Natal experiences neutral vertical motion whilst the Western Cape is characterised by weak subsidence at 500 hPa (Fig. 4.11b). The weak positive vertical motion anomaly observed in Figure 4.12e over KwaZulu/Natal could not yield rains as the deformation of the geopotential field was not supportive of such conditions.

Convergence is observed over KwaZulu/Natal at 200 hPa (Fig. 4.11c) and the anomaly field (Fig. 4.11f) confirms this.

#### 4.3.2.4 COMPOSITE VECTORS OF THE 200 hPa HORIZONTAL WIND AND WATER VAPOUR FLUX

The horizontal wind field vectors at 200 hPa show westerlies throughout the domain analysed (Fig. 4.12a). Convergence occurs north of 20°S and divergence further south. The mean wind vector shows an anomalous anticyclonic circulation over South Africa.

The integrated vectors of water vapour flux between 850 and 300 hPa show a northward flux of water vapour over the eastern coastal areas of South Africa and some advection towards land by the sea breeze over Durban (Fig. 4.12b).

A southward advection of water vapour from the tropical latitudes is more favourable for wet conditions than its northward-flowing counterpart. Water vapour flux is predominantly westerly and strongly zonal south of 35°S.

#### 4.3.2.5 VORTICITY, VORTICITY OF WVF, PRECIPITABLE WATER AND DIVERGENCE OF WVF

Weak cyclonic vorticity at 200 hPa is observed south of Durban and positive values (anticyclonic) are found elsewhere (Figs. 4.13a). A south-east to north-west oriented negative anomaly field is observed (Fig. 4.13d) which concurs with the south-east to north-west oriented negative divergence field at 200 hPa (Fig. 4.13c) and early summer NDVI pattern (Fig. 4.15b). Steep positive vorticity gradients are observed north of Durban extending into Zimbabwe and Mozambique.

Anticyclonic water vapour flux is observed over most of southern Africa (Fig. 4.13b). Over the north-western parts of the subcontinent and the south-west Indian Ocean between 25° and 15°S cyclonic vorticities occur coincident with convective activity. Positive anomalies south of Durban and negative fields northward are both sources of vapour inflow into that region (Fig. 4.13e). Even though the vorticity field is favourable for wet conditions to some degree, the air is deficient of water vapour throughout the continent (Fig. 4.13c and f). It is only in the convective belt north of 15°S that precipitable waters of 50 mm are observed. Therefore, even areas where convergence fields were favourable for realisation of instability, the atmosphere is dry.

This study concurs with Rocha and Simmonds (1997a) that precipitable water is lower than normal over south-eastern Africa (region 2 in their study) during dry summers. Rocha and Simmonds' (1997a) correlation analysis indicates that over the Indian Ocean, east of Madagascar, the relationship is

negative. Areas of positive gpm anomalies is observed to coincide with areas of reduced precipitable water.

The composite for divergence of WVF shows a large cyclonic anomaly near Madagascar (Fig. 4.14), resulting in a reduction in moisture advection into the subcontinent across the eastern coast. Along the Mozambique Channel, wind anomalies have a southerly component (Fig. 4.12a) which concurs with wind anomalies typical of ENSO years reported by Lindesay (1988).

#### 4.3.2.6 THE 1992/93 SUMMER OLR AND NDVI

Figures 4.15a and b are satellite-derived NDVI anomalies for early summer of 1992/3 and late summer of 1993. In the early summer period the vegetation is brown over most of South Africa, particularly over KwaZulu/Natal, the Eastern and Northern Cape, and the Northern Province. A SE to NW oriented wave-train pattern is discernible from Fig. 4.15a with a wet core over the Zambezi wedged in between the dry Lesotho and Malawi cores.

The late summer anomaly saw a reduction in the domain of dry conditions. The KwaZulu/Natal coastal region remained the most "brown" area over South Africa. To the north of South Africa the domain of greenness expanded equatorward with core areas over Botswana, and Mozambique. This implies that countries neighbouring South Africa which were hit by the 1992/93 drought reverted to normal conditions earlier.

#### 4.4 CONCLUSION

This chapter has presented the anomaly patterns, with respect to the historical mean for the period 1980-1994, for summer of 1992/93 and composite phases, as well as the circulation patterns of two extreme months

in the drought period. The results of the study are in agreement with results previously undertaken on drought and related circulation patterns by other authors.

The 1992/93 DJF anomalies indicate that warming occurred over the Indian Ocean where a low prevailed. Low-level westerly anomalies and upper-level easterly anomalies developed off east Africa, hence dry conditions occurred. Rainfall over SE Africa and KwaZulu/Natal in the 1992/93 summer period was below normal as shown by water vapour fluxes, precipitable water and vorticity. Surface temperatures were abnormally high during the dry spell.

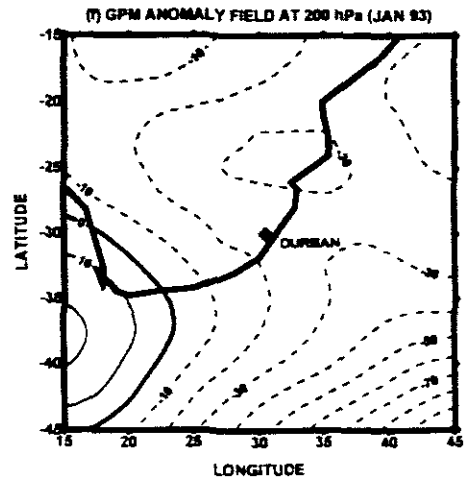
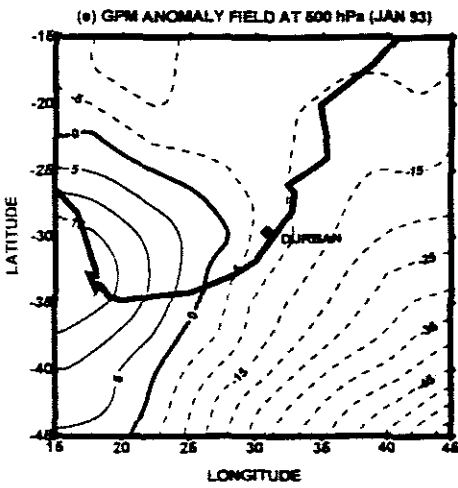
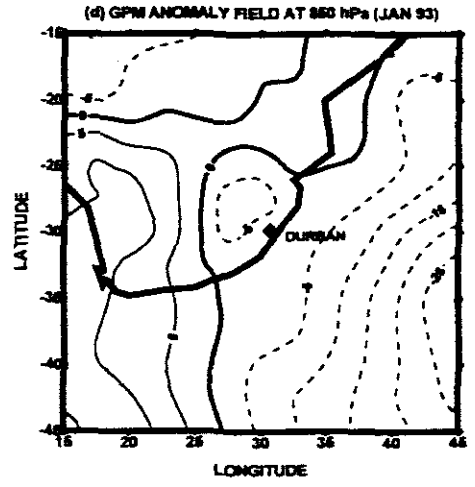
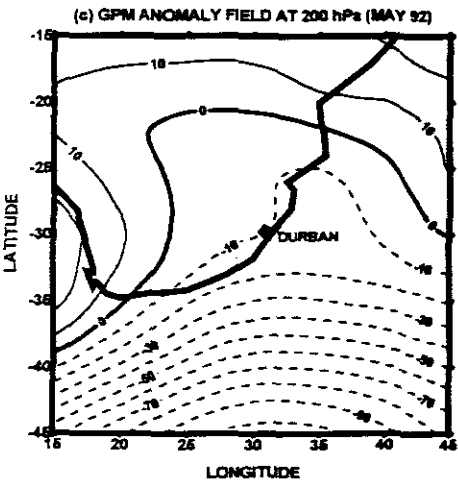
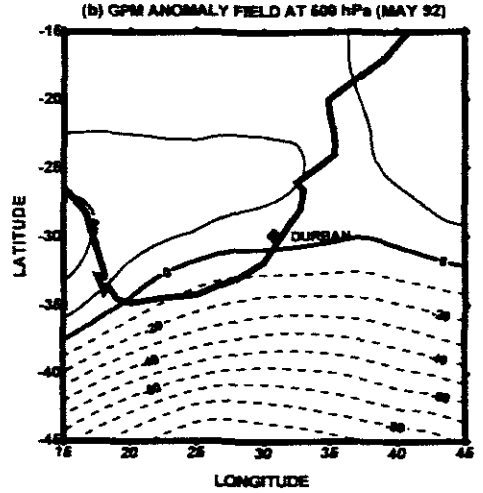
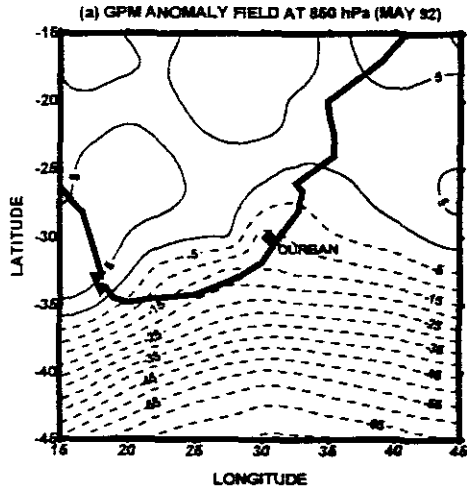


Fig. 4.1: Geopotential heights and anomalies (gpm) (with respect to the ECMWF 1980-94 long-term mean) at 850, 500 and 200 for May 1992 and January 1993.

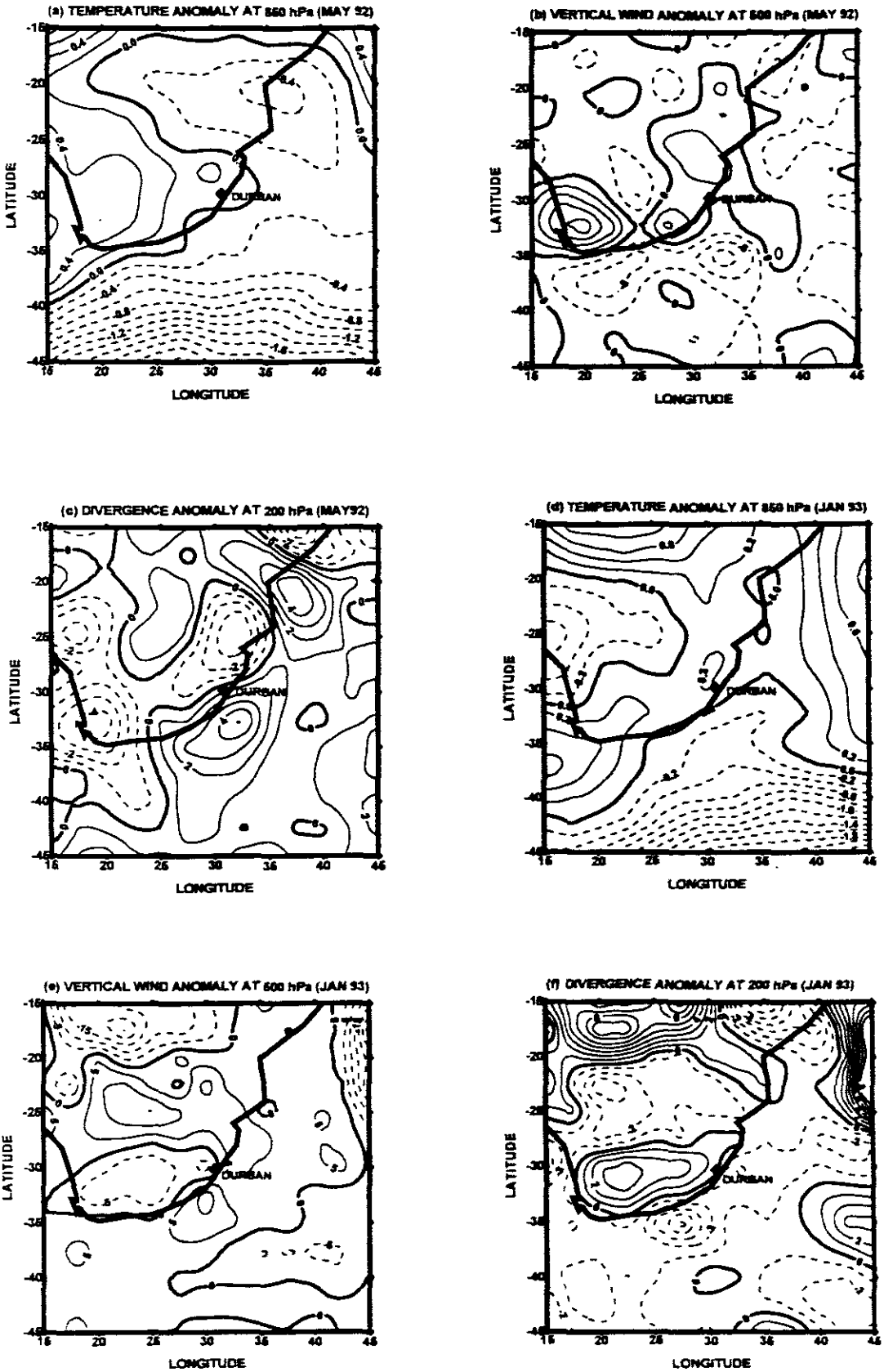


Fig. 4.2: Anomalies of temperature ( $^{\circ}\text{C}$ ) (with respect to the ECMWF 1980-94 long-term mean) at 850 hPa, vertical motion ( $\text{Pa s}^{-1}$ ) at 500 hPa and divergence ( $10^{-6} \text{ s}^{-1}$ ) for May 1992 and January 1993.

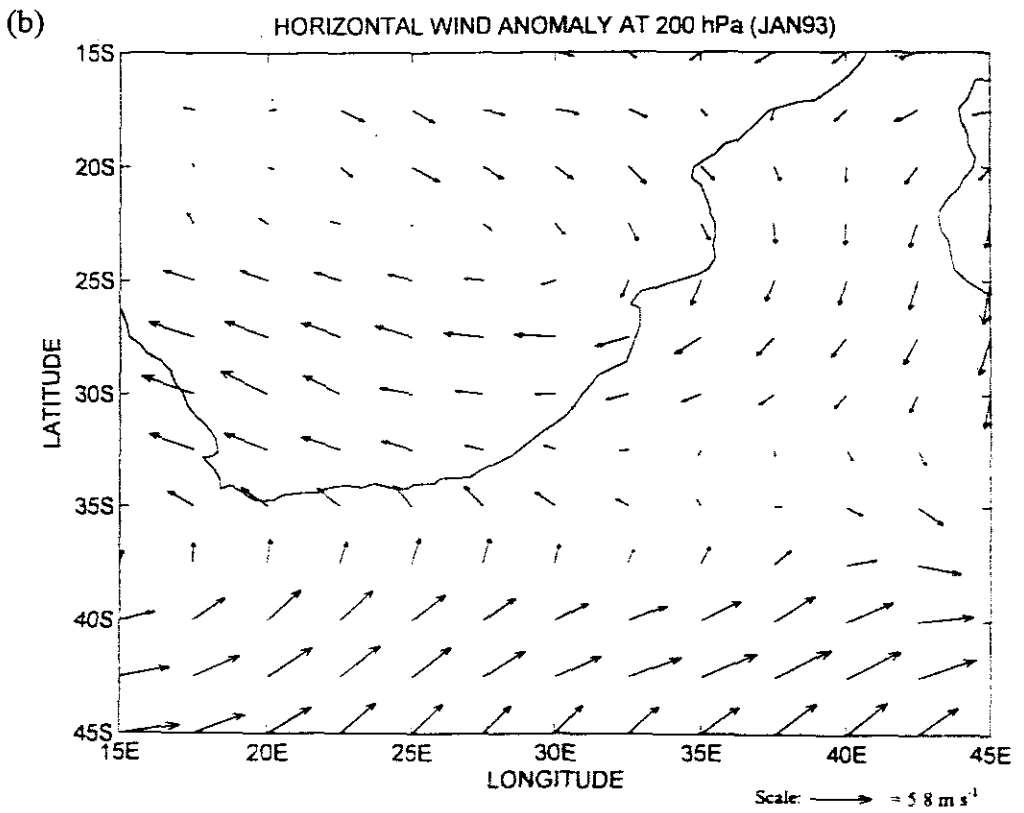
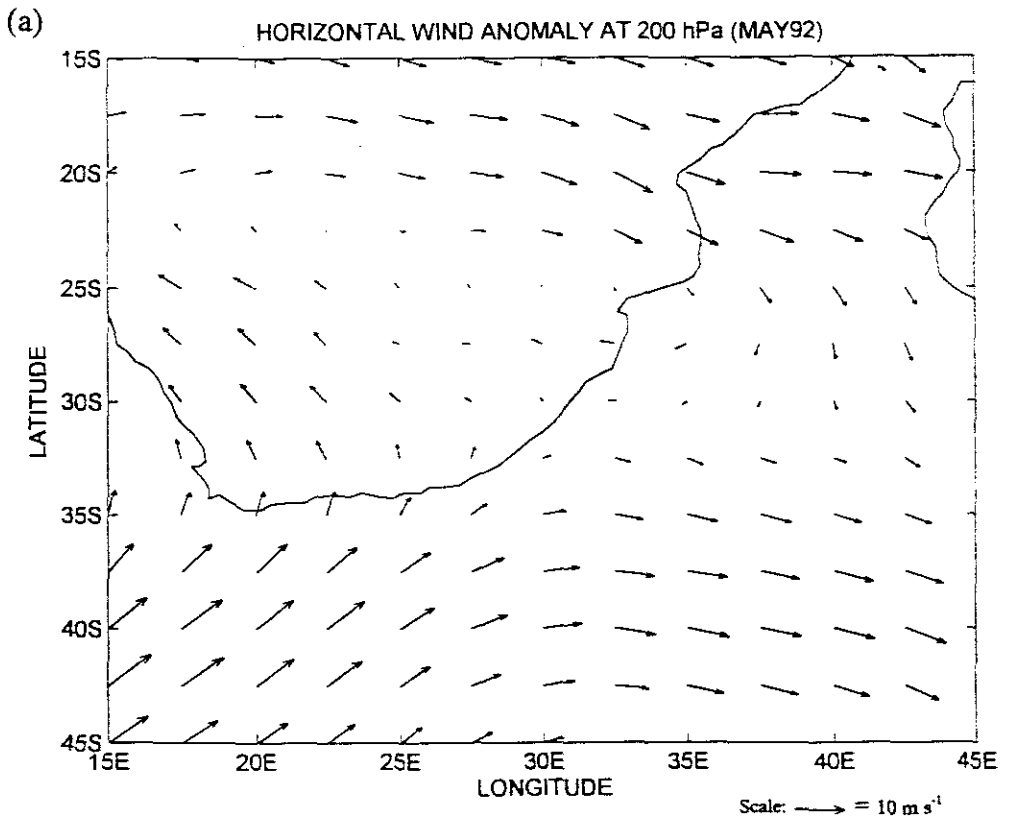


Fig. 4.3: Horizontal wind anomaly vectors (from the ECMWF 1980-94 mean) at 200 hPa for (a) May 1992, and (b) January 1993.

**WINTER**

**WATER VAPOUR FLUX ANOMALY (MAY 92)**

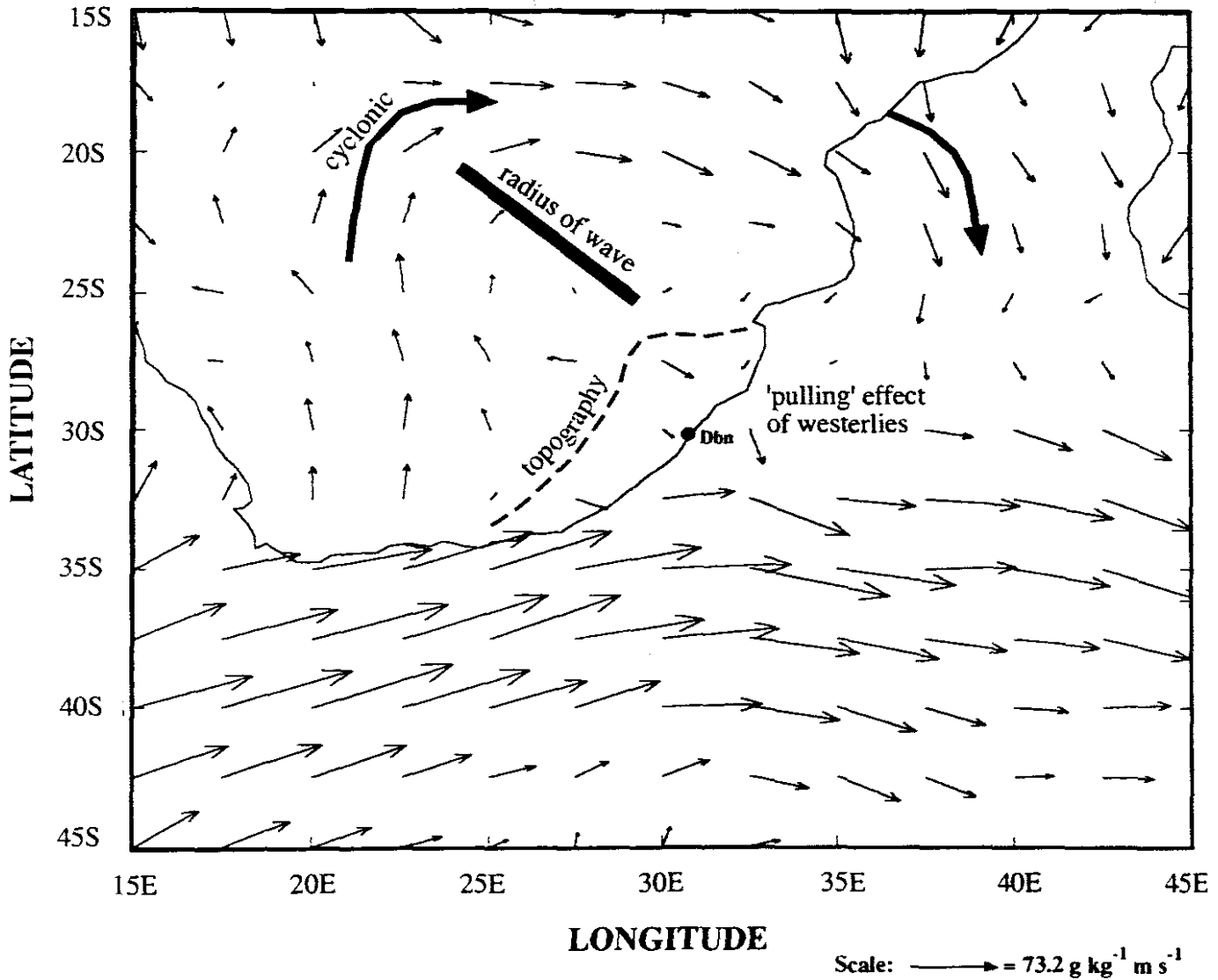


Fig. 4.4: Anomaly (from the 1980-94 mean) of water vapour flux vectors integrated between 1000 and 300 hPa for May 1992.

# SUMMER

## WATER VAPOUR FLUX ANOMALY (JAN 93)

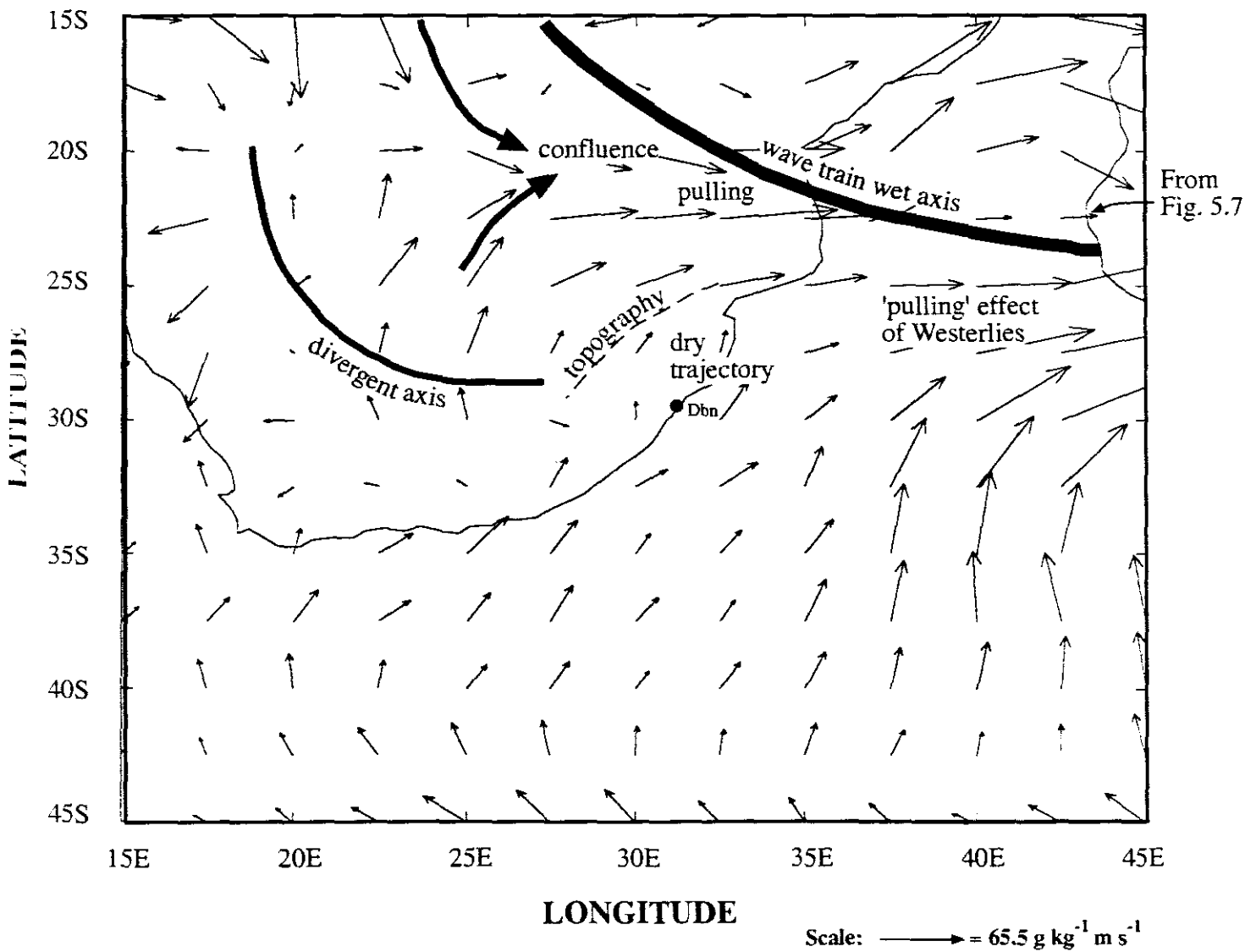


Fig. 4.5: Anomaly (from the 1980-94 mean) of water vapour flux vectors integrated between 1000 and 300 hPa for January 1993.

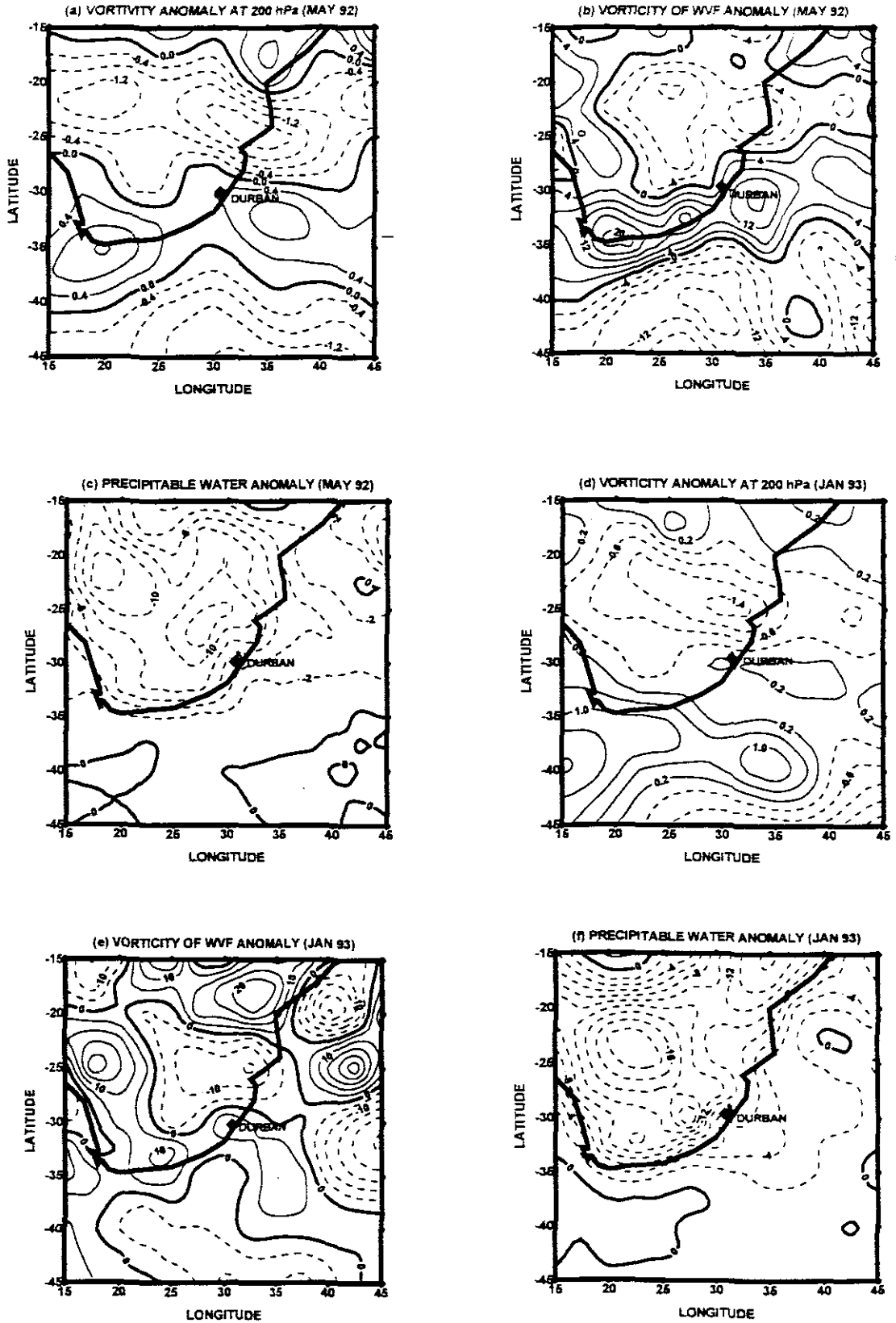
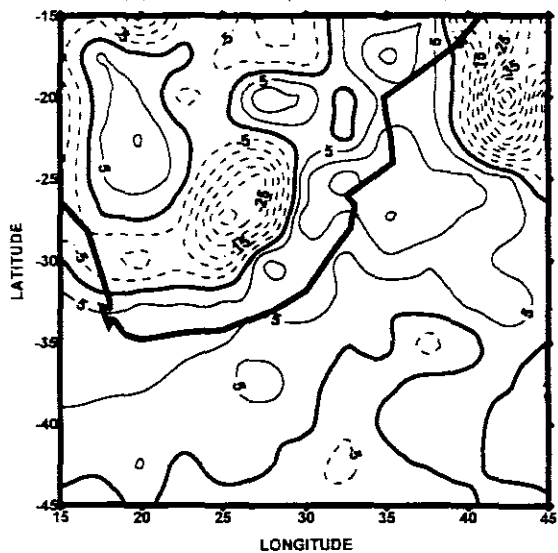
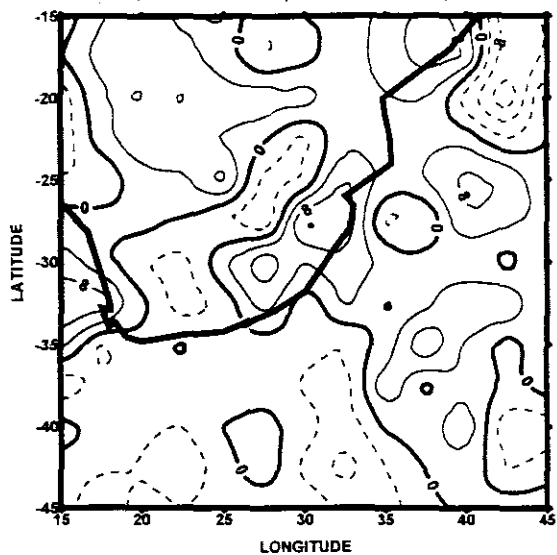


Fig. 4.6: Anomalies (from the ECMWF 1980-94 mean) of vorticity ( $10^{-6} \text{ s}^{-1}$ ) at 200 hPa, integrated vorticity of water vapour flux ( $10^{-6} \text{ g kg}^{-1} \text{ s}^{-1}$ ) between 1000-500 hPa and integrated precipitable water (mm) between 1000-300 hPa for May 1992 and January 1993.

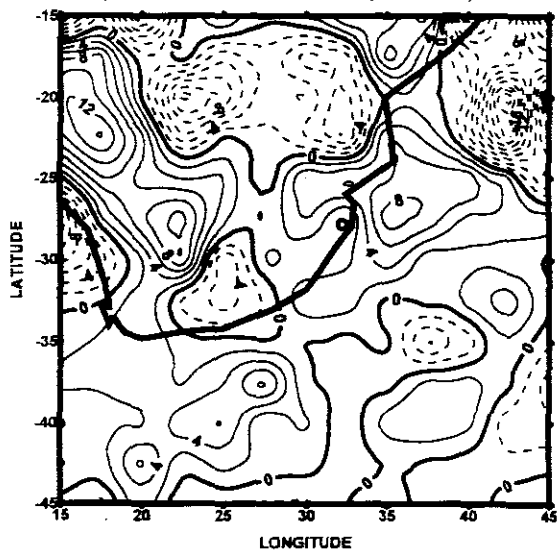
(a) DIV. OF WVF (JAN MEAN 1993)



(b) DIV. OF WVF (MAY MEAN 1992)



(c) ANOMALY DIV. OF WVF (JAN. 1993)



(d) ANOMALY DIV. OF WVF (MAY 1992)

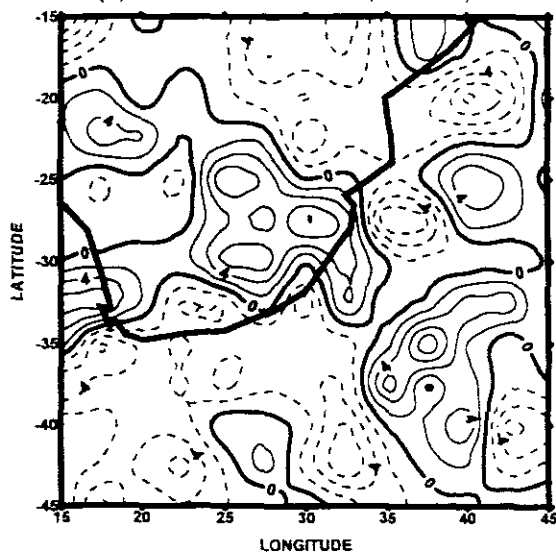


Fig. 4.7: Means and anomalies (from the ECMWF 1980-94 mean) of divergence of water vapour flux integrated between 1000 and 300 hPa for May 1992 and January 1993.

OLR TIME SERIES (DEC 92-FEB 93) 30S,30E  
(30E, 30S)

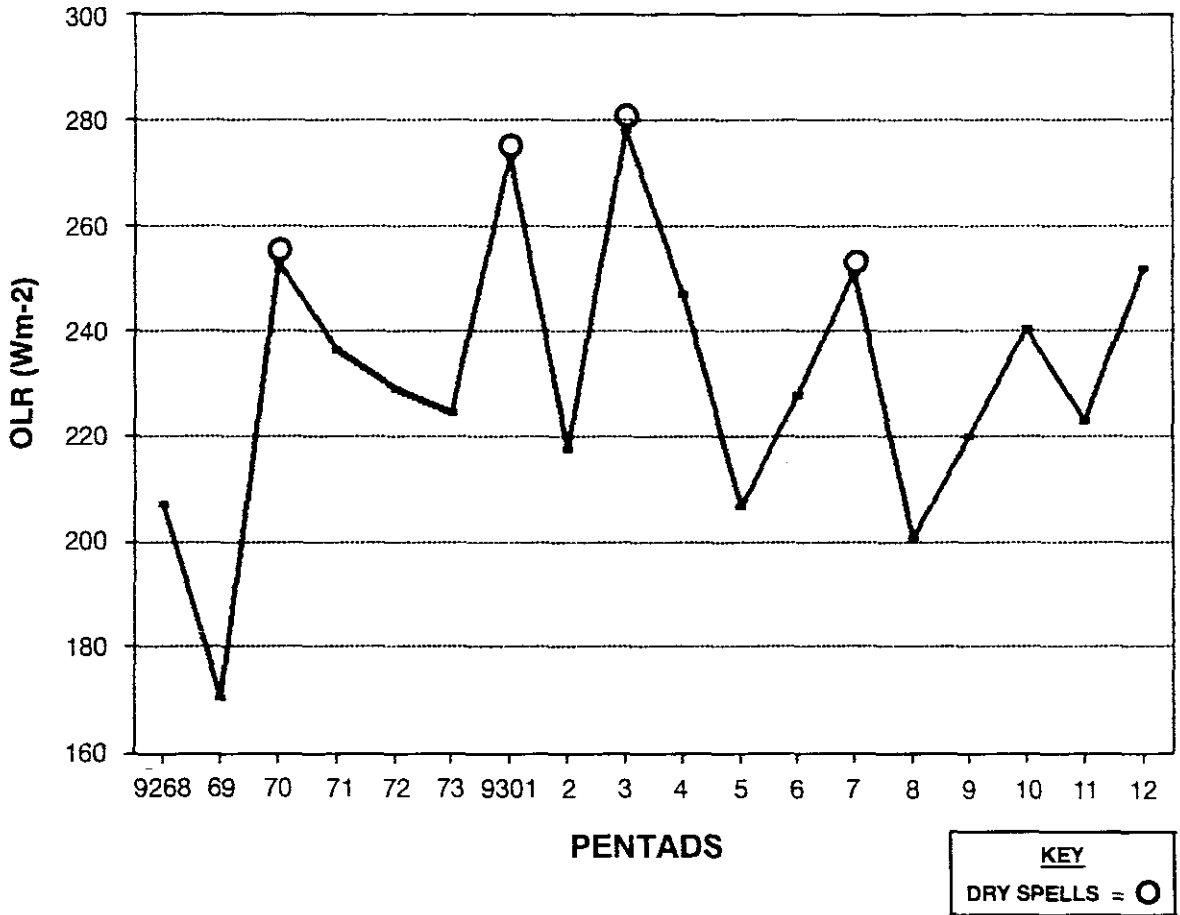


Fig. 4.8: OLR time series for Dec 92 – Feb 93 (30°S, 30°E). Pentads 70 (1992), 01, 03, 07 and 12 (1993) were selected for the dry spell analysis.

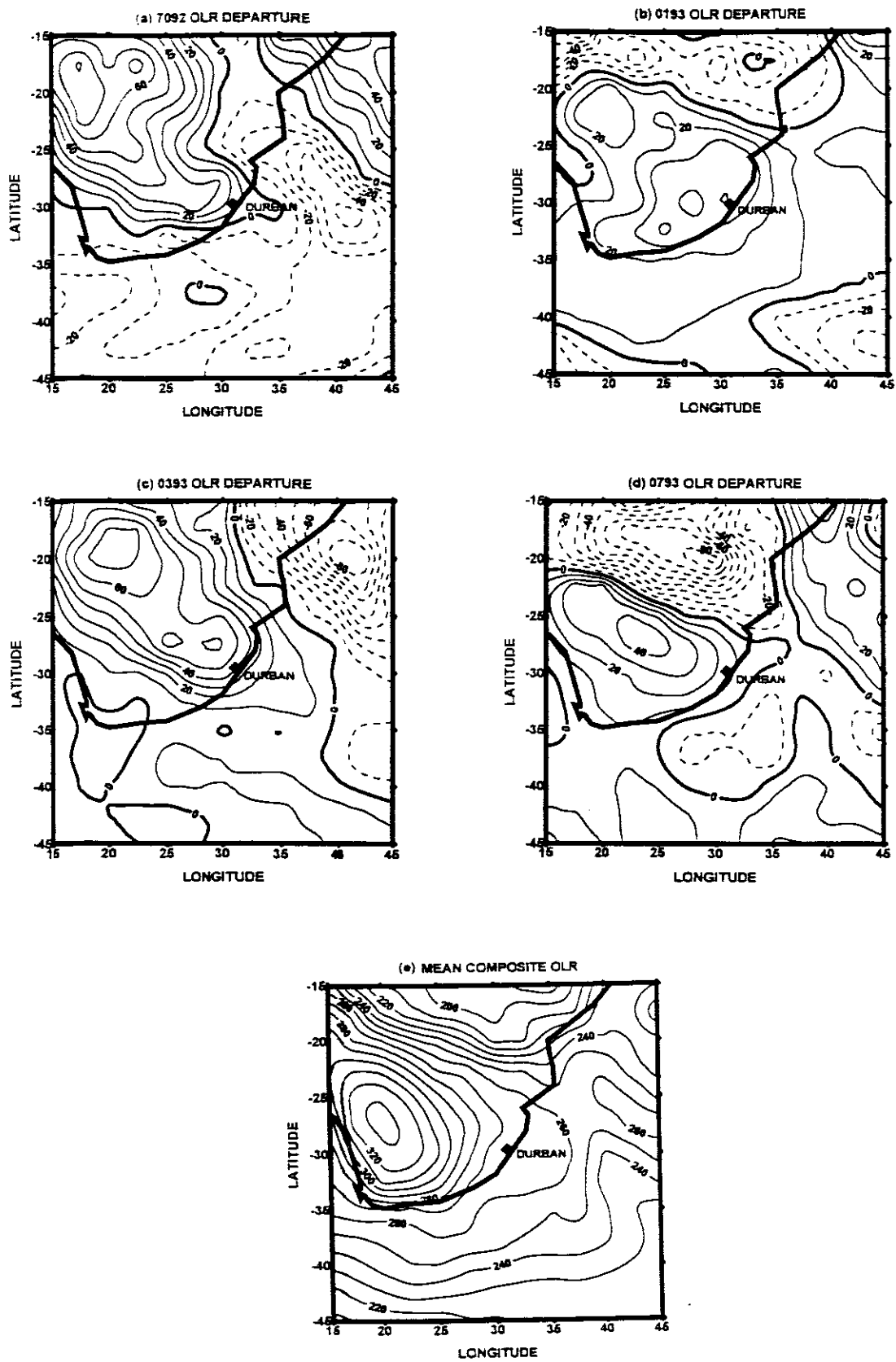


Fig. 4.9: (a-d) OLR departures ( $W m^{-2}$ ) from the 1980-94 DJF mean for pentads 70 (1992), 01, 03, 07 and 12 (1993); (e) mean composite OLR for DJF pentads (a-d).

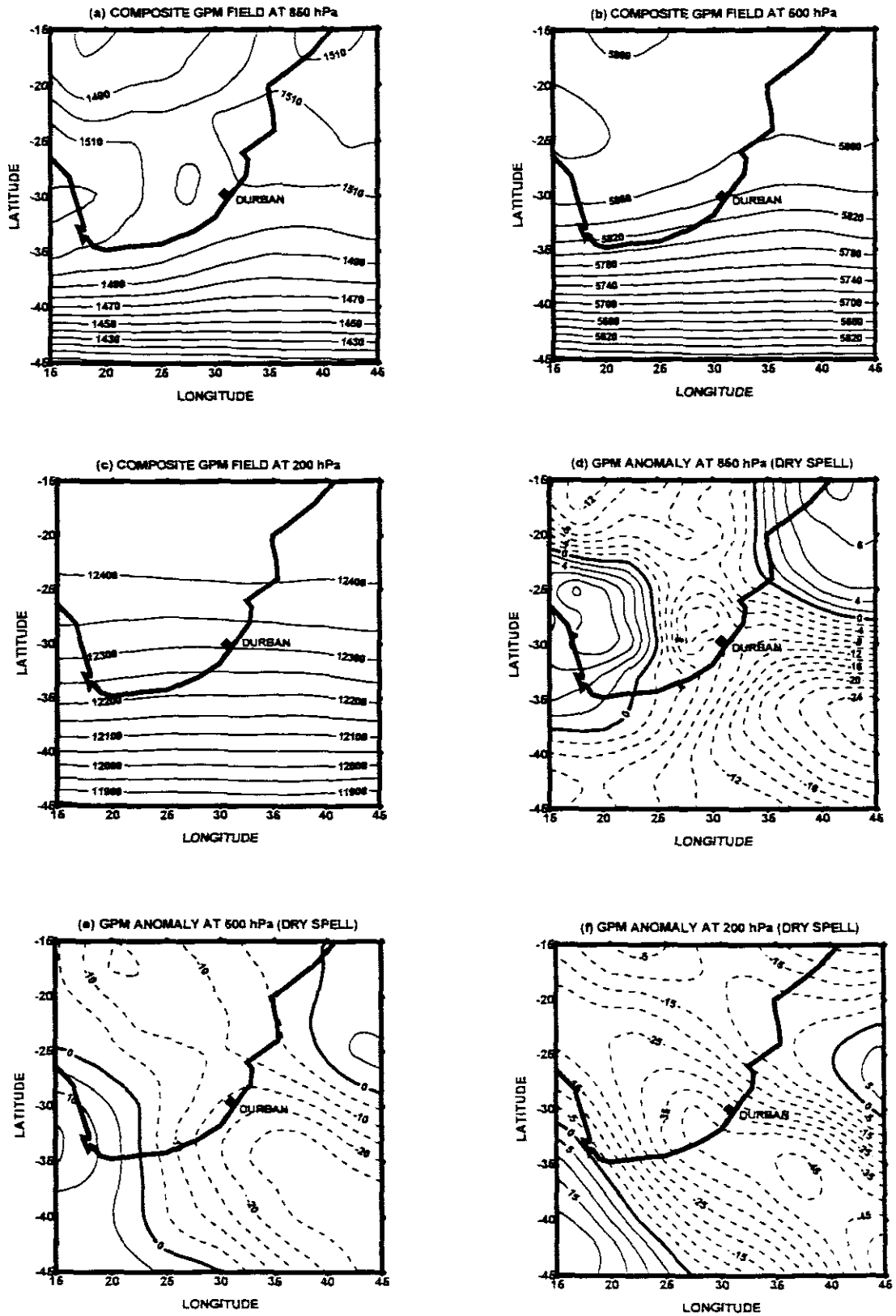


Fig. 4.10: Pentad composite geopotential heights and anomalies (gpm) (from the 1980-94 DJF mean) at 850, 500 and 200 hPa for DJF 1992/93 dry spell.

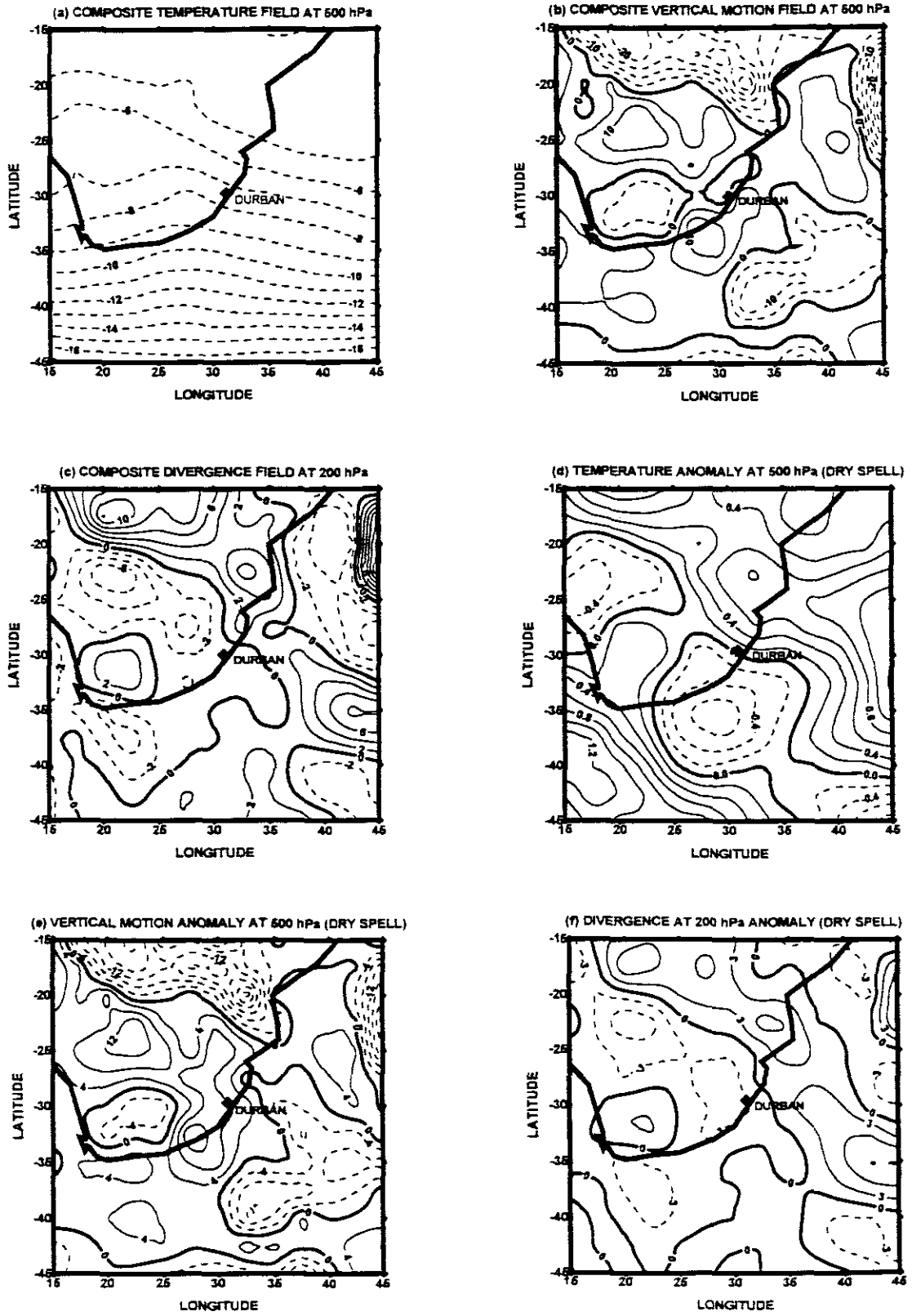


Fig. 4.11: Pentad composites and anomalies of temperature ( $^{\circ}\text{C}$ ) (form the 1980-94 DJF mean) at 500 hPa, vertical wind ( $\text{Pas}^{-1}$ ) at 500 hPa and divergence ( $10^{-6} \text{ s}^{-1}$ ) at 200 hPa for DJF 1992/93 dry spell.

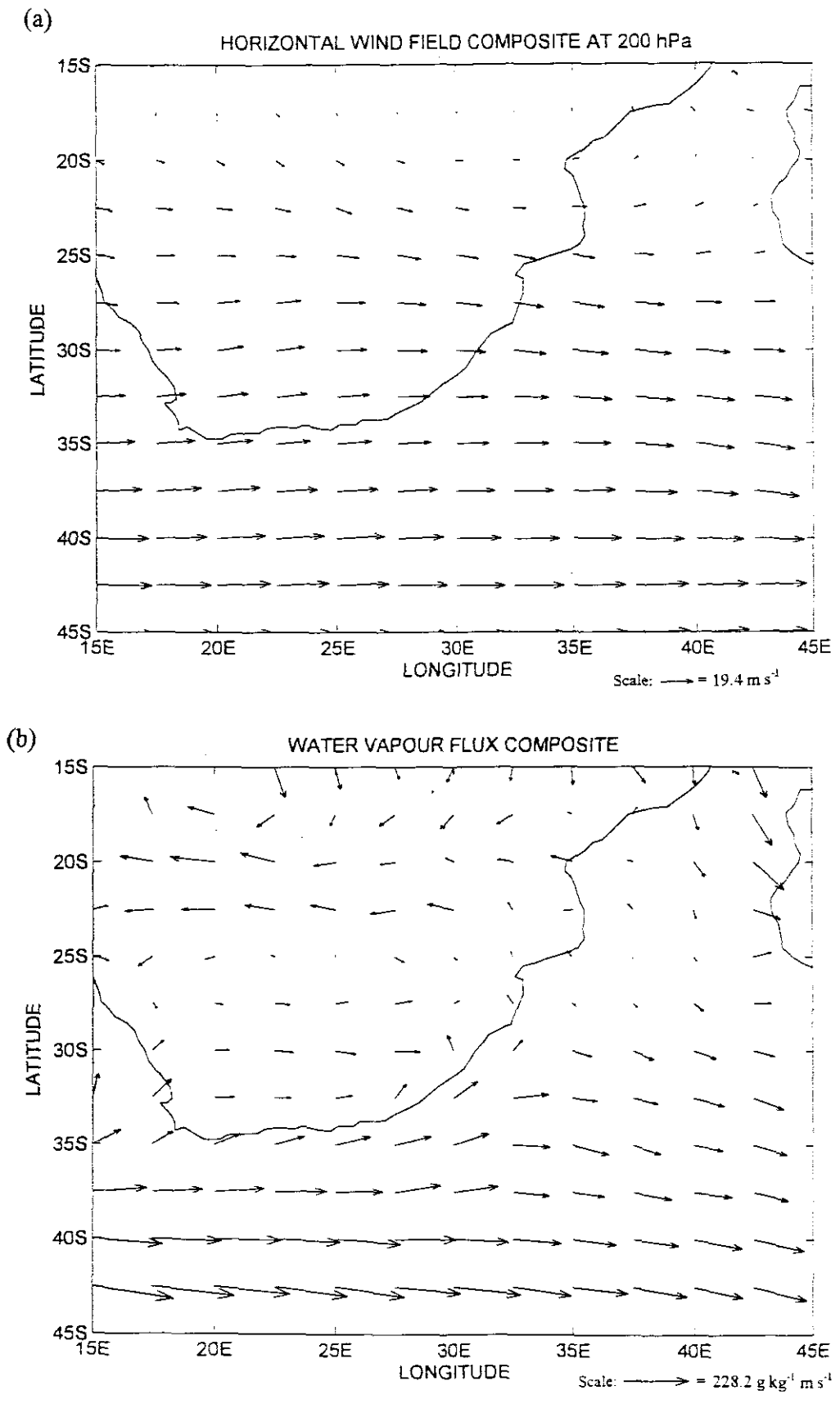


Fig. 4.12: Composite of (a) horizontal wind field vectors at 200 hPa, and (b) water vapour flux vectors integrated between 1000 – 300 hPa, for the DJF 1992/93 dry spell.

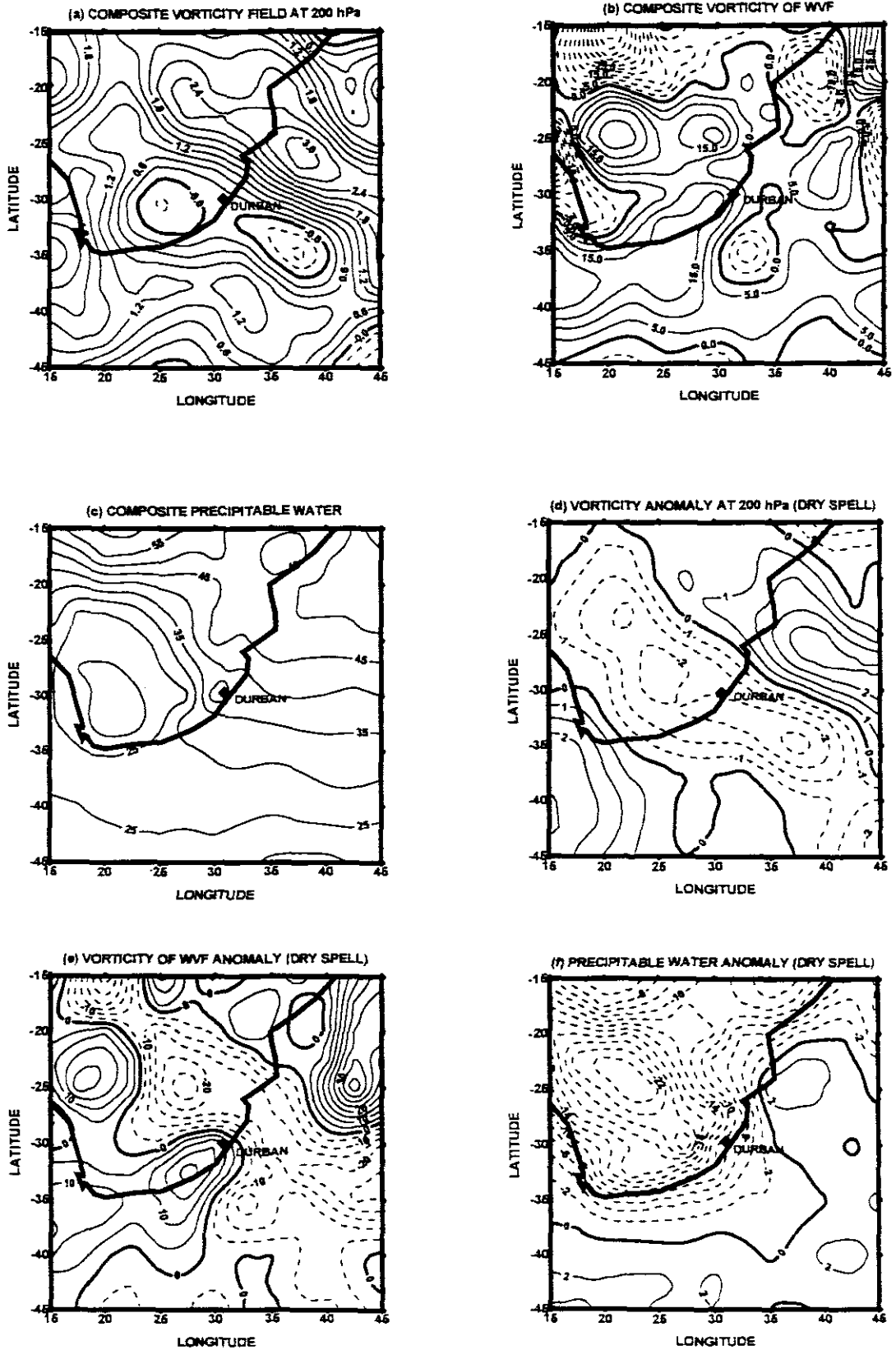


Fig. 4.13: Pentad composites and anomalies (from the 1980-94 DJF mean) of vorticity ( $10^{-6} \text{ s}^{-1}$ ) at 200 hPa, integrated vorticity of water vapour flux ( $10^{-6} \text{ g kg s}^{-1}$ ) between 1000 – 500 hPa and integrated precipitable water (mm) between 1000 – 300 hPa for DJF 1992/93 dry spell.

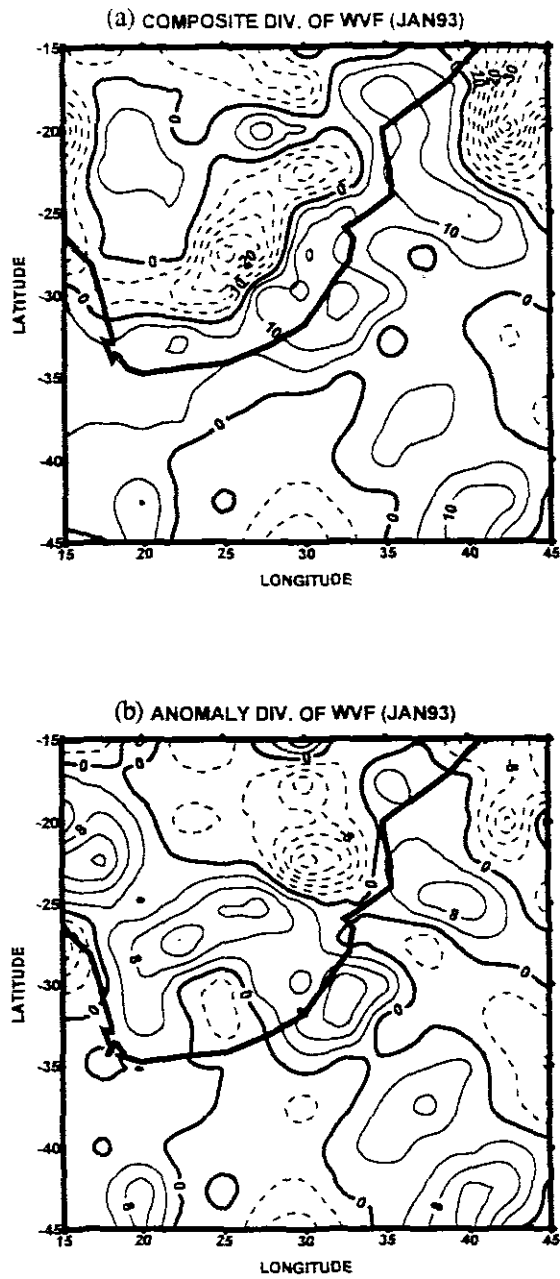


Fig. 4.14: Pentad composite and anomaly (from the 1980-94 DJF mean) of divergence of water vapour flux integrated between 1000 – 300 hPa for DJF 1992/93 dry spell.

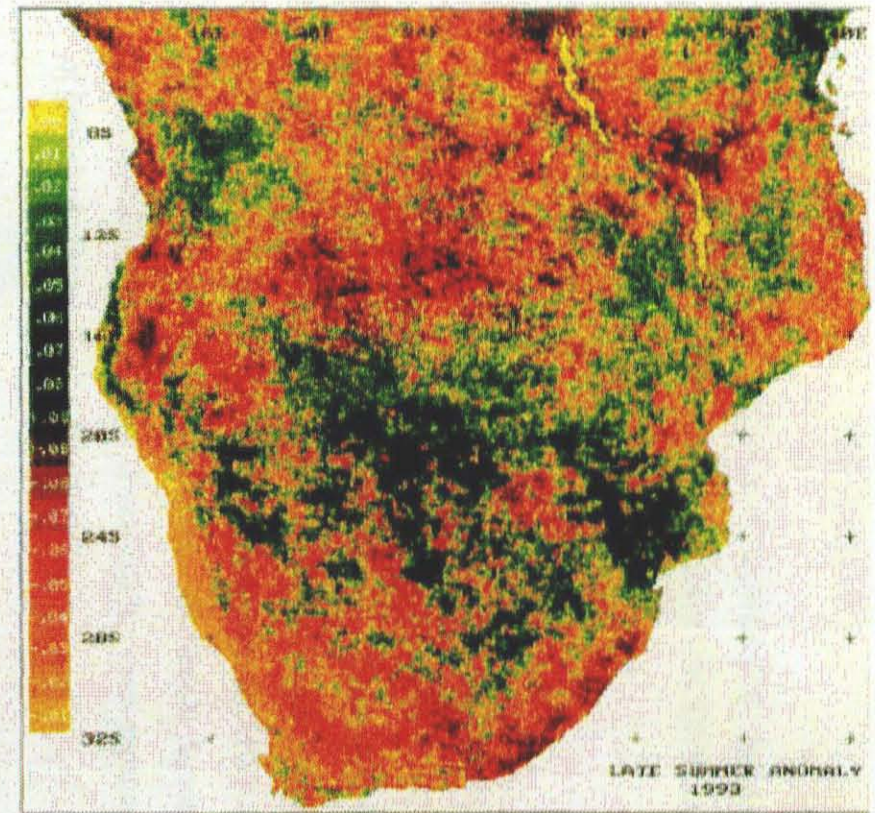
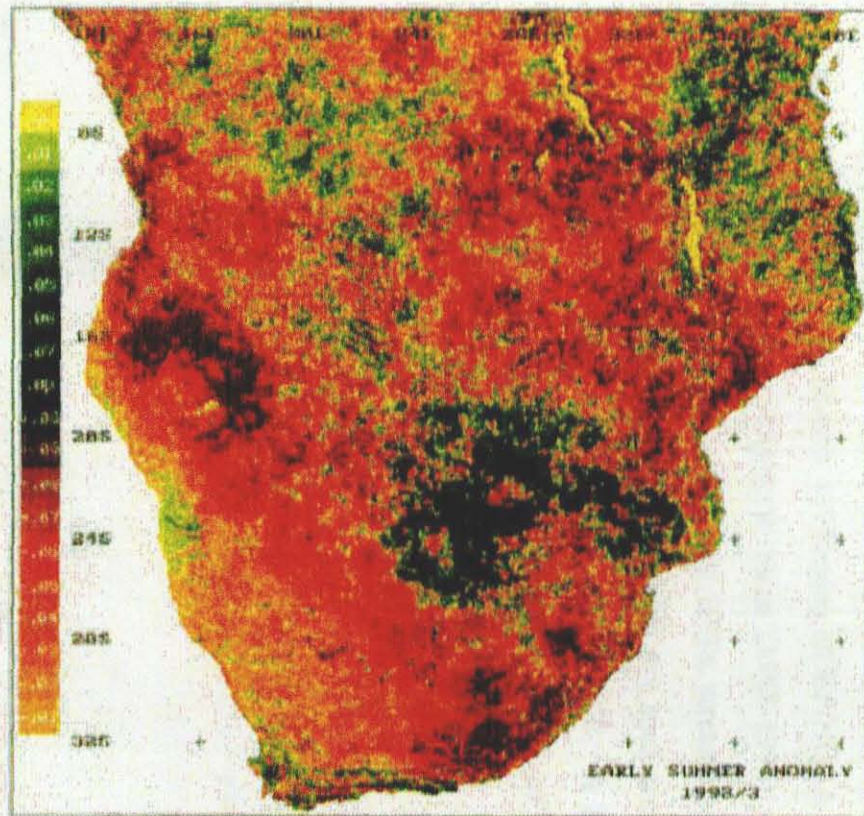


Fig. 4.15: Satellite photographs of the anomalies of normalised difference vegetation index (NDVI) over southern Africa for the 1992/93 early summer, and late summer periods. Green (brown) areas are wet (dry).

## CHAPTER 5

### 5: HEMISPHERIC SCALE COMPOSITE MEAN AND ANOMALY ANALYSIS OF THE 1992/93 DROUGHT (NCEP/NOAA)

#### 5.1 INTRODUCTION

Anomalies in precipitation and temperature of South Africa during the period of the 1992/93 drought can be associated with changes in the atmospheric circulation around the hemisphere. A further analysis of the 1992/93 summer dry spell is considered in this Chapter using NCEP/NOAA data. Most of the results obtained from parameters analysed in Chapter 4 using the ECMWF data, are compared with output from the NCEP/NOAA dataset. Additional parameters are also analysed. The latitude/longitude window of analysis has been expanded to identify the origin of hemispheric forces driving the drought.

#### 5.2 DATA AND METHODOLOGY

An analysis of the 1992/93 drought scenario has been undertaken for the dry summer (DJF) spell and January 1993 using NCEP/NOAA data. Composite means and departures from the long-term mean (1968-1996) of geopotential height, precipitable water, wind vectors, omega, SSTs, streamfunction, velocity potential and mean OLR pattern for the 1992/93 DJF dry spell are presented below. The domain for the analysis is 20°N, 60°S; 40°W, 90°E. A hemispheric domain for SSTs has been considered within the latitude domain 20°N, 40°S. Output from these analyses is compared with ECMWF results.

## 5.3 RESULTS

### 5.3.1 ANOMALY FIELDS

#### 5.3.1.1 GEOPOTENTIAL HEIGHTS

January 1993 pressures at 850 hPa are observed to be anomalously positive over the continent of Africa, reaching values of 5 over the interior parts of South Africa and Botswana (Fig. 5.1). Anomalously negative geopotential heights are observed over the South Atlantic and South Indian Oceans separated by a north-south oriented ridge of high pressure. The strength of below normal pressures for the South Atlantic and South Indian cells intensify at 500 and 200 hPa (Figs. 5.2 and 5.3). The meridionally aligned circulation of above normal pressures is also intensified at these upper levels but its sphere of influence is limited to the western parts of South Africa as a weak below-normal cell sets in over the eastern parts of South Africa. The gpm field is similar in all respects to the ECMWF output (Fig. 4.1d-f) with strong zonal pressure gradients to the south of South Africa and persistent high continental pressures in both analyses. In both ECMWF and NCEP/NOAA data (Fig. 4.1d and 5.1b) reduced atmospheric thickness is observed to the south of South Africa and to the south-east of Madagascar. The SE-NW oriented low pressure trough at 850 hPa is weaker over KwaZulu/Natal in the NOAA results than in ECMWF data. At all three levels, the compressed gradient south of the continent is a dominant feature.

Geopotential height fields show consistency with the low phase of the SOI during the period 1992/93 drought period. Higher geopotential heights occur over the continent during the drought period and lower heights over Gough Island. During the drought period the equatorward momentum flux over South Africa increased and the poleward flow of momentum across Gough Island was also increased resulting in a westerly anomaly. The increased zonal westerly flow is consistent

with the northward displacement of the South Atlantic Anticyclone during dry periods over the summer rainfall region of southern Africa .

#### 5.3.1.2 WIND VECTORS

Westerlies are prevalent at 850, 500 and 200 hPa to the south of South Africa during the 1992/93 dry summer season (Figs. 5.4, 5.5 and 5.6). At 850 hPa anticyclonic overturning occurs with the northward recurving of winds to the south coupled with westward flowing winds over the interior parts of South Africa. Easterlies at 20°S recurve southward over the Mozambique Channel. Another limb of these southward flowing winds joins the continental anticyclonic winds as offshore flow over KwaZulu/Natal, whilst a major limb joins the cyclonic anomaly flow commencing at 40°S over Marion Island. A compressed pressure gradient, in association with jet stream winds of as much as  $40 \text{ m s}^{-1}$  at the 200 hPa level, is observed to the south of South Africa. The anticyclonic wind vectors cover a domain as large as 20°W to 30°E suggesting that the drought was a response to a hemispheric-scale disturbance of the atmosphere.

Westerly zonal anomalies occur over the entire southern Africa except to the south over Marion Island. At 200 hPa the meridional wind is more northerly over tropical Africa hence confluent and more southerly over subtropical latitudes. The boundary at about 20°S is thus a region of 200 hPa convergence that enhances subsidence and dry conditions at the surface. The zonal and meridional wind components are consistent with an anomalous local subsiding limb of the north-south Hadley cell over the eastern parts of South Africa.

### 5.3.1.3 OUTGOING LONGWAVE RADIATION

OLR values over South Africa average between 270 and 280  $\text{W m}^{-2}$  (Fig. 5.7a) whilst low values between 200 and 220  $\text{W m}^{-2}$  are obtained over 40°E, 20°S indicating convection there. KwaZulu/Natal sits in a zone of weak positive OLR anomalies (Fig. 5.7b). The strongly compressed thermal gradient to the south of South Africa is also revealed in the OLR pattern in association with the pressure pattern presented in the preceding section. In general, higher OLR values and stronger gradients occur over the continent of Africa relative to the surrounding oceans. Local convection over the continent, however occurs such as over Kenya and Tanzania where reduced OLR values are found. An E-W gradient along 50°E in Fig. 5.7b coincides with strong gradients of the velocity potential (Fig. 5.13b) and streamfunction (Fig. 5.14b) in this region. Centres of action at 50°E, 5°N; 0°, 0° and at 70°E, 15°S produce teleconnections and an alternating + and - OLR wave train pattern as shown in Fig. 5.7b.

### 5.3.1.4 PRECIPITABLE WATER

One of the meteorological factors responsible for the 1992/93 drought in KwaZulu/Natal is a reduction in water vapour from the Indian Ocean north of Mozambique. Precipitable water, for the layer 850-300 hPa, is ~ 30 mm over this region (Fig. 5.8a). The same pattern is discernible from Figure 4.13c even though the lengths of analysis periods are not the same in these two datasets. The anomaly of columnar precipitable water is negative throughout the region south of 15°S reaching values of about -2 over KwaZulu/Natal (Fig. 5.8b). The Angola Low indicates above-normal precipitable water in contrast to values of -3 over the Indian Ocean to the east of Madagascar. A positive core to the south-east of Madagascar teleconnects an equatorial core and a NW-SE pattern of wave trains is established as shown in Fig. 5.8b. This alignment of the wet axis is in agreement with the dislocation of major cloud bands eastward during dry years over southern

Africa suggested by Harrison (1986).

#### 5.3.1.5 VERTICAL MOTION

Vertical motion is strongly suppressed over KwaZulu/Natal and most of southern Africa south of 20°S (Fig. 5.9a and b). Positive anomalies occur between 10° and 20°S east of 50°E. Negative vertical motion and anomalies are dominant over the Atlantic Ocean.

#### 5.3.1.6 STREAMFUNCTION

Two cells of negative streamfunction (anticyclonic) at the lower 0.995 sigma level are located over the Indian and Atlantic Oceans (Fig. 5.10a). The streamlines are positive and more zonal to the south of 40°S and gradients there are very strong. The anomaly pattern shows negative values to the east of southern Africa and positive values to the west (Fig. 5.10b). Therefore anticyclonic tendencies prevail over the southern Africa and the surrounding oceans. A cyclonic anomaly axis along 40°S is in agreement with constricted gradients and below-normal pressure to the south of South Africa revealed by 850 hPa geopotential height analysis (Fig. 4.10a and c and 5.1). A prominent centre of action (negative streamfunction) at 15°S, 65°E is produced by descending motion of the Hadley cell whose rising limb, hence positive streamfunction, is over the Zambezi.

At the upper 0.2101 sigma level the streamfunction is consistently zonal with constricted gradients to the south of the continent (Fig. 5.11a) as in the pressure and OLR fields. The anomaly pattern to the west of southern is meridionally positive to the west of 10°W and negative between 10°W and 20°E with the core axis at 0°E. To the east of southern Africa a more incoherent pattern of zonal alternating positive and negative anomalies is apparent. Over southern Africa the streamfunction field and its anomaly favour cyclonic motion at this level.

### 5.3.1.7 VELOCITY POTENTIAL AND DIVERGENCE

Strong divergence associated with negative velocity potential values and centred at 0°E is observed over western parts of southern Africa at the lower 0.995 level (Fig. 5.12a). Velocity potential gradients are stronger to the west of this core than to the east. The gradients, however, become weak and positive to the east of 20°S over southern Africa. Anomalies of velocity potential at the 0.995 level indicate convergent flow (+) over the whole domain analysed, particularly along 40°S, except to the east of 40°E (Fig. 5.12b). An ENSO event is expected to a pattern different to the anomaly field depicted in Fig. 5.13b.

At the upper 0.2101 sigma level the velocity potential field is positive over southern Africa and the Atlantic Ocean, but negative over the South Indian Ocean (Fig. 5.13a). Convergence, therefore at the upper levels of the atmosphere, which feeds divergence at the surface (Fig. 5.12a), is reflected by the velocity potential gradient field. A convergent core is centred over 70°E and the pattern is anomalously divergent throughout the upper atmosphere from 25-40°E north of 20°S (Zambezi).

A strong velocity potential gradient is observed between 50 and 60°S at the 0.2101 level. At this period SSTs are cool to the east (Fig. 5.14). Wet conditions are also observed over the Zambezi (in antiphase with KwaZulu/Natal) suggesting that a zonal Walker cell at this latitude was driving such conditions over this area (Fig. 5.15).

### 5.3.1.8 SEA SURFACE TEMPERATURES

SST anomalies over the southern hemisphere are shown in Figure 5.8a. Anomalous warming of the Pacific and South Indian during the drought period is evident. Cooler SSTs occur in the eastern Atlantic and warmer in the western parts of the Atlantic Ocean. The increase in the low-level southerly meridional wind anomaly and higher sea surface temperatures over the southern Benguela system observed in 1992/93 is a typical feature of dry years (Tyson, 1986). Figures 5.1b and 5.14 suggest evidence that during dry summer seasons the weakening of the South Atlantic Anticyclone is associated with a northward displacement of the subtropical ocean convergence and cooler SSTs in the eastern Atlantic at about 10°S-15°W between 20° and 30°S. The change in SSTs to the east of Madagascar ( $\partial SST/\partial y$ ) has no influence on the thermal wind ( $\partial u/\partial z$ ) as higher wind speeds are located poleward from the surface to upper levels (Figs. 5.4 to 5.6).

### 5.3.1.9 SURFACE AIR TEMPERATURE

An alternating pattern of above- and below-normal air temperatures is observed over the oceans to the south of the continent in sympathy with pressure changes discussed in the preceding section (Fig. 5.15). KwaZulu/Natal experiences abnormally high surface air temperature departures of the order of 0.5 to 1. This is less than the positive departures above 2 obtained from surface measurements (Fig. 3.3). The underlying reason is that model-interpolated data has a poor resolution compared to surface data. The temperature gradient over the western sections of South Africa is stronger than over the eastern parts due to the influence of the Kalahari Desert. Below normal temperature departures of ~1 are centred over the Sahel and strong gradients here at the time of the drought, are worth noting. The tropical-subtropical dipole is evident in Figure 5.15. Summer temperature fields show a pattern of north-south reversal, such that temperatures increase during

drought over tropical and subtropical Africa and decrease in temperate latitudes south of Africa.

### 5.3.2 VERTICAL SECTIONS ANOMALY FIELDS

Meridional and zonal cross-sections of vertical motion, streamfunction, velocity potential,  $u$  and  $v$  wind components are analysed for  $30^{\circ}\text{E}$  and  $50^{\circ}\text{E}$  at the  $50^{\circ}\text{S}$  to  $5^{\circ}\text{S}$  latitude band, and  $30^{\circ}\text{S}$  and  $15^{\circ}\text{S}$  for longitude band stretching from  $0^{\circ}$  to  $90^{\circ}\text{E}$ , respectively. These are areas that have been observed to have conspicuous features during the 1992/93 drought over KwaZulu/Natal which need further analysis. Further analyses on zonal vertical sections are given in the Appendix (Figs. A1 to A10).

#### 5.3.2.1 VERTICAL MOTION

Meridional cross-section of vertical motion at  $30^{\circ}\text{E}$  shows subsidence motions at the surface over parts of southern Africa, particularly those to the south of  $25^{\circ}\text{S}$  (Fig. 5.16a). Vertical motion sets in above the 800 hPa level in the zone north of  $20^{\circ}\text{S}$ . A meridional dipole is thus evident in the omega field over southern Africa with  $20^{\circ}\text{S}$  as a boundary between these opposing fields of action.

The analysis of zonal section of vertical motion at  $15^{\circ}\text{S}$  (Fig. 5.16b) undertaken on the basis of the streamfunction and velocity potential anomaly fields (Figs. 5.10 to 5.13) shows sinking motion anomalies over the Indian Ocean consistent with lower than normal SSTs (Fig. 5.14) in this area. Vertical motion is enhanced over the Zambezi consistent with the OLR (Figs. 4.8 and 5.7) and geopotential height (Figs. 4.9 and 5.1 to 5.3) anomaly fields. This therefore suggests that a zonal cell characterised by a descending limb at this latitude over the Indian Ocean and rising limb over centered at  $25^{\circ}\text{E}$  at this latitude governs wetness over the Zambezi region while depriving the southern parts of southern Africa of rainfall.

### 5.3.2.2 ZONAL WINDS

Zonal winds between 30 and 27°S in the 30°E longitude band are westerly to the 700 hPa level over KwaZulu/Natal (Fig. 5.17a and b). A similar pattern of the dominance of surface westerlies conducive to the occurrence of dry conditions is obtained in the 60°E longitude (Fig. 5.18a and b). At upper levels easterlies prevail thus suggesting that the QBO contributed to the occurrence of drought over KwaZulu/Natal during the 1992/93 summer season. Easterlies cover a greater thickness of the atmosphere north of 20°S. This is an area of enhanced convective activity.

### 5.3.2.3 MERIDIONAL WINDS

Meridional wind cross-sections at the 60°E longitude south of 30°S are southerly at the surface and northerly further north (Fig. 5.19a). These winds are associated with an equatorward transfer of momentum which is opposed to wet conditions over KwaZulu/Natal. At the 15°S two opposing cells are located over the Indian Ocean east of 60°E at upper levels (Fig. 5.19b). The polarity of meridional wind regimes at this latitude and further south highlights the role winds play in the occurrence of dry and wet conditions.

### 5.3.2.4 VELOCITY POTENTIAL AND DIVERGENCE

The zonal cross-section of velocity potential at 30°S indicates a dipole pattern with 50°E marking the boundary (Fig. 5.20b). A divergent field is prominent from the surface to upper levels while convergence occurs to the east of 50°E over the whole atmosphere. Such a pattern is typical of El Niño years. Divergence is dominant in the meridional cross-section over the subcontinent in the area south of 20°S (Fig. 5.20a). Opposing centres of action at 40°S at the surface and 10°S at

200 hPa concur with the surface convergent flow at midlatitudes and equatorial southern Africa shown previously in the geopotential, streamfunction and velocity potential anomaly fields.

#### 5.3.2.5 STREAMFUNCTION

Negative anomalies of the streamfunction are obtained between 35°S and 15°S associated with anticyclonic circulation at the 50°E longitude (Fig. 5.21a). These are areas where negative SSTs are observed. Thus this is supporting the Hadley cell hypothesis as the driving mechanism behind drought over the parts of southern Africa south of 20°S. Positive streamfunctions south of 40°S reflect the cyclonic anomaly obtained in the geopotential field.

Positive streamfunction anomaly in the zonal cross-section at 15°S supports an upward Hadley cell overturning over the northern sections of southern Africa whilst negative anomalies between 50 and 65°S support the subsidence limb of the Hadley cell over the Indian Ocean at this latitude (Fig. 5.21b).

#### 5.4 CONCLUSION

During the 1992/93 drought season, positive pressure anomalies set in over KwaZulu/Natal and interior parts of South Africa and a strongest anomalies were over the south-western ocean area. At the 500hPa level, geopotential height anomalies occurred over much of the subcontinent and strongest negative anomalies were observed to the south-west of southern Africa, with weaker negative anomalies occurring over the adjacent southern and south-western ocean areas.

The 1992/93 drought over KwaZulu/Natal was accompanied by a strengthening of the westerlies. The drought period was characterised by winds of a predominantly

southerly component over the eastern interior parts of South Africa which limited the occurrence of rainfall. One important feature of the atmospheric circulation that had an influence on the occurrence of drought over KwaZulu/Natal during the 1992/93 summer season is the Hadley overturning between 15°S latitude and 35°S (Fig. 5.16). A series of teleconnections and wave train patterns have been observed in the OLR and precipitable water anomaly fields suggesting that the 1992/93 drought over KwaZulu/Natal was a response to hemispheric scale disturbances.

ECMWF and NCEP/NOAA datasets produce similar results in overall. Insignificant local inconsistencies occur with some parameters. It is however found that the 1992/93 drought was not a strong El Nino-induced climatic event. There are signs observed in the analysis showing resemblance to an El Nino type of influence but some parameters do not exhibit the expected patterns typical of ENSO. It is concluded that westerly mid-latitude winds an influence in the occurrence of drought during the 1992/93 summer season than SSTs.

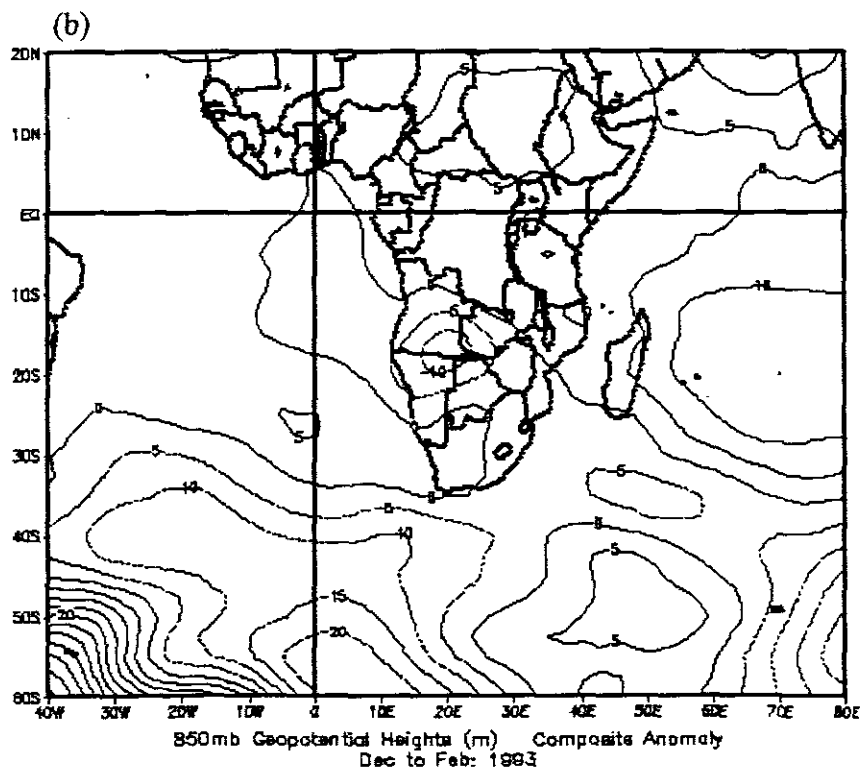
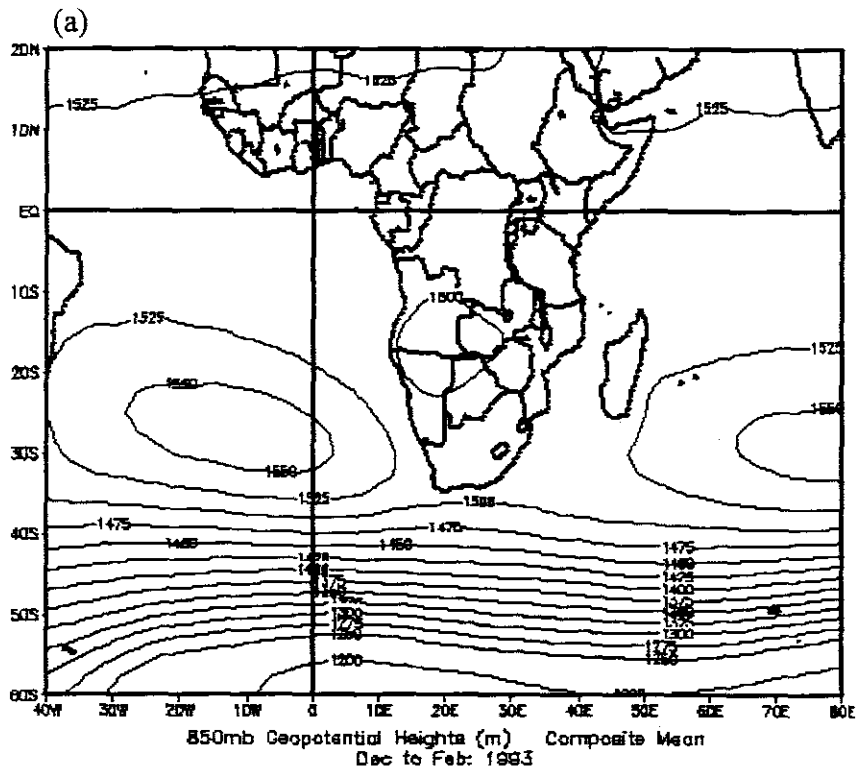


Fig. 5.1: Geopotential heights (a) mean and (b) anomaly at 850 hPa for DJF 1992/93.

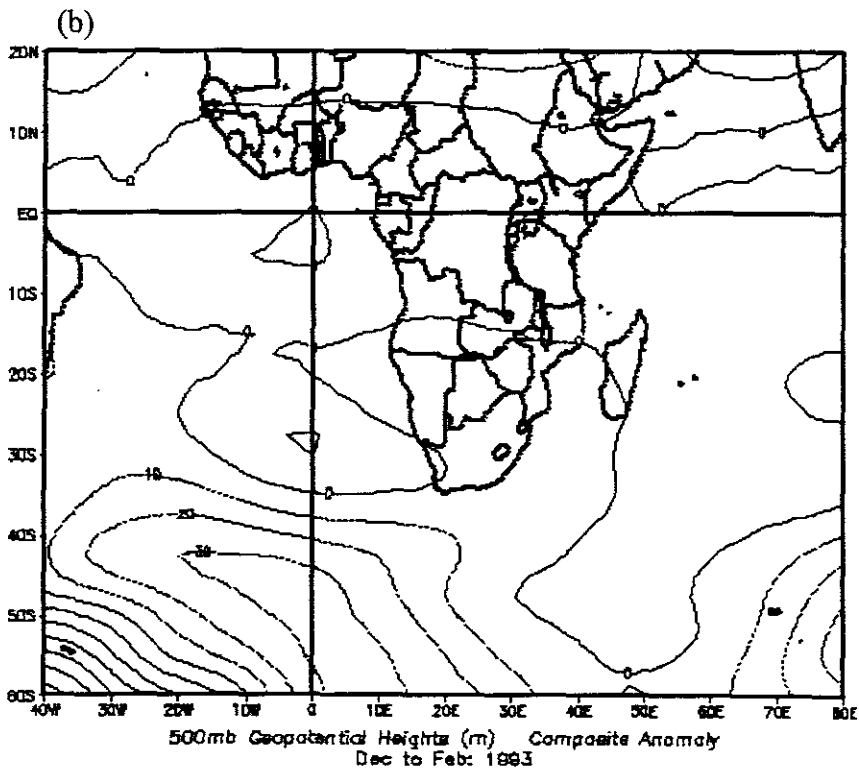
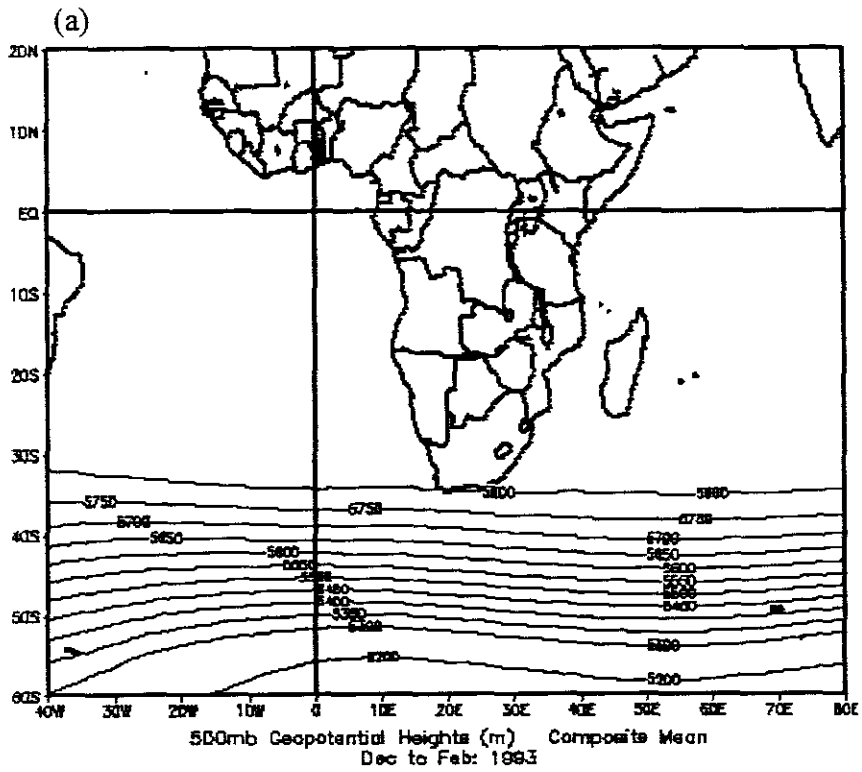


Fig. 5.2: Geopotential heights (a) mean and (b) anomaly at 500 hPa for DJF 1992/93.

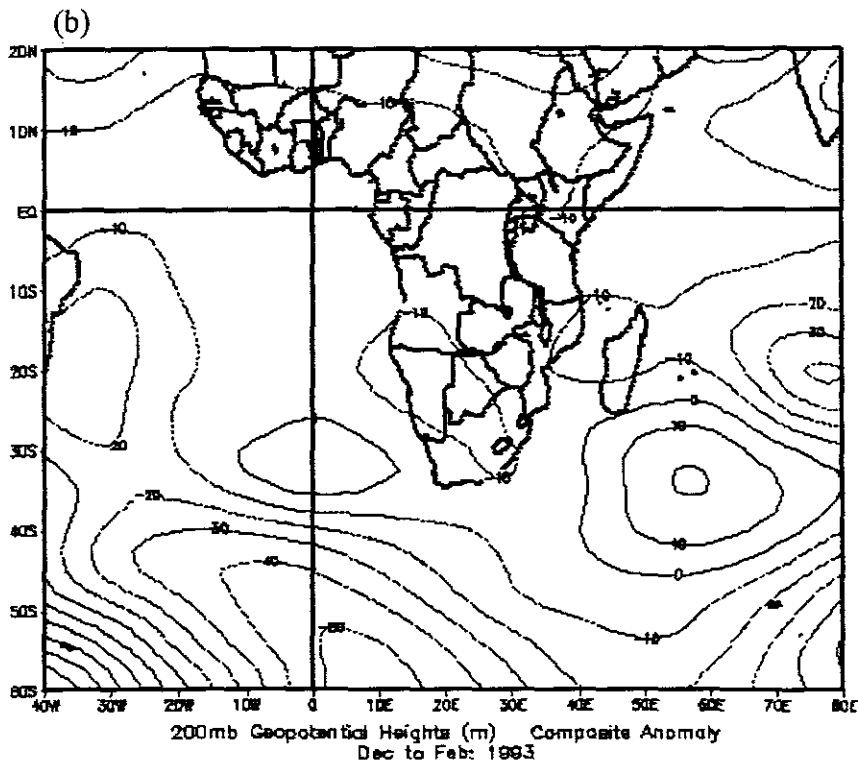
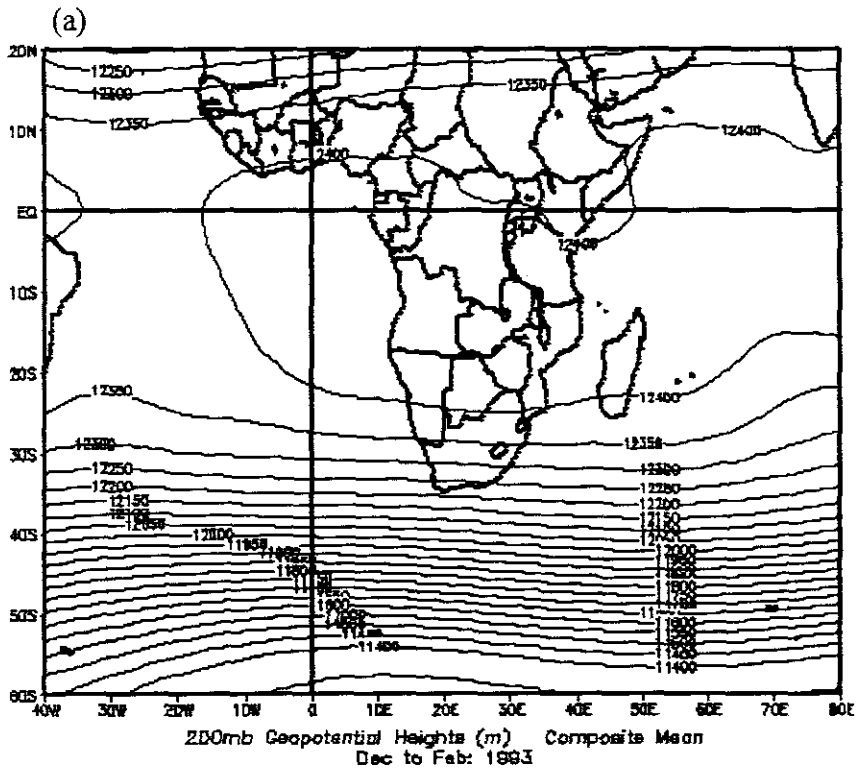


Fig. 5.3: Geopotential heights (a) mean and (b) anomaly at 200 hPa for DJF 1992/93.

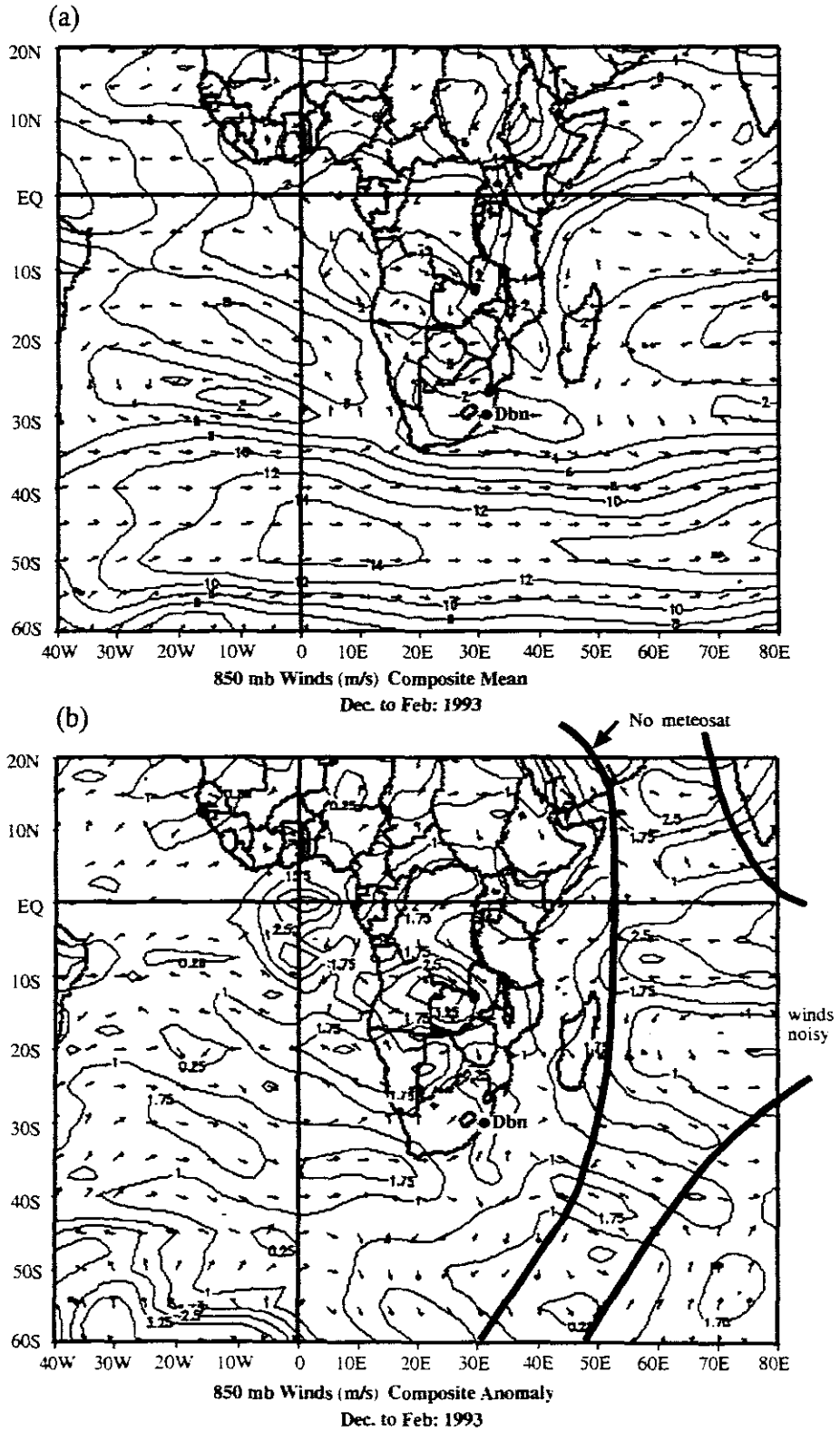


Fig. 5.4: (a) Mean and (b) anomalies of wind vectors and speed ( $\text{m s}^{-1}$ ) at 850 hPa for DJF 1992/93.

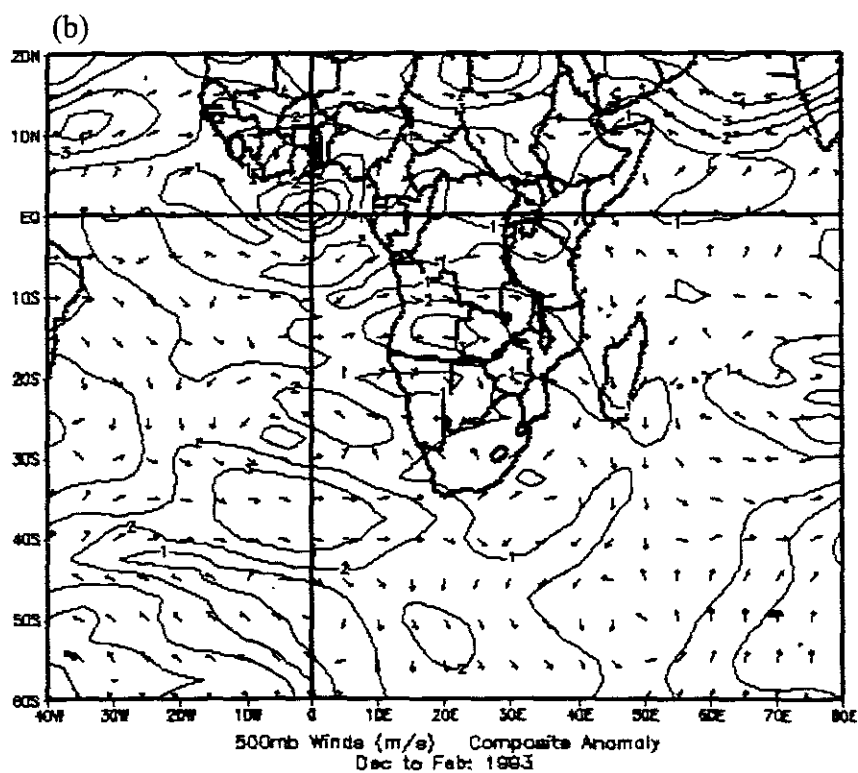
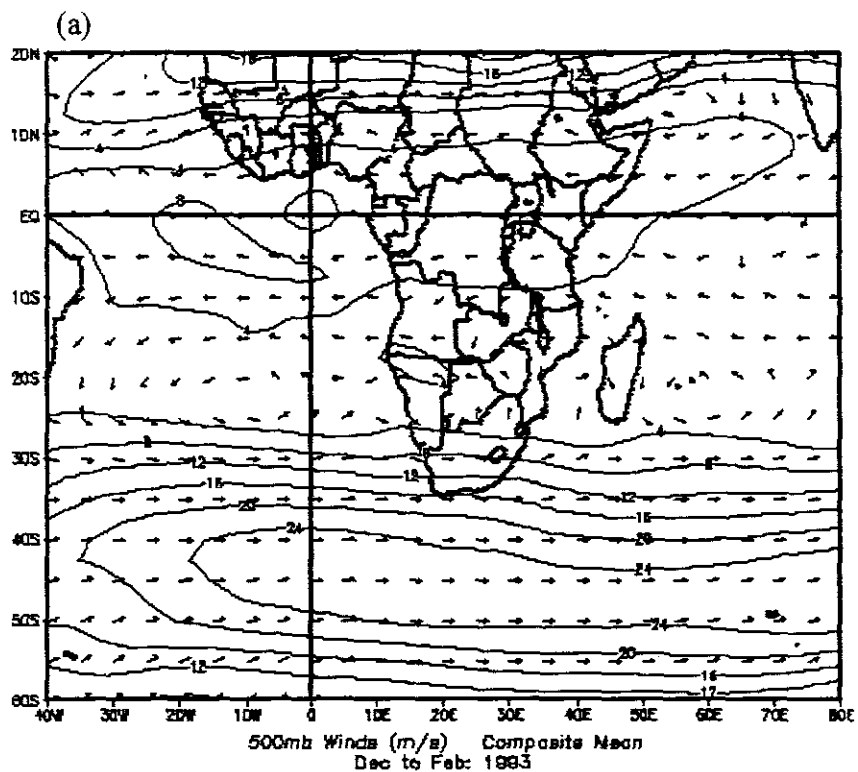


Fig. 5.5: (a) Mean and (b) anomalies of wind vectors and speed ( $\text{m s}^{-1}$ ) at 500 hPa for DJF 1992/93.

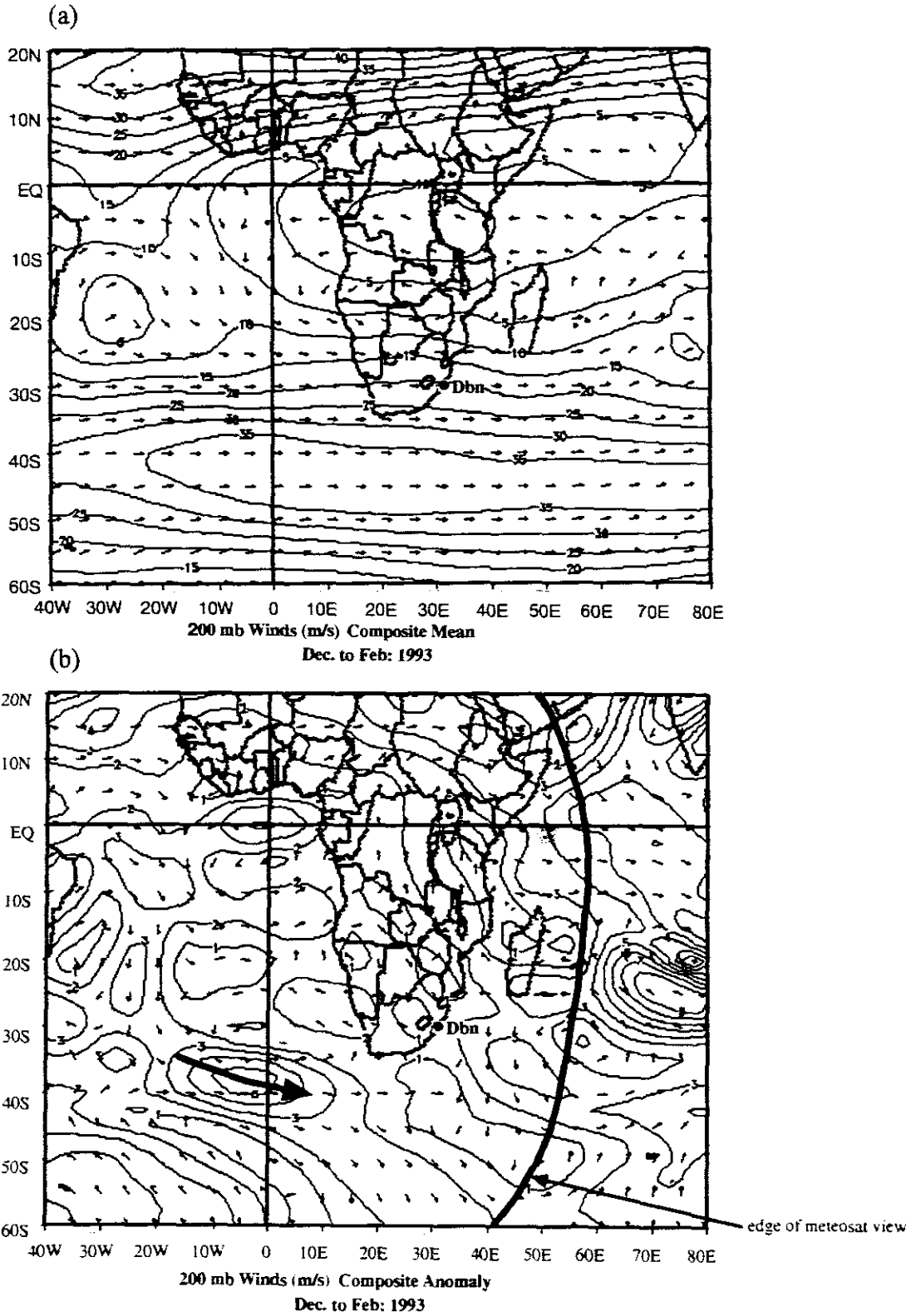


Fig. 5.6: (a) Mean and (b) anomalies of wind vectors and speed ( $\text{m s}^{-1}$ ) at 200 hPa for DJF 1992/93.

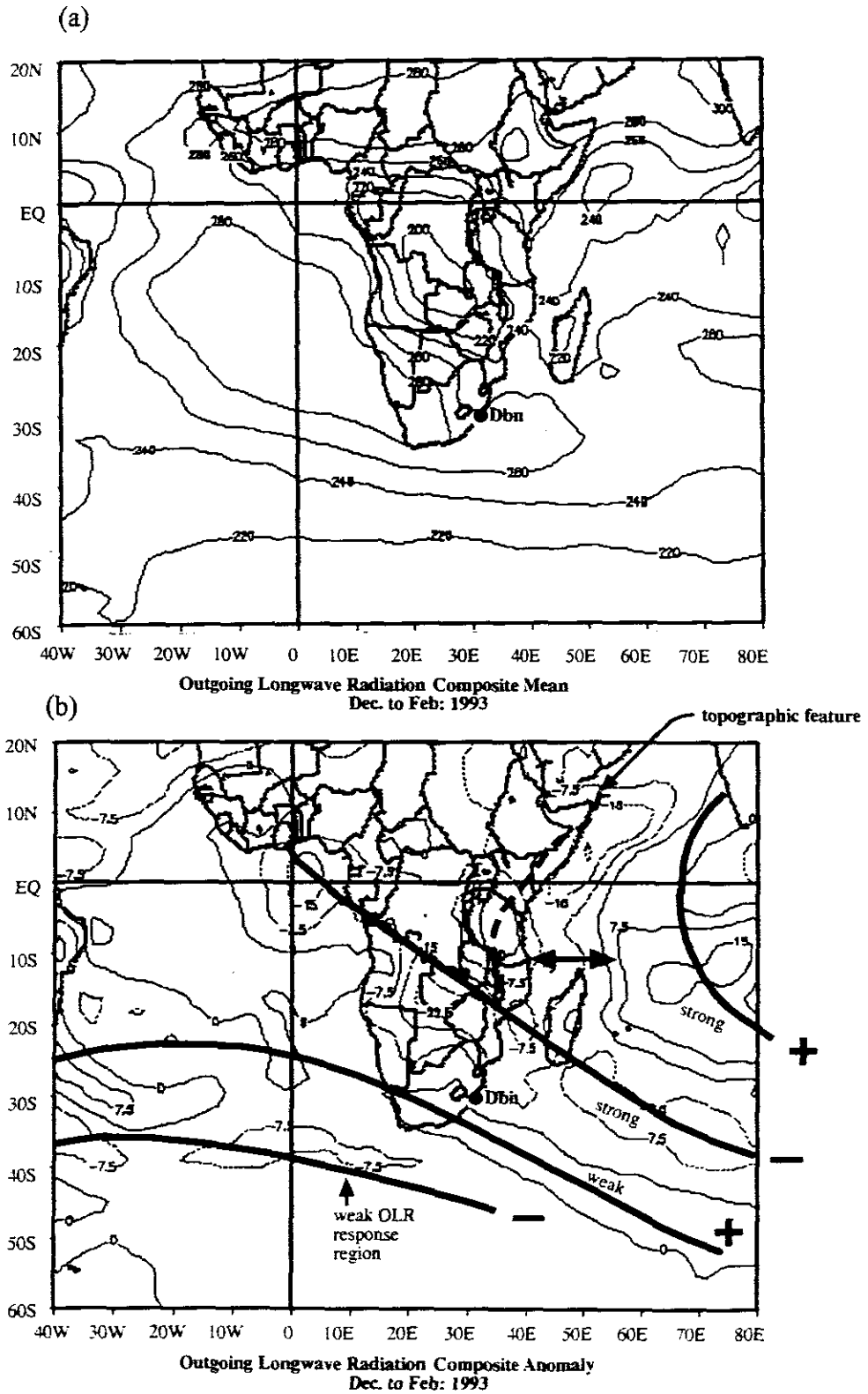


Fig. 5.7: (a) Mean and (b) anomalies of OLR ( $\text{W m}^{-2}$ ) for DJF 1992/93.

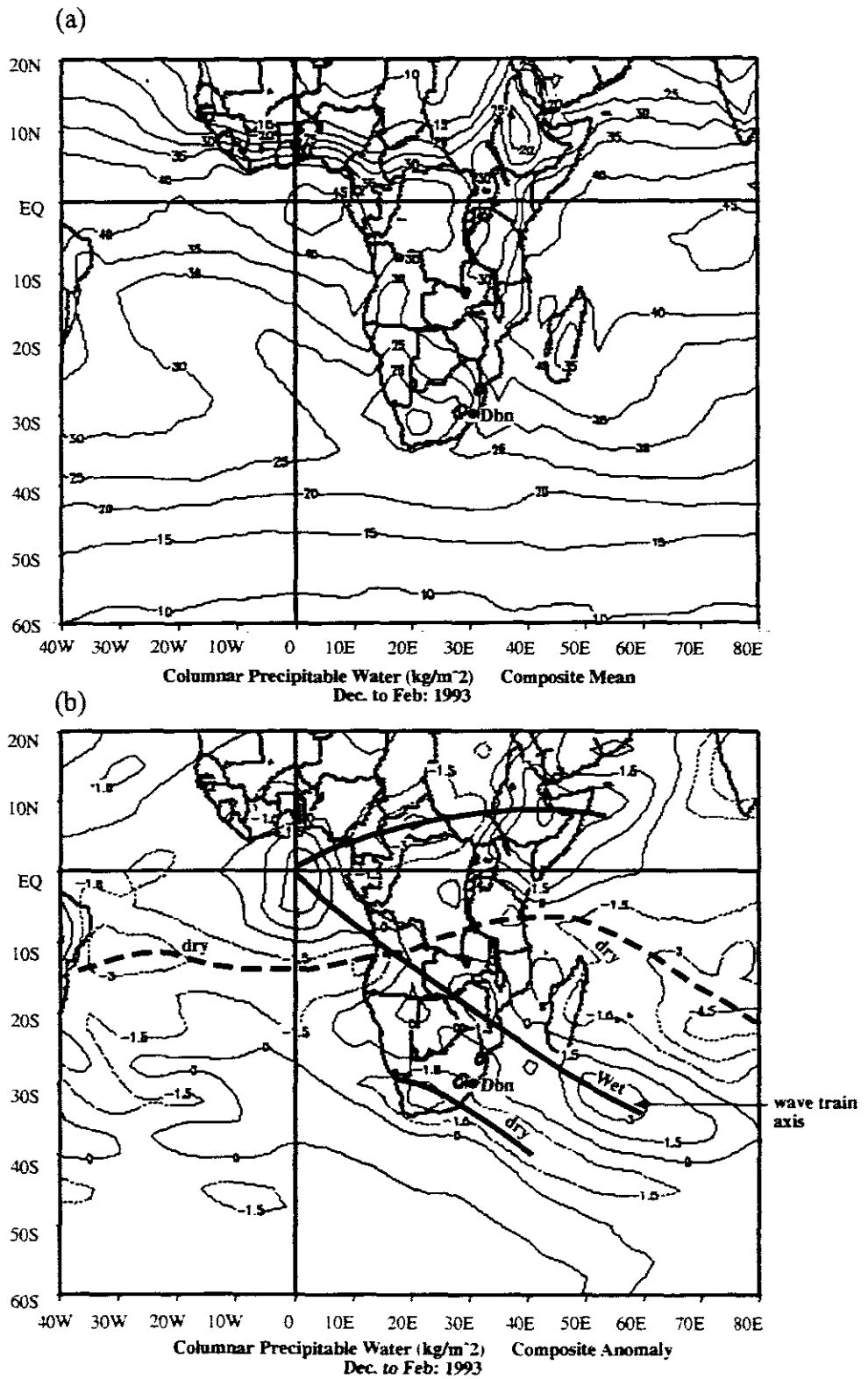


Fig. 5.8: Columnar precipitable water ( $\text{kg m}^{-2}$ ) (a) mean and (b) anomaly for DJF 1992/93.

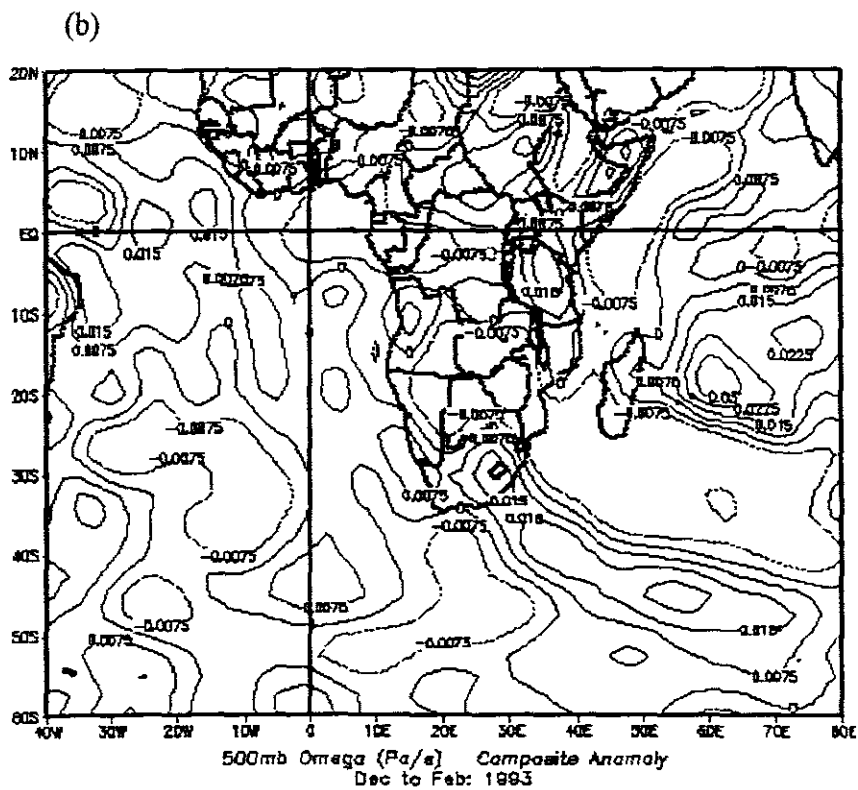
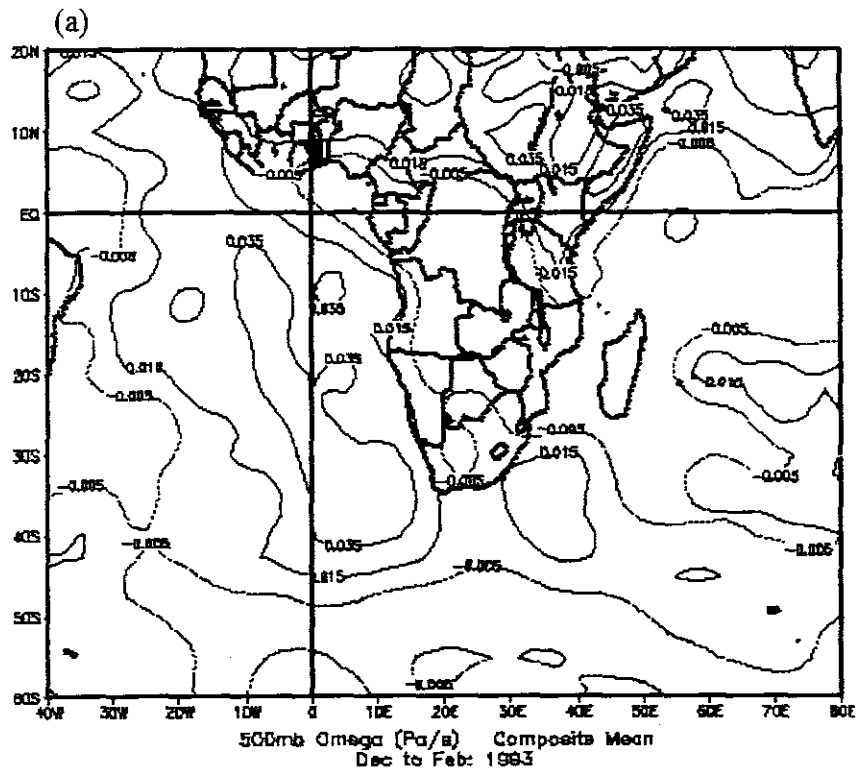


Fig. 5.9: (a) Mean and (b) anomalies of vertical motion ( $\omega$ ,  $\text{Pa s}^{-1}$ ) at 500 hPa for DJF 1992/93.

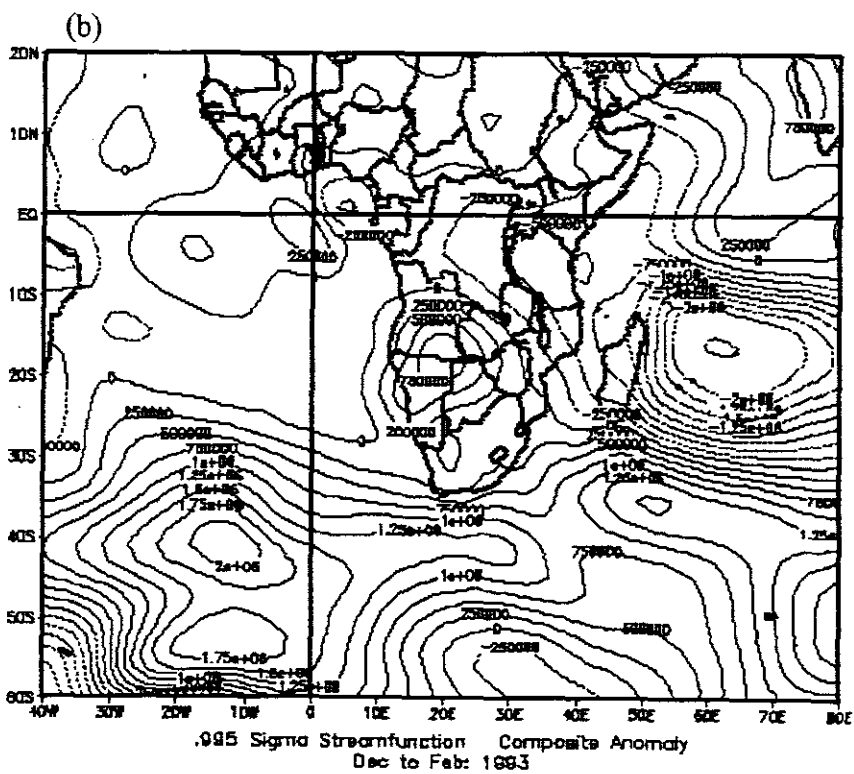
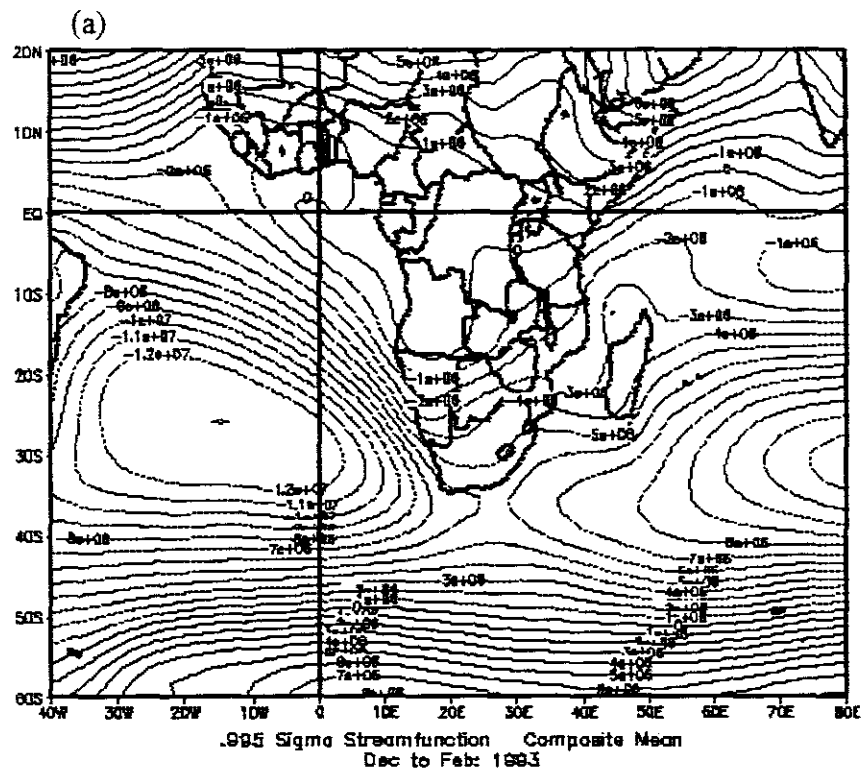


Fig. 5.10: Streamfunction (a) mean and (b) anomalies at the 0.995 sigma level for DJF 1992/93.

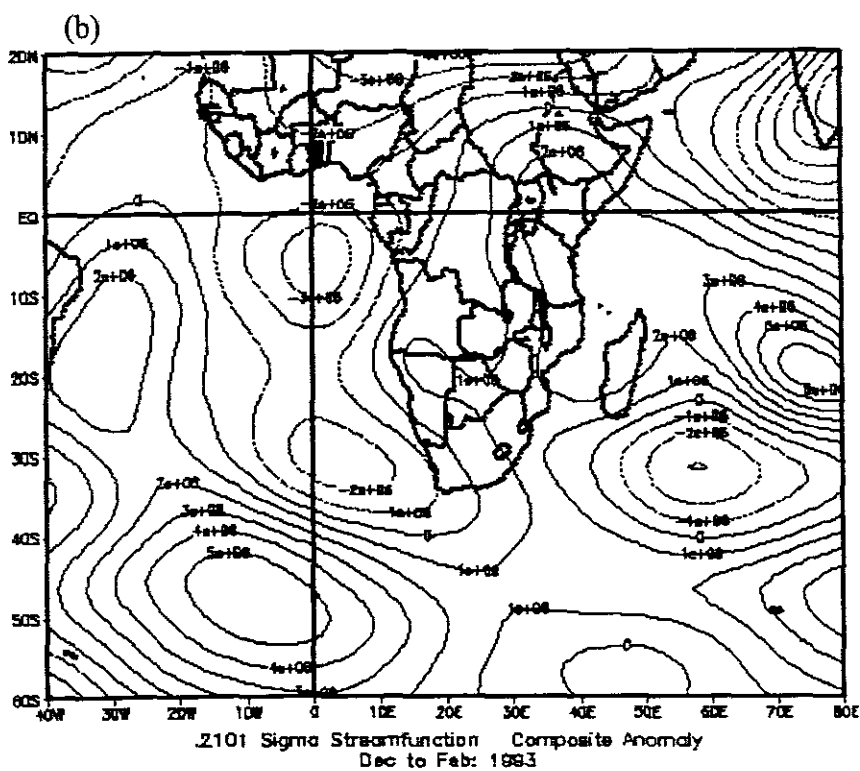
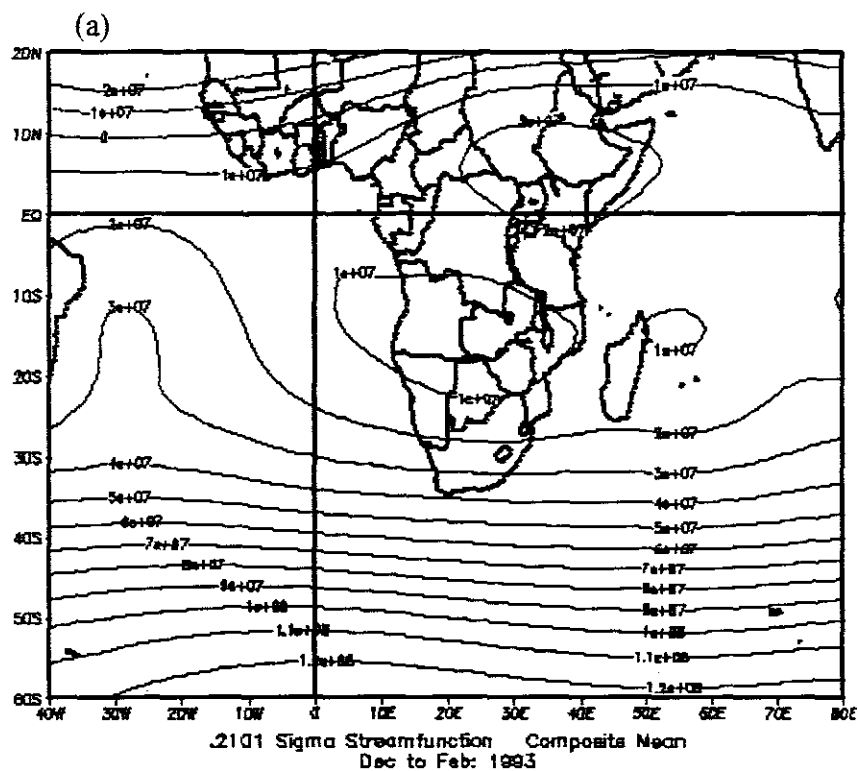


Fig. 5.11: Streamfunction (a) mean and (b) anomalies at the 0.2101 sigma level for DJF 1992/93.

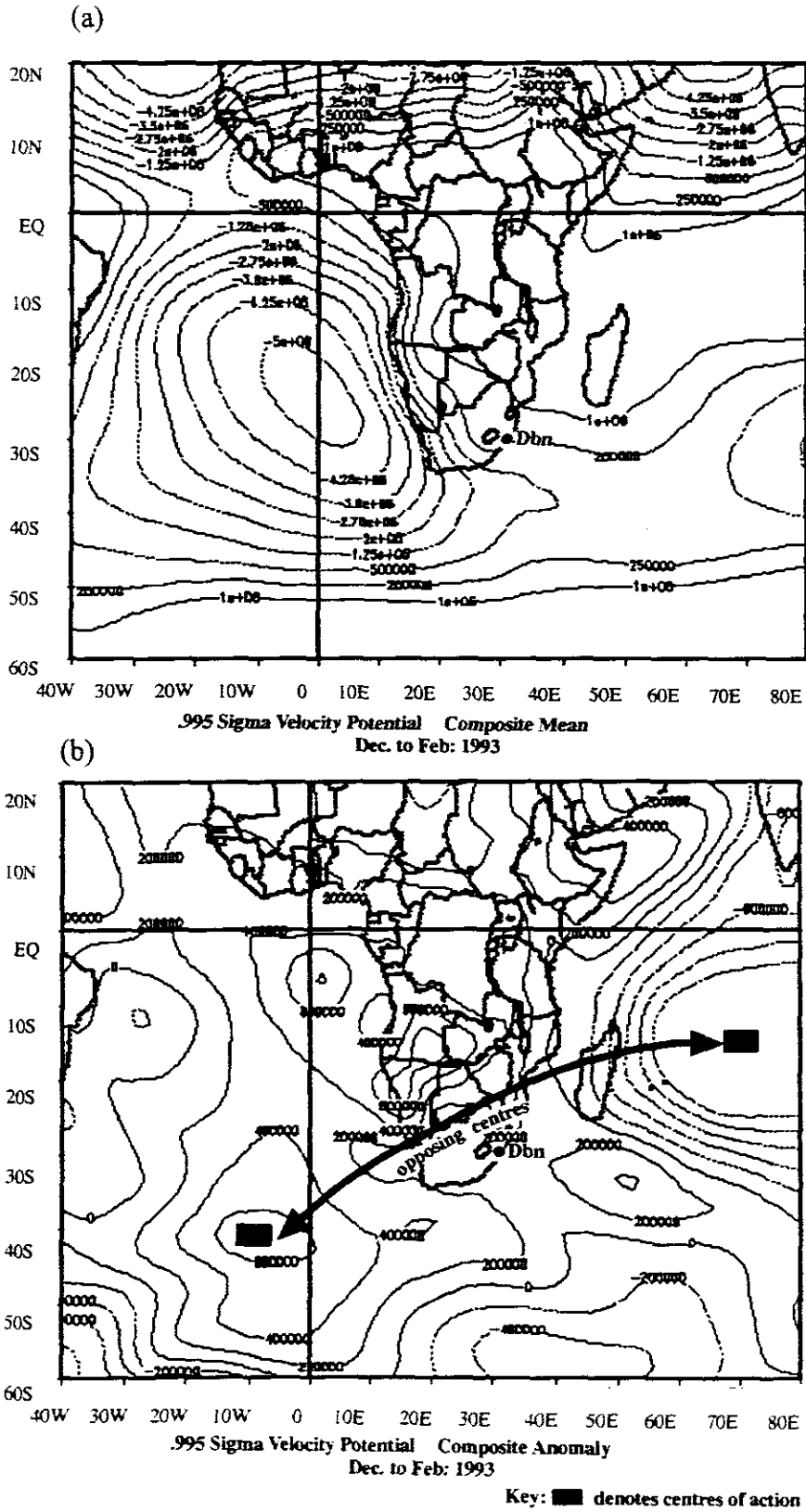


Fig. 5.12: Velocity potential ( $\text{m}^2 \text{s}^{-1}$ ) (a) mean and (b) anomalies at the 0.995 level for DJF 1992/93.

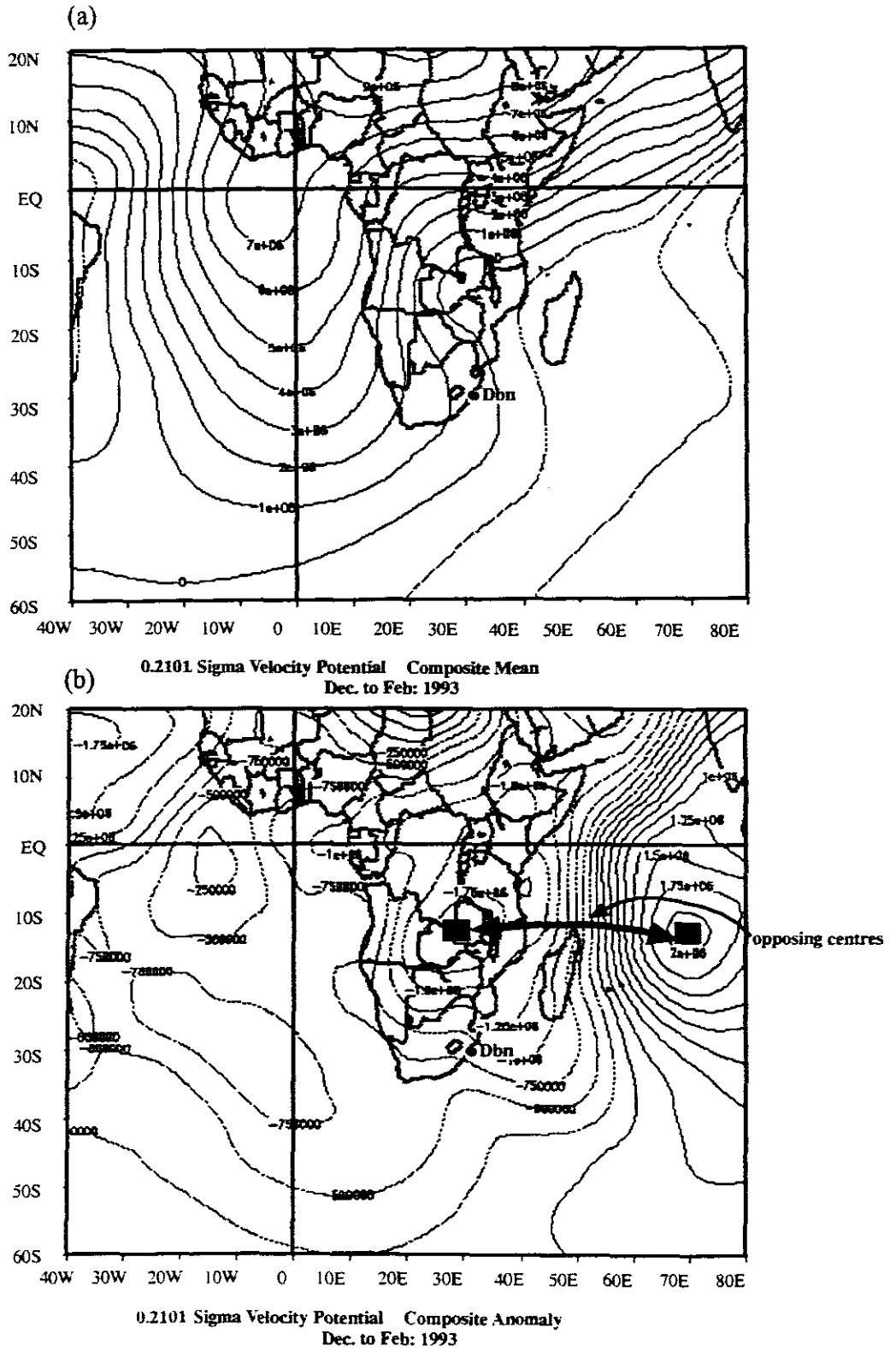


Fig. 5.13: Velocity potential ( $\text{m}^2 \text{s}^{-1}$ ) (a) mean and (b) anomalies at the 0.2101 sigma level for DJF 1992/93.

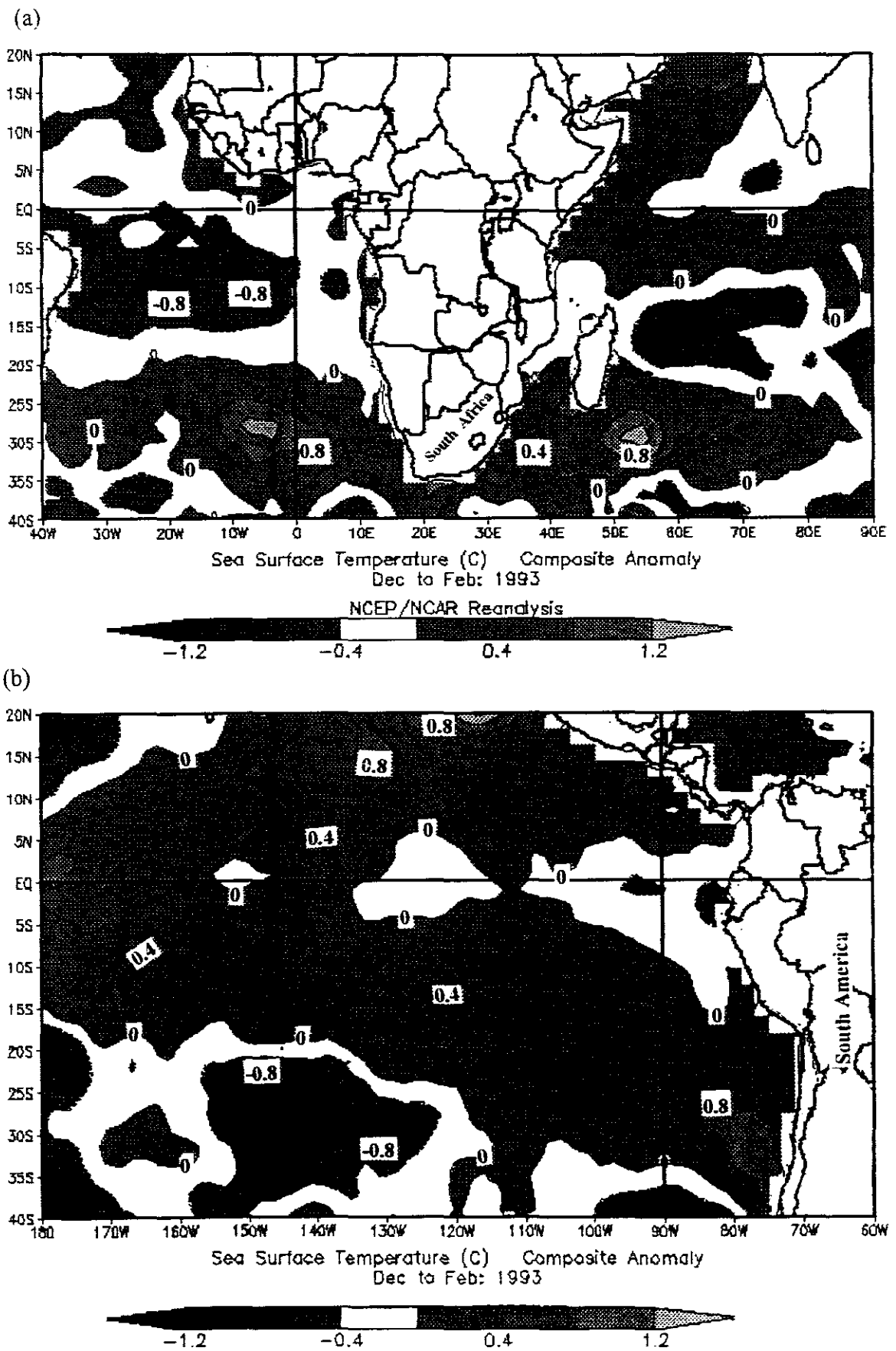


Fig. 5.14: (a) Atlantic and Indian, and (b) Pacific Ocean anomalies of sea surface temperature during DJF 1992/93.

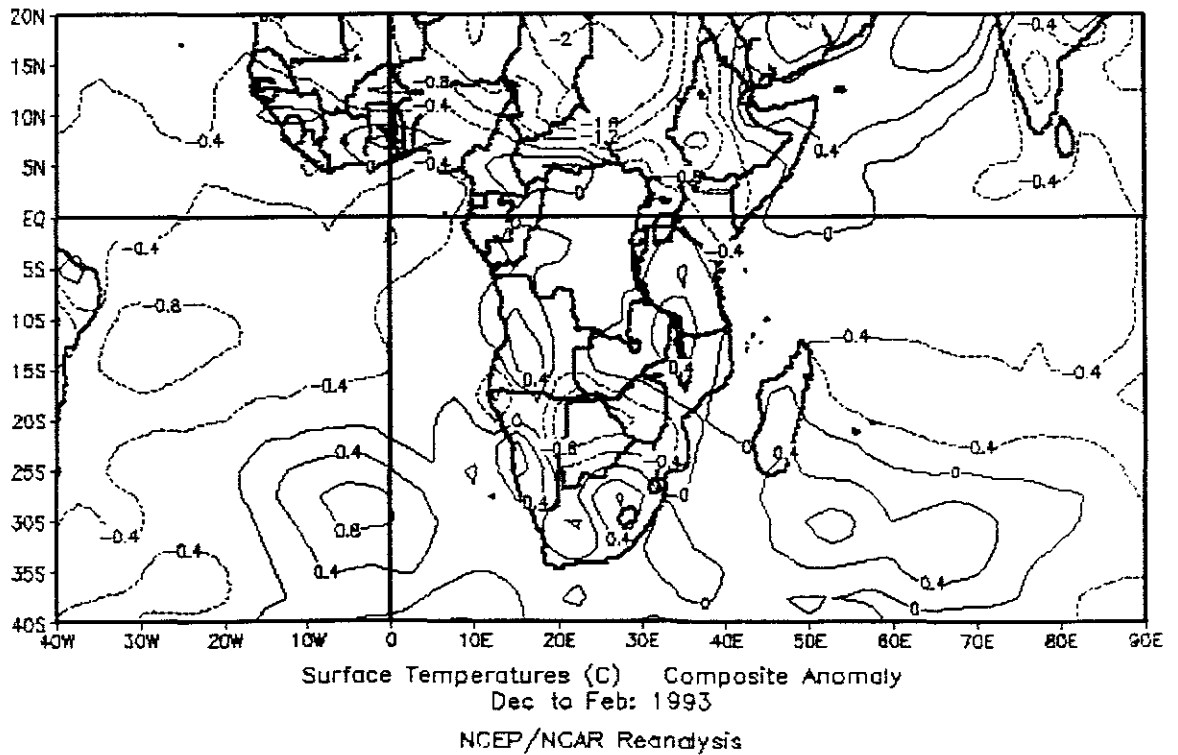
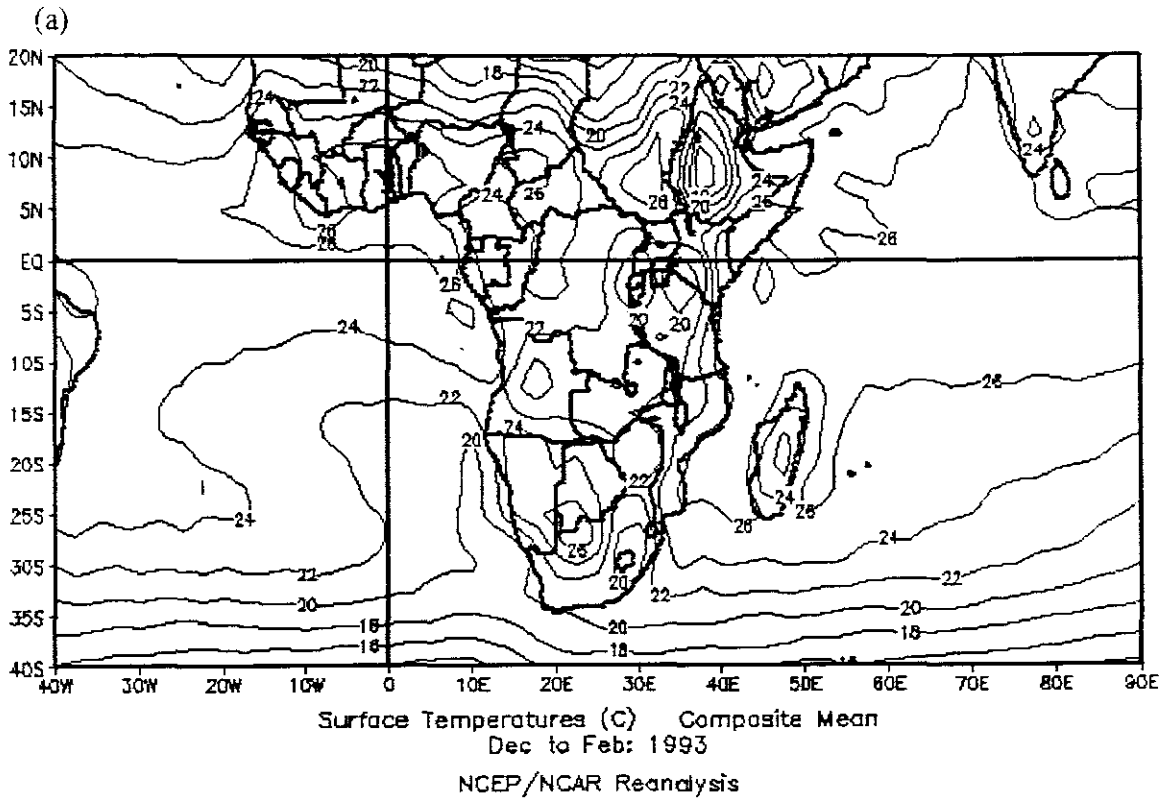


Fig. 5.15: (a) Mean and (b) anomalies of air temperature at 1000 hPa over land and sea during DJF 1992/93.

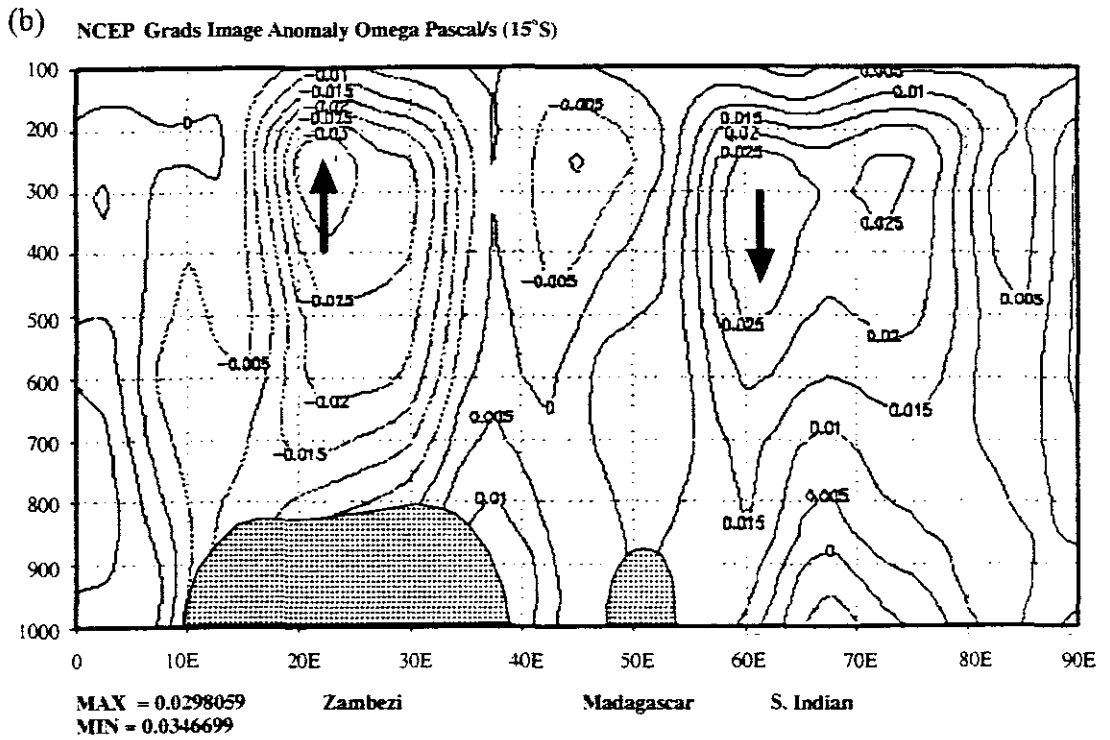
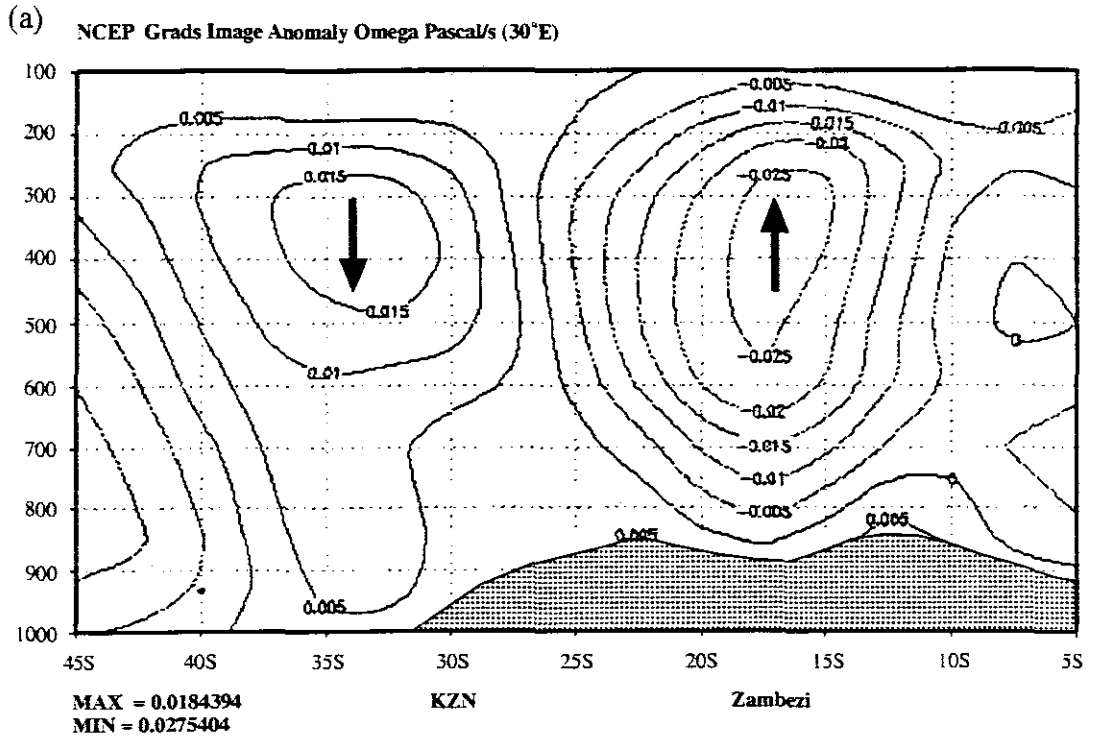
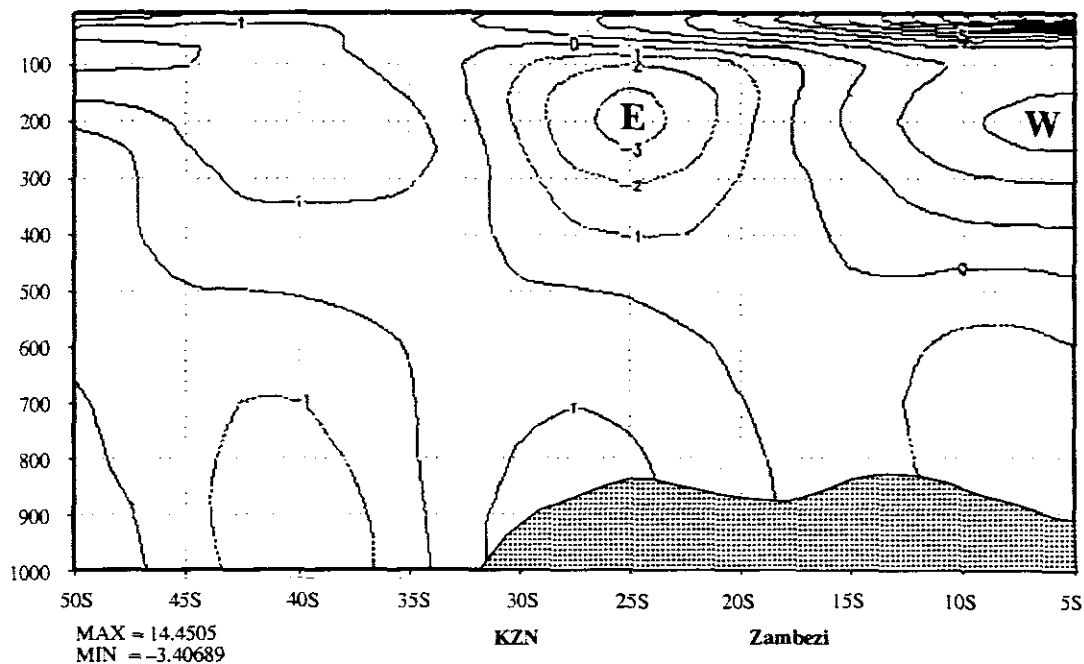


Fig. 5.16: DJF 1992/93 vertical motion (omega) anomalies between 1000 and 100 hPa levels at (a) 30°E and (b) 15°S.



(a) t: Averaged over Dec 1992 to Feb 1993  
NCEP Grads Image Anomaly uwnd m/s



(b) t: Averaged over Dec 1992 to Feb 1993  
NCEP Grads Image Anomaly uwnd m/s

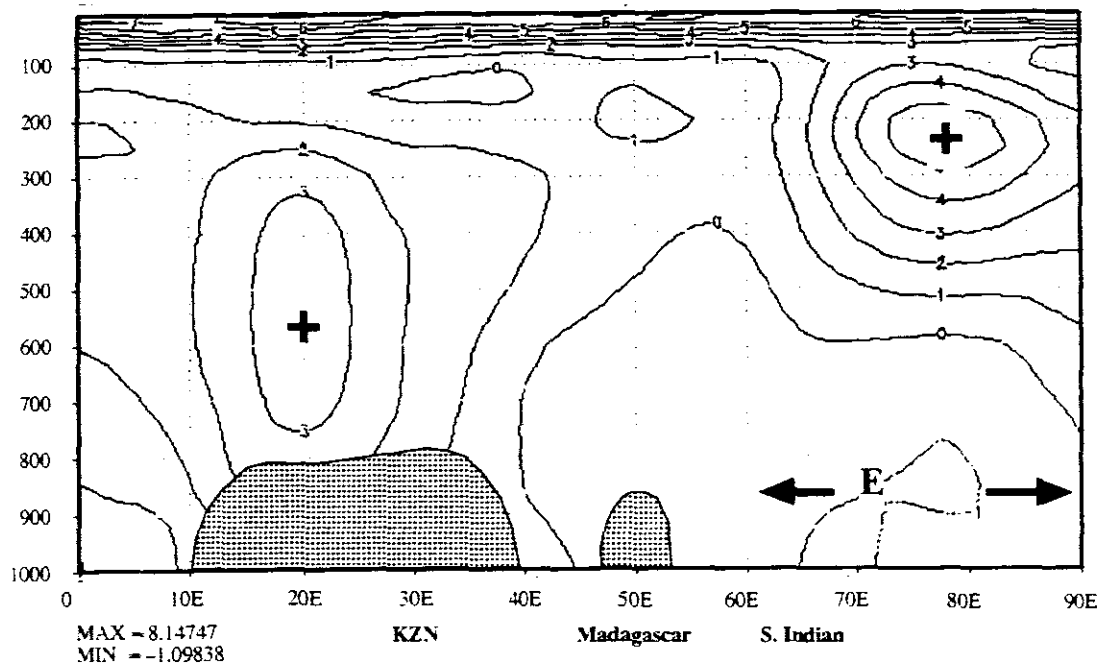


Fig. 5.18: DJF 1992/93 zonal wind anomalies between 1000 and 10 hPa levels at (a) 60°E and (b) 15°S.

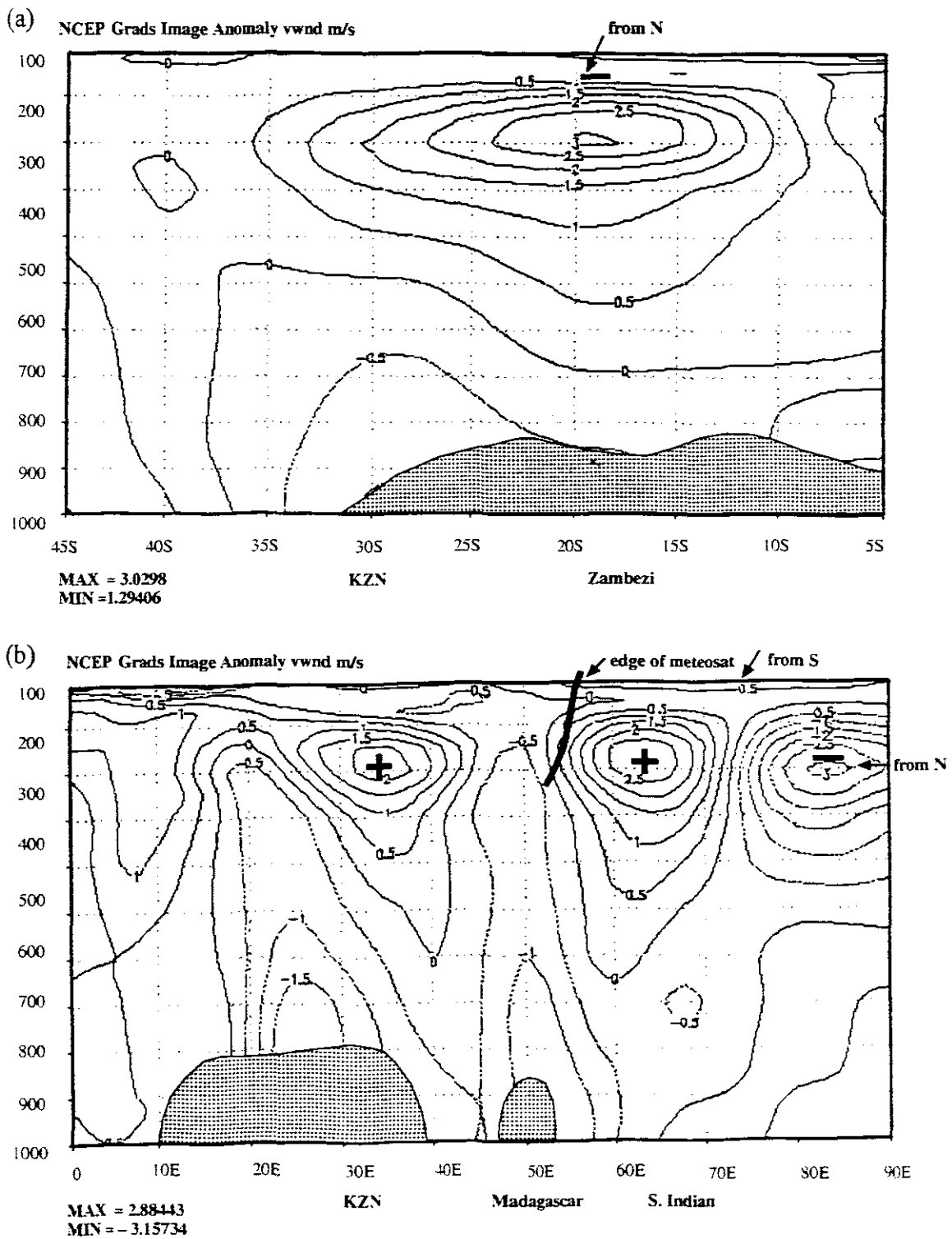
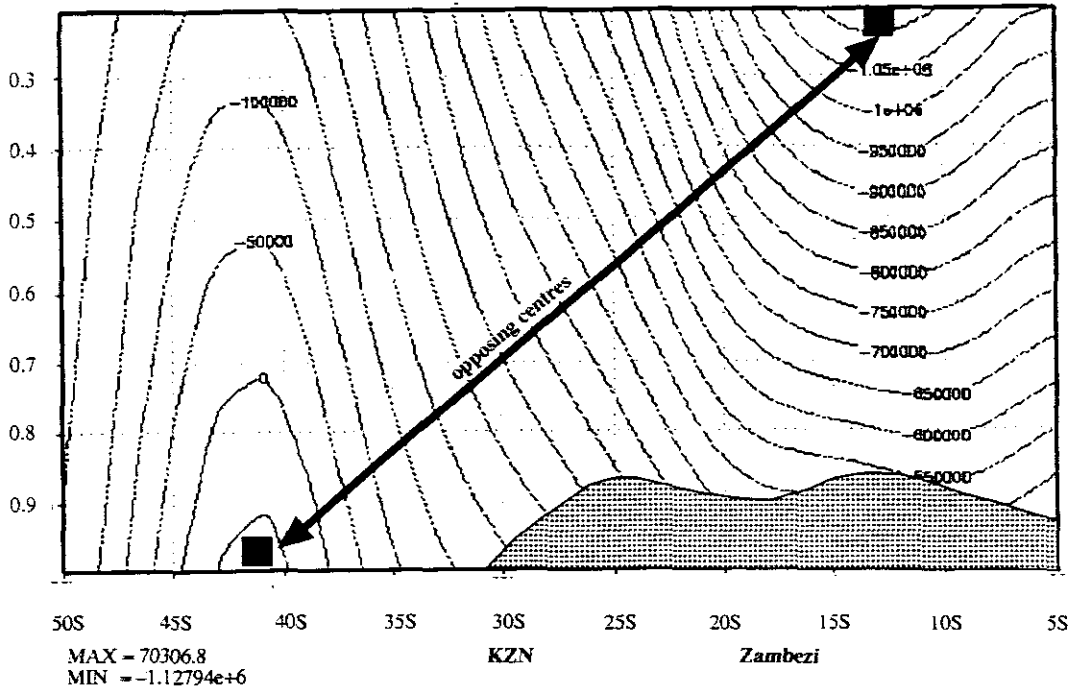


Fig. 5.19: DJF 1992/93 meridional wind anomalies between 1000 and 100 hPa levels at (a) 60°E and (b) 15°S.

(a) t: Averaged over Dec 1992 to Feb 1993  
NCEP Grads Image Anomaly  $\text{chi m}^2/\text{s}$



(b) t: Averaged over Dec 1992 to Feb 1993  
NCEP Grads Image Anomaly  $\text{chi m}^2/\text{s}$

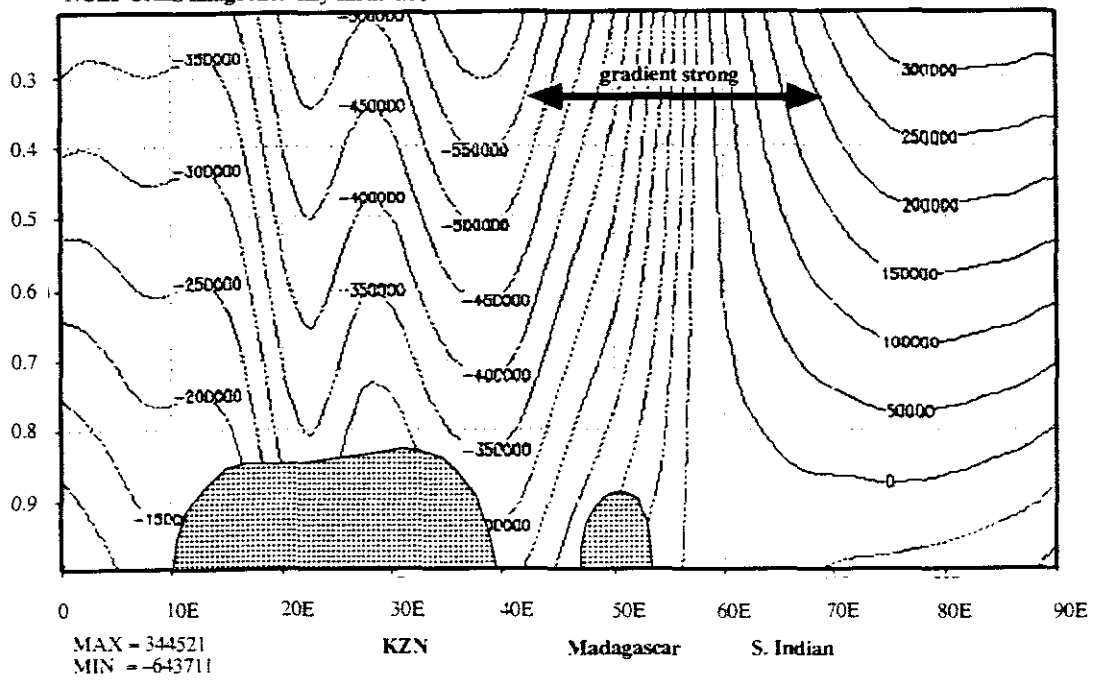
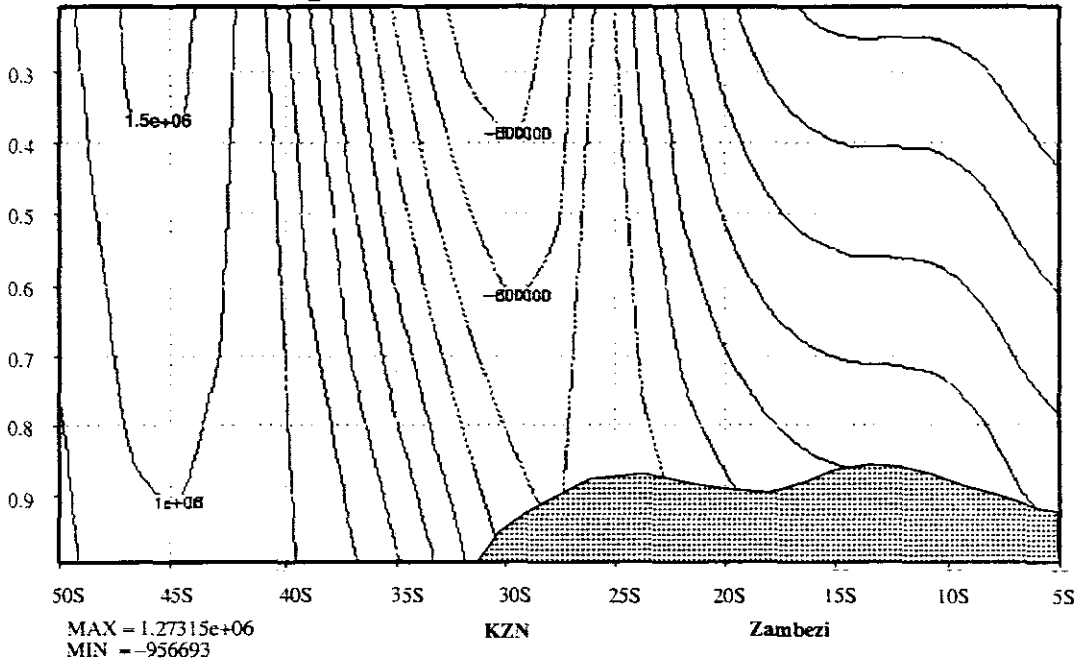


Fig. 5.20: DJF 1992/93 velocity potential anomalies between the 0.9950 and 0.2101 levels at (a) 30°E and (b) 30°S.

(a) t: Averaged over Dec 1992 to Feb 1993  
NCEP Grads Image Anomaly psi m<sup>2</sup>/s



(b) t: Averaged over Dec 1992 to Feb 1993  
NCEP Grads Image Anomaly psi m<sup>2</sup>/s

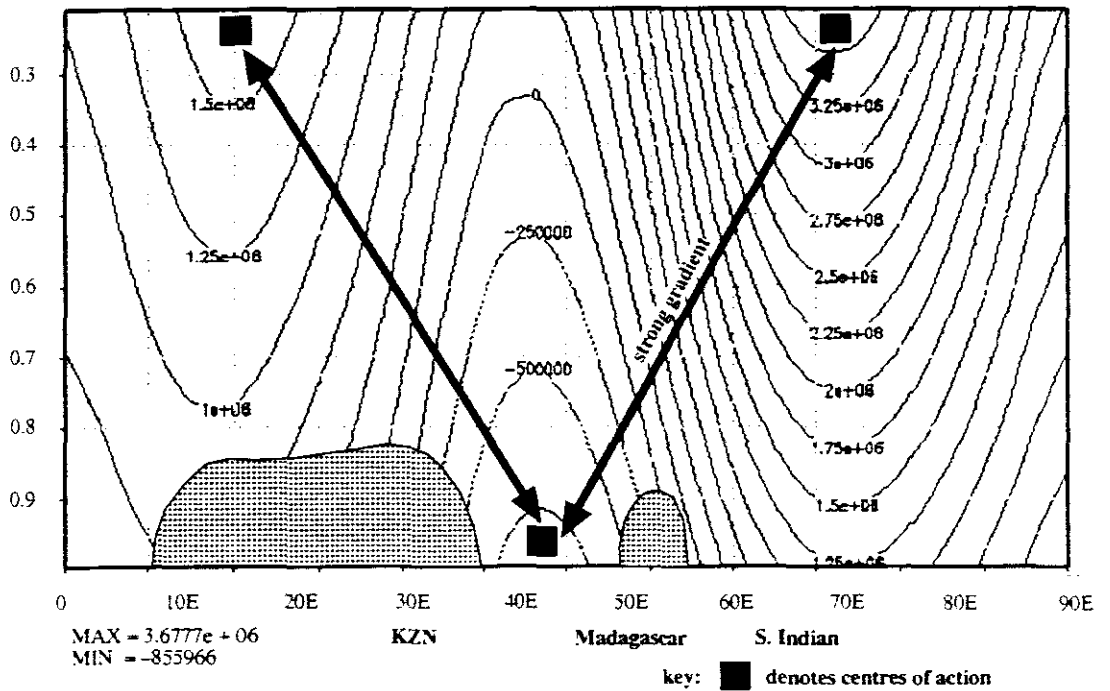


Fig. 5.21: DJF 1992/93 streamfunction anomalies between the 0.9950 and 0.2101 levels at (a) 60°E and (b) 15°S.

## **Chapter 6**

### **6: CAUSES OF THE 1992/93 DROUGHT**

#### **6.1 INTRODUCTION**

Climatological analysis in Chapters 4 and 5 indicates that subsidence and very dry conditions were obtained over the south-east and southern parts of southern Africa during the drought period of 1992/93. The objective of this Chapter is to integrate the results obtained from the ECMWF and NCEP/NOAA datasets in a form that generally describes the causes of the 1992/93 drought over KwaZulu/Natal. An analysis of the antecedent SON climatic conditions is undertaken to establish the 'memory' in the circulation structure carried to the DJF dry period. Temperature, relative humidity, wind speed, and dew point temperature station data for Estcourt, Cedara (Pietermaritzburg) and Durban obtained from the South African Weather Bureau are used to quantify evaporative losses and associated boundary layer conditions over KwaZulu/Natal.

#### **6.2 ANTECEDENT (SON) CONDITIONS**

##### **6.2.1 GEOPOTENTIAL HEIGHTS**

Pressure is anomalously high over the Indian and Atlantic Oceans from the surface to 200 hPa whilst low pressure anomalies are obtained over southern Africa during the antecedent SON period (Fig. 6.1a-c). At the same latitudes where high pressure anomalies are centred ( $50^{\circ}\text{S}$ ), low pressure anomalies are observed during the dry summer (DJF) period (Figs. 5.1b, 5.2b and 5.3b). The high pressures over the surrounding oceans intensify with height during SON. The compressed pressure gradient to the south of South Africa has

similar strength in SON and DJF seasons from 850 hPa to 200 hPa levels (Figs. 5.1-5.3 and 6.1-6.3). This suggests that a semi-stationary Rossby wave in the westerlies had a contribution to the occurrence of drought in 1992/93 over KwaZulu/Natal and other parts of southern Africa.

## 6.2.2 WIND VECTORS

There are no significant differences in the mean wind vector regimes from the surface to upper levels during SON and DJF (Figs 5.4-5.6 and Figs. 6.4-6.6). Anomalies of surface winds are easterly throughout southern Africa and the surrounding oceans except the eastern parts of South Africa where westerlies prevail (Fig. 6.4b). Anticyclonic anomalies are observed over the Indian and Atlantic Oceans and cyclonic circulation occurs between 25 and 45°S. The topographic effect on winds, divergence and offshore flow over KwaZulu/Natal are apparent in the Figure. Wind vector anomalies at the surface during SON 1992/93 show a different flow pattern to the DJF pattern where cyclonic anomalies occurred south of 20°S west of 20°E and anticyclonic anomalies occurred to the west of 30°S north of 40°S (Fig. 5.4b). Winds are westerly to the south of South Africa between 30 and 40°S during the peak summer season while the domain of westerly winds is narrow and restricted only to the eastern parts of KwaZulu/Natal during the antecedent SON period. It is thus concluded that the widening of the westerly wind anomaly domain during the DJF season contributed to the occurrence of drought over KwaZulu/Natal and other parts of southern Africa.

Wind vector anomalies south of 20°S at 500 and 200 hPa levels during SON (Figs. 6.5b and 6.6b) show an inverse pattern to the DJF pattern (Figs. 5.5b and 5.6b). To the north of 20°S the wind anomaly pattern is comparable during the antecedent and peak summer seasons. The change in wind regime is thus a contributory factor to the occurrence of drought south of 20°S.

### 6.2.3 OUTGOING LONGWAVE RADIATION

Mean OLR over KwaZulu/Natal is of the order of  $\sim 15 \text{ W m}^{-2}$  higher during SON compared to DJF (Figs. 5.7a and 6.7a). The OLR anomaly field is negative throughout southern Africa and the surrounding oceans during the pre-summer period (Fig. 6.7b). Over KwaZulu/Natal anomaly values of  $-4$  are obtained in contrast to positive values of the order of  $3$  obtained during the peak dry summer period (DJF). The atmospheric wave train pattern during SON is aligned in the same axis as in the DJF season but the anomaly values are higher in the latter season. This is an indication that even during the pre-summer season convection is suppressed over KwaZulu/Natal and parts of southern Africa south of  $20^{\circ}\text{S}$  shown in the previous Chapter.

### 6.2.4 SEA SURFACE TEMPERATURES

The strength of cool SSTs in the Indian Ocean between  $70$  and  $80^{\circ}\text{S}$  during SON is lesser than during the DJF period (Fig. 6.8). At the same time, the strength of warming anomaly to the south of Madagascar increases from the SON (maximum anomaly of  $0.3$ ) to DJF (maximum of  $1$  at  $40^{\circ}\text{S}$ ) period. The Atlantic Ocean is cool north of  $20^{\circ}\text{S}$  and warm southward. During SON cool SSTs are observed throughout the South Atlantic Ocean.

The equatorial Pacific is cool during SON while warming occurs during the drought season. The warming is too small a magnitude ( $\sim 0.3$ ) to be considered an El Nino type of signal for southern Africa. The prominent SST signal is that of the immediate oceans, particularly the Indian Ocean, that bore an effect on drought over southern Africa. The Atlantic and Indian Oceans

are indicating a weak anti-phase pattern. The warming of the Indian Ocean to the south-west of Madagascar may be responsible for the 'pulling effect' of water vapour flux from KwaZulu/Natal (Figs. 4.4 and 4.5) to this region of warm SSTs. The cool SSTs to the west of Madagascar between 15 and 20°S induced a westward directed zonal cell at these latitudes.

#### 6.2.5 PRECIPITABLE WATER

Mean precipitable water over KwaZulu/Natal are of the order of  $\sim 6 \text{ kg m}^{-2}$  lower during the antecedent period relative to the peak summer period (Figs. 5.8a and 6.9a). This suggests that the low pressure anomalies observed in the geopotential height field were a dry system. The anomaly field shows a wave train pattern oriented to a similar axis to the DJF pattern (Figs. 5.8b and 6.9b). No propagation of these wave trains is observed. The values of below normal precipitable water within these axes increase to the peak summer season.

#### 6.2.6 VERTICAL MOTION (OMEGA)

An alternating south-north pattern of negative and positive vertical motion wave trains are obtained in the vertical motion mean and anomaly fields, mainly south of 10°S (Fig. 6.10a and b). Subsidence occurs over eastern parts of South Africa having intensified during the peak summer period (Fig. 5.9b). A strong anomaly gradient at 30°S/35°E implies divergence and strong offshore winds over KwaZulu/Natal during the SON period. This gradient is, however not observed during the DJF season but strong subsidence (positive vertical motion) anomalies in this area still persist.

Cross -sections at 30°E and 15°S are indicative of the alternating patterns of subsidence and rising motions similar to the DJF omega structure (Figs. 6.11 and 5.16). The descending (rising) motion is sustained over the Zambezi

(South Africa) as during the peak summer period. The persistence of the north-south overturning between these areas implicates the Zambezi's drainage of water vapour flux from the south into its rising cell in the occurrence of the drought.

#### 6.2.7 STREAMFUNCTION

The streamfunction anomaly field shows anticyclonic motion centred at 50°S over the Indian and Atlantic Oceans and cyclonic anomalies over southern Africa at the 0.2101 (surface) and 0.995 (upper) sigma levels (Fig. 6.12a and b). The high pressure anomalies over the surrounding oceans are centred at 30°S. These circulation patterns are in agreement with the geopotential anomaly field during the pre-summer SON season. It is the southward migration of anticyclonic anomalies over the oceans of South Africa which allowed for low pressure systems to set in over southern Africa thus giving a circulation regime slightly opposite to the peak summer pattern.

#### 6.2.8 VELOCITY POTENTIAL

Surface velocity potential anomaly field is divergent over the Indian and Atlantic Oceans and convergent over the subcontinent (Fig. 6.13a). At upper levels, convergence sets in over the surrounding oceans (Fig. 6.13b). Weak convergence occurs over land south of 20°S and strong convergence occurs northward. A wave train pattern is discernible at the 0.995 (0.2101) sigma level such that a south-east to north-west oriented convergent (divergent) anomaly running through southern Africa is located between divergent (convergent) anomaly fields over the Indian and Atlantic Oceans. During the peak summer season, the Indian and Atlantic Ocean circulations were anti-phase at the surface and upper levels (Fig. 5.12b and 5.13b), but show in-phase tendencies in the pre-summer velocity potential anomaly field (Fig. 6.13b).

## 6.3 DISCUSSION OF 1992/93 (DJF) DROUGHT

### 6.3.1 JET STREAM INFLUENCE

The dominant climatic feature during the 1992/93 summer drought is negative geopotential anomalies to the SW of Africa, associated with increased upper westerly flow and low amplitude transient Rossby waves. As a result of the persistence of these perturbations, an unstable vortex of low pressure occurred to the south of the continent and anticyclonic activity, blocking the zonal passage of storms, dominated the interior of South Africa.

A compressed thermal gradient to the southeast of South Africa between 30° and 35°S at 200 hPa occurred during the dry 1992/93 summer period as a result of the southward shift of the subtropical jet stream and northward shift of the subpolar jet (Fig. 6.14a) caused by the warm SSTs between 40 and 80°E at 30°S (westerly thermal wind) and cooler SSTs between 50 and 120°E at 10°S. This coincided with an upper-level anticyclone centred at about 25°S. The two jet streams dilated to the east of 35°S and the northward movement of the subtropical jet coupled with cyclonic motion to the east of Madagascar at about 20°S, 45°E produced wet conditions there. A positive (negative) V wind component to the south-west (south-east) of South Africa and a negative (positive) V component to the north-west (north-east) produced a northward (southward) directed pressure gradient which was conducive to the occurrence of the dry circulation regime over southern Africa. A high centred over Botswana and low south of South Africa suggests a transfer of kinetic energy from the interior lands to the south of South Africa.

*This therefore suggests that the subtropical jet stream shifted southward over southern Africa during dry 1992/93 summer period while the subpolar jet*

shifted further equatorward. Barclay's (1992) dry troughs analysis also suggests this pattern. Diagnostic models presented in Figures 6.14a and b describe the unique circulation structure of the 1992/93 drought season.

Mulenga's (1998) PC5 shows a strong U wind component to the south of South Africa during the drought period of 1992/93 consistent with the compressed geopotential gradient to the south of South Africa. Weak vertical motion observed over South Africa was not favourable to convection and hence dry conditions prevailed.

A shift in the position of the subtropical jet stream and its wave 6 pattern produced a diminution of summer rainfall in association with warming of the south-east Indian Ocean. A ridge in the analysis situated at 30°E is not favourable for an influx of moist air from the Mozambique Channel. It is associated with the location of the descending Hadley limb over South Africa and the reduction of rainfall (whilst a trough to the east of Madagascar enhances rainfall) over most parts of southern Africa south of 20°S. Figure 6.14b is a model indicating the influence of winds and Indian SSTs on rainfall over southern Africa during the 1992/93 drought season. Cooler SSTs over the east coupled with a strong velocity potential anomaly gradient (Fig. 5.13) generate easterly anomalies over the Zambezi (Fig. 5.17a) and ascent there (while enhancing descent at 30°S) (Fig. 5.16a).

#### 6.3.1.1 JET STREAM DYNAMICS

The distribution of divergence and convergence at jet stream level can be inferred from the vorticity equation  $\partial/\partial t (\zeta+f) = -(\zeta+f) \text{DIV}$  (Hastenrath, 1991), where  $f$  is the Coriolis parameter,  $\zeta = -\partial u/\partial y$  is relative vorticity, and DIV divergence. From the isotach pattern in Fig 6.15,  $\zeta$  is positive to the right of the jet axis and negative to the left. The largest value of  $\zeta$  occurs at

the longitude of the jet maximum. The absolute vorticity  $\zeta_a = (\zeta + f)$  is largest positive to the right of the jet maximum, and smallest positive (or negative) to the left. As the left-hand term of the vorticity equation denotes the rate of change of absolute vorticity following the motion, the sign convention for the left-hand side dictates divergence in the left rear (IV = South Africa) and convergence in the left front (III = Indian Ocean) quadrant. To the left of the jet axis  $\zeta$  has a sign opposite to  $f$ , making  $\zeta_a$  less positive, so that convergence occurs in the right rear (I) and divergence in the right front (II) quadrant.

The vector difference from the geostrophic wind (Haltiner and Williams, 1980; Holton, 1972; Palmén and Newton, 1969) dictates an increase in wind speed along the direction of flow in the entrance region of the jet, so that the geostrophic departure is such that there is a transfer of momentum from South Africa to the south of the continent. Conversely, deceleration takes place in the exit region, corresponding to a geostrophic departure vector directed northward from the Southern Ocean. These cross circulations are consistent with the surface convergent and divergent patterns over Madagascar and South Africa, respectively, in the 1992/93 mid-summer period presented in the previous Chapter.

The Rossby wave during the 1992/93 summer drought had a zonal wavelength of  $\sim 4 \times 10^3$  km ( $L_x$ ) and latitudinal width of  $\sim 2 \times 10^3$  km ( $L_y$ ). The calculated wave speed relative to the zonal flow from the equation for a Rossby wave  $c_x - u = - [\beta / (k^2 + m^2)]$  (Fleagle and Businger, 1980; Haltiner and Williams, 1980; Holton, 1972; Palmén and Newton, 1969; Panchev, 1985), where  $c_x$  is zonal phase speed,  $u$  the mean zonal wind velocity,  $\beta = \partial f / \partial y$  (the rate of change of the Coriolis parameter with latitude,  $k (\equiv 2\pi/L_x)$  and  $m (\equiv 2\pi/L_y)$  the zonal and meridional wave-numbers, respectively, is  $2.4 \text{ m s}^{-1}$ . This suggests that this synoptic scale Rossby wave moved very slowly, hence the below-normal rainfall event persisted from 1991 to 1994 over

KwaZulu/Natal (Fig. 3.6).

### 6.3.2 TROPICAL INFLUENCES

Over most parts of the summer rainfall region of South Africa, enhanced rainfall is associated with airflow with a northerly component at both the surface and at 500 hPa. These rain-bearing winds are consistent with deep tropical low-pressure disturbances which extend to at least 500 hPa, either in the form of easterly waves or lows forming over Botswana and adjacent regions (D'Abreton and Tyson, 1996; Preston-Whyte and Tyson, 1988). The absence of these winds during the 1992/93 dry summer period thus limited moisture influx into KwaZulu/Natal. The advection of dry air from the south sweeping through the Karoo into KwaZulu/Natal contributed to drought conditions. The hemispheric wave trains in water vapour are part of the 'atmospheric conspiracy' to inflict dry conditions over KwaZulu/Natal (Fig. 5.7b). Major water vapour source regions for South Africa are east Africa and the Indian Ocean south of the Equator. The south-westerly transport of dry subsiding air from the direction of Gough Island in the South Atlantic Ocean into South Africa has been shown to be a feature of no-rain days (D'Abreton and Tyson, 1996). Thus, the moisture-laden air from the tropical region in the north would have been conducive to rainfall.

Water vapour flux values were very low, more typical of winter. Values of  $8 \text{ g kg}^{-1} \text{ m s}^{-1}$  were observed over KwaZulu/Natal and Namibia in contrast with values exceeding  $50 \text{ g kg}^{-1} \text{ m s}^{-1}$  over the Cape and Mozambique coasts and the Congo Basin. The area of water vapour flux values  $< 15 \text{ g kg}^{-1} \text{ m s}^{-1}$  extended from 15 to 33°S and 15 to 35°E, covering most of southern Africa. In such a dry environment even relatively strong uplift could not initiate the convective rainfall typical of summer.

A dipole in the velocity potential field is observed (Fig. 5.13b). This dipole meant the advection of moisture from the Indian Ocean into the Zambezi while depriving areas south of 15°S of rainfall. At lower levels, a large cyclonic gyre that developed over the southern Mozambique Channel in the 1992/93 mid-summer modulated moisture flux into Madagascar while depriving South Africa of rainfall. This reinforces the observation that a north-eastward advection of dry subtropical air from the South Atlantic was a limiting factor in dry mid-summer of 1992/93.

### 6.3.3 EFFECTS OF LOCAL TOPOGRAPHIC CIRCULATIONS

Low level southerly flow along the eastern Escarpment persisted over KwaZulu/Natal. These winds were light and variable and topographically induced descent of air was pronounced during the 1992/93 dry summer event. Meso-scale circulation over KwaZulu/Natal is well documented (Preston-Whyte, 1968a and b, 1969, 1974 and 1975; Preston-Whyte and Diab, 1980; Preston-Whyte, Diab and Tyson, 1977; Tyson, Preston-Whyte and Diab, 1976; Tyson and Preston-Whyte, 1972). Under strong north-east gradient wind conditions the amplitude of the diurnal variation of wind direction is reduced and components of air movement normal to the coast are weak. The dominance of anticyclonic conditions and the entrainment of local winds into the gradient wind produced increased stability.

The local effects of topography on rainfall over KwaZulu/Natal during the 1992/93 drought season is apparent from winter and summer anomaly fields (Figs. 4.4 and 4.5). To the east of the KwaZulu/Natal escarpment, water vapour is 'pulled' offshore under the influence of westerlies. To the west of the topographic feature, water vapour is drained into the cyclonic wave-path at 20°S. Both these effects kept KwaZulu/Natal dry. The flow is along the topographic gradient in the summer anomaly field (Fig. 4.5) implying that large-scale effects were important in depriving KwaZulu/Natal of rainfall. As

a result of confluence at 20°S (Figs. 4.3a and 4.7) a wave train axis of wet conditions (Fig. 5.7b) is observed in this region while a divergent axis to the south produces a below-normal rainfall scenario.

Evaporative losses over KwaZulu/Natal calculated from the Meyer Equation  $E = c(e_s - e_a)(1 + V/10)$ , where  $c \approx 0.36$ ,  $e_s$  is saturation vapour pressure,  $e_a$  is vapour pressure and  $V$  is wind speed (Schulz, 1976) for different places in a transect from the Escourt to Durban, are given in Table 6.1. Evaporation is higher over Durban indicating that the drought effect was more pronounced over coastal areas of KwaZulu/Natal. Above normal surface temperatures over southern Africa led to such high evaporative losses which contributed to a decline in agricultural production, vegetation cover, and dam and stream-flow levels presented in Chapter 3.

Average daily specific humidities for the 1992/93 DJF season estimated from  $q = 0.622e/(p-0.378e)$  (Byers, 1959; McIlveen, 1986; Preston-Whyte and Tyson, 1988) are  $1 \times 10^{-2}$ ,  $1.6 \times 10^{-2}$  and  $1.8 \times 10^{-2}$  g kg<sup>-1</sup> over Escourt, Cedara and Durban, respectively. Higher values over Durban and Cedara may be due to the local ocean effect. Any form of precipitation was not possible under an atmosphere so extremely dry.

#### 6.3.4 BUDGET CALCULATIONS

Comparisons of the magnitudes of the anomalies for the analysed variables and their respective composite means for SON 1992 and DJF 1992/93 for KwaZulu/Natal and others teleconnection centres are given in Table 6.2a and b. The budget calculations have been computed as ratios of anomalies with respect to composite means for the specific meteorological variables analysed. Variables displaying greatest departures from their composite means ( $\geq 10^\circ$ ) are velocity potential, vertical motion and streamfunction. Of interest to note

is that vertical motion had departures of the order of  $10^1$  over KwaZulu/Natal during DJF and  $10^0$  at  $60^\circ\text{E}$ ,  $15^\circ\text{S}$  during SON 1992 and DJF 1993 thus reinforcing the N-S Hadley overturning as important in depriving the eastern parts of South Africa of rainfall. This and the evidence presented previously suggests that kinematic (rotational) properties of the circulation structure had more contribution to the occurrence of the drought than thermodynamic properties. Positive (negative) vertical motion over KwaZulu/Natal (Zambezi) was a response to these kinematic adjustments over southern Africa, and hence the north-south Hadley overturning between South Africa and the Zambezi implied an anti-phase circulation regime. This together with mesoscale internal dynamics in the meteorological structure of KwaZulu/Natal, sustained the drought for at least three years (Fig. 3.6).

### 6.3.5 REGIONAL CLIMATIC PATTERNS

Regional climatic patterns inimical to wet conditions in KwaZulu/Natal in 1992/93 can be summarised as:

- (i) a subtropical upper trough anomaly over eastern Africa;
- (ii) A low to the south of South Africa enhancing the transfer of momentum to the south;
- (iii)  $> 5 \text{ m s}^{-1}$  stronger upper level westerly winds to the south;
- (iii) weak marine winds and cool sea temperatures to the south-west and east;
- (iv) a more intense anticyclonic gyre in the south-west Indian Ocean;
- (v) an upper level anticyclonic vorticity anomaly across the mid-latitudes;
- (vi) surface divergence and upper convergence of the order of  $2 \times 10^6 \text{ s}^{-1}$  over KwaZulu/Natal.
- (vii) upper level north-westerly flow anomaly to the south-east;
- (viii) a non-convective band that extends north-west-south-east into the mid-latitudes;
- (ix) an association with drought off equatorial east Africa;
- (x) upper velocity potential dipole and Indian ITCZ to Zambezi;

(xi) wave trains and teleconnections with other centres of action in the region.

These patterns limit the development of cut-off low pressure systems, ridging anticyclones and tropical-temperate trough formation which are major rainfall-producing circulation systems over KwaZulu/Natal.

#### 6.4 SYNTHESIS

The analysis of the 1992/93 drought presented in the preceding sections of this thesis also occurred during the 1982/83 drought when, *inter alia*, pressures increased over South Africa, the upper circulation dominated by westerlies and low-level southerly flow persisted over the Mozambique Channel. Anticyclonic vorticity and subsidence via upper level convergence during the 1992/93 drought period suppressed convection in the manner similar to that of the 1982/83 drought period. The OLR series of February 1983 is similar in its pattern and magnitude to that presented in the preceding Chapter of this thesis.

Figure 6.17 is a conceptual model of meteorological influences producing below normal rainfall scenario over KwaZulu/Natal and Table 6.3 details the jet stream effect on rainfall of the eastern South Africa. During the 1992/93 summer season the region of ascent in the western limb of the Indian Ocean cell of the Walker circulation was eastward. The analyses point to the relocation of the locus of major convective activity and heat release eastward, westerlies dominant over Africa at 200 hPa, continental convection reduced, the meridional flux of energy over southern Africa having diminished, and the meridional temperature gradient increased as suggested by Harrison (1986) and Preston-Whyte and Tyson (1988). The westerly storm tracks moved north and decreased advection of thermal vorticity weakened westerly disturbances. Because of the eastward movement of the region of major convective activity, cloud bands formed preferentially over the Madagascar

region while most of central southern Africa lost its major contributor to annual rainfall.

Drier conditions therefore set in over large areas of South Africa (Figs. 4.15a and b) as the thermal low weakened and pressure increased over land. A negative surface pressure anomaly occurred near Gough Island and a positive anomaly in the vicinity of Marion Island in agreement with Tyson (1986). The intrusion of subtropical westerly flow above 500 hPa observed in the analysis is a feature typical of the global El Niño dry season (Jury and Lyons, 1994) and has been found to reduce the potential for development and maintenance of tropical cyclones and subsequently affecting their frequency, intensity and regional impact (Parker and Jury, 1997).

Jury's (1992) pre-summer (October-November 1991 period) analysis shows that SST in the central Indian Ocean had departures of 1 above normal, while low level westerly anomalies and upper level easterly anomalies developed off east Africa. Analysis of the 1992/93 summer seasons indicates a warming anomaly of the order of  $\sim 0.3$  above normal. Surface air temperatures were about 2 above normal during the 1992 pre-summer season (Jury, 1992) in contrast to lesser anomalies ( $\sim 1$ ) during the 1992/93 peak summer season obtained from surface measurements presented in Chapter 3. A weak ENSO influence is observed in the analysis whilst the QBO played no role in inducing drought over KwaZulu/Natal. SSTs are warm to the SE of Africa and this has been shown to be a characteristic feature of a below normal rainfall scenario over the SE Africa region by Jury (1992). As the Indian Ocean to the south-east of South Africa (PC7 region in Mason *et al.* (1994) SST analysis) warms and cools so the pattern of baroclinic westerly waves over the country adjusts. Anomalous warming is associated with an easterly movement of the locus of most frequent occurrence of upper-level wave troughs as discussed in Chapter 2.

OLR analysis indicates that convection was strongly suppressed. OLR values exceeded  $240\text{Wm}^{-2}$  over most of southern Africa during the 1992 /93 summer (Figs. 4.9 and 4.8). Positive OLR anomalies of over 40 were reached (Fig. 4.9) as a result of sinking motions and increased anticyclonic vorticity. The OLR analysis shows a local dipole formed with positive anomalies indicating sinking motions over the South Africa in contrast with negative anomalies and rising motions over the Mozambique Channel ( $40^{\circ}\text{E}$ ) during the drought period.

## 6.5 CONCLUSION

The causes of the 1992/93 drought over KwaZulu/Natal can be summarised as follows:

1. The 1992/93 dry event was dominated by an upper level acceleration of westerly flow across a trough over South Africa. The upper circulation was dominated by a stationary wave in the westerlies over the South Atlantic which brought dry air to KwaZulu/Natal. Anticyclonic vorticity and subsidence via upper level convergence suppressed convection over KwaZulu/Natal.
2. Winds had a major influence in the production and persistence of the drought over KwaZulu/Natal through the northward (southwards) movement of the subpolar (subtropical) jet streams.
3. Wave trains have been observed in some of the variables analysed but no propagation of these systems occurred from the antecedent period SON to the DJF period. SON analysis suggests that the strength of dryness was intensifying with time.

4. A significant 'memory' was thus carried to the DJF from the SON period. The widening of the westerly wind anomaly domain and Indian Ocean cool and warm SST 'spots' during the DJF season, relative to SON, provide the most obvious evidence of this. A semi-stationary Rossby in the westerlies wave with a speed of  $2.4 \text{ m s}^{-1}$  is implicated in to the occurrence of drought in 1992/93 over KwaZulu/Natal and other parts of southern Africa.
  
5. The QBO and El Nino did not imposed significant influences on rainfall over South Africa. The prominent SST signal is that of the immediate oceans, particularly the Indian Ocean, that bore an effect on drought over southern Africa.
  
6. The cool SSTs to the west of Madagascar between 15 and 20°S induced a westward directed zonal cell at these latitudes producing an anti-phase mode in the circulation structure of South Africa and the Zambezi.
  
7. The deficiency of moist inflows from the major water vapour source regions of east Africa and the Indian Ocean south of the Equator was one of the dominant limiting factors to rainfall production.
  
8. The kinematic (rotational) properties of the circulation structure had more contribution to the occurrence of the drought than thermodynamic properties. The north-south Hadley overturning between South Africa and the Zambezi which developed as a result of the kinematic adjustments and the internal dynamics in the meteorological structure of the 1992/93 period over KwaZulu/Natal both explain the occurrence of drought during this period.

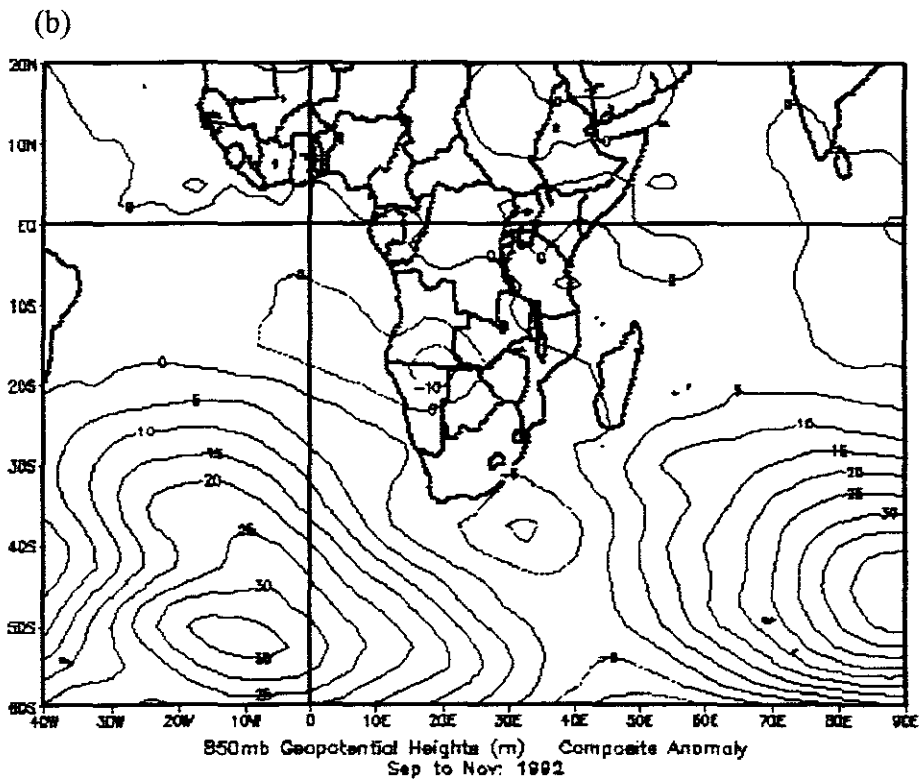
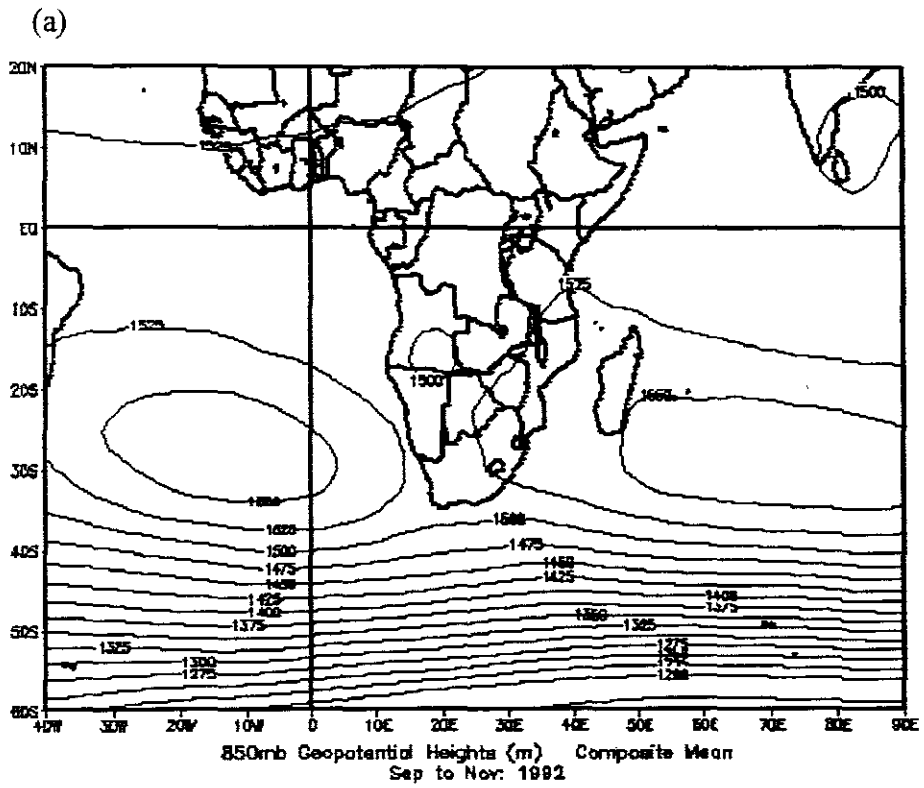


Fig. 6.1: Geopotential heights (a) mean and (b) anomaly at 850 hPa for SON 1992.

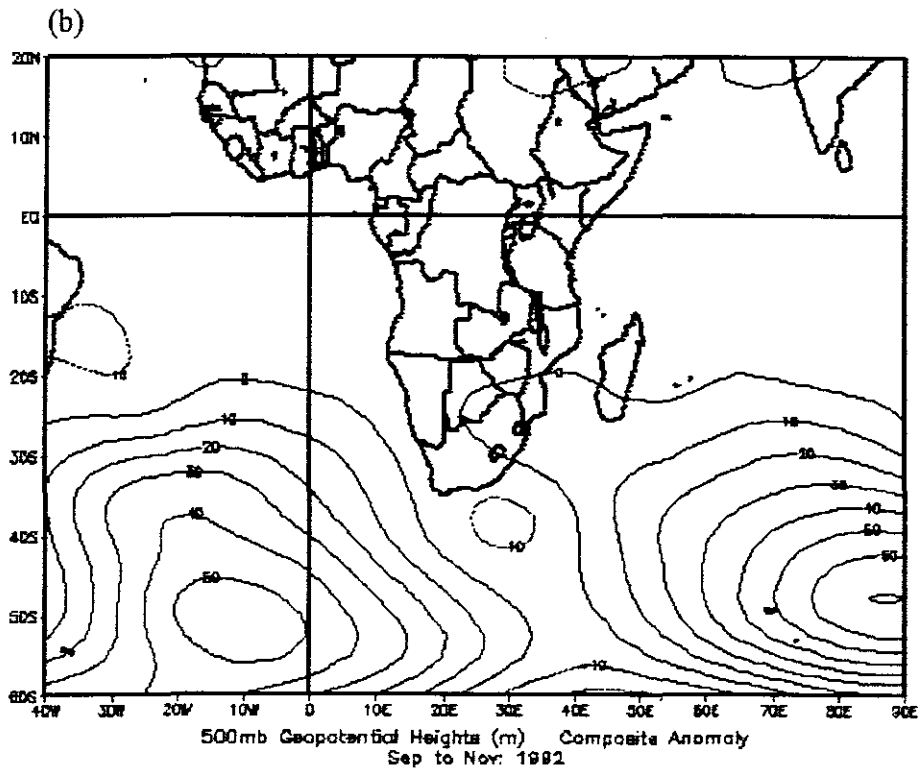
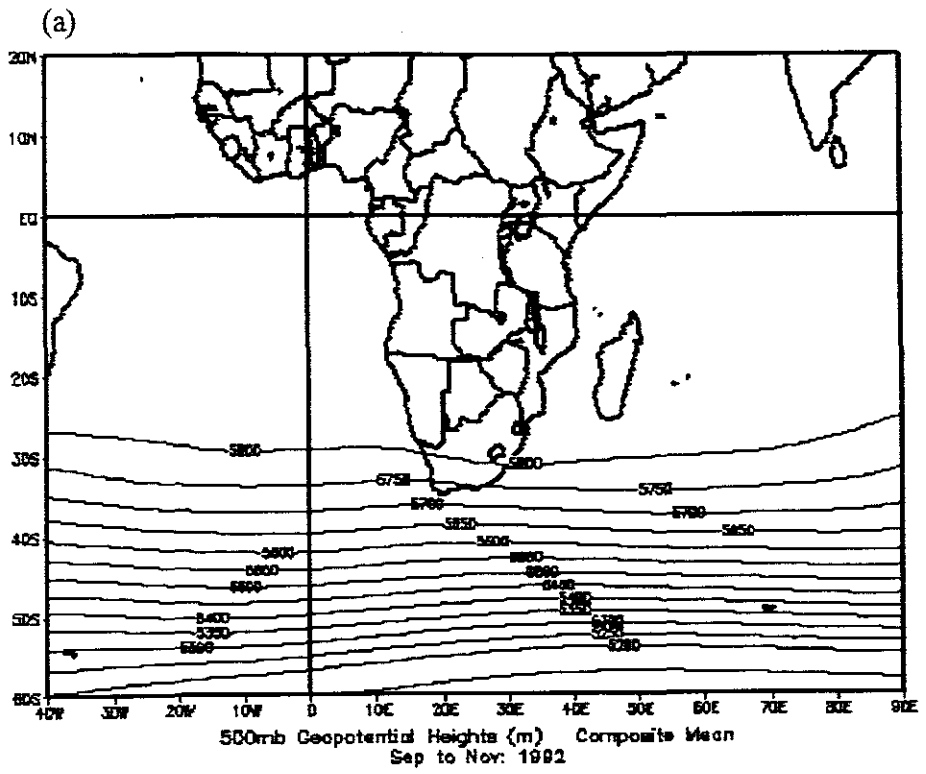


Fig. 6.2: Geopotential heights (a) mean and (b) anomaly at 500 hPa for SON 1992.

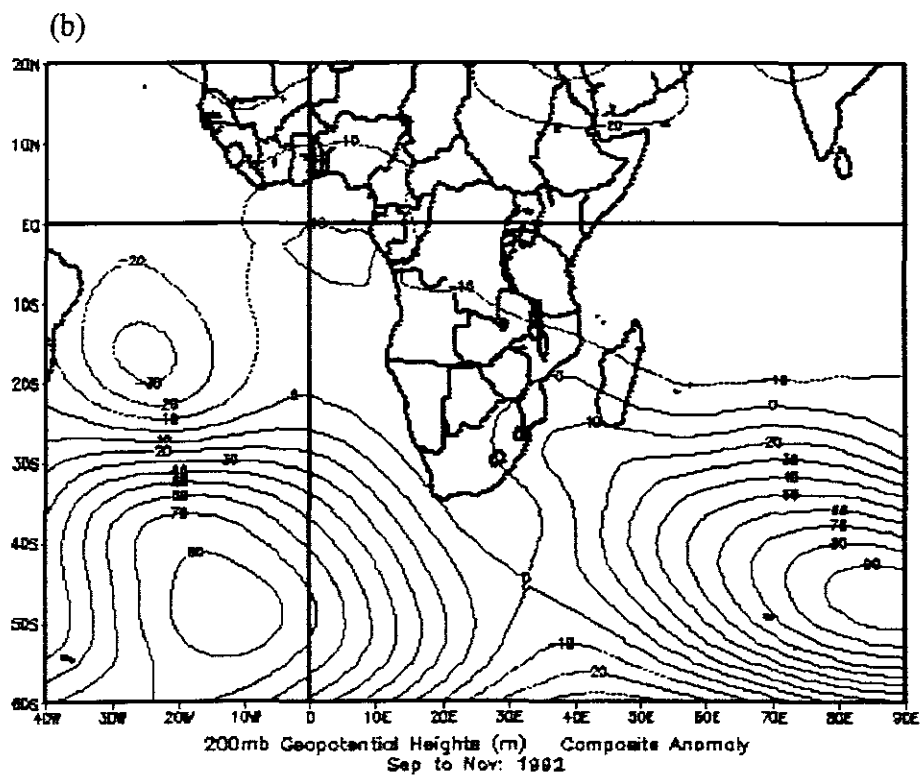
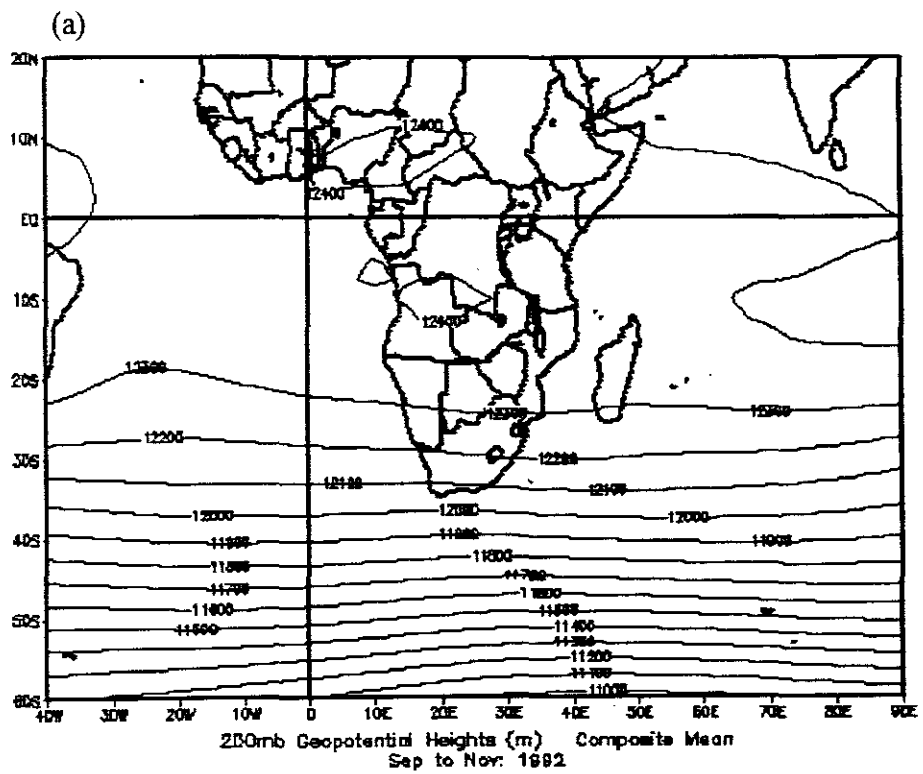


Fig. 6.3: Geopotential heights (a) mean and (b) anomaly at 200 hPa for SON 1992.

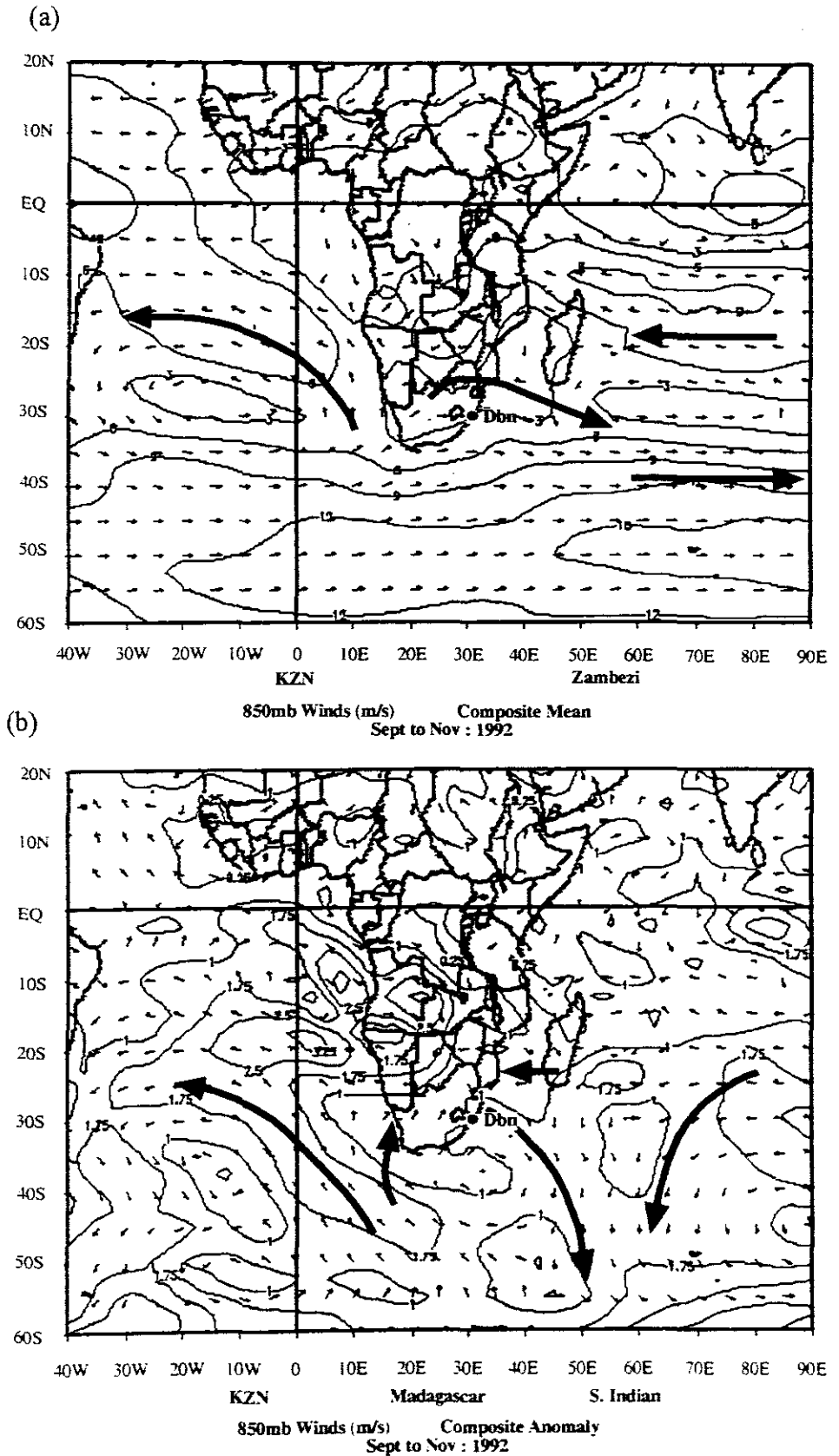


Fig. 6.4. (a) Mean and (b) anomalies of wind vectors and speed ( $\text{m s}^{-1}$ ) at 850 hPa for SON 1992.

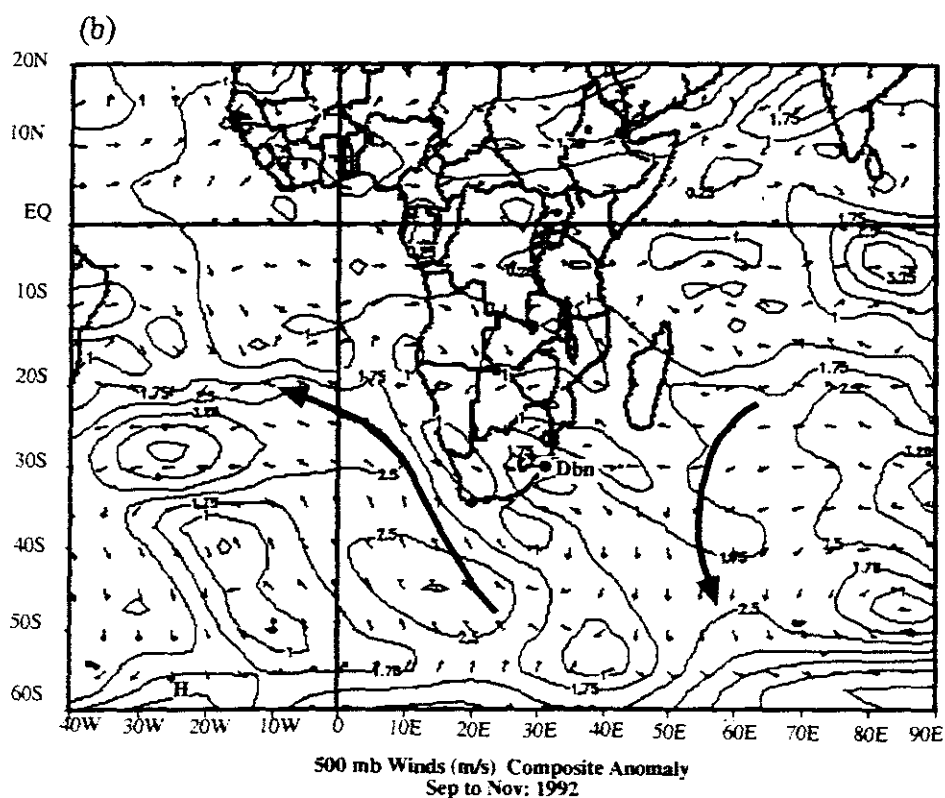
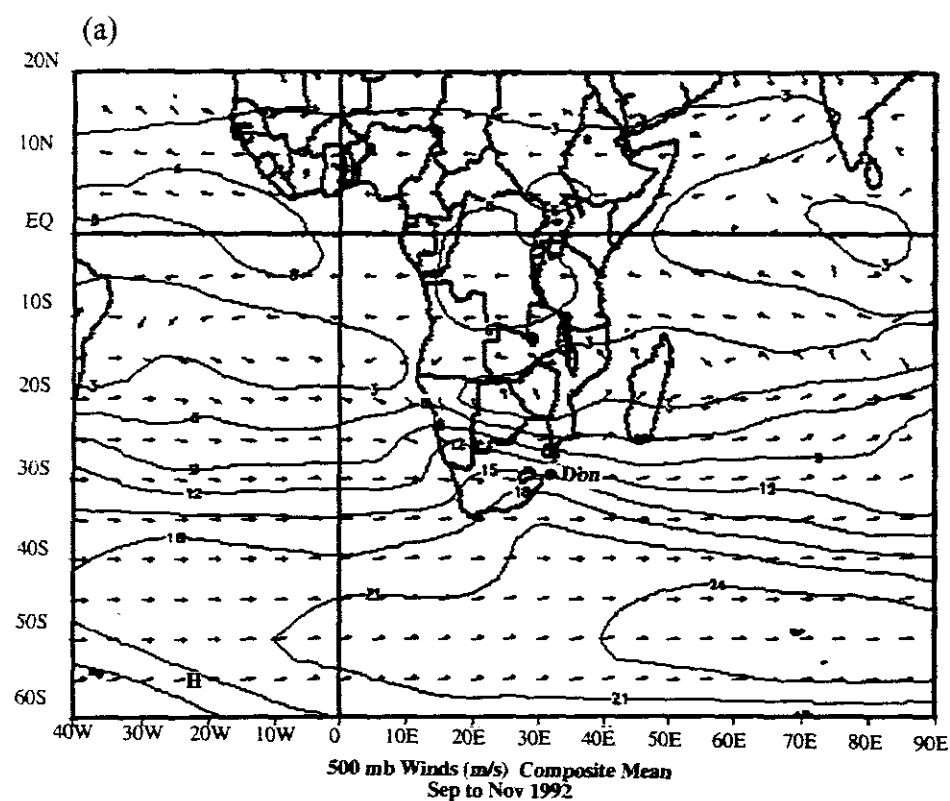


Fig. 6.5: (a) Mean and (b) anomalies of wind vectors and speed ( $\text{m s}^{-1}$ ) at 500 hPa for SON 1992/93.

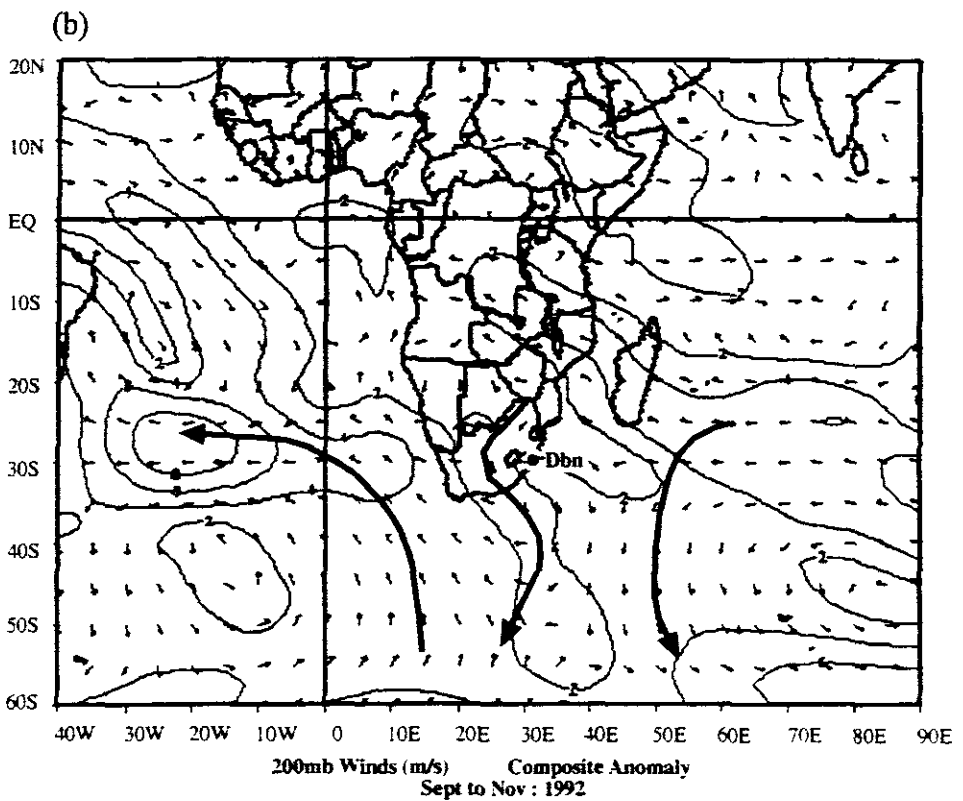
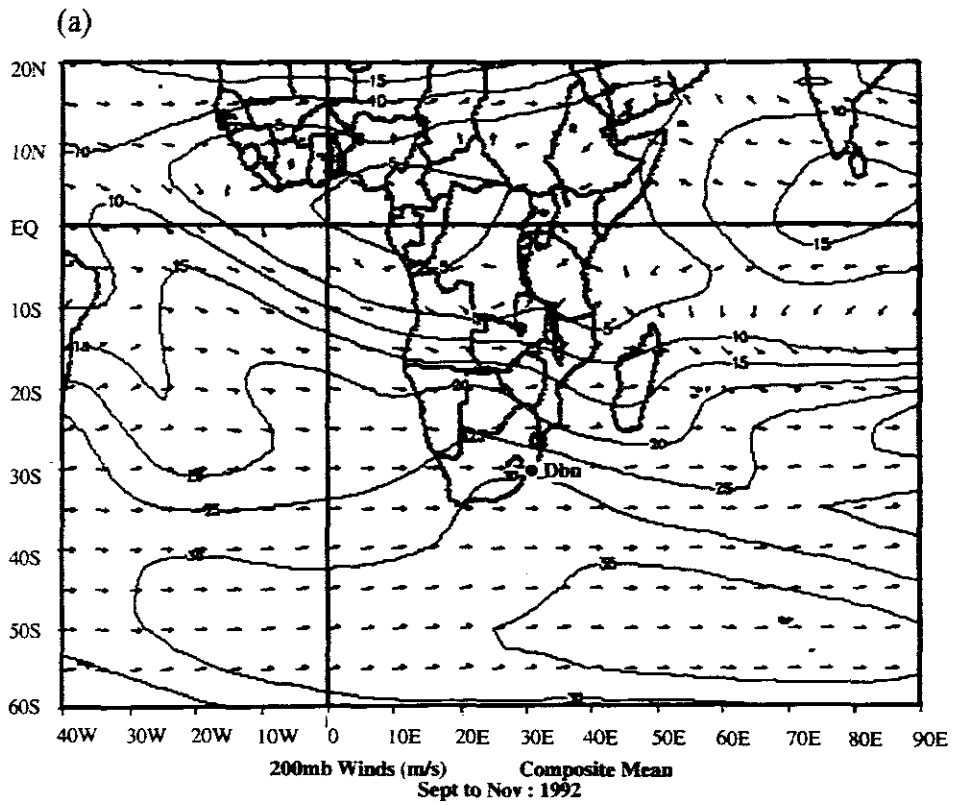


Fig. 6.6: (a) Mean and (b) anomalies of wind vectors and speed ( $\text{m s}^{-1}$ ) at 200 hPa for SON 1992.

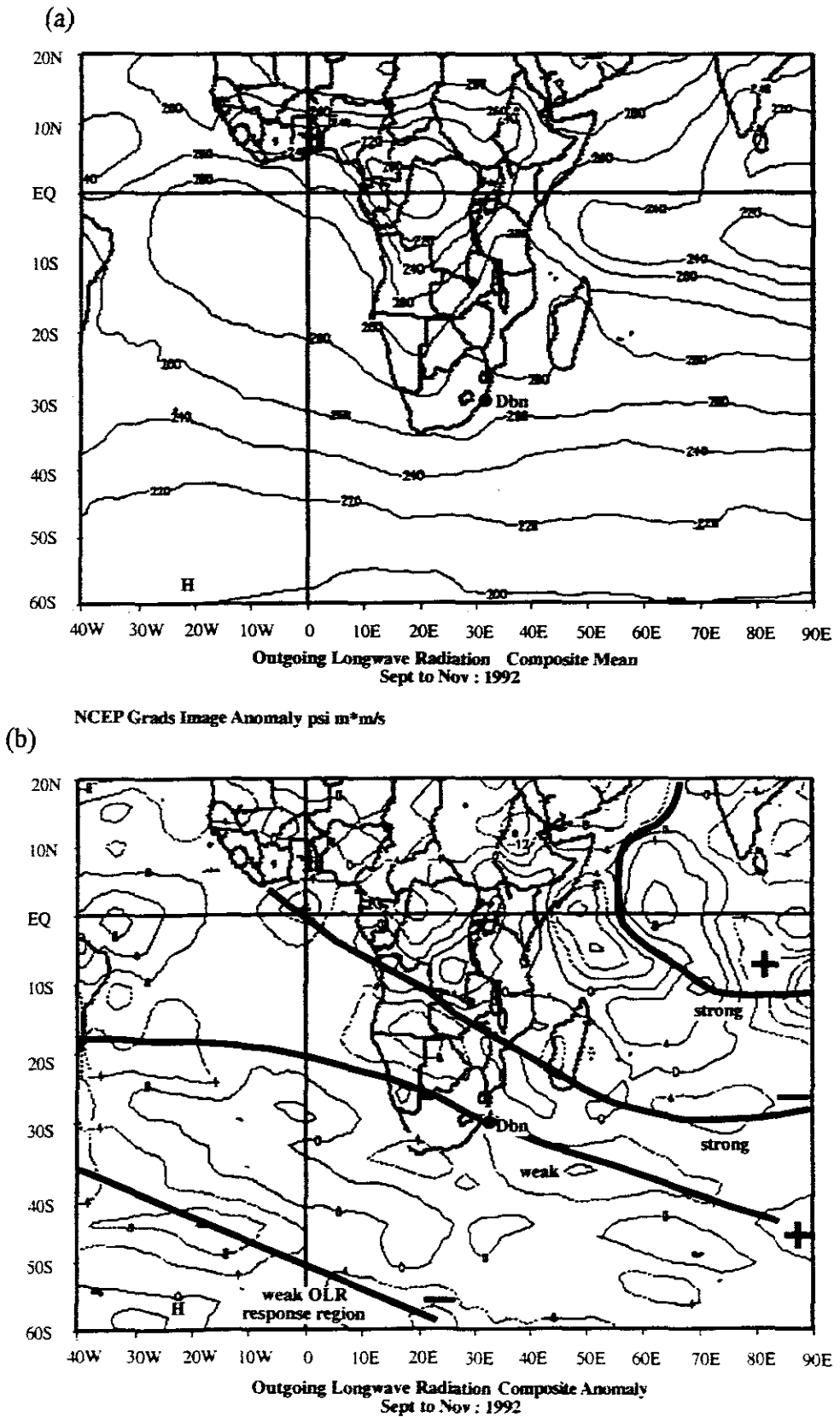


Fig. 6.7: (a) Mean and (b) anomalies of OLR ( $\text{W m}^{-2}$ ) for SON 1992.

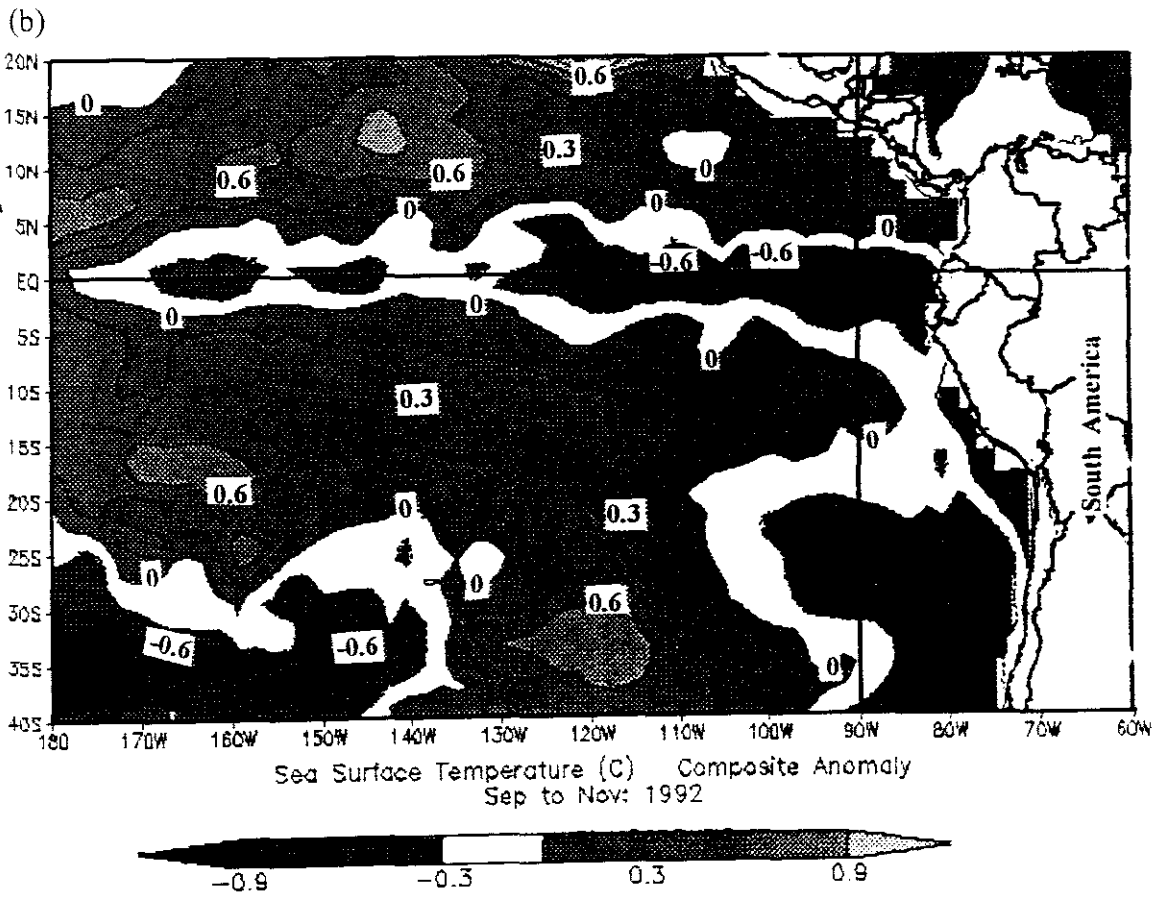
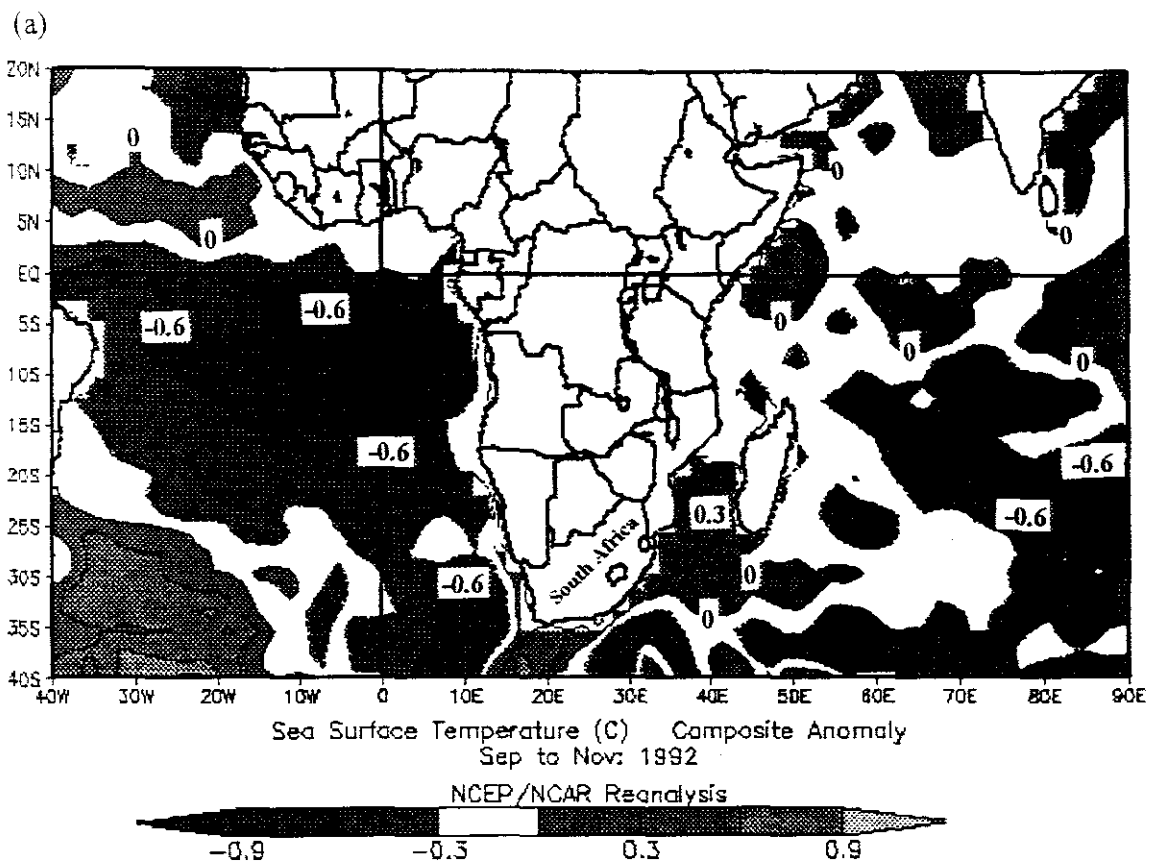


Fig. 6.8: (a) Atlantic and Indian, and (b) Pacific Ocean anomalies of sea surface temperature during SON 1992.

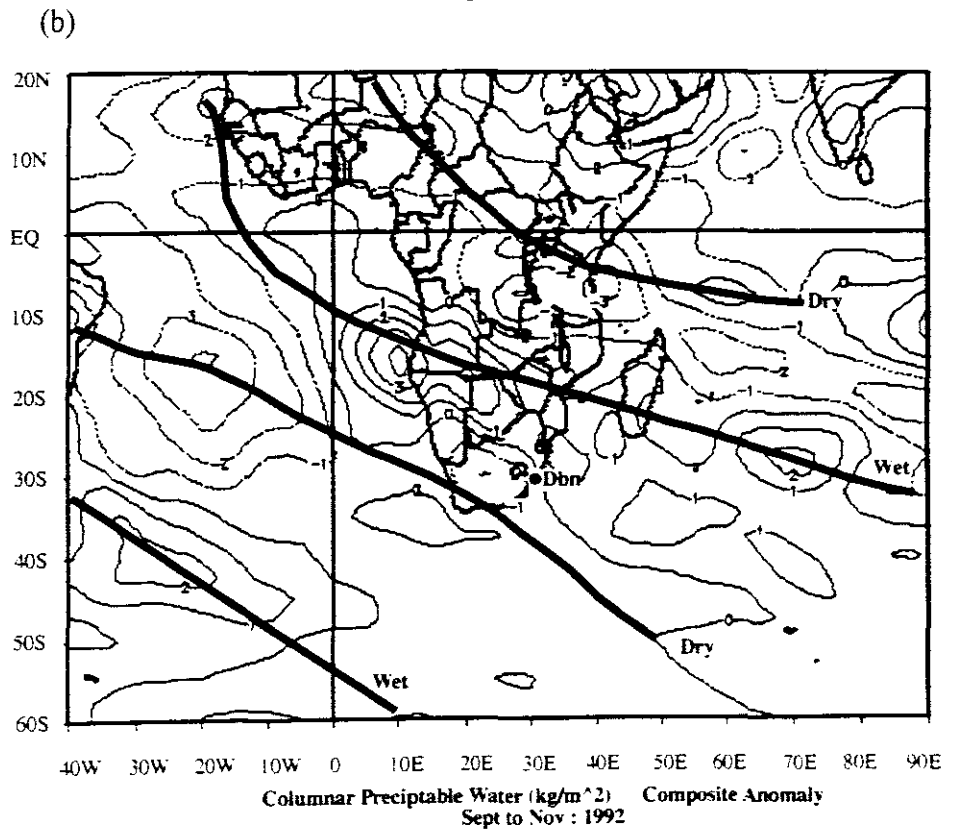
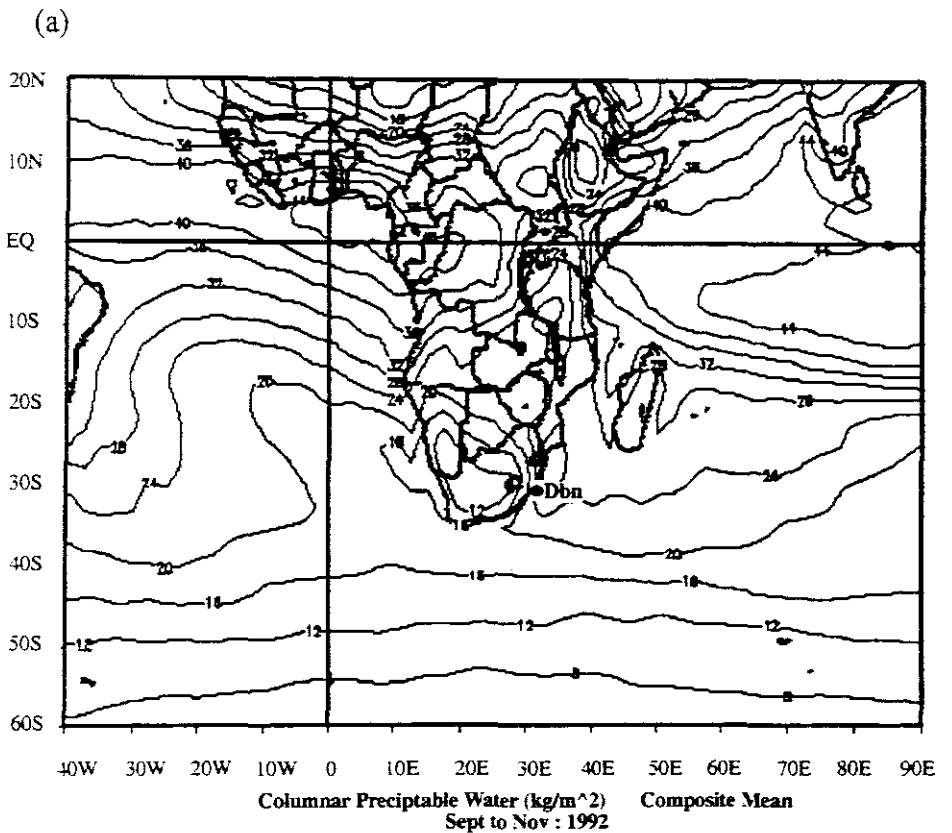


Fig. 6.9: Columnar precipitable water ( $\text{kg m}^{-2}$ ) (a) mean and (b) anomaly for SON 1992.

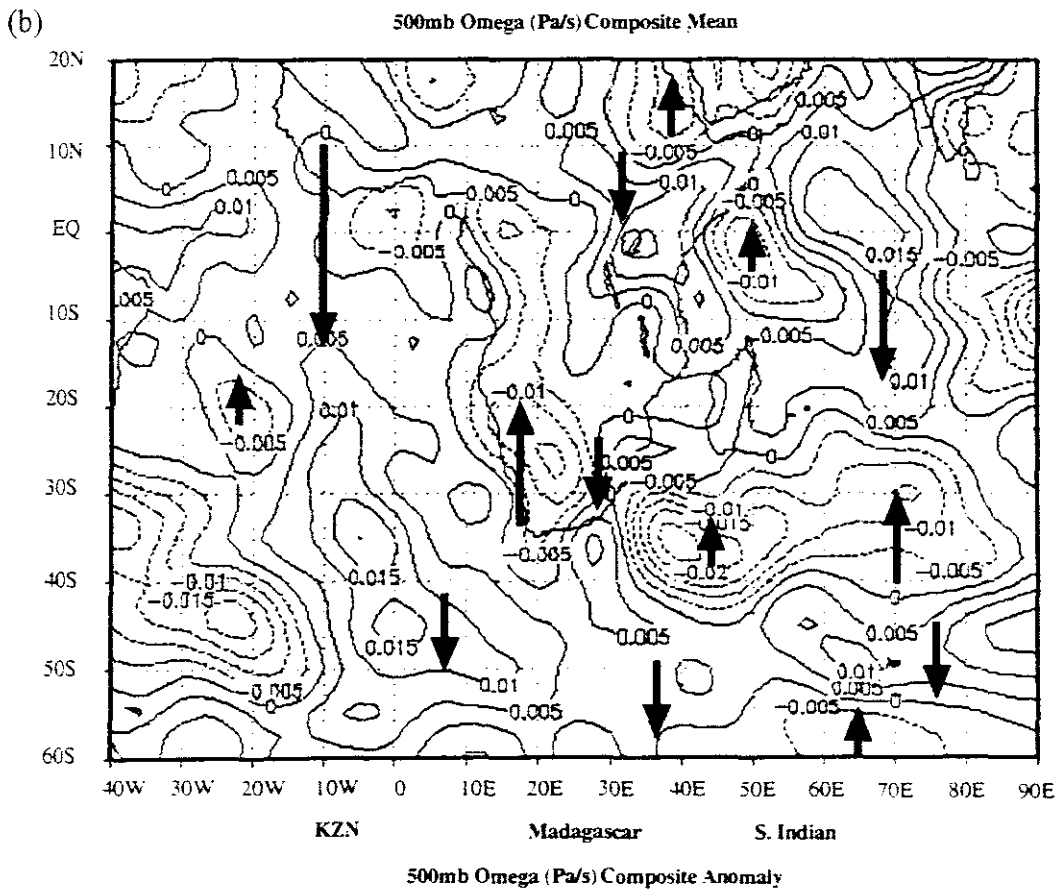
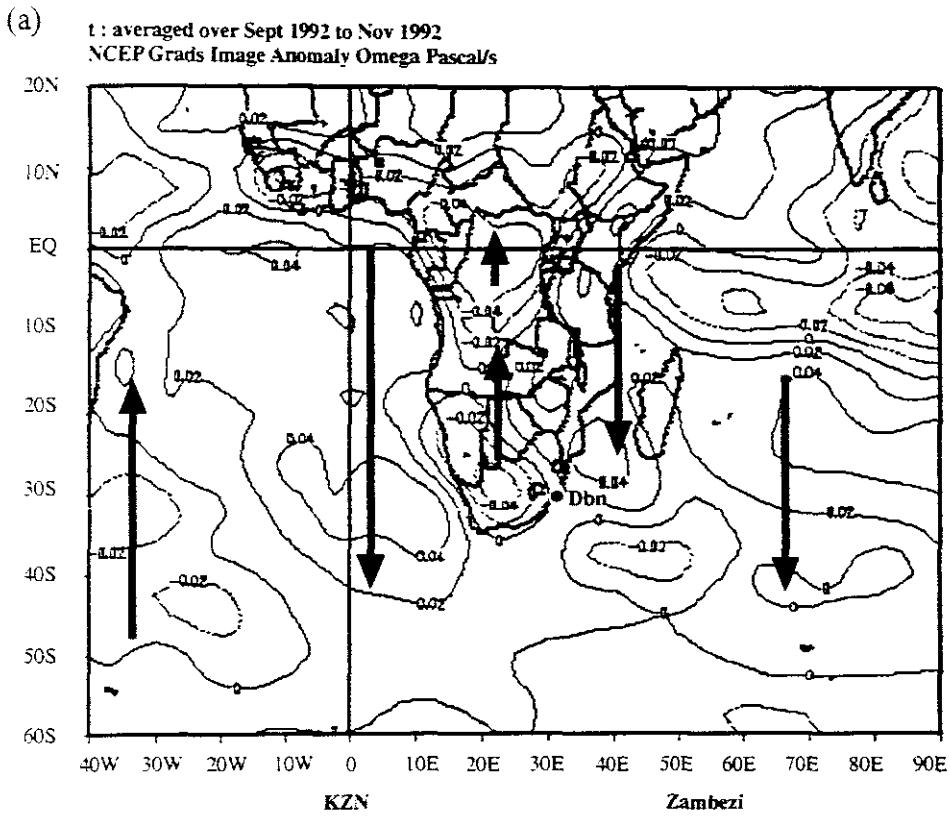
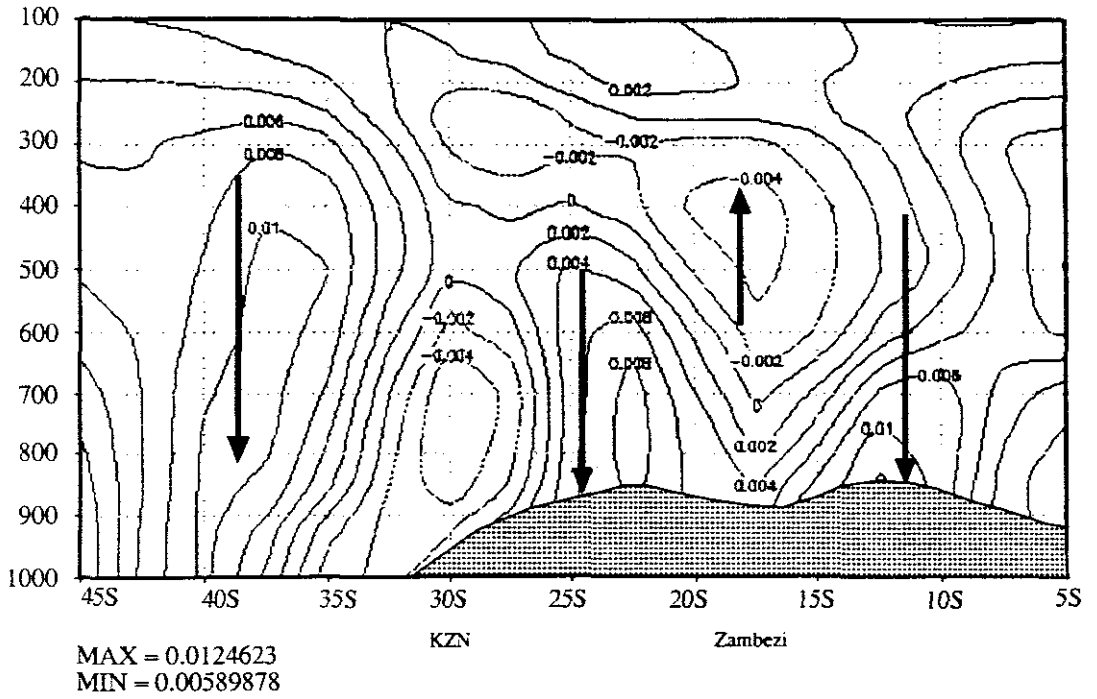


Fig. 6.10: (a) Mean and (b) anomalies of vertical motion (omega, Pa s<sup>-1</sup>) at 500 hPa for SON 1992.

(a)  $\omega$  averaged over Sept 1992 to Nov 1992  
NCEP Grads Image Anomaly Omega Pascal/s



(b)  $\omega$  averaged over Sept 1992 to Nov 1992  
NCEP Grads Image Anomaly Omega Pascal/s

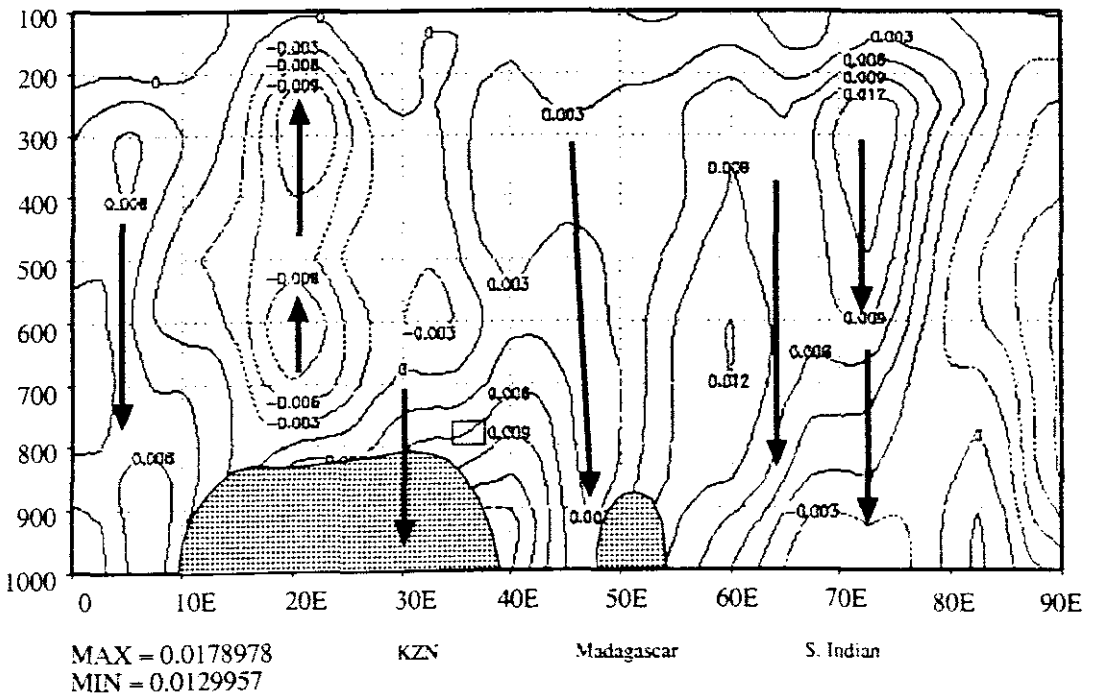


Fig. 6.11: SON 1992 vertical motion (omega) anomalies between 1000 and 100 hPa levels at (a) 30°E and (b) 15°S.

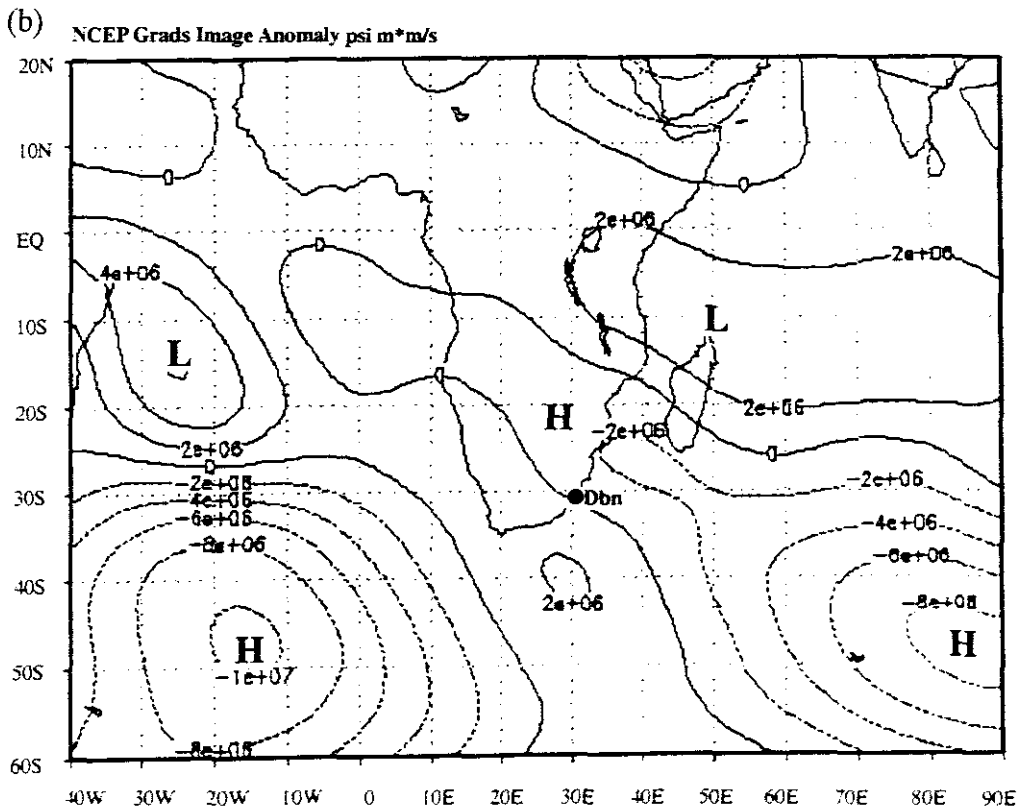
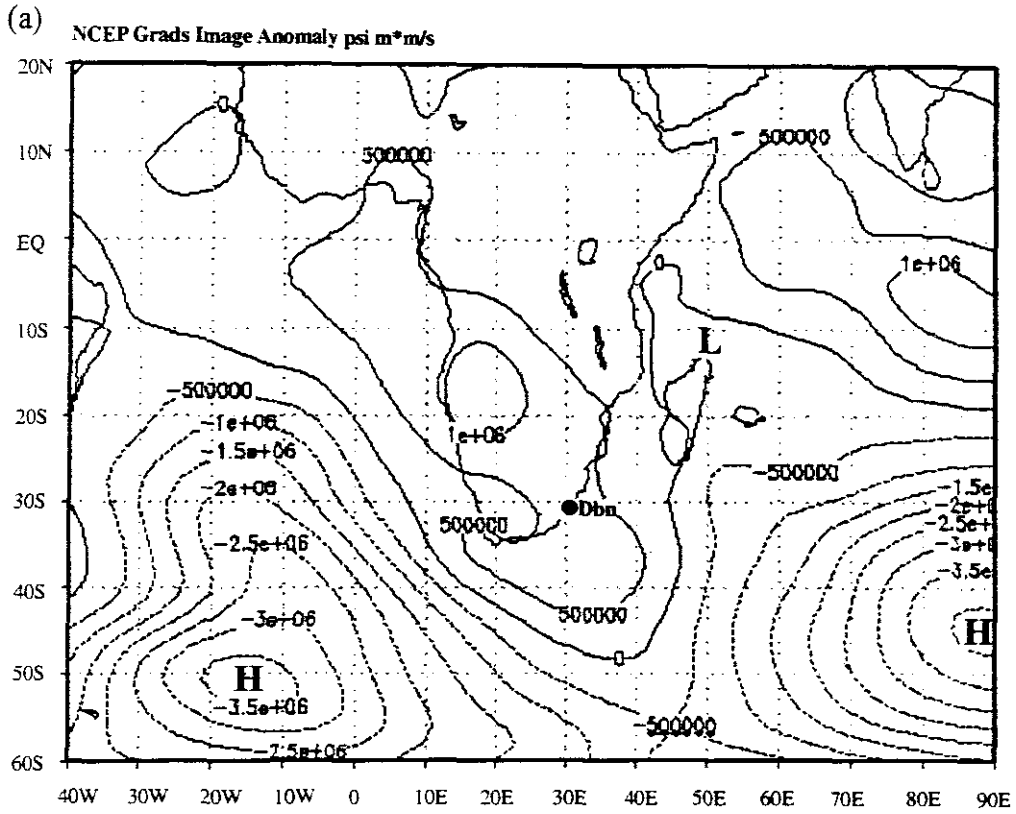


Fig. 6.12: Streamfunction anomalies at the (a) 0.995, and (b) 0.2101 sigma levels for SON 1992/93.

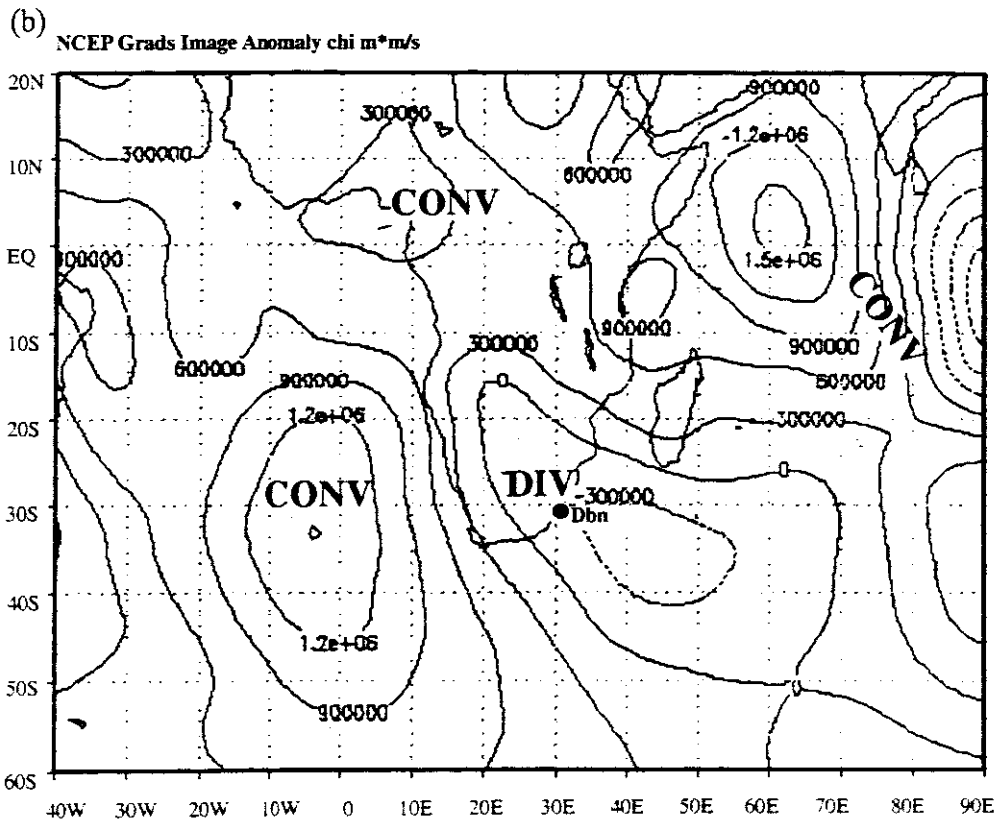
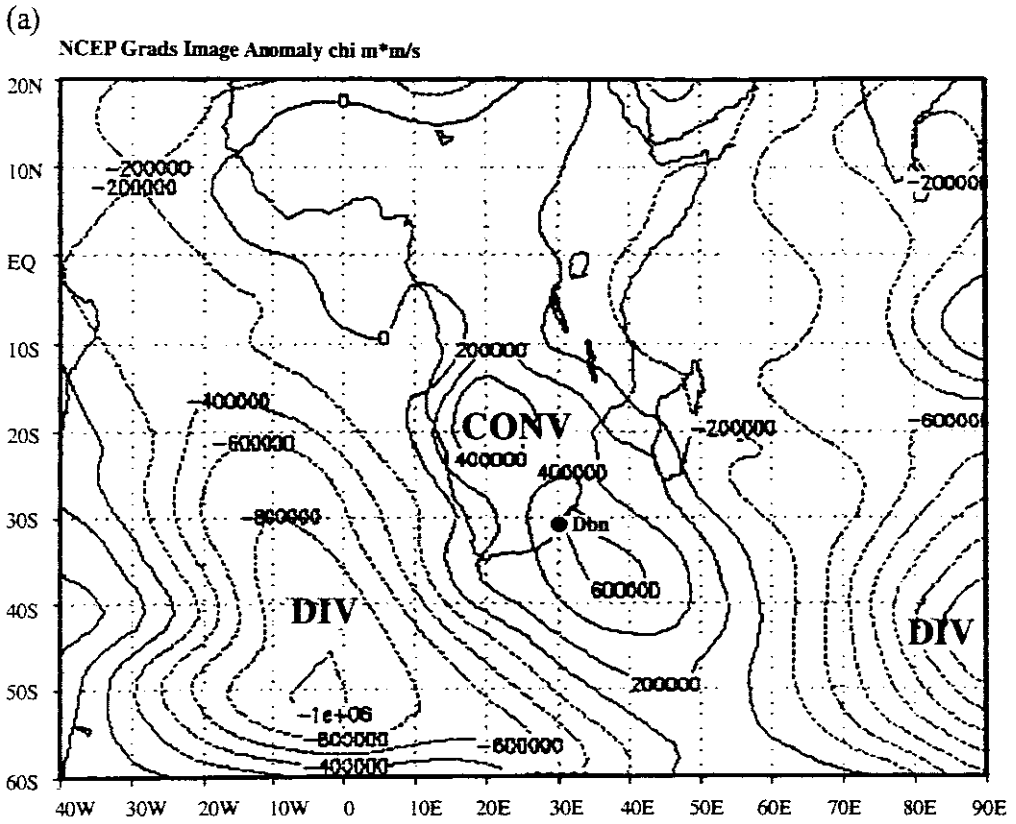


Fig. 6.13: Velocity potential anomalies at the (a) 0.995, and (b) 0.2101 sigma levels for SON 1992/93.

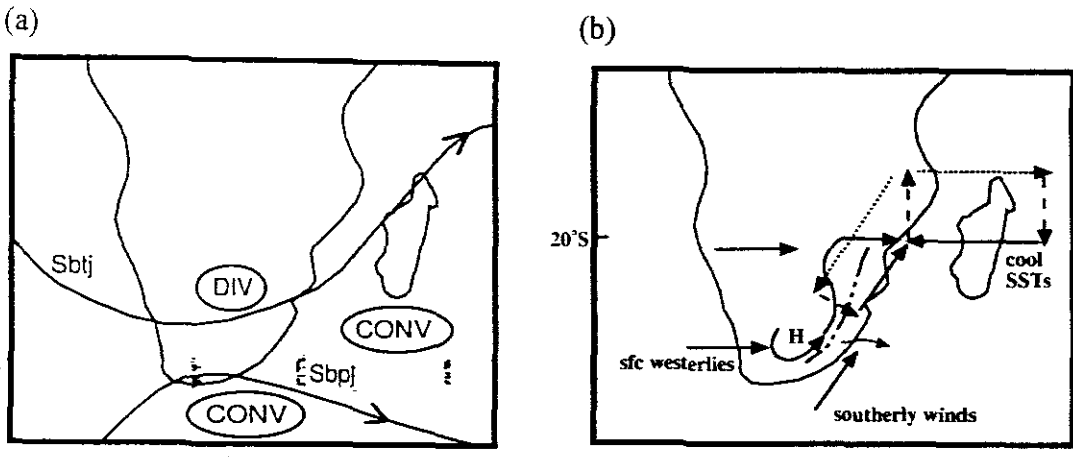


Fig. 6.14: Schematic illustrations of (a) the positions of the subtropical and subpolar jet streams, and (b) wind circulation pattern during the dry 1992/93 summer period. In (b) surface winds are solid bold, upper-level winds are dotted, and ascending and descending motions are indicated by broken lines.

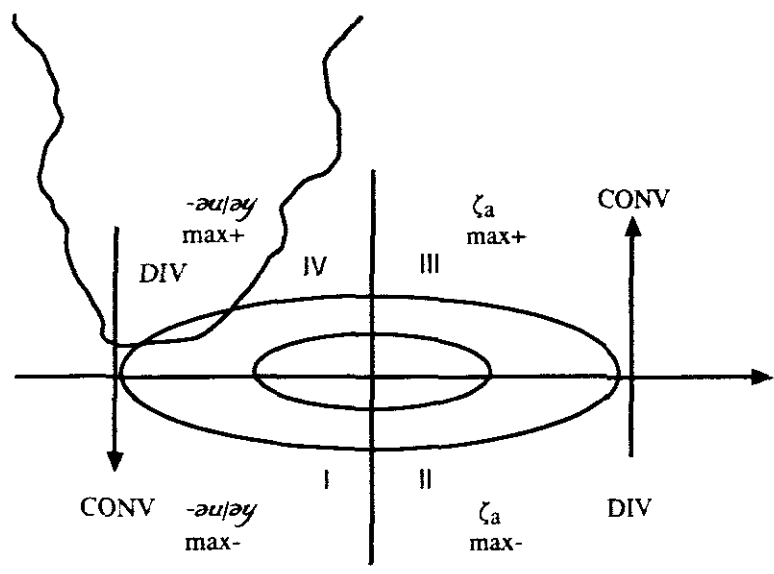


Fig. 6.15: Scheme of westerly jet producing dry conditions over South Africa. Arrow indicates easterly flow direction and jet axis, and the elliptical circles are isotachs, with largest values at the origin of the rectangular coordinate systems. I, II, III and IV are right rear, right front, left front, and left rear quadrants, respectively.

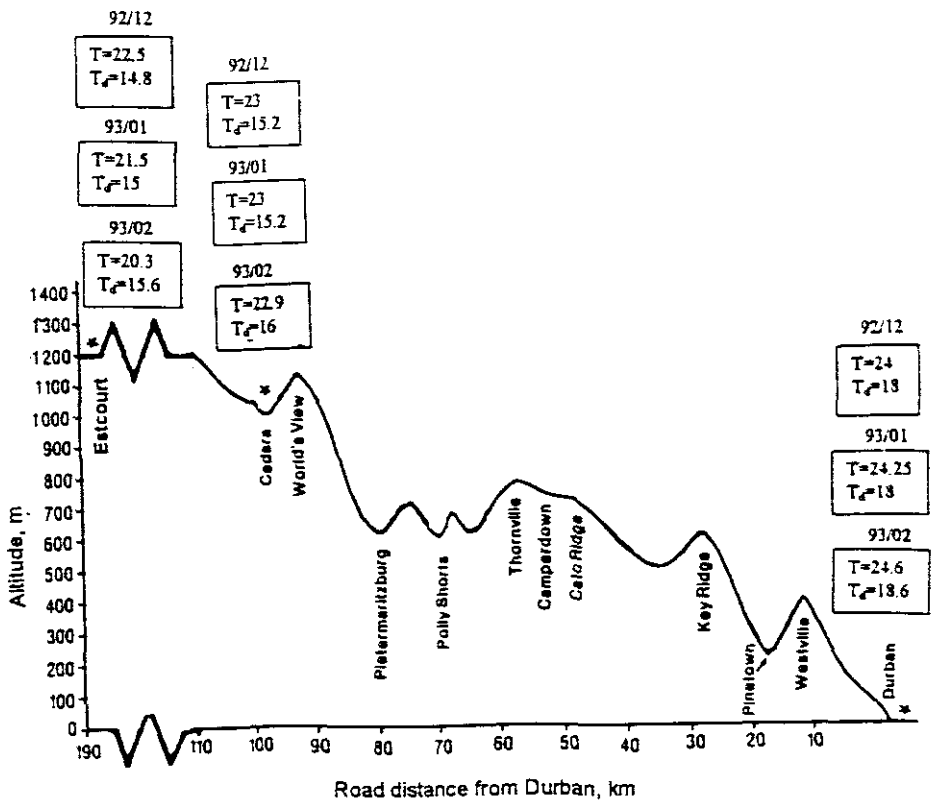


Fig. 6.16: Air and dew-point temperature variations over KwaZulu/Natal along a section from Escourt to Durban during DJF 1992/93. The warming effect with altitude decrease is apparent from the Figure. The altitude profile has been adapted from Preston-Whyte and Tyson (1988).

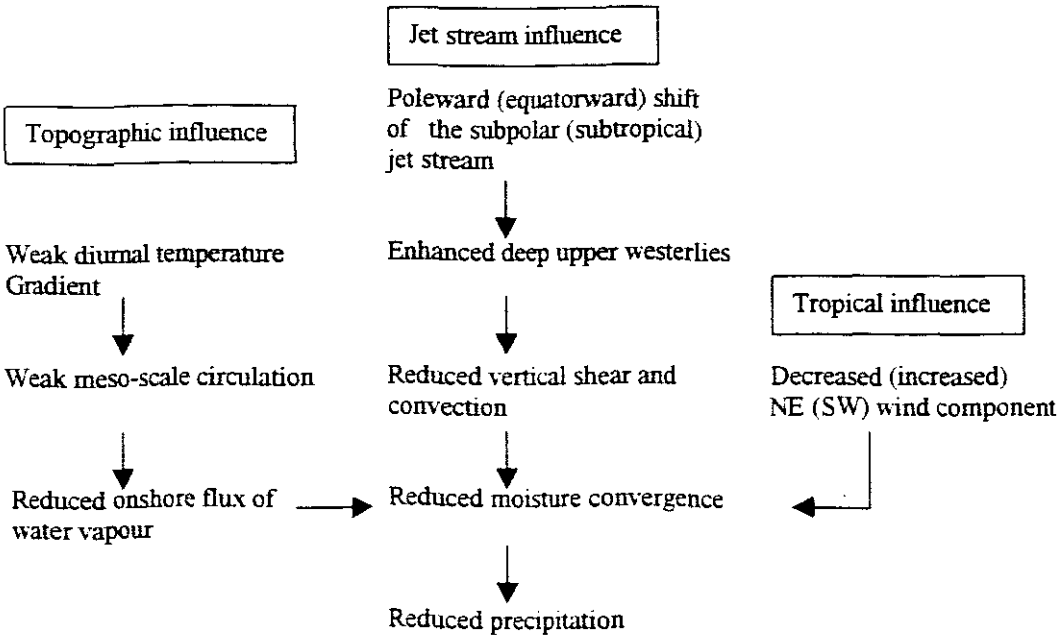


Fig. 6.17: Conceptual model of the influences of jet streams, meso-scale circulation and tropical effects on mid-summer rainfall over KwaZulu/Natal.

Table 6.1: Evaporative losses per day over KwaZulu/Natal during the 1992/93 dry summer.

Station	Period	Mean temp. (°C)	RH (%)	$e_s$ (mb) *	$e_a$ (mb)	Mean wind speed ( $m s^{-1}$ )	Evap./day (mm) **
Escourt	1992/12	22.53	50.0	27.247	13.62	2.83	6.3
	1993/01	21.51	53.8	25.635	13.79	3.14	5.6
	1993/03	20.34	61.0	23.959	14.61	2.75	4.3
Cedara	1992/12	20.38	61.0	24.107	14.71	3.12	4.4
	1993/01	20.05	59.8	23.518	14.06	3.33	4.5
	1993/03	19.67	62.8	22.942	14.41	3.92	4.3
Durban	1992/12	23.94	61.1	29.652	18.12	4.17	5.9
	1993/01	24.22	56.1	30.191	16.94	3.14	6.3
	1993/03	24.57	58.2	30.923	18.00	2.75	5.9

\* Obtained from Smithsonian Meteorological Tables.

\*\* Calculated from the Meyer Equation (Schulz, 1976).

Table 6.2a: SON 1992 and DJF 1992/93 departures of meteorological fields from their respective composite means for KwaZulu/Natal in descending order.

Variable	SON 92	DJF 92/93
Vertical motion	$2.5 \times 10^{-1}$	$-1.5 \times 10^1$
Velocity potential at 0.9995 sigma level	$-1.1 \times 10^{-1}$	$1 \times 10^0$
Velocity potential at 0.2101 sigma level	$-6 \times 10^{-2}$	$-6.7 \times 10^{-1}$
Wind vectors at 850 hPa	$3.3 \times 10^{-1}$	$1.3 \times 10^{-1}$
Wind vectors at 500 hPa	$1.2 \times 10^{-1}$	$1.3 \times 10^{-1}$
Wind vectors speed at 200 hPa	$8 \times 10^{-2}$	$5 \times 10^{-2}$
Precipitable water	$4 \times 10^{-2}$	$-3.3 \times 10^{-2}$
Streamfunction at 0.995 sigma level	$-5.6 \times 10^{-2}$	$-5 \times 10^{-2}$
Streamfunction at 0.2101 sigma level	$-1 \times 10^{-1}$	$5 \times 10^{-2}$
OLR	$1.4 \times 10^{-2}$	$9.6 \times 10^{-3}$
Geopotential height at 850 hPa	$3 \times 10^{-3}$	$3 \times 10^{-3}$
Geopotential height at 500 hPa	$9 \times 10^{-4}$	$9 \times 10^{-4}$
Geopotential height at 200 hPa	$4 \times 10^{-4}$	$8 \times 10^{-4}$

Table 6.2b: SON 1992 and DJF 1992/93 departures of meteorological fields from their respective composite means for core centres of activity and areas and those indicating teleconnections to the 1992/93 KwaZulu/Natal drought structure in descending order.

Variable	Area	SON 92	DJF 92/93
Vertical motion	60°E, 20°S	-2.5x10 <sup>0</sup>	-3x10 <sup>0</sup>
Velocity potential at 0.9995 sigma level	10°W, 10°S	3.3x10 <sup>-1</sup>	-5.7x10 <sup>-1</sup>
	0°E, 30°S	8.9x10 <sup>-2</sup>	-9.4x10 <sup>-1</sup>
	60°E, 20°S	5x10 <sup>-1</sup>	10 <sup>0</sup>
Velocity potential at 0.2101 sigma level	15°S, 60°E	1.2x10 <sup>-1</sup>	-1.3x10 <sup>0</sup>
	0°E, 20°S	1.7x10 <sup>-1</sup>	-1.3x10 <sup>-1</sup>
	30°E, 15°S	4.3x10 <sup>-1</sup>	-1.8x10 <sup>0</sup>
Streamfunction at 0.995 sigma level	0°E, 15°S	1.4x10 <sup>-1</sup>	-2.1x10 <sup>-2</sup>
	60°E, 15°S	1.33x10 <sup>0</sup>	5x10 <sup>-1</sup>
Streamfunction at 0.2101 sigma level	20°W, 30°S	-6.7x10 <sup>-2</sup>	5x10 <sup>-2</sup>
	60°E, 30°S	-6.7x10 <sup>-2</sup>	-6.7x10 <sup>-2</sup>
	60°E, 15°S	2x10 <sup>-1</sup>	3x10 <sup>-2</sup>
Zonal wind vectors and speed at 850 hPa	35°S-50°S, 0°-40°E	+1.5x10 <sup>-1</sup>	+1.5x10 <sup>-1</sup>
	20°E-20°S	+5.4x10 <sup>-1</sup>	+6.3x10 <sup>-1</sup>
	60°E-15°S	-1.1x10 <sup>-1</sup>	-1.7x10 <sup>-1</sup>
Zonal wind vectors and speed at 500 hPa	35°S-50°S, 0°-40°E	+8.3x10 <sup>-2</sup>	+8.3x10 <sup>-2</sup>
	20°E-20°S	+8.3x10 <sup>-2</sup>	+6.3x10 <sup>-2</sup>
	60°E-15°S	-8.3x10 <sup>-2</sup>	-6.3x10 <sup>-2</sup>
Zonal wind vectors and speed at 200 hPa	35°S-50°S, 0°-40°E	+6.7x10 <sup>-2</sup>	+5.7x10 <sup>-2</sup>
	20°E-20°S	-2x10 <sup>-1</sup>	-1.3x10 <sup>-1</sup>
	60°E-15°S	-1.3x10 <sup>-1</sup>	-6.7x10 <sup>-1</sup>
SSTs	E and SE of Madagascar	1.3x10 <sup>-2</sup>	4.8x10 <sup>-2</sup>
	60°E-90°E at 20°S	-4.4x10 <sup>-2</sup>	4.8x10 <sup>-2</sup>

Table 6.2b continued.

Variable	Area	SON 92	DJF 92/93
Precipitable water (wave trains in Figs. 5.8 and 6.9)	20°W-15°E at 10°S	$-3.1 \times 10^{-2}$	$4.8 \times 10^{-2}$
	Dry axis over South Africa	$-4.2 \times 10^{-2}$	$-3.3 \times 10^{-2}$
	Wet axis over Zambezi	$7.1 \times 10^{-2}$	$7.5 \times 10^{-2}$
OLR (regions in Fig. 5.7 and 6.7)	10°S-20°S, 40°W-80°E dry axis	$-8.3 \times 10^{-2}$	$-1.5 \times 10^{-2}$
	Weak -ve OLR response	$-3.6 \times 10^{-2}$	$-3.1 \times 10^{-2}$
	Weak +ve OLR response	$1.5 \times 10^{-2}$	$9.6 \times 10^{-3}$
	Strong -ve OLR response	$-3.3 \times 10^{-2}$	$-3.4 \times 10^{-2}$
	Strong +ve OLR response	$3.1 \times 10^{-2}$	$6.3 \times 10^{-2}$
	Geopotential height at 850 hPa	30°E, 40°S	$-3.4 \times 10^{-3}$
0°E, 30°S		$9.7 \times 10^{-3}$	$6.5 \times 10^{-4}$
60°E, 30°S		$6.5 \times 10^{-3}$	$3.3 \times 10^{-3}$
Geopotential height at 500 hPa	30°E, 40°S	$-1.8 \times 10^{-3}$	$-1.8 \times 10^{-3}$
	0°E, 30°S	$3.5 \times 10^{-3}$	$1.7 \times 10^{-4}$
	60°E, 30°S	$1.7 \times 10^{-3}$	$4.3 \times 10^{-4}$
Geopotential height at 200 hPa	30°E, 40°S	-----	$-8.3 \times 10^{-4}$
	0°E, 30°S	$2.5 \times 10^{-3}$	$8.1 \times 10^{-5}$
	60°E, 30°S	$8.2 \times 10^{-4}$	$8.1 \times 10^{-4}$

Table 6.3: Conceptual model of jet streams influence on mid-summer rainfall over eastern parts of South Africa.

Compressed thermal gradient over South Africa



Increased upper westerlies



Divergence over South Africa



Dry Conditions

## Chapter 7

### 7: SUMMARY AND CONCLUSIONS

#### 7.1 SUMMARY

Subsidence and very dry conditions were obtained over KwaZulu/Natal during 1992/93. Low level southerly flow persisted over the Mozambique Channel and winds were light and variable over the eastern parts of South Africa, hence topographically induced uplift was absent during this event. The upper circulation was dominated by a stationary wave in the westerlies over the South Atlantic which brought dry air to KwaZulu/Natal. In the 200 hPa wind field the major development was a surge of westerlies over the equatorial South Atlantic. Anticyclonic vorticity and subsidence via upper level convergence suppressed convection over the KwaZulu/Natal.

Average water vapour flux over the drought period was very low, more typical of winter, spreading eastward from Namibia in contrast with higher values over the Cape and Mozambique coasts and the Congo Basin. The area of water vapour flux values  $< 5 \text{ g kg}^{-1}$  extended from 20 to 30°S and 17 to 27°E, covering most of KwaZulu/Natal and the plateau of southern Africa. In such a dry environment even relatively strong uplift could not initiate the convective rainfall typical of summer. Positive anomalies occurring in the Indian Ocean suggest an eastward shift of convergence and convection. Water vapour flux anomalies are dominated by Jury's (1992) north-south dipole. This dipole shows increased precipitable water over the equatorial band and less values over parts of Africa south of the Congo basin. Vertical (Hadley) overturning has been found to be operating during the 1992/93 dry summer season. Water vapour flux, OLR, streamfunction and velocity potential anomalies display wave train patterns over southern Africa

suggesting that the 1992/93 drought was a response to hemispheric-scale disturbances in the circulation structure.

During the 1992/93 drought period prominent easterly vector anomalies, previously related to a subtropical anticyclonic gyre in the South Indian Ocean and relaxation of the equatorial monsoon in a study by Jury *et al.* (1996a) have been observed over the tropical Indian Ocean (0-10°S, 40°-80°E). A midlatitude anticyclonic gyre is located over southern Africa. A moist axis lies NE-SW over Madagascar whilst a negative precipitable water anomaly exists over southern Africa.

The 200 hPa wind and vertical motion anomalies in both ECMWF and NCEP/NOAA datasets indicate westerly anomalies occurring throughout southern Africa. Weaker easterlies at 200 hPa have been related to a lower frequency of easterly wave and cloud band formation over the subcontinent, resulting in below average rainfall over the summer rainfall region of South Africa (Harrison, 1983; 1986). Westerly surface wind anomalies across much of the eastern coast of southern Africa have been reported to occur when the SSTs are abnormally warm in the central equatorial Pacific. Westerly anomalies are also observed at 200 hPa over most of the tropical Atlantic and Indian Oceans. A strong anticyclone is centred over Botswana. Relatively weak upper circulation anomalies are evident in the tropics.

Vertical motion field is relatively neutral over KwaZulu/Natal. Alternating axes of uplift and subsidence anomalies are found in the South Indian Ocean. Subsidence anomalies occur over most of South Africa (and southern Africa). Vertical uplift anomalies occur in bands at 20°S. Prominent sinking motion occurs from 15-30°S and upward anomalies near the equator and 40°S where lows are situated. ECMWF and NCEP/NOAA datasets are in agreement that the 1992/93 drought was not a strong El Nino-induced climatic event. There are signs observed in the analysis showing resemblance to an El Nino type of

influence but some parameters such as SSTs are not dominant to suggest a consistent pattern typical of the ENSO.

Based on these results a circulation hypothesis governing dry and wet conditions over South Africa is suggested. The strong pressure and thermal gradients observed to the south of South Africa suggest the southward (northward) movement of the subtropical (subpolar) jet stream.

## 7.2 RECOMMENDATIONS

Most drought-related studies in South Africa describe its temporal behaviour and the associated anomalies over the country and surrounding oceans (Jury and Levey, 1993; Jury and Lutjeharms, 1993; Tyson, 1984; 1986). Studies concentrating on drought impact assessment are limited. This thesis has given a detailed analysis of the historical context of the 1992/93 drought using historical data and has outlined the cause and structure of the drought using surface and upper-level meteorological data, as well as its impacts. It is believed that the study will assist in the further understanding of mechanisms governing drought-producing systems which can aid improved forecasting skills.

It has been an objective of the project to gauge the severity of the 1992/93 drought on agricultural output in KwaZulu/Natal. The study notes the following points pertinent to the objectives outlined in Chapter 1 and related to the potential benefits of timely ENSO forecast:

1. Earlier forecasting and response could reduce costs through earlier food acquisition efforts. A greater window of response will provide more time to budget for and organise the flow of drought-related goods.
2. An accurate drought forecast will enable farmers in marginal growing areas not to waste time or money planting crops that would likely not grow, nor spend resources on a second planting that would likely fail.

3. An ENSO forecast will allow for some degree of changes in crop mix, planting times, and other practices for those farmers with flexible operations. Farmers using short-maturing crop hybrids which might have had enough moisture from the early rains to produce a reasonable crop will help reduce the dependence of the country on costly imports.

4. Water authorities will be forewarned and measures taken timely to ensure adequate supplies to the public through water scheme agreements with neighbouring states unlikely to be affected by the drought. This may call for cooperation in research between South Africa and its neighbours, particularly those with large water reserves and characterised by an inverse climatic regime to South Africa's.

5. With improved drought forecasting water restrictions may be put in place earlier before drought commences. This will ensure that more water is available when drought reaches a peak thus putting less inconvenience to the public.

It is thus recommended that:

1. Drought coping strategies be developed. This may contribute to desertification control strategies at the same time as helping to recover desert land for future agricultural uses. Effective management of drought requires frequent preventive measures, forecasting capabilities and contingency plans for mobilising needed resources for mitigation, relief and recover operations. Drought points out vividly to the interrelationship among resources and underlines the importance of perceiving resource scarcity as a problem of total resource management.

2. In reducing vulnerability to drought emphasis must be on the drought-resistant crops that perform much better than sensitive crops such as maize.

3. Bureaucrats and extension officers must be trained on how to interpret ENSO forecasts and communicate the risks of drought to local farmers. Formal structures or processes must be in place to disseminate ENSO information.

4. Once drought has been forecast, it is imperative that modelling of streamflow and dam inflow levels be undertaken for accurate information on how stringent water cuts are to be.

5. The more challenging questions that are still a subject of research are: what are the dynamic and thermodynamic forces which produce the anomalies in the general circulation regime of the atmosphere and their synoptic byproducts, and why do these anomalies persist? These questions are to be answered for improved forecasting skills to be realised. This calls for further research in this field. There is a need also to develop capabilities to forecast decadal rainfall variability in the same way that forecast seasonal changes can be made, so that strategies can be implemented to minimise these effects (on crops, etc.) and take greater advantage of improved conditions when they occur.

### 7.3 CONCLUSION

Drought-producing systems are well-known and documented. The study has confirmed most of this work. While ENSO features are generally confined to the central and eastern Pacific Ocean, their effects are felt around the globe in the form of teleconnections. The 1992/93 drought period did not bear a prominent ENSO signal. Winds had a profound influence on the occurrence of drought through their moisture advection capability. Wave trains revealed by OLR, water vapour flux, streamfunction and velocity potential anomaly fields over southern Africa and the surrounding oceans point at disturbances of hemispheric magnitude as contributors to the 1992/93 drought.

Furthermore, the 1992/93 drought owes its origin and persistence to the zonal cell characterised by a rising limb over the Zambezi and subsidence over the Indian Ocean in a pattern indicated in Figure 6.14a.

The 1992/93 drought has been shown in the thesis to have had dramatic deleterious effects on KwaZulu/Natal's economy. Through its influence on the economy and because of its magnitude and persistence, the drought is expected to have adversely affected food availability and prices, employment, access to imports, government expenditures, availability of social services, and credit sources to a degree surpassing previous droughts in the last three decades.

Prediction of the occurrence of drought by the SAWB and researchers in various institutions locally and internationally has been successful and attempts to increase forecast skill are under way. Post season analysis and verification of simulations have also been done and forecast errors analysed with a view to refinement of models. As a result the model outputs have improved. Jury (1997), for example reports that of the 21 target forecasts issued in 1995, only the 1996 summer rainfall in northern Namibia was over-predicted (Jury, 1997). Despite the success achieved in respect of drought-prediction, there is a need to further the understanding of drought-producing processes to improve the lead time and develop prediction models with improved certainty of the occurrence or non-occurrence of prolonged dry (and wet) event years. It is believed that the results of this study will highlight some of the information required to fulfill improved drought forecasting skill.

## REFERENCES

- Adedoyin, A, 1997: On African easterly waves, squall lines, global sea-surface temperature anomalies and climate change in tropical Africa, *Fifth international conference on southern hemisphere meteorology and oceanography, 7-11 April 1997*, Pretoria, South Africa, pp280-281.
- Allan, R; Lindesay, J and Parker,D, 1997, The global ENSO picture: Interdecadal variability, *Fifth international conference on southern hemisphere meteorology and oceanography, 7-11 April 1997*, Pretoria, South Africa, pp186-187.
- Anyamba, A and Eastman, JR, 1997: Time-space examination of ENSO-related patterns from vegetation index time series for Africa, *Fifth international conference on southern hemisphere meteorology and oceanography, 7-11 April 1997*, Pretoria, South Africa, pp338-339.
- Barclay, JJ, 1992: *Wet and dry troughs over southern Africa during early summer*, Msc thesis, University of Cape Town.
- Barnston, AG (ed), 1997: El Nino/Southern Oscillation (ENSO) diagnostic advisory, *Experimental long-lead bulletin*, 6(4), NOAA, Washington, p1.
- Botha, P, 1995: The convention to combat desertification in countries experiencing serious drought and/or desertification particularly in Africa, *Proceedings of the National Research and Development Workshop on the assessment and monitoring of desertification in South Africa*, Pretoria, South Africa, pp10-16.
- Bruyere, CL, 1997: Severe haistorm activity over South African Highveld: Utilising the Clark model to numerically simulate selected case days, *Fifth international conference on southern hemisphere meteorology and oceanography, 7-11 April 1997*, Pretoria, South Africa, pp57-58.

Byers, HR, 1959: *General Meteorology*, McGraw-Hill Book Company, Inc., New York, Toronto, London, 540pp.

Camp, KTG, 1997: *The Bioresource Groups of KwaZulu/Natal*, Cedara Report No. N/A/97/6, KwaZulu/Natal Department of Agriculture, Pietermaritzburg, South Africa.

Camp, KGT; Manson, AD; Smith, JMB; Guy, RM and Milborrow, DJ, 1995: *The Bioresource Units of KwaZulu/Natal*, Cedara Report No. N/A/95/32, KwaZulu/Natal Department of Agriculture, Pietermaritzburg, South Africa.

Cane, MA; Eshel, G, and Buckland, RW, 1994: Forecasting Zimbabwean maize yield using eastern equatorial Pacific sea surface temperature, *Nature*, 370, pp204-205.

Cavalcanti, IFA, 1997: Southern hemisphere climate variability and anomalies over South America, *Fifth international conference on southern hemisphere meteorology and oceanography, 7-11 April 1997*, Pretoria, South Africa, pp93-94.

Cervera, JA, 1983: Drought characterisation and impact mitigation measures in Mexico, in Yevjevich, V; da Cunha, L and Vlachos, E, (eds), *Coping with droughts*, Water resources Publications, Michigan, USA, pp259-2269.

Charney, JG, 1975: Dynamics of deserts and droughts in the Sahel, *Quart. J. Roy. Meteor. Soc.*, 101, pp193-202.

CLIVAR, World Climate Research Programme, Initial Science Plan, 1995.

Crimp, SJ, 1997: Modelling sea-surface temperature anomaly effects on South African rainfall using a mesoscale model, *Fifth international conference on southern hemisphere meteorology and oceanography, 7-11 April 1997*, Pretoria, South Africa, pp122-123.

Crimp, SJ; van den Heever, SC; D'Abreton, PC; Tyson, PD and Mason, SJ, 1996: *Final Report: Mesoscale modelling of rainfall-producing systems over southern Africa*, A report to the Water Research Commission, 396pp.

D'Abreton, PC and Tyson, PD, 1996: Three-dimensional kinematic trajectory modelling of water vapour transport over southern Africa, *Water SA*, 22(4), pp297-306.

de Coning, E, 1997: Heavy rains and floods in South Africa during January and February 1996: An isentropic perspective, *Fifth international conference on southern hemisphere meteorology and oceanography, 7-11 April 1997*, Pretoria, South Africa, pp11-12.

Dewey, G., 1993: The crop, *South African Sugar Journal*, 1993, volume17.

Diab, RD; Preston-Whyte, RA and Washington, R, 1991: Distribution of rainfall by synoptic type over Natal, *International Journal of Climatology*, 11, pp877-888.

Dilley, M, 1996: Usefulness of climate forecasting information for drought mitigation and response from a donor's standpoint, *Draft report on the Workshop in reducing climate-related vulnerability in southern Africa held in Zimbabwe from 1-4 October 1996*, Zimbabwe, pp30-37.

Eakin, H, 1996: Comments on National and regional institutional capacity for the dissemination and interpretation of long-lead climate information, *Draft report on the Workshop in reducing climate-related vulnerability in southern Africa held in Zimbabwe from 1-4 October 1996*, Zimbabwe, pp38-46.

Eastman, JR and Anyamba, A, 1997: The spatial manifestation of ENSO-related drought and drought precursors in southern Africa, *Fifth international conference on southern hemisphere meteorology and oceanography, 7-11 April 1997*, Pretoria, South Africa, pp336-337.

Edwards, M, 1997: Heavy rain and floods in South Africa during February 1996: Synoptic review, *Fifth international conference on southern hemisphere meteorology and oceanography, 7-11 April 1997*, Pretoria, South Africa, pp7-8.

Experiment Station of the SA Sugar Association, 1977: Sugar cane production in South Africa, *Bulletin of the Experiment Station of the SA Sugar Association*.

Farmer's Weekly, 1993: Planning for drought as a natural phenomenon - 2 survival strategies, *Farmer's Weekly*, 19 March 1993, pp46-47.

Financial Mail, 1993a: The weather - Good news for farmers, *Financial Mail*, 129(7), p13.

Financial Mail, 1993b, GDP - Windfalls and rainfall, *Financial Mail*, 129(8), p35.

Financial Mail, 1993c: Summer crop: Dancing in the rain, *Financial Mail*, 130(9), p92.

Financial Mail, 1993d: Agriculture: Badly managed farms, *Financial Mail*, 130(1), pp68-69.

Fleagle, RG and Businger, JA, 1980: *An introduction to atmospheric physics*, Academic Press (Harcourt Brace Jovanovich Publishers), Orlando, San Diego, 432pp.

Folland, CK; Palmer, TN and Parker, DE, 1986: Sahel rainfall and worldwide sea temperatures 1901-85, *Nature*, 320, pp602-607.

Garstang, M; Brier, G; Kelbe, B and Diab, R, 1983: Synoptic controls and long-term periodicity in southern hemisphere rainfall, *American Meteorological Society: First international conference on southern hemisphere meteorology*, Boston, Massachusetts, USA, pp127-129.

Gittens, C, 1993: Drought is inevitable - How do you handle it?, *Farmer's Weekly*, 12 February, 1993, pp12-13.

Glantz, MH, 1987: Drought and economic development in Sub-Saharan Africa, in Wilhite, DA; Easterling, WE and Wood, DA, *Planning for drought – Toward a reduction of societal vulnerability*, Westview Press, Inc., Frederick A. Praeger Publisher, Colorado, USA, pp298-316.

Glantz, MH, 1996: Assessing the use and value of ENSO information for food security in southern Africa, *Draft report on the Workshop in reducing climate-related vulnerability in southern Africa held in Zimbabwe from 1-4 October 1996*, Zimbabwe, pp51-52.

Glantz, M; Betsill, M and Crandall, K, 1997: *Food security in southern Africa- Assessing the use and value of ENSO information*, National Centre for Atmospheric Research, Environmental and Societal Impacts Group, USA, pp142.

Goddard, L and Graham, NE, 1997: GCM-based climate forecasts over southern Africa, *Fifth international conference on southern hemisphere meteorology and oceanography, 7-11 April 1997*, Pretoria, South Africa, pp87-88.

Godefroy, SJ, 1992: *The polycyclic aromatic hydrocarbon content and mutagenicity of the residue from cane burning and vehicle emissions*, Unpublished Msc thesis, Department of Chemistry and Applied Chemistry, University of Natal.

Gondwe, M and Jury, MR, 1997a: Sensitivity of vegetation (NDVI) to climate over southern Africa: Relationships with rainfall and OLR, *Fifth international conference on southern hemisphere meteorology and oceanography, 7-11 April 1997*, Pretoria, South Africa, pp85-86.

Gondwe, MP and Jury, MR, 1997b: Sensitivity of vegetation (NDVI) to climate over southern Africa: Relationships with summer rainfall and OLR, *South Africa Geographical Journal*, 79(1), pp52-60.

Haltiner, GJ and Martin, FL, 1957: *Dynamical and physical meteorology*, McGraw-Hill Book Company, Inc., New York, Toronto, London, 470pp.

Haltiner, GJ and Williams, RT, 1980: *Numerical Prediction and dynamic meteorology*, John Wiley & Sons, New York, 477pp.

Hargraves, R and Jury, M, 1997: Composite meteorological structure of flood events over the eastern mountains of South Africa, *Water SA*, 23(4), pp357-363.

Harrison, MSJ, 1983: The Southern Oscillation, zonal equatorial circulation cells and South African rainfall, *American Meteorological Society: First International Conference on Southern Hemisphere Meteorology*, Boston, Massachusetts, pp302-305.

Harrison, MSJ, 1986: *A synoptic climatology of South African rainfall variations*, Unpublished PhD thesis, University of Witwatersrand, 341pp.

Hastenrath, S, 1983: Towards the monitoring and prediction of northeast Brazil droughts, *American Meteorological Society: First international conference on southern hemisphere meteorology*, Boston, Massachusetts, USA, pp116-117.

Hastenrath, S, 1991: *Climate dynamics of the tropics*, Kluwer Academic Press, Dordrecht, Boston, London, 488pp.

Hastenrath, S, 1995: Recent advances in tropical prediction, *Journal of Climate: American meteorological Society*, 8(6), pp1519-1532.

Hastenrath, S, 1987: The drought of northeast Brazil and their prediction, in Wilhite, DA; Easterling, WE and Wood, DA, *Planning for drought – Toward a reduction of societal vulnerability*, Westview Press, Inc., Frederick A. Praeger Publisher, Colorado, USA, pp45-60.

Hastenrath, S; Greischar, L and van Heerden, J, 1995: Prediction of the summer rainfall over South Africa, *Journal of Climate: American Meteorological Society*, 8(6), pp1511-1518.

Hattle, A and Webster, P, 1983: Development of a drought management strategy: A Namibian case study, in Yevjevich, V; da Cunha, L and Vlachos, E, (eds), *Coping with droughts*, Water resources Publications, Michigan, USA, pp270-289.

Heathcote, RL, 1991: Managing the droughts? Perceptions of resource management in the face of the drought hazard in Australia, Henderson-Sellers, A and Pitman, AJ (eds), *Vegetatio*, 91, Kluwer Academic Publishers, Belgium, pp219-230.

Hess, SL, 1959: *Introduction to theoretical meteorology*, Holt, Rinehart and Winston, New York, 362pp.

Hewson, BC, 1997: GCM derived climate change impacts on regional climate variability, *Fifth international conference on southern hemisphere meteorology and oceanography, 7-11 April 1997*, Pretoria, South Africa, pp24-25.

Hidore, JJ, 1983: Coping with drought in Sahel, in Yevjevich, V; da Cunha, L and Vlachos, E, (eds), *Coping with droughts*, Water resources Publications, Michigan, USA, pp290-309.

Hirst, AC and Hastenrath, S, 1983: On mechanisms of sea surface temperature anomalies in the Angola-Tropical Atlantic sector, *American Meteorological Society: First international conference on southern hemisphere meteorology*, Boston, Massachusetts, USA, pp130-131.

Hoffman, MT, 1995: Desertification of the Karoo, South Africa: A review of recent research and current status of the debate, *Proceedings of the National Research and Development Workshop on the assessment and monitoring of desertification in South Africa*, Pretoria, South Africa, pp21-38.

Holton, JR, 1972: *An introduction to dynamic meteorology*, Academic Press, New York and London, 319pp.

Hudson, DA and Hewitson, 1997: Climate change over southern Africa, *Fifth international conference on southern hemisphere meteorology and oceanography, 7-11 April 1997*, Pretoria, South Africa, pp347-348.

Hulme, M, (Ed.), 1996: *Climate change and southern Africa: An exploration of some potential impacts and implications for the SADC region*, Climatic Research Unit of East Anglia, Norwich, UK, pp9-61.

Hunt, BG, 1991: The simulation and prediction of drought, Henderson-Sellers, A and Pitman, AJ (eds), *Vegetatio*, 91, Kluwer Academic Publishers, Belgium, pp89-103.

Hunt, BG, 1997: Natural climatic variability, *Fifth international conference on southern hemisphere meteorology and oceanography, 7-11 April 1997*, Pretoria, South Africa, pp17-18.

Joubert, AM, 1997: Projections of anthropogenically-induced climate change over southern Africa, *Fifth international conference on southern hemisphere meteorology and oceanography, 7-11 April 1997*, Pretoria, South Africa, pp37-38.

Jury, MR, 1992: A climatic dipole governing the interannual variability of convection over the SW Indian Ocean and SE Africa region,, *Trends in Geophys Res.*, 1, pp165-172.

Jury, MR, 1993: A thermal front within the marine atmospheric boundary layer over the Agulhas Current south of Africa: Composite aircraft observations, *Journal of Geophysical Research*, 29(C2), pp3297-3304.

Jury, MR, 1995: A review of research on ocean-atmosphere interactions and South African climate variability, *South African Journal of Science*, 92, pp289-294.

Jury, MR, 1996a: *Atlas of climate fluctuations and impacts over southern Africa, 1975 - 1994*, Data report on satellite and vegetation analyses at inter-annual and intra-seasonal scales prepared under the auspices of the WRC projects, University of Cape Town.

Jury, MR, 1996b: Long-range climate forecasting and user needs in southern Africa, *Draft report on the Workshop in reducing climate-related vulnerability in southern Africa held in Zimbabwe from 1-4 October 1996*, Zimbabwe, pp16-23.

Jury, MR, 1996c: Regional teleconnection patterns associated with summer rainfall over South Africa, Namibia and Zimbabwe, *International Journal of Climatology*, 16, pp135-153.

Jury, MR, 1997: Long-range forecasting of South African summer rainfall using ENSO teleconnections, *Fifth international conference on southern hemisphere meteorology and oceanography, 7-11 April 1997*, Pretoria, South Africa, pp103-104.

Jury, MR and Levey, K, 1993: The climatology and characteristics of drought in the Eastern Cape of South Africa, *International Journal of Climatology*, 13, pp629-641.

Jury, MR; Pathack, B and Waliser, D, 1993: Satellite OLR and microwave data as a proxy for summer rainfall over subequatorial Africa and adjacent oceans, *Int. J. Climatol.*, 13, pp257-269.

Jury, MR and Levey, KM, 1997: Vertical structure of the atmosphere during wet spells over southern Africa, *Water SA*, 23(1), pp51-55.

Jury, MR; Levey, KM and Makarau, A, 1996a: *Mechanisms of short-term rainfall variability over southern Africa*, Final Report to the Water research Commission.

Jury, M; Pathack, B, Rautenbach, CDW and van Heerden, J, 1996b: Drought over South Africa and Indian Ocean SST: Statistical and GCM results, *The Global Atmosphere and Ocean System*, 4, pp47-63.

Jury, MR and Lutjeharms, JRE, 1993: The structure and possible forcing mechanisms of the 1991-92 drought in southern Africa, *S Afr Nat Sci Technol*, 12, pp8-16.

Jury, MR and Lyons, W, 1994: Contrasting synoptic weather events over southern Africa in the dry summer of 1983, *South African Geographical Journal*, 76(1), pp6-10.

Jury, MR and Majodina, M, 1997: Preliminary climatology of southern Africa extreme weather, *Theor. Appl. Climatol.*, 56, pp103-112.

Jury, MR; McQueen, C and Levey, KM, 1994: SOI and QBO signals in the African region, *Theor. Appl. Climatol.*, 50, pp103-115.

Jury, MR; Mulenga, HM; Mason, SJ and Brandao, A, 1997: *Development of an objective statistical system to forecast summer rainfall over southern Africa*, Report to the Water research Commission by the Department of Oceanography, University of Cape Town, WRC Report No. 672/1/97, 45pp.

Jury, MR and Parker, B, 1997: *Long range prediction of Gauteng winter temperature: Pattern recognition and objective models*, Paper under review.

Jury, MR, Valentine, HR and Lutjeharms, JRE, 1993: Influence of the Agulhas Current on summer rainfall along the south-east coast of South Africa, *J. Appl. Meteorol.*, 32, pp1282-1287.

Jury, MR, Weeks, S and Gondwe, MP, 1997: Satellite-observed vegetation as an indicator of climate variability over southern Africa, *South African Journal of Science*, 93, pp34-38.

Klopper, E, 1997: Seasonal temperature prediction in South Africa, *Fifth international conference on southern hemisphere meteorology and oceanography*, 7-11 April 1997, Pretoria, South Africa, pp101-102.

Kousky, JV, 1997: A comparison of model forecast precipitation with satellite rainfall estimates for the African continent, *Fifth international conference on southern hemisphere meteorology and oceanography*, 7-11 April 1997, Pretoria, South Africa, pp198-199.

Kousky, VE; Cavalcanti, IF and Gan, MA, 1983: Contrasts between wet and dry periods within the 1981 rainy season in northeast Brazil, *American Meteorological Society: First international conference on southern hemisphere meteorology*, Boston, Massachusetts, USA, pp112-115.

Kroese, NJ, Mittermaier, MP and Terblanche, DE, 1997: The flood event during February 1996 in the Vaal River catchment: A radar, rainfall and streamflow study, *Fifth international conference on southern hemisphere meteorology and oceanography*, 7-11 April 1997, Pretoria, South Africa, pp13-14.

Kruger, AC, 1997: Time trends in rainfall records in South Africa for the period 1930-1995, *Fifth international conference on southern hemisphere meteorology and oceanography*, 7-11 April 1997, Pretoria, South Africa, pp266-167.

Landbouweekblad, 1993: Finansies en ekonomie - 'n Tweede droogte: Verdere ramphulp onontbeerlik, *Landbouweekblad*, 5 February 1993.

Landman, WA, 1994: Forecasts of South African summer rainfall using canonical correlation analysis, *Experimental Long-Lead Forecast Bulletin*, 3(3), pp28.

Landman, WA, 1997: A study of the predictability of the equatorial Indian Ocean sea-surface temperatures, *Fifth international conference on southern hemisphere meteorology and oceanography*, 7-11 April 1997, Pretoria, South Africa, pp140-141.

Landman, WA; Brooks, DDG and Bartman, AG, 1997: Different modes of evolutionary global-scale sea-surface temperature variability, *Fifth international conference on southern hemisphere meteorology and oceanography, 7-11 April 1997*, Pretoria, South Africa, pp81-82.

Landman, WA; Klopper, E and Bartman, AG, 1997: Rainfall predictions for South Africa's neighbouring countries by means of CCA, *Fifth international conference on southern hemisphere meteorology and oceanography, 7-11 April 1997*, Pretoria, South Africa, pp83-84.

le Roux, SD, 1993: Bioclimatic groups of Natal, in Parsons, MJ (ed), *Maize in Natal: Agricultural production guidelines for Natal*, Cedara Agricultural Development Institute, Pietermaritzburg, South Africa.

Levey, KM, 1994: Data atlas report - Addendum to the MSc thesis: Intra-seasonal oscillations of convection over southern Africa, Report prepared under the auspices of the Water Research Commission Project: Mechanisms of short-term rainfall variability, Oceanography department, University of Cape Town, 91pp.

Levey, KM and Jury, MR, 1997: Educational and technical impact of information exchange via the CTWW Internet website, *Fifth international conference on southern hemisphere meteorology and oceanography, 7-11 April 1997*, Pretoria, South Africa, pp130-131.

Lindesay, JA, 1988: The Southern Oscillation and atmospheric circulation changes over southern Africa, Unpublished PhD thesis, University of the Witwatersrand, 284pp.

Lindesay, JA and Harrison, MSL, 1986: The Southern Oscillation and flow fields over southern Africa, *Reprints of the 2nd International Conference on Southern Hemisphere Meteorology: American Meteorological Society*, pp457-460.

Lindesay, JA and Jury, MR, 1991: Atmospheric circulation controls and characteristics of a flood event in central South Africa, *International Journal of Climatology*, 11, pp609-627.

Lyon, B and Dole, RM, 1995: A diagnostic comparison of the 1980 and 1988 US summer heat wave-droughts, *Journal of climate: American Meteorological Society*, 8 (6), pp1658-1675.

Majodina, M; Jury, MR and Ronault, M, 1997: Tropical air-sea interaction during a cruise in the central Indian Ocean, *Fifth international conference on southern hemisphere meteorology and oceanography, 7-11 April 1997*, Pretoria, South Africa, pp364-365.

Makarau, A., 1995: *Intraseasonal oscillatory modes of the southern Africa summer circulation*, PhD Thesis, Oceanogr. Dept., Univ. Cape Town.

Mallett, JB, 1993: Cultural Practices, in Parsons, MJ (ed), *Maize in Natal: Agricultural production guidelines for Natal*, Cedara Agricultural Development Institute, Pietermaritzburg, South Africa.

Markham, CG and McLain, DR, 1977: Seas surface temperature related to rain in Ceara, north-eastern Brazil, *Nature*, 265, pp320-323.

Mason, SJ, 1992: *Sea surface temperatures and South African rainfall variability*, PhD thesis, University of the Witwatersrand, Johannesburg.

Mason, SJ, 1997: Review of recent developments in seasonal forecasting of rainfall, *Water SA*, 23(1), pp57-62.

Mason, SJ; Joubert, AM; Cosjin, C and Crimp, SJ, 1996: Review of seasonal forecasting techniques and their applicability to southern Africa, *Water SA*, 22(3), pp203-209.

Mason, SJ and Jury, MR, 1997: Climatic variability and change over southern Africa: A reflection on underlying processes, in Tyson, PD (ed.), *Progress in Physical Geography*, 21(1), pp23-50.

Mason, SJ; Lindsay, JA and Tyson, PD, 1994: Simulating drought in southern Africa using sea surface temperature variations, *Water SA*, 20(1), pp14-22.

Matarira, CH and Jury, MR, 1992: Contrasting meteorological structure of intra-seasonal wet and dry spells in Zimbabwe, *International Journal of Climatology*, 12, pp165-176.

McIlveen, JFR, 1986: *Basic Meteorology*, Van Nostrand Reinhold, Wokingham, 457pp.

Meadows, M; Washington, R; Baxter, A and Wynberg, R, 1993: Global warming: The importance of the past in understanding the future, *South African Geographical Journal*, 75(2), pp41-45.

Montecinos, A; Aceituno, P and Diaz, A, 1997: Seasonal diagnostic and forecast of rainfall in subtropical South America based on Pacific SST, *Fifth international conference on southern hemisphere meteorology and oceanography, 7-11 April 1997*, Pretoria, South Africa, pp97-98.

Msengezi, T and Chenje, M, 1994: Climate factor, Chenje, M and Johnson (ed.), *State of the environment in southern Africa*, Penrose Press, Johannesburg, pp87-104.

Mulenga, HM, 1997: Southern African rainfall variability and climate teleconnections, *Fifth international conference on southern hemisphere meteorology and oceanography, 7-11 April 1997*, Pretoria, South Africa, pp194-195.

Mulenga, HM, 1998: *Southern African climatic anomalies, summer rainfall and the Angola low*, PhD thesis, University of Cape Town.

Mullan, AB, Folland, CK, Basnett, TA and Renshaw, AC, 1997: Simulation of multi-decadal climate variability in the South Pacific: 1871-1994, *Fifth international conference on southern hemisphere meteorology and oceanography, 7-11 April 1997*, Pretoria, South Africa, pp35-36.

National Research Council, 1996: *Learning to predict climate variations associated with El Nino and the Southern Oscillation*, National Academy Press, Washington DC, 171pp.

Nicholls, N, 1985: Impact of the Southern Oscillation on Australian crops, *J. Climatol.*, 5, pp553-560.

Nicholls, N, 1987: prospects for drought prediction in Australia and Indonesia, in Wilhite, DA; Easterling, WE and Wood, DA, *Planning for drought – Toward a reduction of societal vulnerability*, Westview Press, Inc., Frederick A. Praeger Publisher, Colorado, USA, pp61-72.

Nicholson, SE, 1983: Rainfall fluctuations in Africa – Interhemispheric teleconnections, *American Meteorological Society: First international conference on southern hemisphere meteorology*, Boston, Massachusetts, USA, pp122-126.

Owen, JA and Ward, MA, 1989: Forecasting Sahel rainfall, *Weather*, 44, pp57-64.

Palmén, E and Newton, CW, 1969: *Climatic circulation systems*, Academic Press, Inc., Hartcourt Brace Jovanovich Publishers, Orlando, 603pp.

Panchev, S, 1985: *Dynamic meteorology*, D. Reidel Publishing Company, Dordrecht, Boston, Lancaster, 360pp.

Parker, BA and Jury, MR, 1997: *Composite structure of tropical cyclones in the south-west Indian Ocean*, Paper under Review, 46pp.

Pathack, B, 1993: *Modulation of South African summer rainfall by global climatic processes*, PhD thesis, University of Cape Town.

Pathack, BMR, 1997: On bogusing and tracking tropical cyclones: A case study, *Fifth international conference on southern hemisphere meteorology and oceanography*, 7-11 April 1997, Pretoria, South Africa, pp134-135.

Pathack, BMR; Jury, MR; Shillington, FA and Courtney, S, 1993: South African summer rainfall variability and its association with the marine environment, *Water Research Commission Report No. 278/1/94.*, Pretoria, South Africa.

Pers. Comm., Chadwick, J, 1998, Director: Growers Services, SA Sugar Growers Association, KwaZulu/Natal.

Peter, BN, 1997: Mass balance in the south Indian Ocean, *Fifth international conference on southern hemisphere meteorology and oceanography, 7-11 April 1997*, Pretoria, South Africa, pp386-387.

Pielke, RA, 1984: *Mesoscale Meteorological Modeling*, Academic Press (Harcourt Brace Jovanovich Publishers), Orlando, San Diego, 612pp.

Power, S; Tseitkin, V; Mehta, V; Torok, S; Lavery, B and Holbrook, N, 1997: Decadal variability in Australian temperature, rainfall and river flow, *Fifth international conference on southern hemisphere meteorology and oceanography, 7-11 April 1997*, Pretoria, South Africa, pp29-30.

Preston-Whyte, RA, 1968a: The nature and significance of early morning winter air movement over Durban Bay, *South African Journal of Science*, pp183-186.

Preston-Whyte, RA, 1968b: Some observations of land breezes and katabatic winds in the Durban area, *South African Geographical Journal*, 3(3), pp227-235.

Preston-Whyte, RA, 1969: Sea breeze studies in Natal, *South African Geographical Journal*, 56, pp39-49.

Preston-Whyte, RA, 1970: Atmospheric pollution and air movement over Durban during winter, *Concept*, 2, pp16-17.

Preston-Whyte, RA, 1974: Land breezes and mountain-plain winds over the Natal coast, *South African Geographical Journal*, 56(1), pp27-33.

Preston-Whyte, RA, 1975: A note on some bioclimatic consequences of coastal lows, *South African Geographical Journal*, 57(1), pp17-20.

Preston-Whyte, RA and Tyson, PD, 1980: Local weather and air pollution potential - The case of Durban, *Environmental Conservation*, 7(3), pp241-244.

Preston-Whyte, RA; Diab, RD and Washington, 1991: Diurnal variation of rainfall events by synoptic type in Natal, *South African Geographical Journal*, 73, pp22-28.

Preston-Whyte, RA; Diab, RD and Tyson, PD, 1977: Towards an inversion climatology of southern Africa - Part II, Non-surface inversions in the lower atmosphere, *South African Geographical Journal*, 59(1), pp45-58.

Preston-Whyte, RA and Tyson, PD, 1988: *The atmosphere and weather of southern Africa*, Oxford University Press, Cape Town, pp178-276.

Rathor, HS; de Araujo, MA and de Mello, CC, 1983: The divergence of water vapour flux during a typical rainy month over northeast Brazil, *American Meteorological Society: First international conference on southern hemisphere meteorology*, Boston, Massachusetts, USA, pp138-142.

Rautenbach, CLdeW, 1997a: A GCM study describing teleconnections between global SST anomalies and copious summer rainfall over southern Africa, *Fifth international conference on southern hemisphere meteorology and oceanography*, 7-11 April 1997, Pretoria, South Africa, pp1-2.

Rautenbach, CJdeW, 1997b: Seasonal variability in observed and GISST simulated rainfall over southern Africa, *Fifth international conference on southern hemisphere meteorology and oceanography*, 7-11 April 1997, Pretoria, South Africa, pp105-106.

Reason, CJC; Allan, RJ; Lindesay, JA and Godfred-Spenning, CR, 1997: Mechanisms associated with low frequency climate variability in the south Indian Ocean region, *Fifth international conference on southern hemisphere meteorology and oceanography, 7-11 April 1997*, Pretoria, South Africa, pp3-4.

Rocha, A and Simmonds, I, 1997a: Interannual variability of south-eastern African summer rainfall - Part I: Relationships with air-sea interaction processes, *International Journal of Climatology*, 17, pp235-265.

Rocha, A and Simmonds, I, 1997b: Interannual variability of south-eastern African summer rainfall - Part II: Modelling the impact of sea-surface temperatures on rainfall and circulation, *International Journal of Climatology*, 17, pp267-290.

Rocha, A and Simmonds, I, 1997c: Rainfall variability over the Sahel and Kalahari regions and its associations with sea surface temperatures, *Fifth international conference on southern hemisphere meteorology and oceanography, 7-11 April 1997*, Pretoria, South Africa, pp7-8.

Rocha, A and Simmonds, I, 1997d: Distinct modes of SST-forced rainfall variability over southern hemisphere continents, *Fifth international conference on southern hemisphere meteorology and oceanography, 7-11 April 1997*, Pretoria, South Africa, pp91-92.

Ronchail, J, 1997: Interdecadal variability of rainfall in Bolivia and sea-surface temperatures, *Fifth international conference on southern hemisphere meteorology and oceanography, 7-11 April 1997*, Pretoria, South Africa, pp99-100.

Rossi, G, 1983: Droughts of Sicily, in Yevjevich, V; da Cunha, L and Vlachos, E, (eds), *Coping with droughts*, Water resources Publications, Michigan, USA, pp244-258.

Sakamoto, CM and Steyaert, LT, 1987: International drought early warning program of NOAA/NESDIS/AISC, in Wilhite, DA; Easterling, WE and Wood, DA, *Planning for drought – Toward a reduction of societal vulnerability*, Westview Press, Inc., Frederick A. Praeger Publisher, Colorado, USA, pp247-272.

Santos, MA; Correia, F; da Cunha, LV, 1983: Drought characterisation and impact assessment: Case study of Portugal, in Yevjevich, V; da Cunha, L and Vlachos, E, (eds), *Coping with droughts*, Water Resources Publications, Michigan, USA, pp219-243.

Schulz, EF, 1976: *Problems in applied hydrology*, Water Resources Publications, Fort Collins, Colorado, USA, pp197-210.

Sivakumar, MVK, 1995: Desert Margins Initiative: An integrated national, regional and international research programme for developing sustainable resource management options to combat land degradation in sub-Saharan Africa, *Proceedings of the National Research and Development Workshop on the assessment and monitoring of desertification in South Africa*, Pretoria, South Africa, pp6-9.

Smith, D, 1978: *Cane sugar world*, Palmer Publications, USA, pp150-155.

Smith, JMB, 1993: Maize yield estimation, in Parsons, MJ (ed), *Maize in Natal: Agricultural production guidelines for Natal*, Cedara Agricultural Development Institute, Pietermaritzburg, South Africa.

South African Weather Bureau, 1992a: Comparison between 1991/92 and the 1982/83 drought, *South African Weather Bureau Newsletter No. 525*, Department of Environmental Affairs, South Africa, p6.

South African Weather Bureau, 1992b: *South African Weather Bureau Newsletter No. 514*, Department of Environmental Affairs, South Africa.

Stephenson, D, 1996: Drought management as an alternative to new water schemes- Theory, *Water SA*, 22(4), pp291-296

Tennant, WJ, 1997: Monthly forecasting in South Africa, *Fifth international conference on southern hemisphere meteorology and oceanography, 7-11 April 1997*, Pretoria, South Africa, pp154-155.

Stringer, ET, 1972: *Foundations of climatology*, WH Freeman and Company, San Francisco, 586pp.

Taljaard, JJ, 1989: Climate and circulation anomalies in the South African region during the dry summer of 1982/1983, *South African Weather Bureau, Technical Paper 21*, Pretoria, South Africa, 45pp.

The South African Sugar Association, 1993a: Rainfall well below average - Drought situation report, *The South African Sugar Association*, May 1993, pp132.

The South African Sugar Association, 1993b: Sugar industry grappling with unparalleled drought, *The South African Sugar Association*, July 1993, p190.

The South African Sugar Association, 1993c: Drought cuts growers revenue by R790 million, *The South African Sugar Association*, July 1993, pp182-186.

The South African Sugar Association, 1993d: Drought has spawned south coast devastation, *The South African Sugar Association*, October 1993, pp296-297.

The South African Sugar Association, 1993e: Sugar price increase, *The South African Sugar Association*, May 1993, p132.

The South African Sugar Association, 1993f: Rural areas in the grip of drought, *The South African Sugar Association*, August 1993, p212.

The South African Sugar Association, 1993g: Changes in global weather patterns, *The South African Sugar Association*, October 1993, p298.

The South African Sugar Association, 1993h: Bitter harvest of a two-year drought, *South African Sugar Association*, August 1993, p222.

The South African Sugar Association, 1993i: Rural communities menaced by drought: "Operation Amanzi" offers a water lifeline, *South African Sugar Association*, September 1993, p262.

The South African Sugar Association, 1993j: First sugar from Australia: Drought results in sugar imports, *South African Sugar Association*, November 1993, p316.

Thiao, W, 1996: Summary of lessons learned from climate prediction for southern Africa in 1992-95, *Draft report on the Workshop in reducing climate-related vulnerability in southern Africa held in Zimbabwe from 1-4 October 1996*, Zimbabwe, pp24-24j.

Thiao, W and Barnston, AG, 1997: Long-lead predictability of summer rainfall in southern Africa, *Fifth international conference on southern hemisphere meteorology and oceanography, 7-11 April 1997*, Pretoria, South Africa, pp156-157.

Trenberth, KE; Branstator, GW and Arkin, PA, 1988: Origins of the 1988 North American drought, *Science*, 242, pp1640-1645.

Tyson, PD, 1972: Observation of regional topographically-induced wind systems in Natal, *Journal of Applied Meteorology*, 11(4), pp643-650.

Tyson, PD, 1986: *Climatic change and variability in southern Africa*, Oxford University Press, Cape Town, 220pp.

Tyson, PD and Preston-Whyte, RA, 1972: Observations of topographically-induced wind systems in Natal, *Journal of Applied Meteorology*, 11(4), pp643-650.

Tyson, PD, Preston-Whyte, RA and Diab, RD, 1977: Towards an inversion climatology of southern Africa - Part I, Surface inversions, *South African Geographical Journal*, 58(2), pp151-163.

United Nations, 1992a: *Agenda 21: The United Nations programme of action from Rio*, United Nations Department of Public Information, United Nations, New York, USA, 294pp.

United Nations, 1992b: *Earth Summit: Convention on Desertification held in Rio de Janeiro, Brazil*, Department of Public Information, New York, USA, 44pp.

van den Heever, SC; D'Abreton, PC and Tyson, PD, 1997: Numerical simulation of tropical-temperate troughs over southern Africa using the CSU RAMS model, *South African Journal of Science*, 93, pp359-365.

Vaides, PJ, 1994: Climate change in southern Africa, *Archimedes*, 36(2), pp10-11.

Valença, A, 1983: Annual rainfall variability in the northeast Brazil, *American Meteorological Society: First international conference on southern hemisphere meteorology*, Boston, Massachusetts, USA, pp134-137.

van Zyl, 1993: Drought doesn't only affect farmers, *Farmer's Weekly*, 10 December 1993, pp40-42.

Verstraete, MM and Schwarts, SA, 1991: Desertification and global change, Henderson-Sellers, A and Pitman, AJ (eds), *Vegetatio*, 91, Kluwer Academic Publishers, Belgium, pp3-13.

Visser, PJM, 1997: Radar reflectivity characteristics of severe storms over the eastern Free State, *Fifth international conference on southern hemisphere meteorology and oceanography, 7-11 April 1997*, Pretoria, South Africa, p115.

Vlachos , E and James, LD, 1983: Drought impacts, in Yevjevich, V; da Cunha, L and Vlachos, E, (eds), *Coping with droughts*, Water resources Publications, Michigan, USA, pp44-73.

Voice, ME and Hunt, BG, 1984: A study of the dynamics of drought initiation using a global general circulation model, *J. Geophys. Res.*, 89, pp9504-9520.

Walker, ND, 1989: *Sea-surface temperature-rainfall relationships and associated ocean-atmosphere coupling mechanisms in the southern African Region*, Unpublished PhD Thesis, University of Cape Town, 173pp.

Whetton, PH, Joubert, AM and Labraga, JC, 1997: Sensitivity of regional climate change simulations to the representation of oceanic processes at high latitudes in the southern hemisphere, *Fifth international conference on southern hemisphere meteorology and oceanography, 7-11 April 1997*, Pretoria, South Africa, pp21-22.

Whitehead, ENC, Crockart, BRI and Parsons, MJ, 1993: Financial aspects of maize production, in Parsons, MJ (ed), *Maize in Natal: Agricultural production guidelines for Natal*, Cedara Agricultural Development Institute, Pietermaritzburg, South Africa.

Wilder, J; Beckford, K; Borenstein, S; Druyan, L; Estrella, A; Hansen, J; Knox, J; Miller, R and Ruedy, R: 1997: Winter forecast by the GISS SI91 model based on fixed SST anomalies, in Barnston, AG (ed): *Experimental long-lead bulletin*, 6(4), NOAA, Washington, pp2-8.

Zambatis, N and Biggs, HC, 1995: Rainfall and temperature during the 1991/92 drought in the Kruger National Park, *Koedoe*, 38(1), pp1-16.

## APPENDIX

## APPENDIX A3

### STATISTICAL PREDICTION OF RAINFALL AND CROP YIELDS:

#### A3.1 RAINFALL PREDICTION

The best fit for JFM ( $r^2 = 71$ ) and NDJ ( $r^2 = 58$ ) rainfall over the Swaziland-KwaZulu/Natal region is obtained, respectively, from the models  $-0.68(aATpc4)-0.37(oSocNs)+0.56(aMaurV)+0.61(oNIv)$  and  $+0.70(Wiv)+0.89(aArBolr)+0.48(SWp)-1.1(SIp)$  ((Jury *et al.*, 1997) (see (see Table A3.1 for predictor definitions).

#### A3.2 MAIZE YIELD

The model defining the best fit ( $r^2 = 84$ ) for maize yield over South Africa is  $-0.29(oQBO_-)-0.31(aIpc2)+0.56(oColr)+0.35(oSIst)$  (Jury *et al.*, 1997) (see (see Table A3.1 for predictor definitions).

#### A3.3 SUGAR CANE YIELD

The model defining the best fit ( $r^2 = 84$ ) for sugar cane yield is  $+0.85(oNIv)+0.31(oSEolr)+0.31(aATpc1)+0.44(oSOI)$  (Jury *et al.*, 1997) (see Table A3.1 for definition of predictors).

Table A3.1: Predictor area definition of South African rainfall, maize and sugar cane yield models. All times are JAS or SON months and most have areas  $> 10^6 \text{ km}^2$  (Source: (Jury *et al.*, 1997).

Predictor/selected	Parameter	Area/borders	Lat. Long
ATpc4 3	Sea surface temp.	SW Atlantic	40°S, 45°W
SocNs 2	Sea surface temp.	Southern Ocean	45°S, 10–40°E
MaurV 1	Sfc meridional wind	Mauritius region	20°S, 62°E
Niv 1	Sfc meridional wind	Northern Indian Ocean	02°N, 70°E
Wiv 1	Sfc meridional wind	Western Indian Ocean	02°S, 47°E
ArBolr 3	Outgoing longwave rad.	Arabian Sea	10°N, 55°E
SWp 2	Air pressure	SW Indian Ocean	27°S, 47°E
Sip 1	Air pressure	South Indian Ocean	12°S, 77°E
QBO 3	Quasi-biennial oscil.	Zonal wind 30hPa	Singapore
Ipc2 1	Sea surface temp.	South Indian dipole	35°S, 50°E
Colr 1	Outgoing longwave rad.	Central Indian Ocean	02°S, 62°E
SIst 1	Sea surface temp.	South Indian Ocean	12°S, 77°E
SOI 3	Southern Oscil. Index	Tahiti-Darwin pressure	West-central Pacific

## APPENDIX A4:

### DEFINITIONS AND CALCULATION OF SOME ATMOSPHERIC VARIABLES

Definition of some of the terms used in Chapters 4 to 6 of the thesis and calculations are summarised below.

#### A4.1 VORTICITY AND DIVERGENCE

Perhaps the terms that have been used very often in the text are vorticity and divergence/convergence as they easily describe the circulation pattern and relate easily to other parameters. Absolute vorticity of a rotating vortex in the earth's atmosphere which itself is rotating is  $\zeta + f$  ——— A4.1

where  $\zeta$  is relative vorticity, and  $f$  is the Coriolis parameter ( $2\omega\sin\phi$ ).

Expressed in  $u$  and  $v$  velocity components, relative vorticity is

$$\zeta = dv/dx - du/dy \quad \text{—————A4.2}$$

which is the difference between the rate of change of the  $v$  (meridional) wind component in the  $x$  direction and the  $u$  (zonal) component in the  $y$  direction (Preston-Whyte and Tyson, 1988).

If a column of air is rotating clockwise, i.e. cyclonically, around a vertical axis, convergence and concentration of mass near the axis of rotation will increase rotation and hence vorticity increases. Cyclonic vorticity is positive or increasing and anticyclonic vorticity is negative or decreasing. The relationship between divergence and vorticity is given by

$$\text{div} = -d\zeta/dt \quad \text{————— A4.3}$$

Thus cyclonic vorticity is associated with negative divergence, i.e. convergence, and anticyclonic vorticity with divergence.

The vorticity equation in the vector form

$$\partial\zeta/\partial t + \mathbf{u}\cdot\nabla(\zeta + f) + w \partial\zeta/\partial z = -(\zeta + f) \nabla\cdot\mathbf{u} + \mathbf{k}\cdot(\partial\mathbf{u}/\partial z \times \nabla\mathbf{w}) - \mathbf{k}\cdot(\nabla\alpha \times \nabla p) \quad \text{---A 4.4}$$

states that the rate of change of the absolute vorticity following the motion is given by the sum of the three terms on the right, viz. the divergence, tilting and solenoidal terms, respectively. For large-scale atmospheric circulations the last two terms die out and only the divergence term remains. Details on vorticity and its conservation are provided in Holton, 1979; Panchev, 1985, Fleagle and Businger, 1980).

#### A4.2 PRECIPITABLE WATER

For a column of air having a cross-sectional area of  $1 \text{ cm}^2$ , the total mass of water vapour contained between the height 0 and the height  $z$  would be

$$W = \int_0^z \rho_w dz \quad \text{(Byers, 1959)} \quad \text{--- A4.5}$$

where  $\rho_w$  is the density of water vapour or absolute humidity. Substituting the hydrostatic equation  $dp = -\rho g dz$ ,

$$W = \int_p^{p_0} (\rho_w/\rho)(1/g) dp \quad \text{(Byers, 1959)} \quad \text{--- A4.6}$$

$$= 1/g \int_p^{p_0} q dp \quad \text{--- A4.7}$$

where  $q$  is specific humidity, defined as  $\rho_w/\rho$ . It is simpler to express the quantity in terms of vapour pressure and pressure. Since  $q = 0.622e/p$ ,

$$W = 0.622/g \int_p^{p_0} e(dp/p) \quad \text{(Byers, 1959)} \quad \text{--- A4.8}$$

$$W = 0.622/g \int_p^{p_0} e(d(\ln p)) \quad \text{(Byers, 1959)} \quad \text{--- A4.9}$$

$W$  is in grams per square centimetre of area.

### A4.3 STREAM FUNCTION

The streamline is a line drawn such that the velocity vectors of all the fluid particles lying on it in a given instant  $t$  should be tangential to it at the corresponding points. The streamlines constructed at  $t = t_1$  and  $t = t_2$ , generally do not coincide. The differential equation of the streamline is

$$dx/u(x, y, t) = dy/v(x, y, t) \quad \text{(Panchev, 1985)} \quad \text{----- A4.10}$$

If  $u, v$  are known functions of  $x, y$ , it could be integrated to yield  $y = y(x, t)$ .

An alternative form of a stream function equation is derived from the definition (non-divergence of the wind field, i.e.  $(u_x + v_y = 0)$  and from equation A4.10. Here  $\partial(-u)/\partial x = \partial v/\partial y$ ,  $v dx + (-u) dy = 0$ , ----- A4.11

hence equation 4.11 may be represented as a differential of some function

$\psi(x, y, t)$ :  $u = -\psi_y$ ,  $v = \psi_x$ ,  $d\psi(x, y, t) = \text{constant}$ .  $\psi(x, y, t)$  is called a stream function. A negative streamfunction is associated with anticyclonic circulation and the opposite applies for a positive streamfunction. Streamfunction analysis for the 1992/93 drought has been done on NCEP/NOAA data and is presented in Chapter 5.

### A4.4 VELOCITY POTENTIAL

Orthogonal to the streamlines is a set of lines in a unit distance proportional to the wind speed to produce a velocity potential  $\phi$  defined by

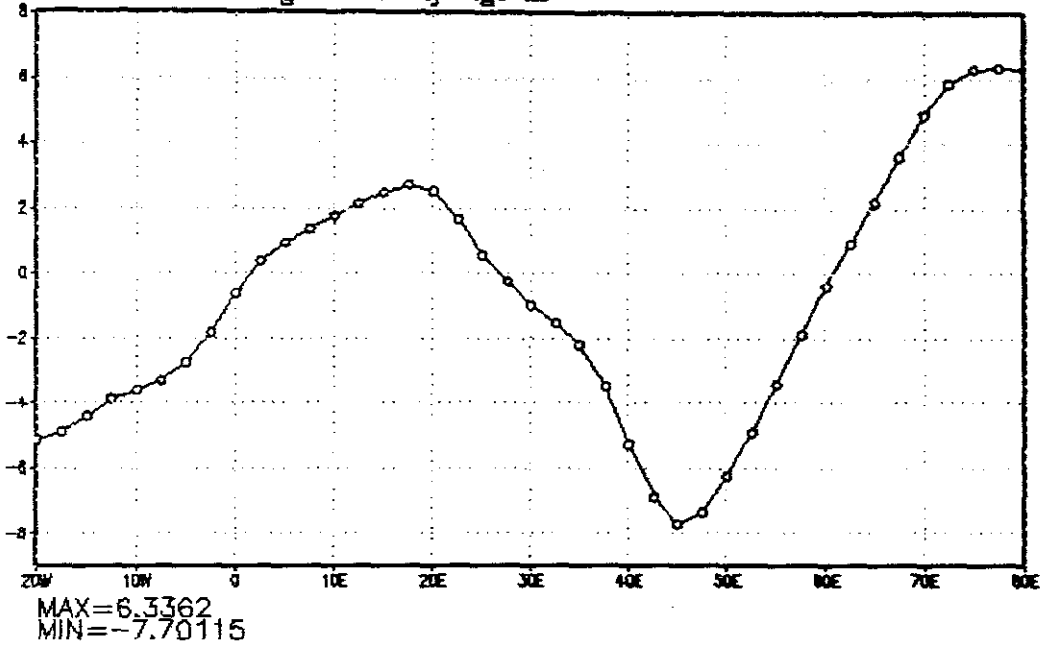
$$u = -\partial\phi/\partial x, \quad v = \partial\phi/\partial y \quad \text{(Byers, 1959)} \quad \text{----- A4.12}$$

If the velocity potential exists, the flow must be irrotational, i.e. the vorticity must be zero. This is shown by obtaining  $\partial v/\partial x$  and  $\partial u/\partial y$  by differentiating equation A4.12 to obtain  $\partial v/\partial x - \partial u/\partial y = 0$  defining irrotational flow. Velocity potential analysis for the 1992/93 drought has been performed on NCEP/NOAA data and is presented in Chapter 5.

(a)

t: averaged over Dec 1992 to Feb 1993

NCEP GrADS image Anomaly hgt m



(b)

t: averaged over Dec 1992 to Feb 1993

NCEP GrADS image Anomaly hgt m

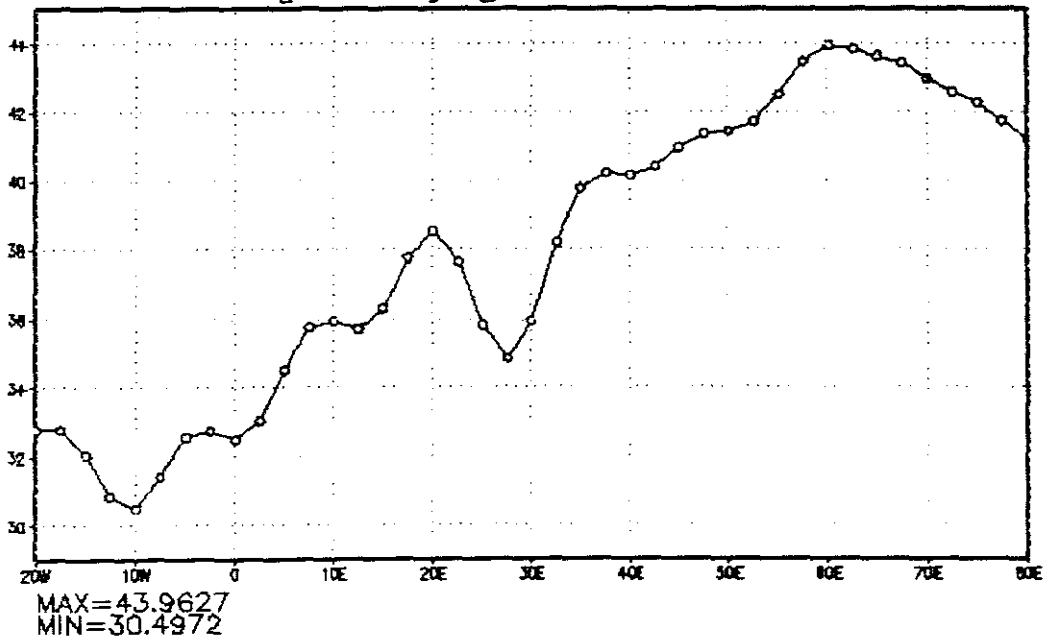
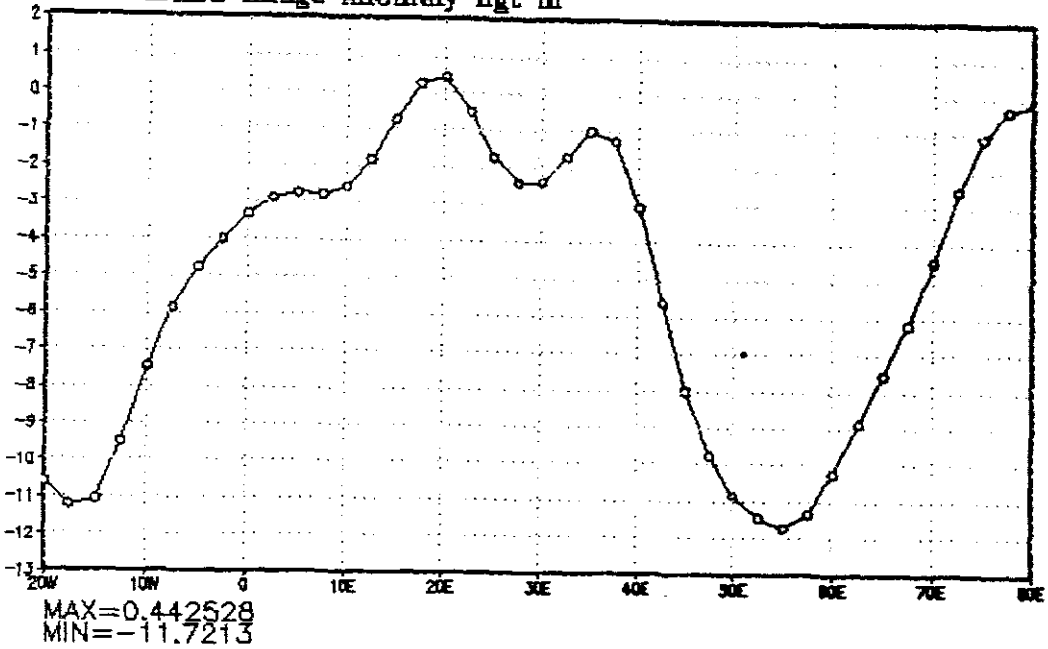


Fig. A4.1: DJF 1992/93 geopotential height anomalies at (a) 30°S latitude at the 1000 hPa level, and (b) 100 hPa level.

(a)

t: averaged over Dec 1992 to Feb 1993

NCEP GrADS image Anomaly hgt m



(b)

t: averaged over Dec 1992 to Feb 1993

NCEP GrADS image Anomaly hgt m

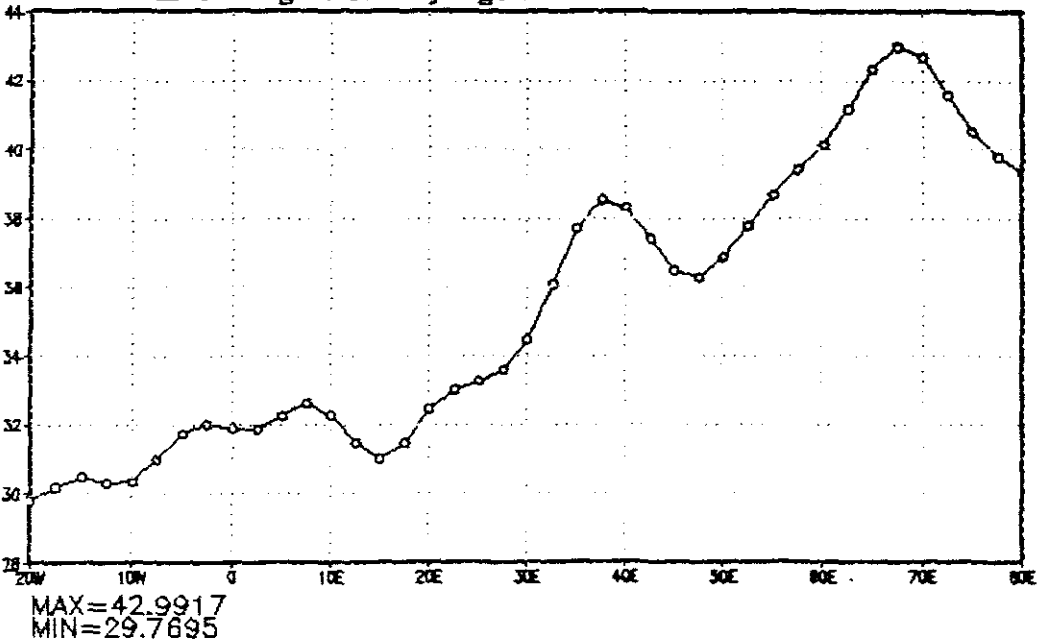
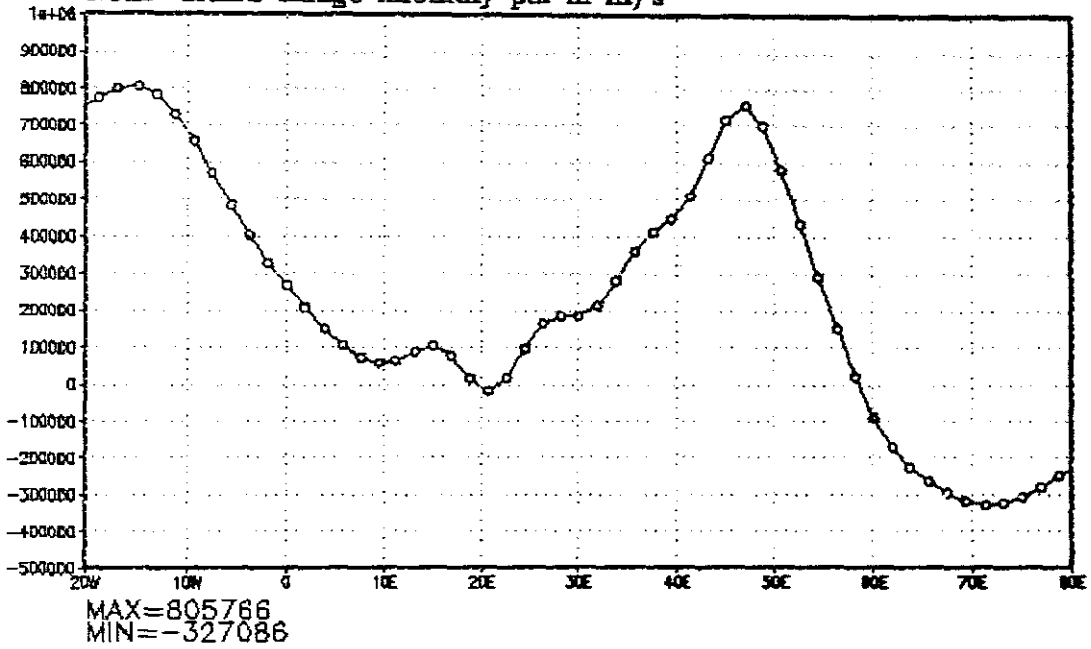


Fig. A4.2: DJF 1992/93 geopotential height anomalies at (a) 35°S latitude at the 1000 hPa level, and (b) 100 hPa level.

(a)

t: averaged over Dec 1992 to Feb 1993

NCEP GrADS image Anomaly psi m<sup>2</sup>/s



(b)

t: averaged over Dec 1992 to Feb 1993

NCEP GrADS image Anomaly psi m<sup>2</sup>/s

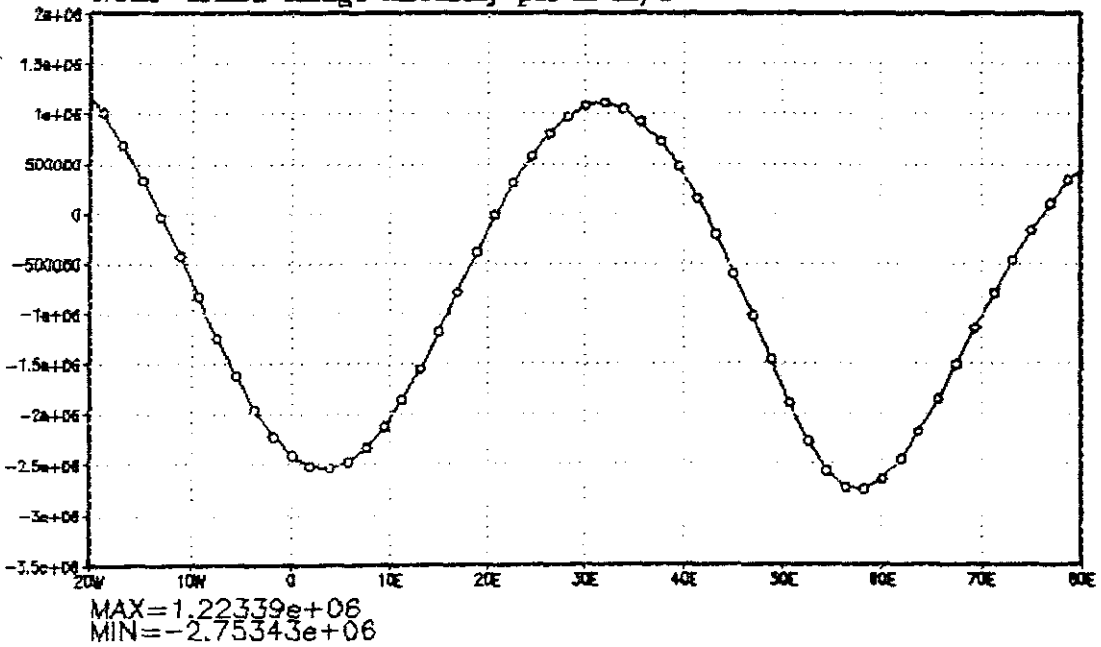
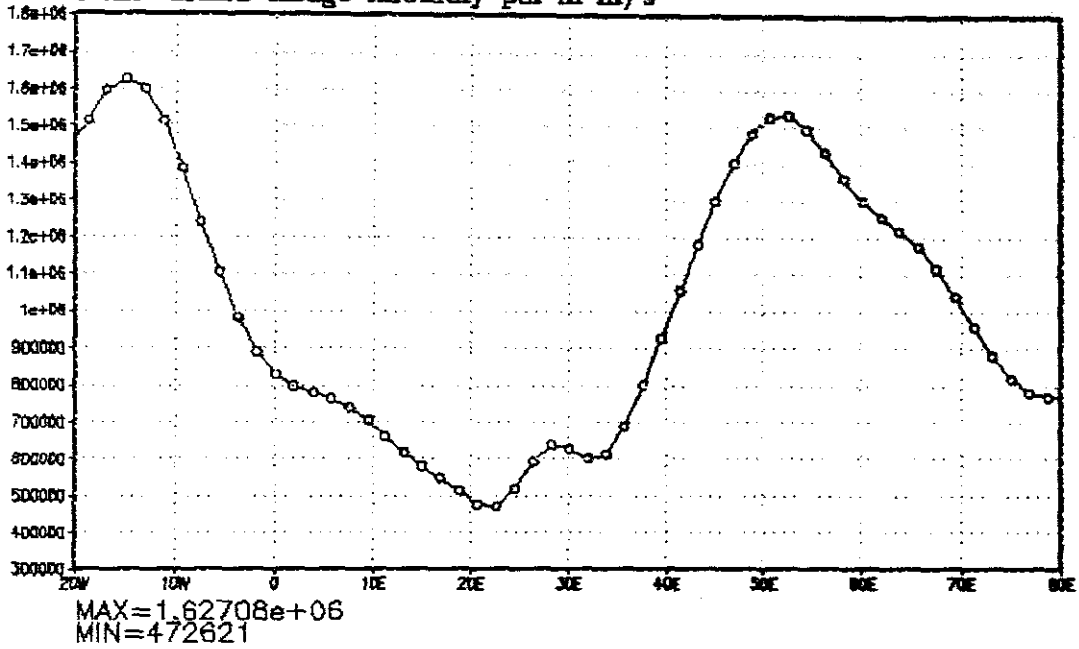


Fig. A4.3: DJF 1992/93 streamfunction anomalies at 30°S latitude at the (a) 0.9950 sigma level, and (b) 0.2101 sigma level.

(a)

t: averaged over Dec 1992 to Feb 1993

NCEP GrADS image Anomaly psi m\*m/s



(b)

t: averaged over Dec 1992 to Feb 1993

NCEP GrADS image Anomaly psi m\*m/s

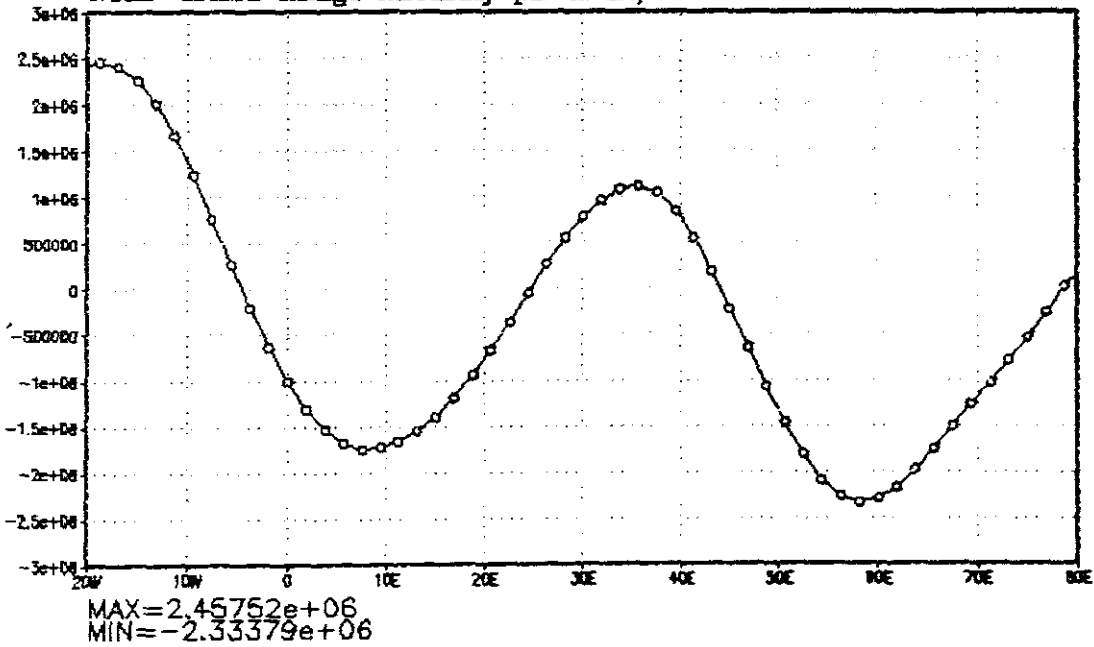
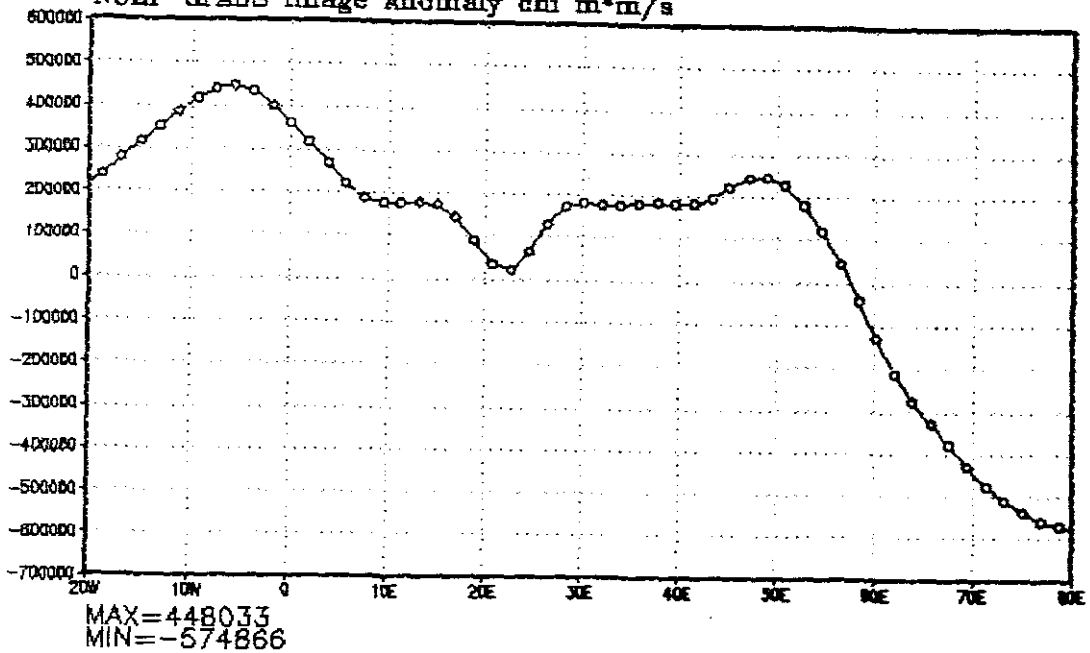


Fig. A4.4: DJF 1992/93 streamfunction anomalies at 35°S latitude at the (a) 0.9950 sigma level, and (b) 0.2101 sigma level.

(a)

t: averaged over Dec 1992 to Feb 1993

NCEP GrADS image Anomaly chi m\*m/s



(b)

t: averaged over Dec 1992 to Feb 1993

NCEP GrADS image Anomaly chi m\*m/s

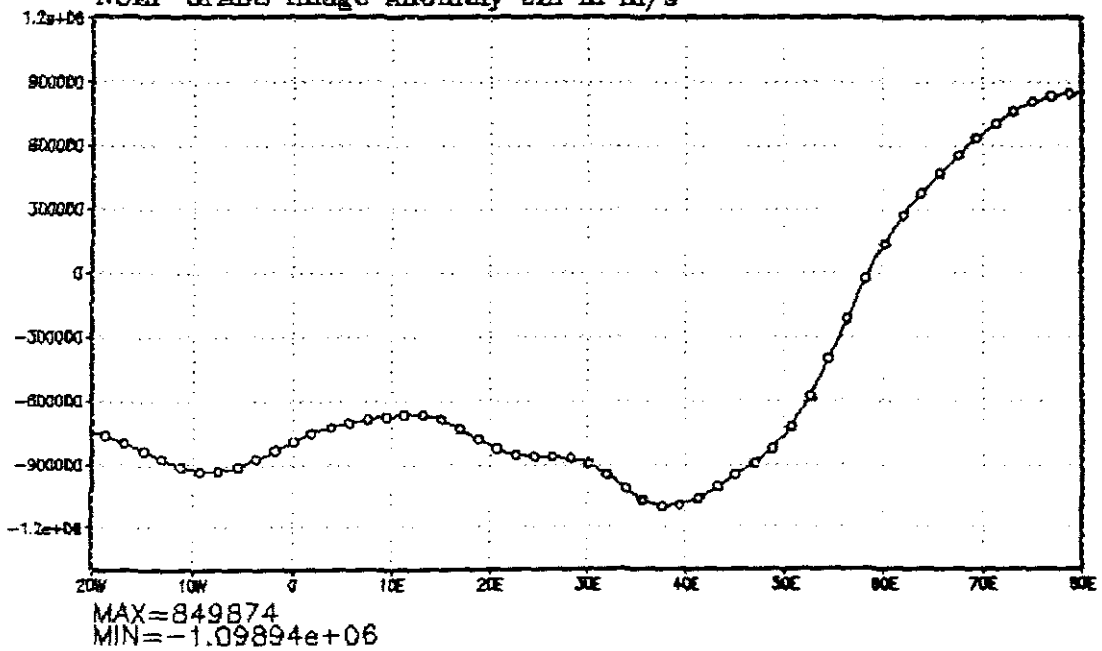
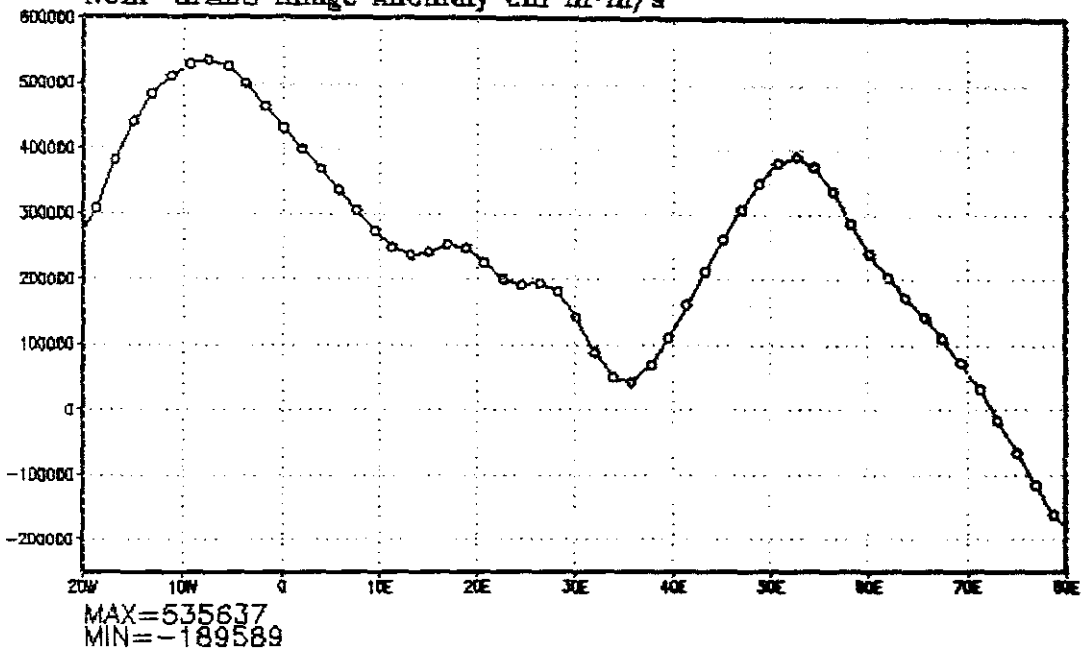


Fig. A4.5: DJF 1992/93 velocity potential anomalies at 30°S latitude at the (a) 0.9950 sigma level, and (b) 0.2101 sigma level.

(a)

t: averaged over Dec 1992 to Feb 1993

NCEP GrADS image Anomaly chi m\*/m/s



(b)

t: averaged over Dec 1992 to Feb 1993

NCEP GrADS image Anomaly chi m\*/m/s

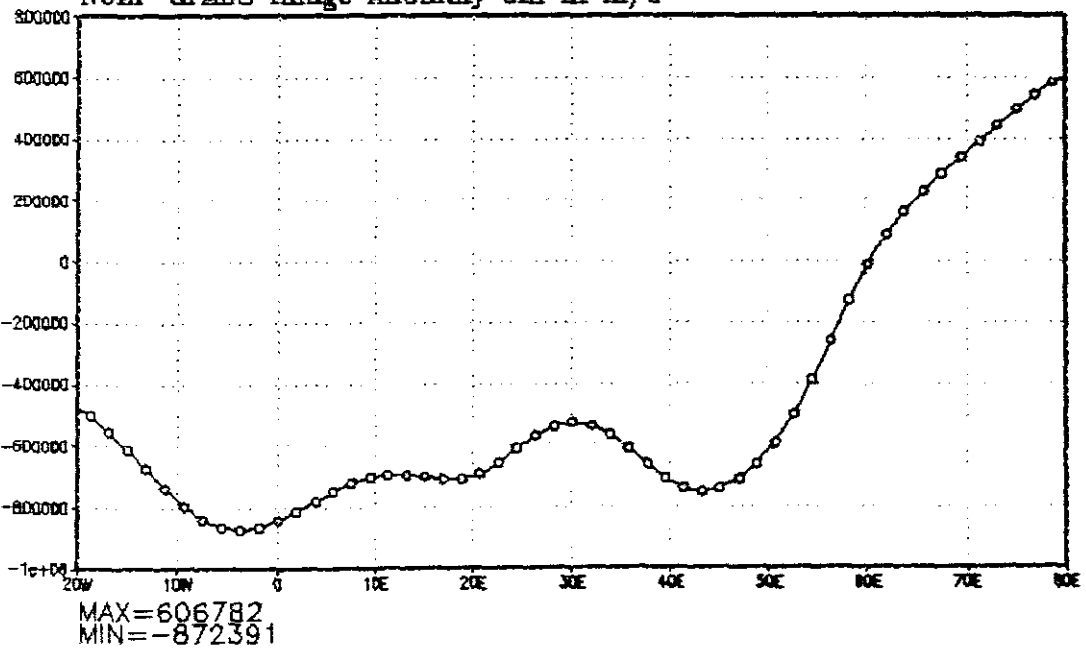


Fig. A4.6: DJF 1992/93 velocity potential anomalies at 35°S latitude at the (a) 0.9950 sigma level, and (b) 0.2101 sigma level.

Table A4.1: Meteorological pentads.

PENTAD	MONTH	DATE	PENTAD	MONTH	DATE
01	JAN	01-05	38	JUL	05-09
02	JAN	06-10	39	JUL	10-14
03	JAN	11-15	40	JUL	15-19
04	JAN	16-20	41	JUL	20-24
05	JAN	21-25	42	JUL	25-29
06	JAN	26-30	43	JUL-AUG	30-03
07	JAN-FEB	31-04	44	AUG	04-08
08	FEB	05-09	45	AUG	09-13
09	FEB	10-14	46	AUG	14-18
10	FEB	15-19	47	AUG	19-23
11	FEB	20-24	48	AUG	24-28
12	FEB-MAR	25-01	49	AUG-SEPT	29-02
13	MAR	02-06	50	SEPT	03-07
14	MAR	07-11	51	SEPT	08-12
15	MAR	12-16	52	SEPT	13-17
16	MAR	17-21	53	SEPT	18-22
17	MAR	22-26	54	SEPT	23-27
18	MAR	27-31	55	SEPT-OCT	28-02
19	APR	01-05	56	OCT	03-07
20	APR	06-10	57	OCT	08-12
21	APR	11-15	58	OCT	13-17
22	APR	16-20	59	OCT	18-22
23	APR	21-25	60	OCT	23-27
24	APR	26-30	61	OCT-NOV	28-01
25	MAY	01-05	62	NOV	02-06
26	MAY	06-10	63	NOV	07-11
27	MAY	11-15	64	NOV	12-16
28	MAY	16-20	65	NOV	17-21
29	MAY	21-25	66	NOV	22-26
30	MAY	26-30	67	NOV-DEC	27-01
31	MAY-JUN	31-04	68	DEC	02-06
32	JUN	05-09	69	DEC	07-11
33	JUN	10-14	70	DEC	12-16
34	JUN	15-19	71	DEC	17-21
35	JUN	20-24	72	DEC	22-26
36	JUN	25-29	73	DEC	27-31
37	JUN-JUL	30-04			